Zeitschrift: IABSE reports = Rapports AIPC = IVBH Berichte
Band: 62 (1991)

Rubrik: Sub-theme 2.4: Dimensioning and detailing

Dimensioning and Detailing

Dimensionnement et conception des détails

Bemessung und Bewehrungsführung

James MacGREGOR
Prof. of Civil Eng.
Univ. of Alberta
Edmonton, AB, Canada

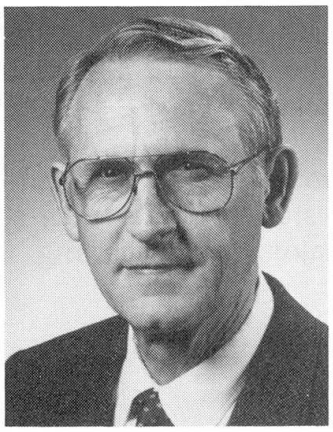

James G. MacGregor is Chairman of the Standing Committee on Structural Design for the National Building Code of Canada. He is Chairman of the Subcommittee on Shear and Torsion for the American Concrete Institute Building Code.

SUMMARY

Current and proposed Canadian, American and European design rules for dimensioning and detailing concrete structures are received and compared. The majority of the discussion deals with shear in B Regions and D Regions. Major areas needing more experimental evidence and synthesis are identified.

RÉSUMÉ

Les normes canadiennes, américaines et européennes visant le dimensionnement et la conception des détails constructifs des structures en béton armé actuellement en vigueur ou simplement proposées, sont passées en revue et comparées. La majeure partie de la discussion touche l'effet tranchant dans les régions B et D. Les zones plus larges nécessitant davantage de résultats expérimentaux et de synthèse sont mises en valeur.

ZUSAMMENFASSUNG

Die derzeit gültigen und die geplanten Regeln kanadischer, amerikanischer und europäischer Normen für die Bemessung und Bewehrungsführung von Betontragwerken werden zusammengestellt und miteinander verglichen. Dabei werden überwiegend die B-Bereiche mit Querkraft und die D-Bereiche behandelt, und die wichtigsten Felder herausgestellt, die eine weitere experimentelle Absicherung und bessere Zusammenfügung erfordern.

1. INTRODUCTION

In the past 15 years there has been a major shift in the design methods for reinforced concrete toward methods based on equilibrium solutions from the theory of plasticity and related simple mechanical models. This paper discusses the current state of the Canadian, American and European design rules for regions subjected to combined shear, moment and axial load. Four specific documents are discussed: the 1984 Canadian Standards Association (CSA) code[1], a 1987 draft of Chapter 11 (Shear and Torsion) of the ACI Code[2] prepared by a subcommittee of ACI Committee 318 but never finally adopted, the First Draft of the Chapter 6 (Verification of the Ultimate Limit States) of the CEB-FIP Model Code 1990[3] and a design method proposed by Collins and Mitchell.[4]

This paper is not intended to be an endorsement of one or other set of design rules, but rather a critique of the state-of-the-art. In spite of the great progress made in recent years, there are major areas needing more experimental evidence and synthesis.

2. DEFINITION OF CONCEPTS

2.1 Dimensioning and Detailing

Dimensioning and *detailing* refer to the process of selecting the dimensions of members and joints within a structure and selecting the amount, the layout, the position and the details of the reinforcement. Traditionally, dimensioning or design has been taken to mean the selection of overall sizes and reinforcement amounts at highly stressed sections and detailing has dealt with selection of the bends, cut-off points, joints and the like. In North America, dimensioning was the job of the engineer, detailing was the job of the reinforcement fabricator. This is an incorrect division since the details of the reinforcement in the discontinuities control the strengths of these regions and hence must be considered by the structural engineer.

2.2 D Regions and B Regions

In 1982 Schlaich and Weischede[5,6] introduced the concept of *D regions* and *B regions* where D stands for discontinuity or disturbed and B stands for beam, bending or Bernoulli. D regions, extending a distance equal to the member depth away from a discontinuity such as a change in section, concentrated load or reaction, were assumed to carry load primarily by strut-and-tie action with significant in-plane load components. The regions between D regions were termed B regions. Here beam theory applied as did truss analogies such as those developed at the turn of the century by Ritter and Mörsch or the more refined plastic truss analogies[7]. This classification scheme permitted a major step forward in our understanding of the design of concrete members and our ability to write design rules for such members.

2.3 Full Member Design and Sectional Design

Truss and strut-and-tie models require consideration of the entire member in the design process. In such methods, a truss which is in equilibrium with the loads is developed. This one model allows consideration of internal forces due to shear,

flexure and axial loads. Such a design procedure will be referred to as *full-member design*. In a full-member design procedure, such things as the extension of flexural reinforcement resulting from the presence of shear forces, are accounted for automatically. A drawback of such methods is that a different set of internal forces and hence member sizes results from each loading case. As a result, multiple load cases must each be considered separately and different loading cases may require different truss layouts. Such an approach is generally too tedious for the design of conventional beams.

The traditional design process for reinforced concrete, particularly in North America, assumes that a beam can be designed section by section for the worst combination of flexure and shear at that section. Generally it is assumed that flexure and shear can be decoupled and considered separately - first designing for flexure using the moment envelope, then designing for shear using the shear envelope. The interaction of shear and flexure is ignored, or dealt with empirically, or considered using equations derived from truss concepts. Such a design procedure is referred to as a *section-by-section design* or *sectional design*. Sectional design procedures generally do not work in D regions.

2.4 Compressive Strength of Cracked Concrete

The concrete in the cracked web of a beam is subjected to diagonal compressive stresses which are parallel or nearly parallel to the inclined cracks. One must know the crushing strength of this concrete to prevent web crushing failures. The strength of this concrete is variously related to (a) the presence or absence of cracks and/or the orientation of these cracks, (b) the tensile *strain* perpendicular to the compressive stress averaged over a width including several cracks, or (c) the transverse tensile *stress*.

2.4.1 Stress Limited as a Function of Presence of Cracks - The 1978 CEB Model Code[8] limited the diagonal compressive stress in the web to $f^*_{cd} = 0.6\, f_{cd}$ where f_{cd} was the design compressive strength. This valve was also used in Reference 7. Schlaich et. al.[6] propose

$f^*_{cd} = 1.0\, f_{cd}$ for uniaxial compression,
$= 0.8\, f_{cd}$ if transverse tensile strains cause cracking parallel to the strut with normal crack width,
$= 0.6\, f_{cd}$ for skew cracking of normal width or struts crossed by skew reinforcement
$= 0.4\, f_{cd}$ for skew cracks of unusual width.

Schäfer, Schelling and Kuchler[9] reported tests of ten specimens and reviewed data from five other test series and reaffirmed the above rules. The First Draft of the CEB-FIP Model Code 1990[3] defines f^*_{cd} as:

$$f^*_{cd} = \alpha\left[0.85\left(1 - \frac{f_{ck}}{250}\right)\right] f_{cd} \qquad (1)$$

where $\alpha = 1.0$ for uncracked zones or zones with cracks at angles greater than 45° to the direction of the compressive stresses and 0.7 for zones with cracks at less than 45° to the compression. For 30 MPa concrete and $\alpha=0.7$ this works out to 0.524 f_{cd}. Regan[10] has shown this to be a lower bound to the web crushing stress in 31 beams which failed by crushing of the web concrete. Rangan[11] compared Eqs. 1 and 2 to 16 tests of prestressed beams which failed by web crushing and reported equally good agreement by either equation.

2.4.2 Stress Limited as a Function of Transverse Strain - In 1978 Collins[12] suggested that the compressive strength of cracked concrete was a function of the strain perpendicular to the direction of the principal compressive stress. The strain used was an average strain based on a gauge length that included several cracks. Collins and Mitchell[13] incorporated these concepts in their Compression Field Theory design method for shear and torsion.

From tests of reinforced concrete panels subjected to in-plane normal and shear stresses Vecchio and Collins[14] derived a relationship between f_{cd}^* and the transverse principal tensile strain, ε_1. The 1984 Canadian code has incorporated the following version of this relationship:

$$f_{cd}^* = \frac{\lambda f_{cd}}{(0.8 + 170\,\varepsilon_1)} \qquad (2)$$

where λ ranges from 1.0 for normal weight concrete to 0.75 for concrete made with lightweight sand and gravel.

2.4.3. Stress Limited as a Function of Transverse Tensile Stress - Kollegger and Mehlhorn[15] tested 55 panels under in-plane compression and transverse tension and reviewed data from several other test series and report a maximum reduction of compressive strength of about 20 percent for panels which failed by crushing of the concrete prior to yield of the reinforcement. They concluded that the effective compressive strength was more accurately described as a function of the transverse tensile stress than the transverse tensile strain.

Agreement must be reached as to the best way of defining the compressive strength of cracked webs. Preferably this should be done at two levels: (a) A theoretically correct definition, and (b) a definition which can be easily applied in the design of beams. For design the author favors the values of f_{cd}^* given in Section 2.4.1.

3. GENERAL REQUIREMENTS OF STRUCTURAL DESIGN CODE CLAUSES

Four general rules should be followed in formulating structural design codes:

1. Wherever possible, code provisions should be based on clearly understood mechanical models.

We have a clear physical model for pure flexure - a beam is a compression force and a tension force which form a couple in equilibrium with the applied moment.

Strain compatibility is invoked. These principles are clearly stated in all modern codes. In the Introductory Report for Sub Theme 2.2, Professor Schlaich has pointed out that the mechanical models needed in design should be "just enough" and not "as much as possible". Too complex models obscure the understanding.

Frequently, concepts derived from full-member models such as strut-and-tie models or truss models are applied in a sectional design procedure. Problems have arisen when the code drafting body has given inadequate attention to the fundamental differences between the two procedures.

2. If it is necessary to introduce empirical constants or expressions or simplifying assumptions, the end result should be as simple as possible.

The derivation of simple rules may take considerable effort on the part of the code writers. The rectangular stress block for flexure[16,17] is a simple approximation to the true stress blocks. This simplicity is based on extensive and thoughtful research, based in turn on a professional understanding of the degree of complexity which could be tolerated in a design office. The existence of computers in design offices does not in itself justify complex empirical expressions.

Generally speaking, shear design equations which involve the longitudinal steel ratio, ρ, or the shear span to depth (M/Vd) ratio are tedious to apply in practice since these quantities change from point to point along the beam and change for different load cases. Questions also arise as to where a reinforcing bar is sufficiently well anchored to be counted.

3. When design shifts from one range to another the design models and/or approximate design expressions should meet at a common point unless there is a mechanical reason why they should not.

4. Ductile modes of failures are preferable to brittle failures. The margin of safety should be greater for brittle failures than for ductile failures.

4 FLEXURE

At points of maximum moment in B regions, with or without axial load, the internal forces are represented by tensile force in the reinforcement and an assumed compressive stress distribution in the compression zone. A linear strain distribution is assumed at such a location. The compressive stresses are related to the strains by the stress-strain curve of the concrete. For design, the stress-strain curve is simplified to one of the forms shown in Fig. 1. The ACI Code, CSA Code and 1978 CEB-FIP Model Code[16] use variations of the rectangular stress block in Fig. 1b. Here the stress intensity, $0.85f'_c$, and the depth of rectangle, $\beta_1 c$, are chosen so that (i) the

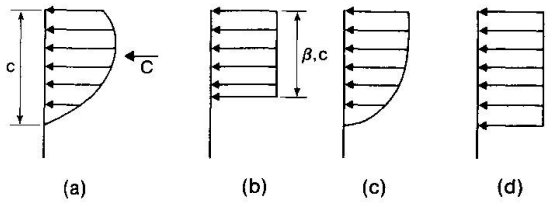

Fig. 1. Compression Stress Blocks

resultant force C, and (ii) the line of action of this force, are the same as for the "real" stress block in Fig. 1a. The same is true of the parabola-rectangle diagram shown in Fig. 1c. Chapter 6 of the First Draft of the CEB-FIP Model Code 1990[3] permits the use of the parabola-rectangle stress-block or the stress block shown in Fig. 1d where the entire compression zone is assumed to be stressed to f_{cd}^{*} given by Eq. 1 with $\alpha = 1.0$. While this results in a compression force approximately the same as Fig. 1b and c, the location of the axis of zero strain is closer to the extreme compressive fiber than in Fig. 1b and c. This will affect the strain in the tension steel and whether the steel yields or not in a given beam or column.

Except as noted here the model for flexure is accurate and well established and needs no further comment.

5. D REGIONS

D or Discontinuity regions are assumed to extend a distance equal to the member depth away from concentrated loads, reactions, changes in cross section and holes. Such regions can be designed using strut-and-tie models. In their introductory reports for this conference Professor Schlaich and Professor Marti describe such models in detail.

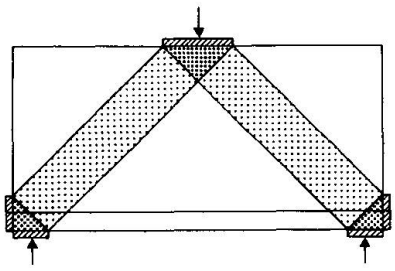

Fig. 2. Strut-and-Tie Models

In their most basic form, strut-and-tie models consist of uniaxially stressed tension ties consisting of normal or prestressed reinforcement, uniaxially stressed concrete compression struts, and joint regions referred to as nodal zones at points where three or more struts meet, or where a combination of three or more struts, ties, or external forces meet. In the example shown in Fig. 2 the compression struts are prismatic with perpendicular ends bearing on the nodal zones. Because this does not truly represent the state of stress in the beam, more complex models or bottle-shaped[6] or fan-shaped struts[18] have been suggested.

Although the nodes have finite width, the strut-and-tie model is analyzed as a pin-jointed truss. Walraven and Lehwalter[19] account for the flexural stresses in the struts due to the continuity at the top joint of Figure 2. They also include a size effect.

5.1 Selection of Strut-and-Tie Models

The procedure for laying out strut-and-tie models involves a graphical procedure to draw a truss in equilibrium with the loads.[20] The procedure involves trial and error because the widths of the struts and the sizes of the nodes depend on the forces in the struts and ties. Recently computer programs have been developed to carry out this process[21,22].

Different designers may come up with different strut-and-tie models. Although the models selected are to some extent self fulfilling prophecies, problems may develop if the model selected in the design differs too much from the natural load carrying

mechanism because the concrete may have inadequate ductility to adapt to the strut arrangement in the model.

Schlaich et al.[6] suggest two guides in selecting a workable strut-and-tie model. First, the compatibility of deformations may be approximately considered by orienting the struts and ties within 15 deg. of the force systems obtained from a linear elastic analysis of uncracked members and connections. Second, the most valid model tends to be the one that minimizes the amount of reinforcement since this corresponds to the minimum strain energy solution.

5.2 Material Strengths

5.2.1 Tension Ties - Tension ties are designed on the assumption they are steel ties stressed to the design yield strength at points of maximum stress. Adequate anchorage must be provided. The tensile resistance of the concrete is not utilized.

5.2.2 Compression Struts - The strength of the concrete in the compression struts is taken as:

$$f^*_{cd} = \nu f_{cd} \qquad (3)$$

where ν is an effectiveness factor in the order of 0.5 to 1.0. The effectiveness factor accounts for: (a) reduction of the useable concrete strength due to cracking of the struts and/or tensile strains or stresses transverse to the struts, and (b) strain gradients across the width of the struts arising from the fact that the strut-and-tie model is not truly a pin-jointed truss.[19] Several approaches to defining ν were given in Section 2.4. The effective compression strength of the concrete making up the compression struts varies from code draft to code draft.

The 1990 Draft of Chapter 6 of the CEB-FIP Model Code 1990[3] assumes the full width of the strut is stressed to f^*_{cd} given by Eq. 1 with $\alpha = 0.7$.

The 1984 Canadian code[1] and the draft code by Collins and Mitchell[4] base the strength of the compression struts, f^*_{cd} , on Eq. 2 where ε_1 is the *average* strain perpendicular to the strut as illustrated in Fig. 3. This average reflects the restraint that the adjoining concrete gives to the highly stressed concrete in the strut. In a varying strain field the value of the average depends on the gauge length used to define the average. In many D regions there is no rational way of estimating ε_1 in a cracked web. In such cases the Explanatory Notes for the Canadian code[23] suggest

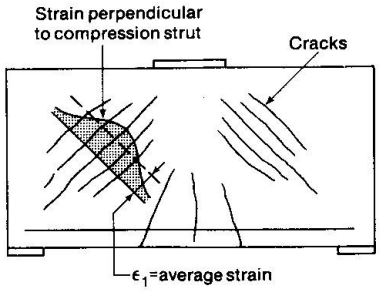

Fig. 3. Definition of ε_1 for D Region

$$\varepsilon_1 = \varepsilon_s + (\varepsilon_s + 0.002)/\tan^2 \alpha_s \qquad (4)$$

where ε_s is the average tensile strain in reinforcement crossing the strut at an angle α_s to the axis of the strut. Again there is the problem of how to define ε_s. The

Explanatory Notes suggest ε_s can be taken as f_y/E_s. For 400 MPa steel at angles of 30, 45 and 60 degrees to the strut, Eqs. 3 and 4 and $\varepsilon_s = f_y/E_s$ give f_{cd}^* equal to $0.315\lambda f_{cd}$, $0.55\lambda f_{cd}$ and $0.732\lambda f_{cd}$. Eqn. 4 was derived by Collins and Mitchell[13] using a Mohr's circle for strain.

The 1987 draft ACI Code Chapter 11[2] expresses f_{cd}^* in a cracked beam web as

$$f_{cd}^* = \frac{\phi f_c' (\theta_{st} - 10)}{(50 + f_y/2000)} \qquad (5)$$

for reinforced concrete where ϕ is a resistance factor equal to 0.85, f_c' is the cylinder compressive strength, θ_{st} is the angle between the tension tie and the compression strut in degrees and f_y is the yield strength in psi. Equation 5 was derived from Eqs. 3 and 4 to avoid the need to compute the strain ε_1.

Since there is no simple procedure for obtaining ε_1 the writer prefers to define f_{cd}^* using expressions similar to Eqs. 1 or 2.

More data is required on the effects of compression steel and confining reinforcement in struts. Analytical solutions must be checked experimentally.

5.2.3 Nodal Zones - The strength of concrete in the nodal zones depends on: (a) the confinement of the zones by reactions, compression struts, prestress anchorage plates, reinforcement from the adjoining members and hoop reinforcement; (b) the effects of strain discontinuities within the nodal zone when ties strained in tension are anchored in, or cross, a compressed nodal zone; (c) the splitting stresses and hook bearing stresses resulting from the anchorage of the reinforcing bars of a tension tie in or immediately behind a nodal zone; (d) the weakening effects of grouted or ungrouted prestressing ducts which frequently extend through a nodal zone.

Chapter 6 of the First Draft of the CEB-FIP Model Code 1990[3] requires that the forces in the struts and ties be anchored and balanced in the nodal regions. The Commentary on this section of the draft Model Code states that compressive stresses within the nodes normally only need to be checked at nodes where concentrated loads are applied to the surface of the structural element by means of bearing plates, anchor plates or supports. They also may need to be checked at discontinuities such as holes or corners. The bearing stress is limited to

$$f_{b1} = \alpha\beta f_{cd} \qquad (6)$$

where α = 1.0 at nodes where only compression struts meet and 0.8 for nodes at which main tension bars are anchored, and β allows up to a four times increase in the bearing stress if the member is wider than the bearing plate. Transverse reinforcement is required in cases where β is greater than 1.0. Prestressing ducts

crossing the nodal zone are assumed to weaken the nodal zone. No guidance is given for compressive stresses in nodal zones which are not bearing areas.

Except where special confining reinforcement is provided, the 1984 Canadian code[1] and the new draft by Collins and Mitchell[4] limit the concrete compressive stresses in nodal zones to:

$0.85f_{cd}$ in nodal zones bounded by compression struts or bearing areas;
$0.75f_{cd}$ in nodal zones anchoring only one tension tie,
$0.60f_{cd}$ in nodal zones anchoring tension ties in more than one direction.

These values were selected empirically to reflect items (a) to (c) above.

The author does not know of any published experimental study of the strength of nodal zones. This is a major drawback in the development of strut-and-tie models for D regions. Another area needing study is the strength of nodal zones in members comprised of precast and cast-in-place concrete.

The strengths chosen for concrete in nodal zones must be compatible with other similar situations in structures such as the transmission of column load through building floors where, for example, the ACI and CSA codes allow a nodal zone stress of $\phi 1.4f'_c$ where ϕ is a resistance (safety) factor.

5.3 Serviceability

None of the three documents under consideration adequately treat the Serviceability Limit State for D regions. The major serviceability condition is inclined crack width at service loads. The 1990 draft of Chapter 6 of the CEB-FIP Model Code 1990 suggests that an SLS check can normally be avoided if the secondary and main reinforcement together are oriented at the direction of the linear elastic stress fields.

The CSA Code and the ACI draft do not consider the serviceability of D regions. Means for doing this need to be developed.

6. B REGIONS

B regions are regions of structural members where conventional beam theory or the Ritter, Mörsch or Thürlimann types of truss analogies apply. These regions can be designed by full-member design procedures although most commonly they are designed by sectional design procedures some of which are derived from truss analogies.

6.1 Basic Design Models

The Simplified Methods of the 1987 ACI Code draft[2] and the 1984 Canadian code[1] assume that a portion of the factored shear V_u is resisted by "shear in the concrete",

V_c, and the rest is resisted by stirrups, V_s. V_c is constant for all values of V_u and V_s is calculated using a 45 deg. truss.

Chapter 6 of the First Draft of the CEB-FIP Model Code 1990[3], the General Methods of the 1984 Canadian code[1] and the 1987 ACI Code draft[2] and the draft by Collins Mitchell[4] are based on the plastic truss model, developed by Thürlimann and his colleagues[7] and shown in Fig. 4. The beam is modelled by a compression chord, shown dashed, a tension chord and a web. The web is assumed to be cracked at θ with the horizontal.

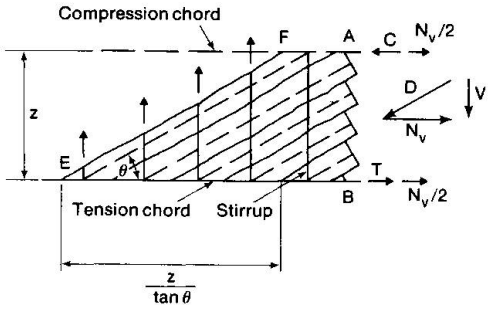

Fig. 4. Plastic Truss Model

The shear, V, acting on section A-B is assumed to be resisted by a diagonal compression force D parallel to the cracks and an axial tension, N_v. The stirrup reinforcement is designed considering the stirrup forces across section E-F in Fig. 4. If θ is less than 45 deg, the shear V_s carried by the stirrups for a given amount and spacing of stirrups exceeds the value used in the Simplified Methods of the ACI and CSA Codes This partially, but not completely, offsets the lack of a V_c term in the so called General Methods. Collins and Mitchell's draft includes a V_c term based on the tension between the cracks.

In design, four modes of failure must be considered: (a) the web must not crush due to the diagonal compression force, D; (b) the longitudinal reinforcement must be able to resist $(T + N_v/2)$, except that, at points of maximum moment, N_v goes to zero; (c) the stirrups must be able to resist V; and (d) the compression chord must be able to resist a compression of C at the points of maximum moment and $(C - N_v/2)$ at other points.

The ambiguity in items (b) and (d), above, results from attempting to express the full-member design concept of a compression fan region at concentrated loads and supports into a sectional design procedure based on a constant angle θ.

The General Method of the Canadian Code has not been widely used because designers regard it to be more complex to apply and because it generally requires more stirrups than the Simplified $(V_c + V_s)$ method.

6.2 Recent Developments in Basic Design Models

The truss model in Fig. 4 assumes that the compression struts are parallel to the direction of cracking and that to stresses are transferred across the cracks. More recent theories have made one of two assumptions: (a) Tensile stresses transverse to the axis of the strut exist at points between the inclined cracks but drop to zero at the cracks, Fig. 5a, (b) Shearing stresses are transferred across the inclined cracks by aggregate interlock or friction, Fig. 5b.

Vecchio and Collins[24] show that these two assumptions are the same or, at least very closely related. Two results of these assumptions are: first, the angle of the principal

compression stress in the web is less than the angle of the cracks θ, and second, the vertical component of the force along the crack in Fig. 5b is

$$V_c = v_{ci} b_w d \qquad (7)$$

assuming v_{ci} is constant.

In the analysis of a beam using the Modified Compression Field theory of Vecchio and Collins[24] a valve of the principal tensile strain ε_1, perpendicular to the cracks, is estimated. From this, the width of the cracks and the average transverse tensile stress in the struts, f_1, are calculated. The transverse tensile stresses and resulting V_{ci} add what amounts to a V_c term.

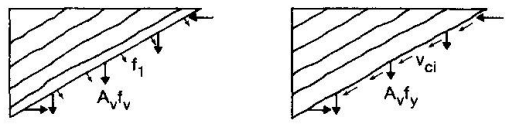

(a) Stresses on a section between two cracks (b) Stresses on a section along a crack

Fig. 5. Modified Compression Field Theory

Dei Poli, Gambarova and Karakoc[25] assume the beam behaves like a plane truss with aggregate interlock shear and compression stresses across the inclined cracks, the latter occurring because the angle of web compression is flatter than the crack angle. This analysis resulted in a V_c term due to the aggregate interlock. This term was larger for parts of beams with web-shear cracking (tension chord of the truss uncracked) than for parts of beams developing flexure-shear cracking (tension chord cracked).

Kirmair and Mang[26], following analyses developed in cooperation with Professor Kupfer found that the V_c term depended mainly on aggregate interlock along the inclined cracks. The amount of interlock was governed by the relative displacement along the cracks. The V_c term was affected by the extension of the tension flange, decreasing as the flange strain increased, similar to Vecchio and Collins'[24] observation.

Reineck and Hardjasaputra[27] also used a truss model with the angle of compression less than the crack angle. Based on the assumption that the cracks open perpendicular to their axis and an assumed stress-strain curve for concrete in compression they derived expressions for the kinematics of the web deformations. Their results were expressed in a series of design charts. Again, the effective value of V_c was found to increase as the longitudinal strain at mid-depth decreased as observed in each of the other three papers mentioned in this section.

Reineck[28] presents an explanation of the shear strength of beams without shear reinforcement based on a tooth model. He concludes that the aggregate interlock shear and dowel action shear along the cracks transfer most of the shear in such beams.

A simple means of computing a realistic V_c term would be a desirable addition to shear design codes. Such a term is important in the design of beams having a factored shear force between one and three times the inclined cracking shear. A large fraction of cast-in-place concrete beams fall in this region. The Collins and Mitchell

draft[4] includes a table of V_c values and special values of V_c for beams without stirrups.

6.3 Web Crushing Strength for Design

Chapter 6 of the First Draft of the CEB-FIP Model Code 1990 uses Eq. 1 with $\alpha = 0.7$ to define the web crushing strength in B Regions. The web crushing strength is reduced if prestressing ducts cross the compression field in the web. The draft accounts for this by reducing the effective web width.

The 1984 Canadian code uses Eq. 2 to define the web crushing strength where ε_1 is computed using:

$$\varepsilon_1 = \varepsilon_x + (\varepsilon_x + 0.002) / \tan^2 \theta \qquad (8)$$

where ε_x is the longitudinal strain at mid-depth of the member when the section is subjected to M_f, N_f and the axial force N_v resulting from the shear, positive when tensile, and θ is the angle between the compression struts and the longitudinal axis. Because Eq. 2 was derived from the average strains in panels subjected to a uniform state of stress and strain, the average longitudinal strain (i.e. at mid-depth) is assumed to be the appropriate value here. This has been experimentally checked in several cases.[29]

The 1987 draft of ACI Chapter 11 uses Eq. 5 to compute the crushing strength of the web. As pointed out earlier this was derived from Eqs. 3 and 4. Alternatively, the ACI draft assumes that the web will not crush if the angle θ satisfies

$$\theta > 15^\circ + \frac{140\, v_n}{f'_c} \qquad (9)$$

for reinforced concrete where v_n is the average shear stress in the web of the beam. This equation was derived in Ref. 13.

The Collins and Mitchell draft [4] presents a table which is entered using v_n and ε_x. Values of θ which satisfy Eqs. 2 and 8 and values of a V_c term computed from the tension between the cracks are obtained from the table. This is done at a number of cross-sections along the beam to reflect changes in v_n and ε_x.

A major difference between Chapter 6 of the First Draft of the CEB-FIP Model Code 1990 and the other three codes is the dependence of f'_{cd} on the angle θ in the latter three. This complicates design but may be necessary to properly reflect the true crushing strength of the web concrete. This discrepancy needs to be resolved.

For beams subjected to very high shears the CSA code[1] requires the web width to be reduced to the width inside the stirrups to account for the spalling of the concrete outside the stirrups observed in tests of beams with closely spaced stirrups subjected to very high shears. This concept is not contained in the other two codes.

6.4 Allowable Angles

The flattest angle θ allowed in Chapter 6 of the First Draft of the CEB-FIP Model Code 1990 is 18.4° (cotan θ = 3). This is currently under discussion by CEB Commission IV. A more stringent limit based on shear transmitted across the original cracks has been proposed by two members of that Commission.

The 1984 Canadian Code allows any angle θ between 15° and 75°. The 1987 ACI draft limited the angle to 25° to 65°. Grob and Thürlimann[6] suggested a limit of cotan θ = 2 (θ = 25.6°) to prevent excessive inclined crack widths.

In the Collins and Mitchell draft[4] the angle θ is chosen from a table to satisfy Eq. 2 and 8.

6.5 Staggering Rules

When a beam is loaded on its top surface and supported at locations on its lower surface, the stirrups within a distance d/tan θ from the support can be designed for the shear at d/tan θ from the support, those between 1 and 2 d/tan θ for the shear at 2d/tan θ and so on. This is referred to as the *staggering rule.* For beams loaded and supported in this way this procedure satisfies equilibrium and has been shown experimentally[29] to produce a safe design. On the other hand, the staggering rule does not satisfy equilibrium for beams both loaded and supported on their bottom surfaces or for beams in which dead load is a major fraction of the total load. The ACI Code has allowed the staggering concept to be used within d (=d/tan 45) from the support since 1963. The General Method of the 1984 Canadian code allows the staggering rule for uniformly loaded beams loaded on their top surface and supported at locations on its bottom surface. It does not give guidance for other cases. The commentary for Chapter 6 of the First Draft of the CEB-FIP Model Code 1990 allows this procedure in the end d/tan θ but does not appear to make it a general rule.

6.6 Prestressed Concrete

One of the most perplexing features in the development of codes for structural concrete is the treatment of shear in prestressed concrete beams. Thus, for example, the CEB-FIP Model Code 1978 presented a Standard Method for design for shear in prestressed concrete which included a V_c term which was larger for prestressed beams than for reinforced concrete and an Accurate Method which for high shears did not include a V_c term and did not recognize any favorable effect of prestress. As a result, the Accurate Method required more stirrups than the Standard Method. Similar arguments have prevented the adoption of the 1987 draft of ACI Chapter 11.

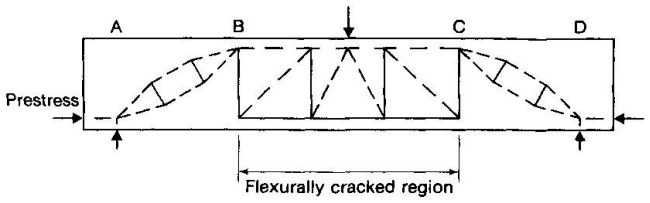

Fig. 6. Truss Model of Prestressed Beam

Schlaich et al.[6] suggest that the load carrying mechanism of a prestressed beam at ultimate loads consists of an inclined

compression strut in the uncracked regions of the beam, AB and CD in Fig. 6, and a truss in the cracked regions, BC. In ACI terminology, regions AB and CD would be subject to web-shear cracking (inclined cracking prior to flexural cracking) while region BC would be subject to flexure-shear cracking (inclined cracking affected by flexural cracking). Stirrups in regions AB and CD prevent widening of the splitting crack (web-shear crack). The main shear carrying mechanism in this region is strut action. In region B-C the stirrups equilibrate all the shear unless account is taken of the shear transferred across the crack interfaces or the tension transverse to the diagonal compression struts.

For uniformly loaded beams Chapter 6 of the First Draft of the CEB-FIP Model Code 1990 identifies two cases. For the normal case the prestress is assumed to carry a portion, λq, of the dead and live loads, q, by the arching action of the compression zone and upward pressure of the tendons as shown in Fig. 7a and b. The remainder of the loads $(1-\lambda)q$ are carried by truss action as shown in Fig. 7c. As a result, stirrups are only required for $(1-\lambda)$ times the shear force.

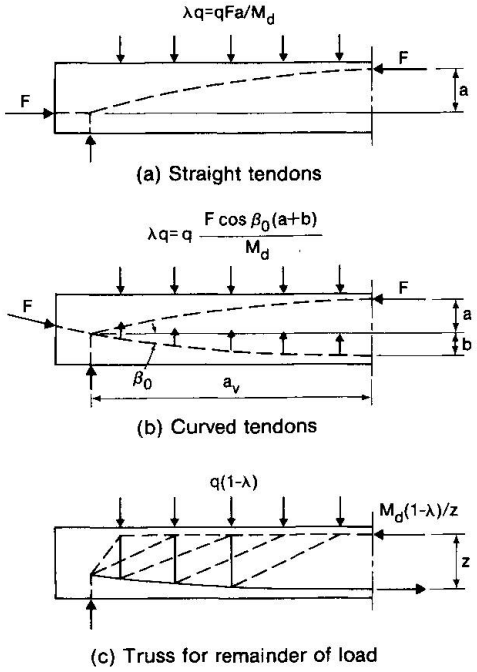

Fig. 7. Prestressed Concrete Draft CEB-FIP Model Code

For thin-webbed beams with massive end blocks, the 1990 draft Model Code assumes the prestress force is applied directly to the top and bottom flanges as shown in Fig. 9. In this case the only part of the transverse load supported by the prestress is that supported by the upward pressure of any curved tendons. No quantitative guidance is given as to whether the models in Fig. 7 or 8 should be used.

It should be noted that this portion of Chapter 6 of the 1990 draft received extensive discussion and may be modified in the final Model Code.

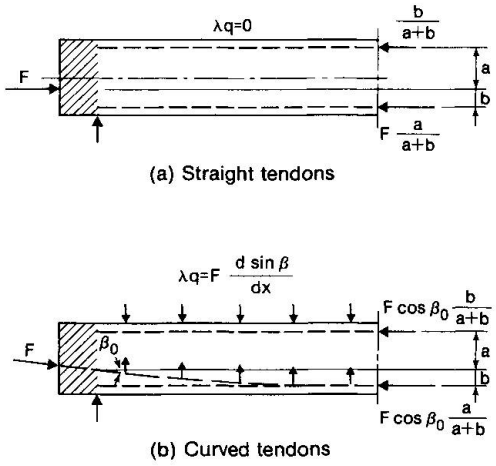

Fig. 8 Prestressed Concrete Beams with Thin Webs and Massive End Blocks

The 1984 Canadian code presents a Simplified Method and a General Method for design of prestressed beams for shear. The Simplified Method is based on the $V_c + V_s$ concept with V_s calculated using a 45 deg

truss. The V_c term is the smaller of the shear causing web-shear cracking and flexure-shear cracking. The General Method is based on the plastic truss model. The General Method has no V_c term and hence does not recognize any favorable effect of prestress except its vertical component, unless a strain compatibility solution is used to compute ε_x in Eq. 13.

The 1987 draft of ACI Chapter 11 follows the same pattern as the 1984 Canadian code although the presentation is simplified to avoid the computation of ε_1.

The Collins and Mitchell draft[4] includes the effects of prestress in the calculation of the value of ε_x at each section and thus accounts for the effects of prestress directly.

6.5 Serviceability

The 1987 ACI Code draft and the 1990 draft of the CEB-FIP Model Code do not consider the width of shear cracks in B regions except through detailing rules. The Simplified Method of the 1984 Canadian code attempts to limit inclined crack width by limiting the maximum shear stress in a beam web. The upper limit was chosen on the basis of limiting the stirrup stress at service loads to 200 MPa. The General Method of the 1984 Canadian code gives a set of "deemed to satisfy" rules. If these are violated, the designer must limit the strain in the stirrups at service loads to 0.001 for interior exposure. A relatively complex equation is given to estimate this strain.[13]

7. MAJOR AREAS NEEDING MORE STUDY

1. Further development of computer programs to lay out and solve strut-and-tie models.
2. A compromise is needed defining the factors which affect the crushing strength of the webs in beams or the struts in strut-and-tie models. The CEB-FIP draft involved concrete strength and a qualitative description of the degree of cracking, the General Method of the CSA code and the Collins and Mitchell draft included concrete type and principal tensile strain, while the ACI code draft included crack angle and reinforcement yield strength as variables.
3. Experimental verification of nodal zone strengths is needed.
4. Simple ways are needed for verifying the serviceability limit states of D regions and B regions. These could take the form of "deemed to satisfy" rules.
5. Recent theories suggest that tension in the concrete between cracks is responsible for V_c, the shear carried by concrete. Simple ways of accounting for this effect are desirable.
6. A major area requiring more study is the enhanced shear strength of prestressed members.
7. Although not discussed in this paper, the full-member design procedures proposed in the CEB-FIP draft Model Code for T-beam flanges need to be made compatible with sectional design procedures for beam webs and the description of the thin-walled tube used in torsion design needs to be standardized (A_o, wall thickness).

8. Designers need more guidance about the design for warping torsion.

REFERENCES

1. CSA Technical Committee on Reinforced Concrete Design, "Design of Concrete Structures for Buildings, CAN3-A23.3-M84", Canadian Standards Association, Rexdale, Ontario, 1984, 221 pp.

2. ACI Committee 318, Subcommittee E, "ACI Change Submittal, Redraft of Chapter 11", June 8, 1987, 36 pp (Personal communication from J.G. MacGregor).

3. Comité Euro-International du Béton, CEB-FIP Model Code 1990, - First Draft, Chapters 6-14 and Appendices, Bulletin d'Information No. 196, March 1990, 100 pp.

4. COLLINS, M.P. and MITCHELL, D., "Prestressed Concrete Structures", Prentice Hall, Englewood Cliffs, 1990, 500 pp.

5. J. SCHLAICH and D. WEISCHEDE, "Detailing of Concrete Structures" (in German), Bulletin d'Information 150, Comité Euro-International du Béton, Paris, March 1982, 163 pp.

6. SCHLAICH, J., SCHÄFER, K. and JENNEWEIN, M., "Towards a Consistent Design of Reinforced Concrete Structures", Journal of the Prestressed Concrete Institute, Vol. 32, No. 3, May-June 1987.

7. GROB, J. and THÜRLIMANN, B., "Ultimate Strength and Design of Reinforced Concrete Beams under Bending and Shear", Publications, International Association for Bridge and Structural Engineering, Zurich, Vol. 36-II, 1976, pp. 107-120.

8. CEB-FIP Model Code for Concrete Structures, Bulletin d'Information 124/125E, Comité Euro-International du Béton, Paris, 1978, 348 pp.

9. SCHÄFER, K., SCHELLING, G. and KUCHLER, T., "Compression and Transverse Tension in Reinforced Concrete Elements" (in German) Deutscher Ausschuss für Stahlbeton No. 408, Beuth Verlag, GmbH, Berlin, 1990, pp 1-85.

10. REGAN, P.E., "Shear Resistance of Members with Shear Reinforcement", Unpublished Memorandum to CEB Commisssion IV, January, 1990.

11. RANGAN, V., "Web Crushing Strength of Reinforced and Prestressed Concrete Beams", Submitted to ACI Structural Journal for Publication.

12. COLLINS, M.P., "Towards a Rational Theory for R C Members in Shear", Journal of the Structural Division Proceedings ASCE, Vol. 104, No. ST4, April 1978, pp. 649-666.

13. COLLINS, M.P. and MITCHELL, D., "Design Proposals for Shear and Torsion", Journal of the Prestressed Concrete Institute, Vol. 25, No. 5, September-October 1980, 70 pp.

14. VECCHIO, F.J. and COLLINS, M.P., "The Response of Reinforced Concrete to In-Plane Shear and Normal Stresses", Publication No. 82-03, Department of Civil Engineering, University of Toronto, March 1982, 332 pp.

15. KOLLEGGER, J. and MEHLHORN, G., "Experimental Investigations into the Compressive Strength of Reinforced Concrete Subjected to Transverse Tension" (in German), Deutscher Ausschuss für Stahlbeton, No. 413, Beuth Verlag, Berlin, 1990, 132 pp.

16. WHITNEY, C.S., "Plastic Theory of Reinforced Concrete Design", Proceedings ASCE, December 1940; Transactions ASCE, Vol. 107, 1942, pp. 251-326.

17. MATTOCK, A.H., KRIZ, L.B. and HOGNESTAD, E., "Rectangular Concrete Stress Distribution in Ultimate Strength Design", ACI Journal, Proceedings, Vol. 57, No. 8, February 1961, pp. 875-926.

18. MARTI, P., "Strength and Deformations of Reinforced Concrete Members Under Torsion and Combined Actions", Bulletin d'Information No. 146, Comité Euro-International du Béton, Paris, Jan. 1982, pp. 97-138.

19. WALRAVEN, J.C. and LEHWALTER, N., "The Bearing Capacity of Concrete Compression Struts in Strut and Tie Models, considering the Example of Short Deep Beams" (in German) Beton-und Stahlbetonbau, Vol. 84, No.4, April 1989, pp 81-87.

20. ROGOWSKY, D.M., and MacGREGOR, J.G., "Design of Reinforced Concrete Deep Beams", Concrete International: Design and Construction, Vol. 8, No. 8, August 1986, pp. 49-58.

21. SCHLAICH, M. and ANAGNOSLOU, G., "Stress Fields for Nodes of Strut-and-Tie Models", Journal of Structural Engineering, ASCE, Vol. 116, No. 1, January 1990, pp. 13-23.

22. HAJDIN, R., "Computer Assisted Design of Reinforced Concrete Walls with Stress Fields" (in German), Report No. 175, Institut für Baustatik und Konstrucktion, Swiss Federal University Zurich, Aug. 1990, 115 pp.

23. COLLINS, M.P., MITCHELL, D and MacGREGOR, J.G., "Explanatory Notes on CSA Standard A23.3-M84", Concrete Design Handbook, Canadian Portland Cement Association, Ottawa, 1985.

24. VECCHIO, F.J. and COLLINS, M.P., "The Modified Compression Field Theory for Reinforced Concrete Elements Subjected to Shear", Journal of the American Concrete Institute, Vol. 83, No. 2, March/April 1986, pp. 219-231.

25. DEI POLI, S., GAMBAROVA, P.G. and KARAKOC, C., "Aggregate Interlock Rule in R.C. Thin-Webbed Beams in Shear" ASCE Journal of Structural Engineering, Vol. 113, No. 1, January 1987, pp. 1-19.

26. KIRMAIR, H. and MANG, R., Shear Carrying Behavior of Slender Reinforced and Prestressed Concrete Beams with Bending and Axial Forces" (in German), Bauingenieur, Vol. 62, April 1987, pp. 165-170.

27. REINECK, K.H. and HARDJASAPUTRA, H., "Consideration of Strains in the Shear Design of Reinforced Concrete and Prestressed Concrete Beams." (in German), Bauingenieur, Vol. 65, February 1990, pp. 73-82.

28. REINECK, K.-H., "A Mechanical Model for the Behaviour of Reinforced Concrete Members in Shear", Ph.D. thesis, Universität Stuttgart, February 1990, 273 pp.

29. MAILHOT, G., "Experiments on the Staggering Concept for Shear Design", Department of Civil Engineering and Applied Mechanics, McGill University, Project Report No. G84-5, March 1985, 96 pp.

NOTATION

c = distance from extreme compression fiber to axis of zero strain

C = resultant compressive force due to flexure

d = effective depth

D = diagonal compressive force in the web of a beam

E_s = modulus of elasticity of reinforcement

f_{bl} = bearing strength

f_{cd} = factored or design strength of concrete

= f_{ck}/γ_m in CEB code, where $\gamma_m = 1.5$

= $0.6f'_c$ in CSA code

f^*_{cd} = effective compressive strength in compression zones or cracked beam webs

f_{ck} = concrete compressive strength from a cylinder test, exceeded by 19 of 20 tests

f'_c = concrete compressive strength from a cylinder test, exceeded by 11 of 12 tests

f_y = yield strength of reinforcement

f_1 = tension transverse to strut

M_f = moment due to factored loads

N_v = axial tensile force due to shear

q = uniform load

T = resultant tensile force due to flexure

v_{ci} = shear stress transferred across an inclined crack

v_n = nominal shear stress in web of beam

V_c = component of shear "carried by concrete"

V_s = shear resisted by stirrups

V_u = shear due to factored loads (ACI code)

α = compressive strength factor

α_s = angle between compression strut and reinforcement crossing it

β = nodal strength factor

β_1 = ratio of depth of rectangular stress block to c

ε_s = strain in reinforcement crossing compression strut

ε_x = average longitudinal strain in web of beam

ε_1 = average principal tensile strain in cracked web

λ = a factor to account for concrete type ranging from 1.0 for normal-weight concrete to 0.75 for structural concrete with lightweight, coarse and fine aggregate (CSA, ACI)

= the fraction of the total load resisted by arching action of the prestress force.

ν = effectiveness factor

ϕ = a resistance factor (ACI)

θ = inclination of compression struts in cracked beam web

θ_{st} = angle between a tension tie and a compression strut

Leere Seite
Blank page
Page vide

Dimensioning and Detailing

Dimensionnement et élaboration des détails constructifs

Bemessung und Konstruktion von Betontragwerken

Peter MARTI
Prof. Dr.
Swiss Fed. Inst. Technol.
Zurich, Switzerland

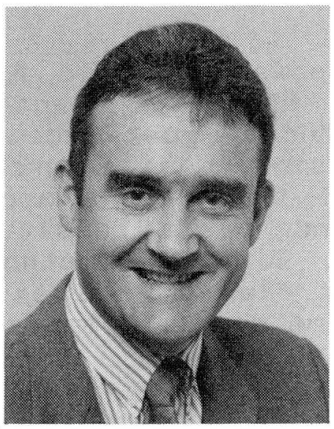

Born in 1949, Peter Marti is a professor of structural engineering at the Swiss Federal Institute of Technology (ETH) in Zurich, Switzerland. Until 1990, Dr. Marti was the chief technical officer of the VSL Group and an executive vice-president of VSL International Ltd., Berne, Switzerland. P. Marti is the chairman of ACI-ASCE Committee 445, Shear and Torsion, and he is a member of several other committees in both Europe and North America.

SUMMARY
Truss model approaches and related theories are presented in an attempt to provide a synthesis of recently-developed methods, permitting a consistent dimensioning and detailing of structural concrete members.

RÉSUMÉ
Un aperçu est donné de quelques travaux récents basés sur des modèles de treillis afin d'arriver à une synthèse permettant un dimensionnement cohérent et une élaboration correcte des détails constructifs des structures en béton.

ZUSAMMENFASSUNG
Fachwerkmodelle und verwandte Verfahren werden im Hinblick auf eine einheitliche Bemessung und Konstruktion von Betontragwerken im Sinne einer Synthese dargestellt.

1. INTRODUCTION

The idea of using truss models for following the flow of internal forces in reinforced concrete structures, which emerged about one hundred years ago, was greatly advanced over the first two decades of this century [23]. Being based on careful observations of the behaviour of actual and test structures as well as a thorough understanding of basic principles, the clarity and the wide range of applicability of these concepts still deserve our admiration.

Truss models provide powerful tools for the structural dimensioning and detailing. Mörsch's classical 45-degree truss model concept has been adopted by most codes of practice as the basis of their shear and torsion design provisions. Unfortunately, the originally simple and transparent approach was obscured by many empirical modifications. As a result, rather than being simple, rational and general, like the methods for the dimensioning of sections subjected to flexure and axial load, shear and torsion design procedures became complex, empirical and restricted.

Despite the unfavourable code developments practising engineers have commonly applied truss models. However, as there was little if any official support, many engineers had some doubts about the justification of their methods. This has changed in recent years. The renewed interest in truss models has led to a universal acknowledgement of their potential but current code revisions have yet to avoid the danger of again introducing too many restrictions for their actual use.

This paper attempts to provide a synthesis of truss model approaches and related theories. The presentation starts with the familiar problem of beams subjected to flexure and shear. Next, geometric and static discontinuity regions are treated, followed by a chapter on the dimensioning of plates and shells for the effects of in-plane and transverse loading. The subsequent discussion of members subjected to combined actions is based on the treatment of plate elements subjected to in-plane forces. Finally, considerations of failure mechanisms involving discrete collapse cracks and slip lines are briefly reviewed and a set of conclusions regarding necessary further developments is given.

2. SHEAR AND FLEXURE IN BEAMS

2.1 Introductory example

To introduce a few basic concepts consider the uniformly loaded I-beam represented in Figs. 1(a) and (b).

Fig. 1(a) shows the expected crack pattern due to the factored load of 200 kNm^{-1}. It consists of vertical flexural cracks at midspan, inclined web shear cracks near the supports and inclined flexure-shear cracks in-between.

The crack pattern suggests that the beam acts like a truss with the flanges forming the chords, the stirrups acting as posts and the web concrete providing the compression diagonals. Three possible truss models for one half of the beam are shown in Figs. 1(c) through (e). In any case, the distributed load has been replaced by statically equivalent single loads and the effective depth of the web, d_v, is equal to 1000 mm since the chords have been assumed to coincide with the flange centres. Resultant truss member forces (in kN) are indicated in the figures. It can be observed that choosing a flatter inclination of the truss diagonals leads to less stirrup reinforcement while more longitudinal reinforcement is required.

Fig. 1(f) shows a discontinuous stress field corresponding to the truss model of Fig. 1(d). Truss diagonals are indicated as lines AL, BJ and DH. While diagonals AL and DH correspond to fan-shaped stress fields in regions AKM and CEGI, diagonal BJ corresponds to a uniformly compressed band of web concrete, ACIK. Finally, truss posts BL and DJ correspond to uniformly distributed stirrups in regions ACKM and CEIK. Thus, truss diagonals and diagonal forces simply represent the lines of action and the magnitudes of the stress resultants in the associated fans or bands. Similarly, truss posts and post forces represent the position and magnitude of the resultant stirrup force within certain beam portions.

Figs. 1(g) and (h) represent the variation of the chord forces according to both the truss model and the discontinuous stress field. It should be noticed that the two diagrams coincide at Sections CK and EI where the stirrup reinforcement is staggered. Furthermore, according to the discontinuous stress field, chord forces vary linearly along boundaries of stress bands, and parabolically along fan boundaries. In either case, the stirrups provide a uniform force but while the shear stresses acting on the chord are uniform for a stress band, they vary linearly along a fan boundary.

On principle, the bottom chord reinforcement may be curtailed such that the provided resistance matches the required resistance according to Fig. 1(g). It can be assumed that the provided resistance varies linearly over the development length of a bar, l_d.

Then, as shown in Figs. 1(i) and (j), two critical cases can be differentiated, where ΔT denotes the resistance provided by the curtailed reinforcement.

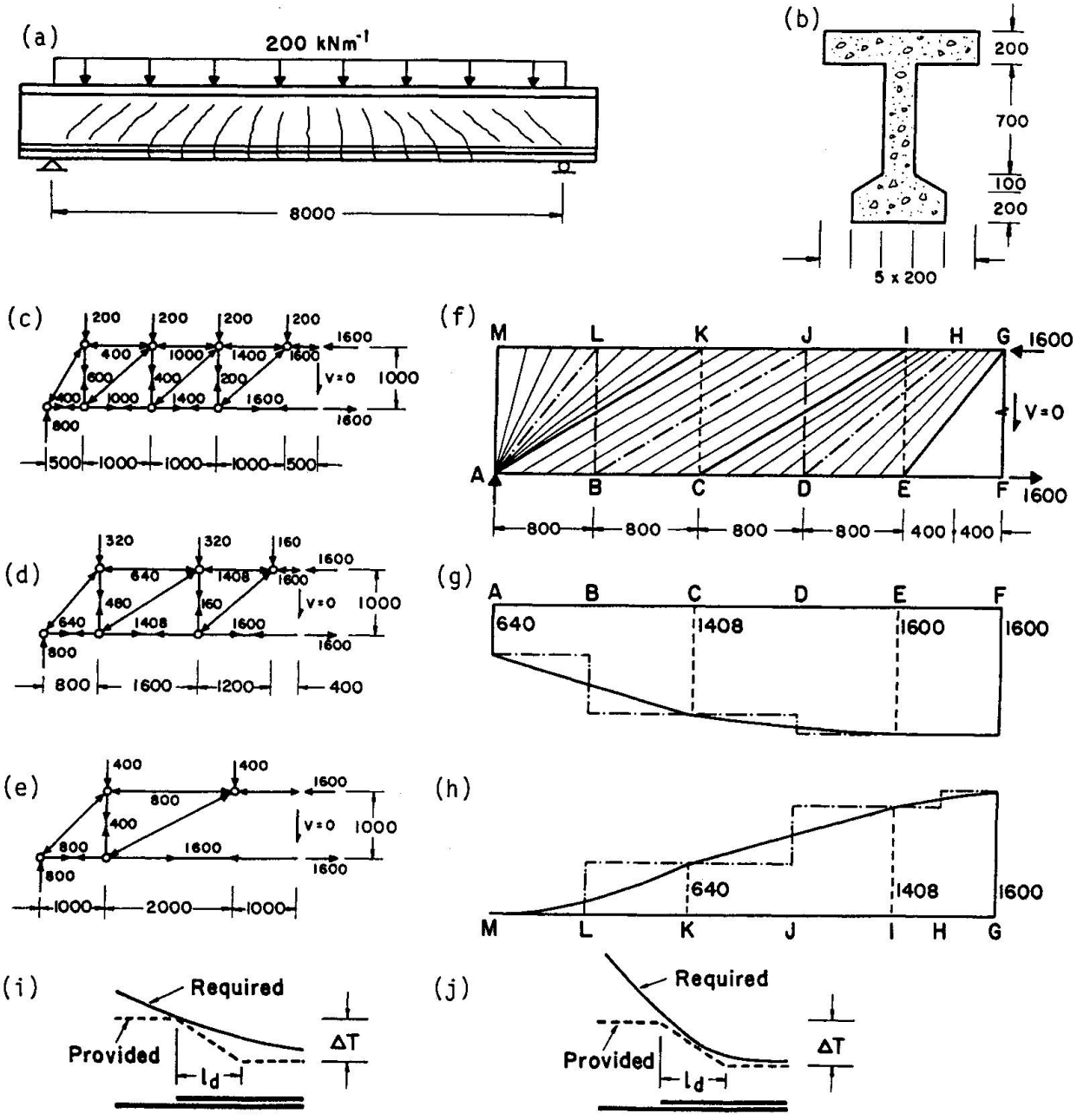

Fig. 1 Uniformly loaded I-beam: (a) Loading and crack pattern; (b) Cross-section; (c) through (e) Truss models; (f) Discontinuous stress field; (g) Required factored resistance of bottom chord; (h) Factored top chord force; (i) Critical condition at bar cutoff; (j) Critical condition within development length.
Note: Forces in kN and dimensions in mm.

Figs. 1(d) and (g) demonstrate that a bottom chord force equal to 40 % of that required at midspan has to be anchored at the support. Assuming a bottom chord reinforcement consisting of eight bars as shown in Fig. 2(a), of which four are anchored behind the support using 90 degree bends as indicated in Fig. 2(b), the other bars may be curtailed.

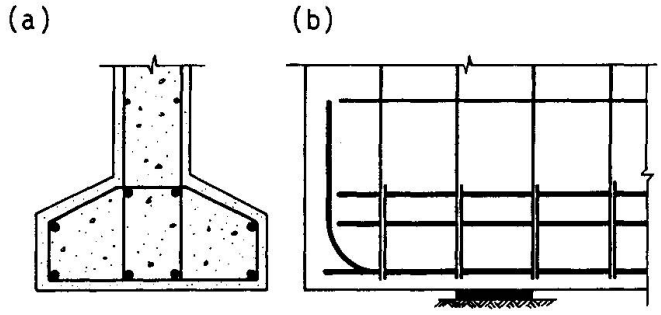

Fig. 2 Detailing of bottom chord reinforcement: (a) Cross-section; (b) Elevation at support.

Fig. 3(a) shows a truss model for the top flange. The compressive force of 1600 kN at midspan is split into two halves applied at the quarter points of the flange width and the shear transfer from the web into the flange is idealised with a series of 45-degree truss models as shown in Fig. 3(b). The resultant shear flow is illustrated by the diagram of Fig. 3(c) which represents one half of the derivative of the function given in Fig. 1(h). Since a 45-degree truss model is used, this diagram also shows the necessary factored resistance of the transverse flange reinforcement and from Fig. 3(b) it is clear that this reinforcement has to be placed at a distance of 200 mm from the location where the shear flow orignates.

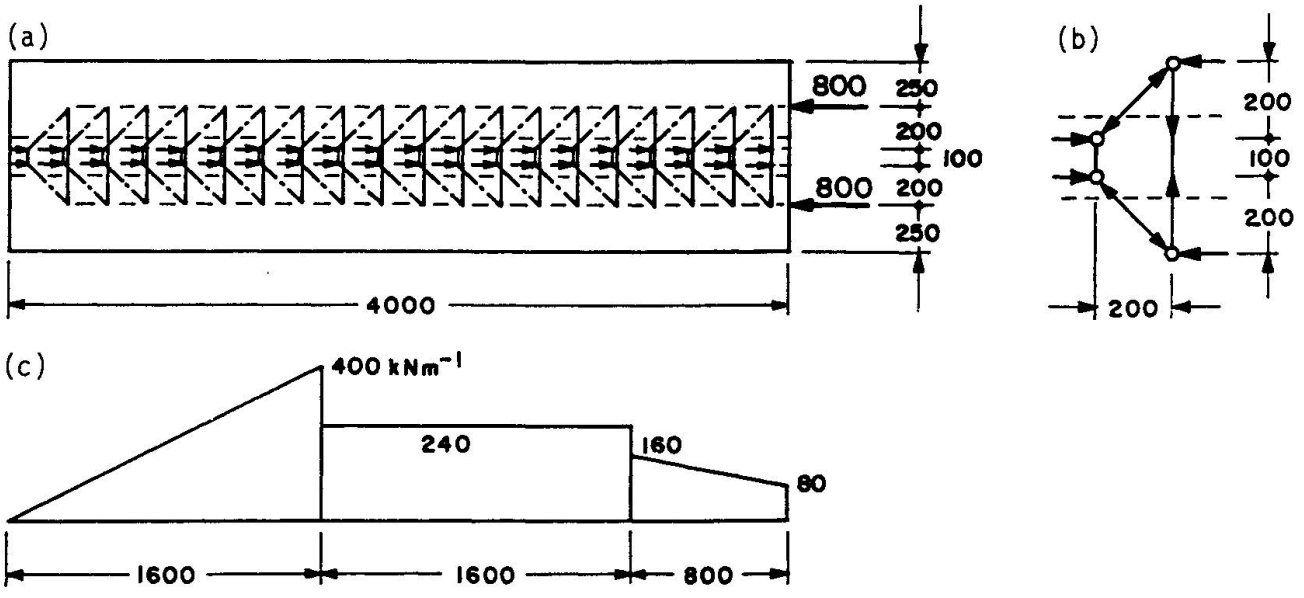

Fig. 3 Truss model for top flange: (a) Overview; (b) Detail; (c) Shear flow between web and either side of flange.

2.2 Continuous beams and general loading

The truss model and discontinuous stress field approaches can easily be generalised for continuous beams and arbitrary loading.

For fixed loads acting on continuous beams the only difficulty consists in determining the support reactions. Once these are known the beam can be subdivided into segments bounded by sections of zero shear force and the different segments can be treated individually. The segments can be considered as free bodies with known forces and moments applied to them. The truss model approach allows to visualise internal force paths in each segment and it indicates how the reinforcement should be detailed such that the envisaged force flow may indeed develop.

Statically indeterminate support reactions are commonly determined by performing a linearly elastic analysis for the uncracked system. However, members usually crack and apart from applied loads there are typically restraints which may cause effects similar to those produced by the loads. Hence, while an elastic analysis provides a statically admissible equilibrium solution for given loads it should be realised that there will always be some redistribution of the internal forces and moments. This redistribution corresponds to a self-equilibriated (or residual) state of stress whose magnitude depends on the loading and restraining history.

Contrary to an analysis of an existing structure where the actual loading and restraining history may be reasonably approximated this is impossible in design. However, well proportioned and detailed structures are capable of adapting to a large variety of imposed actions in a ductile manner, resulting in considerable redistributions of the internal forces and moments. Hence, rather than trying to analyse these redistributions a designer will attempt to achieve a sufficiently ductile behaviour through good detailing, and determine concrete and reinforcement dimensions based on a simple elastic analysis taking some freely assumed redistribution of the internal forces and moments into account.

For variable loads, moment redistribution within certain limits is usually permitted for each individual loading case. Alternatively, moment and shear force envelopes can be adjusted by superimposing a single residual stress state for all loading cases [20]. The differences between the two approaches have not yet been fully investigated, and in conjunction with a discussion of conventional load and resistance factor design, would deserve the attention of researchers.

If deemed necessary, cracked member stiffnesses can be considered to get an estimate for the residual stress state. An interesting possibility to perform such an investigation is to use the truss model used for proportioning the member by assigning appropriate stiffness values to the individual truss members. However, it is

Seite fehlt

Page missing

Page manque

Seite fehlt

Page missing

Page manque

Seite fehlt

Page missing

Page manque

Seite fehlt

Page missing

Page manque

Seite fehlt

Page missing

Page manque

Seite fehlt

Page missing

Page manque

Seite fehlt

Page missing

Page manque

Seite fehlt

Page missing

Page manque

Seite fehlt

Page missing

Page manque

Seite fehlt

Page missing

Page manque

Seite fehlt

Page missing

Page manque

Seite fehlt

Page missing

Page manque

Seite fehlt

Page missing

Page manque

Seite fehlt

Page missing

Page manque

Seite fehlt

Page missing

Page manque

Seite fehlt

Page missing

Page manque

The cover elements are sujected to the membrane forces given in Fig. 13(d) and can be designed according to the principles outlined in Section 4.2 [21].

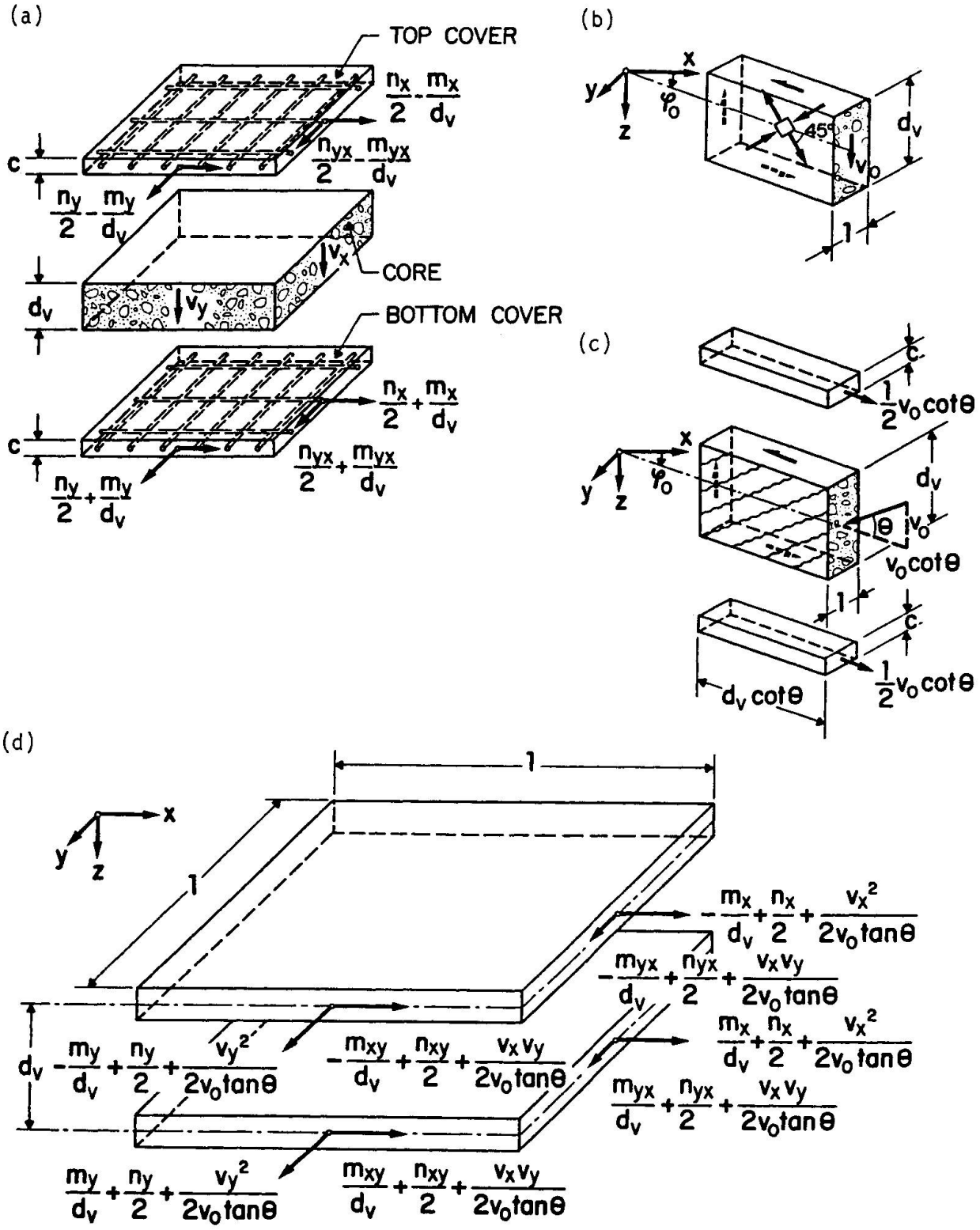

Fig. 13 Limit design of slab elements: (a) Sandwich model; (b) Pure shear in uncracked core; (c) Diagonal compression field in cracked core; (d) Forces acting on cover elements.

Apart from shear transfer in the interior of slabs, shear transfer along slab edges should be considered. Twisting moments at slab edges correspond to a shear force of equal magnitude being transferred along the edge. The analogy to beams subjected to circulatory torsion suggests that slab edges should be similarly reinforced as the side faces of such beams. In particular, the in-plane top and bottom reinforcements perpendicular to the edge must be connected through transverse reinforcements at the edge. The truss model of Fig. 14 illustrates this situation.

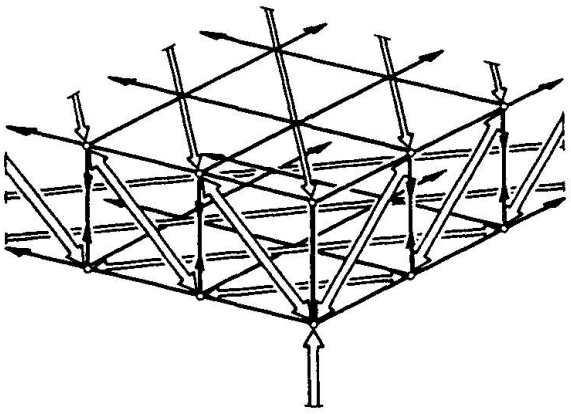

Fig. 14 Truss model for slab corner.

5. MEMBERS SUBJECTED TO COMBINED ACTIONS

5.1 Limit analysis and design

Starting from Fig. 15(a) and connecting several web elements along their stringers, one can build up arbitrary cross-sections which may be subjected to arbitrary combined actions, see Fig. 15(b) and (c). Conversely, arbitrary combined actions can be replaced by a system of axial and shear forces applied to the different stringers and wall elements. For example, side wall 1 in Fig. 15(c) has to resist a shear force of $V_1 = T/(2a_2) - V_y/2$ where the shear is taken as positive if it acts in the direction of the circulatory shear flow $S = T/(2a_1 a_2)$ due to T. Assigning flexural moments and axial load to the stringers, stringer 1 has to take a force of $T_1 = N/4 + M_y/(2a_2) - M_z/(2a_1)$, etc. Alternatively, flexural moments and axial load can be carried by combined axial forces in the stringers and the different wall elements.

Considering a diagonal compression field in each wall element and selecting appropriate inclination angles θ_i, the transverse reinforcements can be designed according to Eq. (1). The axial components of the diagonal compression forces, $V_i \cot\theta_i$, have to be resisted by the adjoining stringers. Thus, for example, stringer 1 of Fig. 15(c) has to resist $T_1 + V_1 \cot\theta_1/2 + V_4 \cot\theta_4/2$.

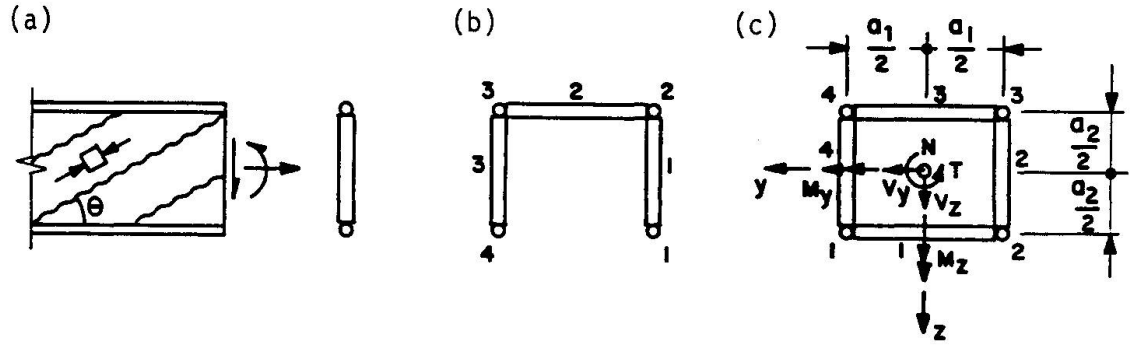

Fig. 15 Subdividing a cross-section into wall and stringer elements: (a) Single web; (b) Open cross-section; (c) Box section.

For a box section subjected to torsion, it is appropriate to assume that the shear flow, due to the torque, acts in the centre planes of the different side walls. A solid cross-section acts like a hollow one since its interior is subjected to triaxial tensile strains. Hence, neglecting the concrete tensile strength, only an exterior tube of diagonally compressed concrete is effective in resisting the torque [16].

Similar to the response to flexure a section subjected to a torsional moment tends to develop as large as possible lever arms of the internal forces resisting the torque. At ultimate, the concrete in the diagonally compressed tube will reach the crushing limit.

In dimensioning a member subjected to combined actions one may start with an estimate of the different wall thicknesses. This determines the lever arms of the internal forces and allows to compute these. Using Eq. (3) the adequacy of the initial estimate can be checked and the procedure can be repeated if necessary. Usually, one iteration is sufficient to get an acceptable solution.

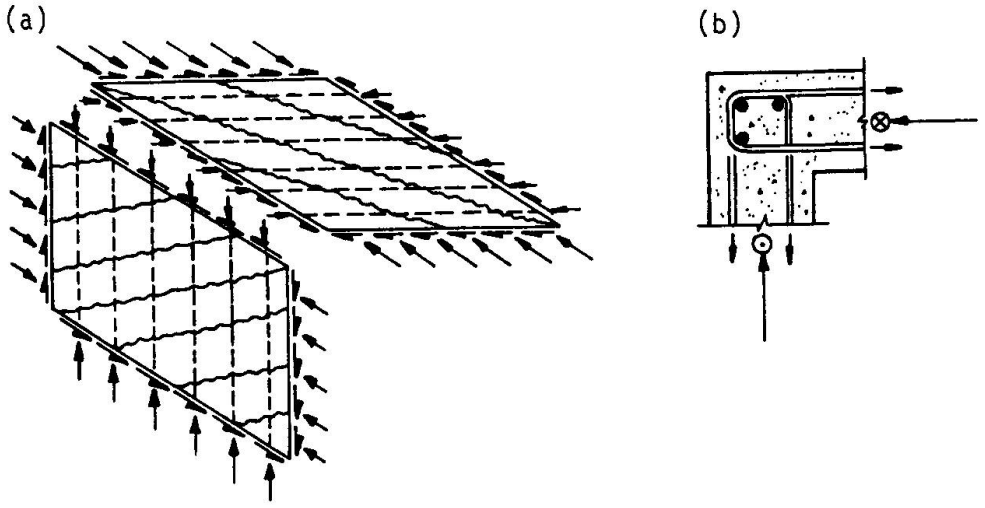

Fig. 16 Connection of wall elements: (a) Force flow; (b) Detailing of transverse reinforcement.

In detailing the transverse reinforcement we have to consider the shear transfer between the interconnected wall elements. Fig. 16(a) illustrates the static conditions and Fig. 16(b) shows an appropriate detail. For ease of placing, hairpin-shaped bars can be spliced with straight bars in the walls.

Similar to the remark made in connection with Fig. 6(f) it can be observed that the tensile strength of the concrete has to be mobilised to activate the cover. In fact, under very high loads the cover may spall off and it would therefore be conservative to use spalled section properties. However, for ease of computation it is advantageous to use unspalled properties along with a cautious assessment of the effective concrete compressive strength f_c.

Interaction equations for the combined action of flexural and torsional moments and axial laods were derived [15,35,37], and collapse mechanisms were found which are compatible with the static conditions discussed above [24,25].

5.2 Deformations

A variety of methods have been devised which permit to compute the deformations of thin-walled box girders subjected to combined actions in the cracked state [16]. Essentially they are based on the compression field approach and use either a space truss [34] or a finite element model [29].

Usually, flexural and axial load deformations dominate and, fortunately, are much easier to predict than the deformations due to shear and torsion. Thus, application of the referenced methods can be restricted to special cases with significant shear and torsional deformations.

6. CONSIDERATION OF FAILURE MECHANISMS

The material presented in the previous chapters is essentially based on the static or lower-bound method of limit analysis. This chapter briefly reviews concepts of the kinematic or upper-bound method of limit analysis. This method has been widely used for slab design [13] but it has not received the same attention for other applications. However, although not normally stated, the familiar shear friction method [1,4] belongs to the category of upper-bound analyses. Furthermore, the analogy to slip line methods used in soil mechanics has been helpful in solving several problems in the area of concrete structures [27,28,20,25].

Using a lower-bound approach, one is forced to follow the flow of forces throughout a member. Hence, such approaches lend themselves

to dimensioning and detailing which must result in enough of the right material at the right place throughout the member. On the other hand, upper-bound methods are primarily suited for analysis, enabling quick checks of essential dimensions and details. Recent developments have favoured the application of static methods, while perhaps, the kinematic methods have been thrust too much into the background. This is unfortunate because there is much to be gained from such considerations.

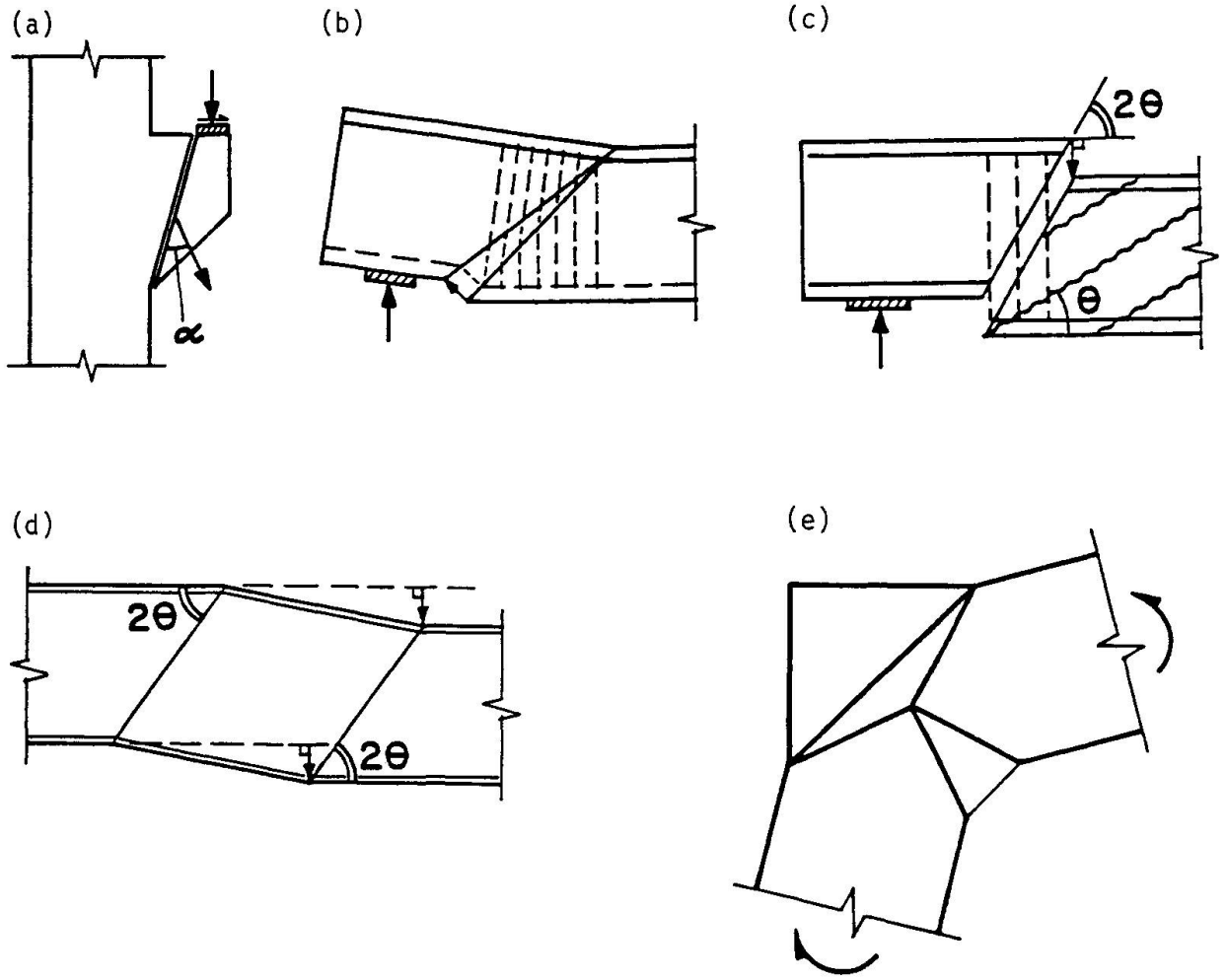

Fig. 17 Failure mechanisms: (a) Discontinuity surface in corbel; (b) Collapse crack in beam; (c) Web crushing mechanism; (d) Web crushing and stirrup yielding in zone of homogeneous deformation; (e) Collapse crack mechanism for knee joint subjected to opening moment [41].

Frequently, we observe that failure of a member occurs at a distinct surface. For example, the corbel shown in Fig. 17(a) may fail along a discontinuity plane extending from the back side of the loading plate to the reentrant corner at the bottom connection of the corbel with the column. At failure, the portion of the corbel under the load moves down and away from the column. The work done by the externally applied load equals the dissipation in the concrete and the reinforcement crossing the discontinuity surface

where all the deformation is concentrated. Considering a relative translation inclined at an angle α to the discontinuity the work as well as the dissipation can be expressed as functions of α and, on account of the upper-bound theorem, the optimum value of α resulting in the lowest upper-bound for the collapse load can be found.

Neglecting the concrete tensile strength and assuming a perfectly plastic behaviour in compression, the dissipation in the concrete per unit area of a discontinuity surface due to a unit relative displacement amounts to $f_c(1 - \sin\alpha)/2$. Thus, for $\alpha = 90$ deg., i.e., a pure crack opening, there is no dissipation in the concrete. Müller [24] introduced the term "collapse crack" for such a situation. Fig. 17(b) shows an example of a collapse crack mechanism. The stirrups as well as the bottom chord reinforcement crossing the collapse crack are yielding while there is no dissipation in the concrete.

Figs. 17(c) and (d) illustrate web crushing mechanisms of a beam in which the stirrups yield, the web concrete crushes and the chord reinforcement remains elastic. These mechanisms correspond to the static conditions underlying Eq. (8) and the inclination of the discontinuity or slip line in Fig. 17(c) is twice that of the associated stress field [3,25]. The mechanism of Fig. 17(d) can be thought of as a series of slip lines similar to that in Fig. 17(c).

Fig. 17(e) shows a collapse crack mechanism for a knee joint. It appears that similar mechanisms could be developed for numerous other practical problems.

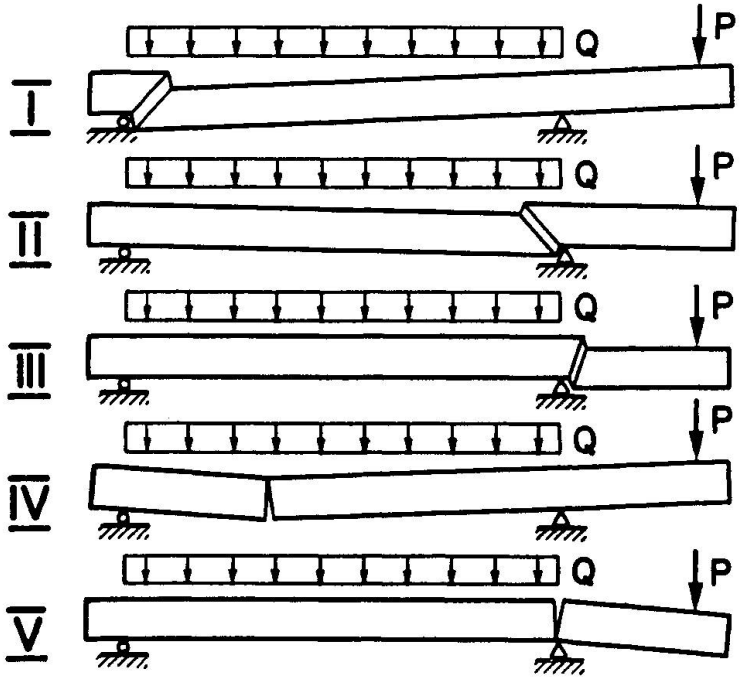

Fig. 18 Failure mechanisms for isostatic beam [6].

Finally, Figs. 18 and 19 illustrate a number of possible collapse crack and web crushing mechanisms for isostatic and continuous girders. Note that flexural failure mechanisms such as Mechanisms IV and V in Fig. 18 are special collapse crack mechanisms. Furthermore, mechanism II in Fig. 19 addresses the problem of insufficient extensions of the longitudinal reinforcement in the vicinity of points of contraflexure, while mechanisms IV and V address the problem of insufficient extensions of the top reinforcement in spans adjoining the most heavily loaded span.

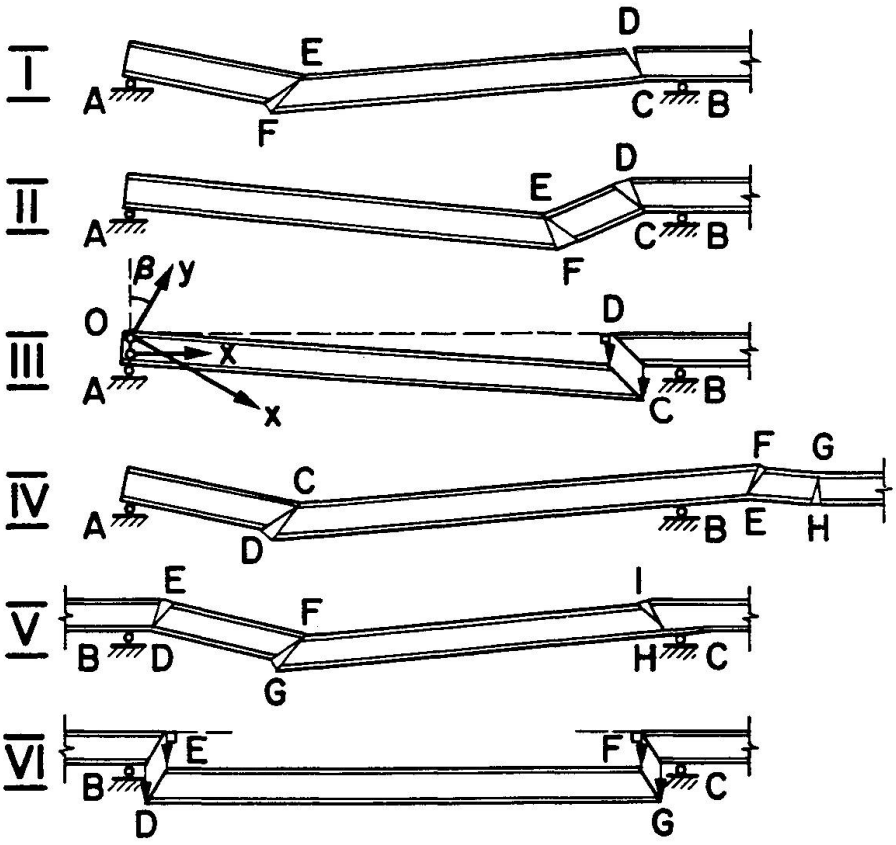

Fig. 19 Failure mechanisms for continuous girders [20].

7. CONCLUSIONS

Truss model approaches and related theories have been presented in an attempt to provide a synthesis of recently developed methods permitting a consistent dimensioning and detailing of structural concrete members. It has been demonstrated that all the different methods supplement each other, having one common base.

Truss or strut and tie model procedures inherently relate to dimensioning and detailing. Having selected initial member sizes application of such procedures is characterised by a trial and adjustment process leading to final dimensions and details. Provision of an adequate minimum reinforcement, development of an appropriate equilibrium model to follow the flow of the internal

forces, and consequent dimensioning and detailing are the essential features in this process.

Major areas deserving further work include:

(i) There is a need for better understanding of bond and development of reinforcement. Associated principles should be brought in line with strut and tie model concepts. This would lead to improved guidance on the effective concrete strength of nodal zones.

(ii) Models for prestressed members are not yet entirely consistent.

(iii) More guidance on the selection of minimum reinforcement is required. Possible restraints, deformations under service conditions, and the contribution of such reinforcement to the ultimate strength as well as its effect on the need for compatibility considerations during the development of strut and tie models should be taken into account.

(iv) Failure mechanism considerations should be further developed to obtain reliable and easily applicable methods for standard design situations.

(v) A compromise is needed regarding simplified design procedures permitted by codes.

(vi) Appropriate information and education of the profession are necessary to make the transition to the envisaged unified design approach for structural concrete possible.

ACKNOWLEDGEMENTS

Discussions with Dr. David Rogowsky contributed much to clarifying the views expressed in this paper. Regina Nöthiger and Viktor Sigrist assisted in preparing the manuscript. Their contribution is also warmly acknowledged.

REFERENCES

[1] ACI Committee 318, "Building Code Requirements for Reinforced Concrete (ACI 318-89) and Commentary - ACI 318R-89", American Concrete Institute, Detroit, 1989, 353 pp.

[2] Baumann, T., "Zur Frage der Netzbewehrung von Flächentragwerken (On the Problem of Net Reinforcement of Surface Structures)", Bauingenieur, Vol. 47, No. 10, Oct. 1972, pp. 367-377.

[3] Braestrup, M.W., "Plastic Analysis of Shear in Reinforced Concrete", Magazine of Concrete Research, Vol. 26, No. 89, Dec. 1974, pp. 221-228.

[4] Canadian Standards Association, "Design of Concrete Structures for Buildings (CAN3-A23.3-M84)", Rexdale, Ontario, 1984, 281 pp.

[5] Comité Euro-International du Béton, "CEB-FIP Model Code 1990", First Draft, Bulletins d'Information, No. 195 and No. 196, Lausanne, March 1990.

[6] Cerruti, L.M., and Marti, P., "Staggered Shear Design of Concrete Beams: Large Scale Tests", Canadian Journal of Civil Engineering, Vol. 14, No. 2, April 1987, pp. 257-268.

[7] Collins, M.P., "Towards a Rational Theory for Reinforced Concrete Members in Shear", Proceedings, ASCE, Vol. 104, No. ST4, April 1978, pp. 649-666.

[8] Collins, M.P., and Mitchell, D., "Shear and Torsion Design of Prestressed and Non-Prestressed Concrete Beams", Journal of the Prestressed Concrete Institute, Vol. 25, No. 5, Sept.-Oct. 1980, pp. 32-100. Also, Discussion, Vol. 26, No. 6, Nov.-Dec. 1981, pp. 96-118.

[9] Collins, M.P., and Mitchell, D., "A Rational Approach to Shear Design - The 1984 Canadian Code Provisions", Journal of the American Concrete Institute, Vol. 83, No. 6, Nov.-Dec. 1986, pp. 925-933.

[10] Collins, M.P., and Mitchell, D., "Prestressed Concrete Basics", Canadian Prestressed Concrete Institute, Ottawa, 1987, 614 pp.

[11] Cook, W.D., and Mitchell, D., "Studies of Disturbed Regions near Discontinuities in Reinforced Concrete Members", ACI Structural Journal, Vol. 85, No. 2, March-April 1988, pp. 206-216.

[12] IABSE, "Colloquium on Plasticity in Reinforced Concrete", Copenhagen 1979, International Association for Bridge and Structural Engineering, Introductory Report, Vol. 28, 1978, 172 pp; and Final Report, Vol. 29, 1979, 360 pp.

[13] Johansen, K.W., "Yield-Line Theory", Cement and Concrete Association, London, 1962, 181 pp.

[14] Kupfer, H., "Erweiterung der Mörsch'schen Fachwerkanalogie mit Hilfe des Prinzips vom Minimum der Formänderungsarbeit (Generalization of Mörsch's Truss Analogy Using the Principle of Minimum Strain Energy)", Comité Euro-International du Béton, Bulletin d'Information, No. 40, Paris, Jan. 1964, pp. 44-57.

[15] Lampert, P., and Thürlimann, B., "Ultimate Strength and Design of Reinforced Concrete Beams in Torsion and Bending", International Association for Bridges and Structural Engineering, Publications, Vol. 31-I, 1971, pp. 107-131.

[16] Marti, P., "Strength and Deformations of Reinforced Concrete Members Under Torsion and Combined Actions", Comité Euro-International du Béton, Bulletin d'Information, No. 146, Jan. 1982, pp. 97-138.
[17] Marti, P., "Basic Tools of Reinforced Concrete Beam Design", Journal of the American Concrete Institute, Vol. 82, No. 1, Jan.-Feb. 1985, pp. 46-56. Also, Discussion, Vol. 82, No. 6, Nov.-Dec. 1985, pp.933-935.
[18] Marti, P., "Truss Models in Detailing", Concrete International: Design and Construction, Vol. 7, No. 12, Dec. 1985, pp. 66-73. Also, Discussion, Vol. 8, No. 10, Oct. 1986, pp. 66-68.
[19] Marti, P., "Staggered Shear Design of Simply Supported Concrete Beams", Journal of the American Concrete Institute, Vol. 83, No. 1, Jan.-Feb. 1986, pp. 36-42.
[20] Marti, P., "Staggered Shear Design of Concrete Bridge Girders", Proceedings, International Conference on Short and Medium Span Bridges, Ottawa, Aug. 1986, Vol. 1, pp. 139-149.
[21] Marti, P., "Design of Concrete Slabs for Transverse Shear", ACI Structural Journal, Vol. 87, No. 2, March-April 1990, pp. 180-190.
[22] Mitchell, D., and Collins, M.P., "Diagonal Compression Field Theory - A Rational Model for Structural Concrete in Pure Torsion", Journal of the American Concrete Institute, Vol. 71, No. 8, Aug. 1974, pp. 396-408.
[23] Mörsch, E., "Der Eisenbetonbau - Seine Theorie und Anwendung (Reinforced Concrete Construction - Theory and Application)", 5th Edition, Vol. 1, Part 2, K. Wittwer, Stuttgart, 1922.
[24] Müller, P., "Failure Mechanisms for Reinforced Concrete Beams in Torsion and Bending", International Association for Bridge and Structural Engineering, Publications, Vol. 36-II, 1976, pp. 147-163.
[25] Müller, P., "Plastische Berechnung von Stahlbetonscheiben und -balken (Plastic Analysis of Reinforced Concrete Walls and Beams)", Institute of Structural Engineering, ETH Zürich, Report No. 83, 1978, 160 pp.
[26] Nielsen, M.P., "On the Strength of Reinforced Concrete Discs", Civil Engineering and Building Construction Series, No. 70, Acta Polytechnica Scandinavica, Copenhagen, 1971, 261 pp.
[27] Nielsen, M.P., "Limit Analysis and Concrete Plasticity", Prentice-Hall, 1984, 420 pp.
[28] Nielsen, M.P., Braestrup, M.W., Jensen, B.C., and Bach, F., "Concrete Plasticity", Special publication, Dansk Selskab for Bygningsstatik, Copenhagen, 1978, 129 pp.
[29] Potucek, W., "Die Beanspruchung der Stege von Stahlbetonplattenbalken durch Querkraft und Biegung (Stresses in Webs of Reinforced Concrete T-beams Subjected to Flexure and Shear)", Zement und Beton, Vol. 22, No. 3, 1977, pp. 88-98.
[30] Rogowsky, D.M., Mac Gregor, J.G., and Ong, S.Y., "Tests of Reinforced Concrete Deep Beams", Journal of the American Concrete Institute, Vol. 83, No. 4, July-August 1986, pp. 614-623.
[31] Schlaich, J., and Weischede, D., "Detailing Reinforced Concrete Structures", Canadian Structural Concrete Conference 1981, Proceedings, Department of Civil Engineering, University of Toronto, Toronto, 1981, pp. 171-198.

[32] Schlaich, J., and Schäfer, K., "Konstruieren in Stahlbetonbau (Detailing in Reinforced Concrete Design)", Betonkalender 1984, Part 2, W. Ernst, Berlin, 1984, pp. 787-1005.

[33] Schlaich, J., Schäfer, K., and Jennewein, M., "Toward a Consistent Design of Structural Concrete", Journal of the Prestressed Concrete Institute, Vol. 32, No. 3, May-June 1987, pp. 74-150.

[34] Thürlimann, B., and Lüchinger, P., "Steifigkeit von gerissenen Stahlbetonbalken unter Torsion und Biegung (Stiffness of Cracked Reinforced Concrete Beams Subjected to Torsion and Flexure)", Beton und Stahlbetonbau, Vol. 68, No. 6, June 1973, pp. 146-152.

[35] Thürlimann, B., Grob, J., and Lüchinger, P., "Torsion, Biegung und Schub in Stahlbetonträgern (Torsion, Flexure and Shear in Reinforced Concrete Girders)", Institute of Structural Engineering, ETH Zürich, 1975, 170 pp.

[36] Thürlimann, B., "Shear Strength of Reinforced and Prestressed Concrete Beams - CEB Approach", Concrete Design: U.S. and European Practices, SP-59, American Concrete Institute, Detroit, 1979, pp. 93-115.

[37] Thürlimann, B., "Torsional Strength of Reinforced and Prestressed Concrete Beams - CEB Approach", Concrete Design: U.S. and European Practices, SP-59, American Concrete Institute, Detroit, 1979, pp. 117-143.

[38] Thürlimann, B., Marti, P., Pralong, J., Ritz, P., and Zimmerli, B., "Anwendung der Plastizitätstheorie auf Stahlbeton (Application of the Theory of Plasticity to Reinforced Concrete)", Institute of Structural Engineering, ETH Zürich, 1983, 252 pp.

[39] Vecchio, F.J., and Collins, M.P., "The Response of Reinforced Concrete to In-Plane Shear and Normal Stresses", Publication No. 82-03, Department of Civil Engineering, University of Toronto, March 1982, 332 pp.

[40] Vecchio, F.J., and Collins, M.P., "The Modified Compression Field Theory for Reinforced Concrete Elements Subjected to Shear", Journal of the American Concrete Institute, Vol. 83, No. 2, March-April 1986, pp. 219-231.

[41] Müller, P., "Consistent Connection Design", Session on 'Innovations in Shear Design', 1990 ACI Annual Convention, Toronto, March 20, 1990.

Leere Seite
Blank page
Page vide

Ductility of Structural Concrete

Ductilité du béton armé

Duktilität von Konstruktionsbeton

Robert PARK
Prof. of Civil Eng.
Univ. of Canterbury
Christchurch, New Zealand

Robert Park has teaching and research interests in structural concrete and in the design for earthquake resistance. He has received a number of awards from the USA, United Kingdom and New Zealand for his research contributions.

SUMMARY
Definitions for the required and available ductility of structural concrete are described. The need for ductility in the design of structures for earthquake resistance is considered, and possible modes of inelastic deformation of moment resisting frames and structural walls are outlined. Procedures for detailing members for ductility are discussed.

RÉSUMÉ
Des définitions concernant la ductilité nécessaire et disponible du béton armé sont présentées; il est nécessaire de tenir compte de la ductilité dans le dimensionnement des structures devant résister aux séismes. On esquisse les modes possibles de déformation plastique des cadres résistant aux moments et des parois armés. On discute des procédés qui permettent d'augmenter la ductilité des éléments de construction.

ZUSAMMENFASSUNG
Definitionen für die erforderliche und verfügbare Duktilität von Konstruktionsbeton werden beschrieben. Es wird die Notwendigkeit begründet, die Duktilität bei der Bemessung von Tragwerken im Hinblick auf eine Erdbebenbeanspruchung zu berücksichtigen und es werden die möglichen Arten nicht-elastischer Verformungen von Rahmentragwerken und Wandscheiben aufgezeigt. Die Vorgehensweise für die konstruktive Durchbildung von Bauteilen zur Errechnung der Duktilität werden diskutiert.

1. INTRODUCTION

The term "ductility" in structural design is used to mean the ability of a structure to undergo large deformations in the postelastic range without a substantial reduction in strength. This can be contrasted with "brittle" behaviour in which the load carrying capacity of the structure decreases sharply when the strength is reached.

In design, consideration of the available ductility of a structure is necessary for the following reasons: (1) to prevent brittle failure, (2) to use distributions of bending moments differing from that obtained from linear elastic structural analysis, and (3) to survive severe earthquake and blast loading.

This paper considers the ductility of structural concrete members and structures. Emphasis is given to aspects of the design of structures for earthquake resistance, since ductility considerations are of paramount importance in the design for earthquake loading.

2. DEFINITIONS FOR REQUIRED DUCTILITY

The required ductility of a structure, element or section can be expressed in terms of the maximum imposed deformation. Often it is convenient to express the maximum deformations in terms of ductility factors, where the ductility factor is defined as the maximum deformation divided by the corresponding deformation present when yielding occurs. The use of ductility factors permits the maximum deformations to be expressed in nondimensional terms as indices of postelastic deformation for design and analysis. Ductility factors have been commonly expressed in terms of the various parameters related to deformations, namely displacements, rotations, curvatures and strains.

The displacement ductility factor is $\mu = \Delta_{max}/\Delta_y$, where Δ_{max} is the maximum displacement and Δ_y is the displacement at yield. The displacement ductility factor μ is shown defined for ideal elastoplastic behaviour in Fig.1.

The rotation ductility factor required of members is θ_{max}/θ_y, where θ_{max} is the maximum rotation at the plastic hinge and θ_y is the rotation in the plastic hinge region at yield. The information most needed by designers is the required curvature behaviour of the critical sections of members in plastic hinge regions, expressed by the curvature ductility factor ϕ_{max}/ϕ_y, where ϕ_{max} is the maximum curvature at the section and ϕ_y is the curvature there at yield.

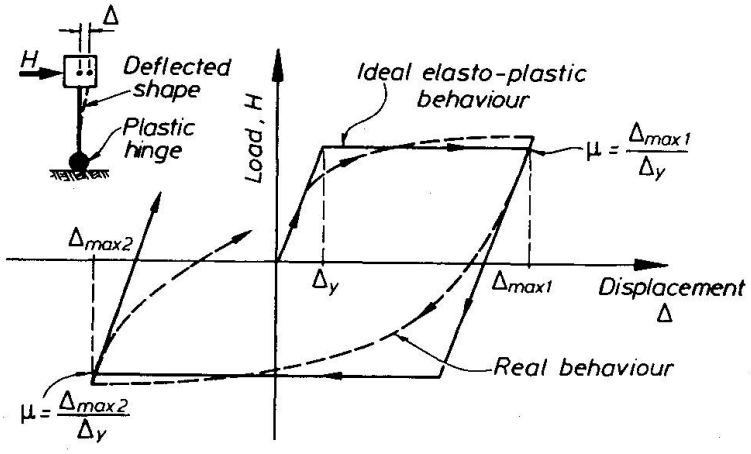

Fig.1 Displacement Ductility Factor

3. DEFINITIONS FOR AVAILABLE DUCTILITY

The ductility required of the structure when loaded into the postelastic range needs to be matched by the available ductility of the structure. Definitions which can be used to estimate the available ductility factor are considered below [2]:

(a) The Definition of the Yield Deformation - When calculating ductility factors the definition of the yield deformation (displacement, rotation or curvature) often causes difficulty since the force-deformation relation may not have a well defined yield point. This may occur, for example, due to nonlinear behaviour of the materials, or due to reinforcing bars at different depths in a structural concrete section reaching yield at different moment levels, or due to plastic hinges in different parts of a structure forming at different load levels. Various alternative definitions which have been used by investigators to estimate the yield displacement are illustrated in Fig.2. These are the displacement when yielding first occurs (Fig.2a), the yield displacement of the equivalent elastoplastic system with the same elastic stiffness and ultimate load as the real system (Fig.2b), the yield displacement of the equivalent elastoplastic system with the same energy absorption as the real system (Fig.2c), and the yield displacement of the equivalent elastoplastic system with reduced stiffness found as the secant stiffness at 75% of the ultimate lateral load H_u of the real system (Fig.2d). The latter definition (Fig.2d) takes the secant stiffness as described in order to include the reduction in stiffness due to cracking near the end of the elastic range. This latter definition is the most realistic definition for the yield displacement for reinforced concrete structures.

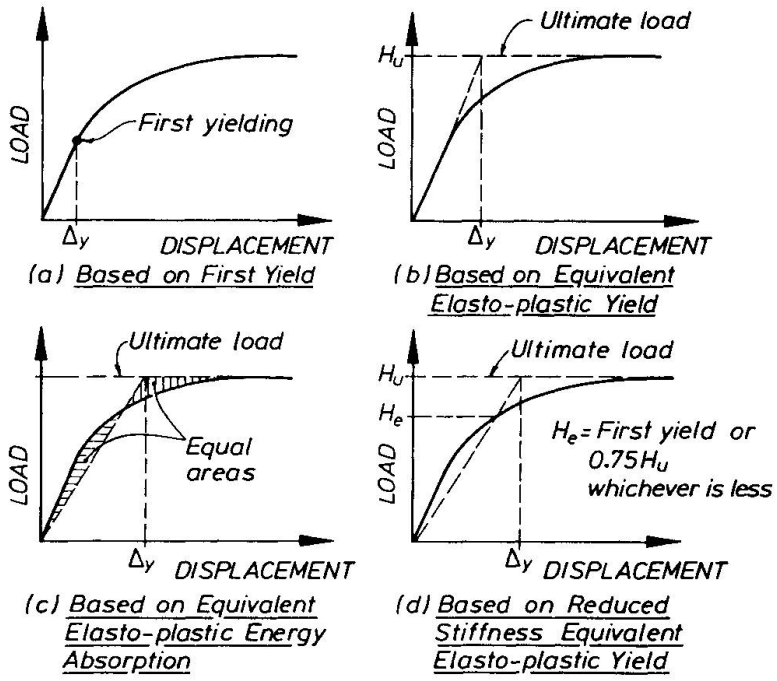

Fig.2 Alternative Definitions for Yield Displacement

(b) Definition of the Maximum Available (Ultimate) Deformation - The maximum available (ultimate) deformation has also been estimated using various assumptions by investigators. Some possible estimates for the maximum available displacement are shown in Fig.3. These are the displacement corresponding to a particular limiting value for the concrete compressive strain (Fig.3a), the displacement corresponding to the peak of the load-displacement relation

(Fig.3b), the postpeak displacement when the load carrying capacity has undergone a small reduction (Fig.3c), and the displacement when the transverse or longitudinal reinforcing steel fractures or the longitudinal compression reinforcement buckles (Fig.3d). When considering the most appropriate definition it should be recognized that most structures have some capacity for deformation beyond the peak of the load-displacement relation without significant reduction in strength. It would be reasonable to recognize at least part of this postpeak deformation capacity. Also, it is evident that the maximum available deformation does not necessarily correspond to a specified extreme fibre concrete compresssive strain. Hence the most realistic definition for the maximum available displacement are given by the criteria shown in Figs. 3c and 3d, whichever occurs first.

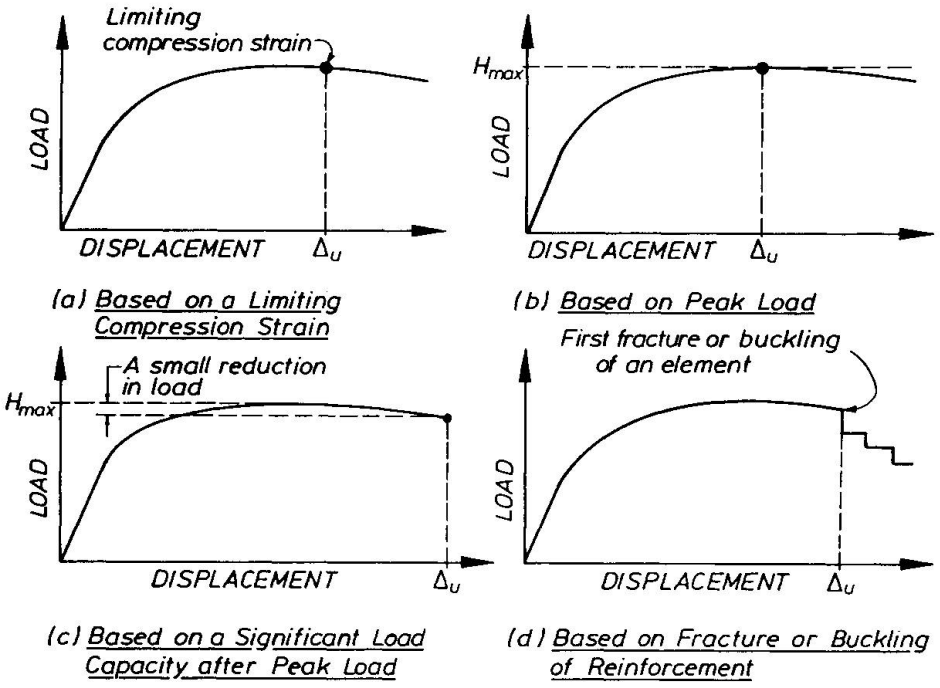

Fig.3 Alternative Definitions for Maximum Available (Ultimate) Displacement

4. DUCTILE DESIGN APPROACH FOR EARTHQUAKE LOADS

4.1 Design Strength and Ductility for Earthquake Loading

In the design of structures for earthquake resistance the emphasis should be placed on good structural concepts and detailing of reinforcement. It is well known that when a structure responds elastically to ground motions during a severe earthquake, the maximum response acceleration may be several times the maximum ground acceleration and depends on the stiffness of the structure and the magnitude of the damping. Generally it is uneconomical to design a structure with adequate strength to respond in the elastic range during a severe earthquake, since that would require very high design earthquake forces. Codes generally recommend lower levels of design earthquake loading which means that the critical regions of the structure need to be detailed to possess sufficient ductility to enable the structure to survive without collapse. For example, the design earthquake loads recommended by the New Zealand general structural design code [3] for ductile structures assumes that the structure is capable of deforming in the postelastic range to a displacement ductility factor of at least $\mu = 4$ to 6 during several cycles of earthquake loading without significant loss of strength.

4.2 Capacity Design

The exact characteristics of the earthquake ground motions that may occur at a given site cannot be predicted with certainty and it is difficult to evaluate all aspects of the complete behaviour of a complex structure when subjected to a severe earthquake. Nevertheless it is possible to design the structure so that it has features that will ensure the most desirable behaviour. The rational approach for achieving this aim in earthquake resistant design is to choose the most suitable mechanism of postelastic deformation for the structure and to ensure by appropriate design procedures that yielding will occur only in the chosen manner during a severe earthquake. This approach is referred to as "capacity design" in New Zealand [3,4].

For moment resisting frames the best means of achieving ductile postelastic deformations is by flexural yielding at selected plastic hinge positions, since with proper design the plastic hinges can be made adequately ductile. The chosen plastic hinge positions are designed for adequate flexural strength and ductility for the code specified loading. Then when designing for shear the design shear forces are calculated on the basis of amplified plastic hinge moments, to take into account the actual quantity of longitudinal reinforcement present, the actual yield strength of that steel being higher than specified and strain hardening of steel at high deformations. If plastic hinges in columns of moment resisting frames are to be avoided, the design bending moments of columns may also need to be amplified to take into account the effects of higher modes of vibration and biaxial earthquake loading as well as beam overstrength [4].

4.3 Preferred Modes of Inelastic Deformation

Fig. 4 shows mechanisms of inelastic deformation which could form in moment resisting frames and structural walls due to the formation of plastic hinges during severe earthquakes. For tall moment resisting frames a beam sidesway mechanism is preferred since it makes more moderate demands on the curvature ductility required at the plastic hinges and ductility is more easily provided in beams than in columns. Collapse of frames during severe earthquakes due to a "soft storey" (column sidesway mechanisms) has commonly been observed. Ductile coupled structural walls (see Fig.4) should preferably be designed so that the coupling beams yield before the walls, and the coupling beams should be detailed for adequate ductility. Ductile cantilever walls should preferably be designed to ensure that flexural yielding occurs. For the substructures of bridges, the mechanisms inelastic deformations sought are similar to those for buildings during severe seismic loading [5].

4.4 Required Plastic Hinge Rotations

The required curvature ductility factor ϕ_u/ϕ_y which should be available at the plastic hinge locations in frames and walls will depend on the many variables involved, such as the geometry of the members and the relative strengths of sections. Codes do not generally expect designers to calculate the curvature ductility factors required at the plastic hinge regions. Instead, adequate ductility is considered to have been provided if the structure resisting seismic forces is detailed for ductility in accordance with the seismic provisions of the code [4].

5. DETAILING OF PLASTIC HINGE REGIONS

5.1 General

The most important design consideration for ductility in the plastic hinge regions of structural concrete members is the provision of adequate longitudinal compression reinforcement as well

as tension reinforcement, and the provision of adequate transverse reinforcement in the form of rectangular stirrups or hoops and cross ties or spirals, in order to act as shear reinforcement, to confine the compressed concrete, and to prevent premature buckling of the compressed longitudinal reinforcement. A centre to centre spacing of transverse bars not exceeding six longitudinal bar diameters in plastic hinge regions is considered to be necessary in order to prevent premature buckling of longitudinal bars during cycles of tension-compression yielding such as is caused by severe earthquake loading [4].

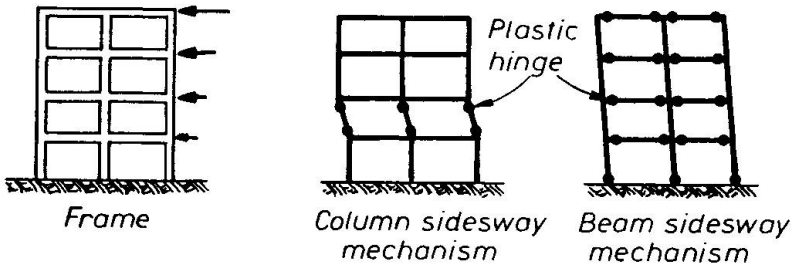

(a) Moment Resisting Frames

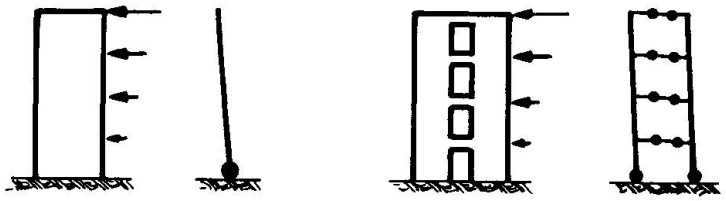

(b) Structural Walls

Fig. 4 Moment Resisting Frames and Walls and Mechanisms of Inelastic Deformation Due to Plastic Hinging During Severe Earthquake Loading

5.2 Ductility Enhancement by Concrete Confinement

The ductility (and strength) of structural concrete members can be greatly improved by confining the compressed concrete using arrangements of closely spaced transverse reinforcement in the form of spirals and circular hoops or rectangular hoops with adequate cross ties. The concrete becomes confined when at strains approaching the unconfined strength the transverse strains become very high and the concrete bears out against the transverse reinforcement, which then applies a passive confining pressure due to the arching of the concrete between the transverse bars and the longitudinal bars. The cover concrete, including that concrete outside the arching forces, is not confined and will be lost as in the case of unconfined concrete.

It is evident from Fig.5 that the confinement of concrete is improved if the transverse and longitudinal reinforcement is placed at relatively close spacing, and if there are a number of longitudinal bars well distributed around the column section and ties across the section, because then the arches between the bars are shallower and hence more of the concrete sections is confined.

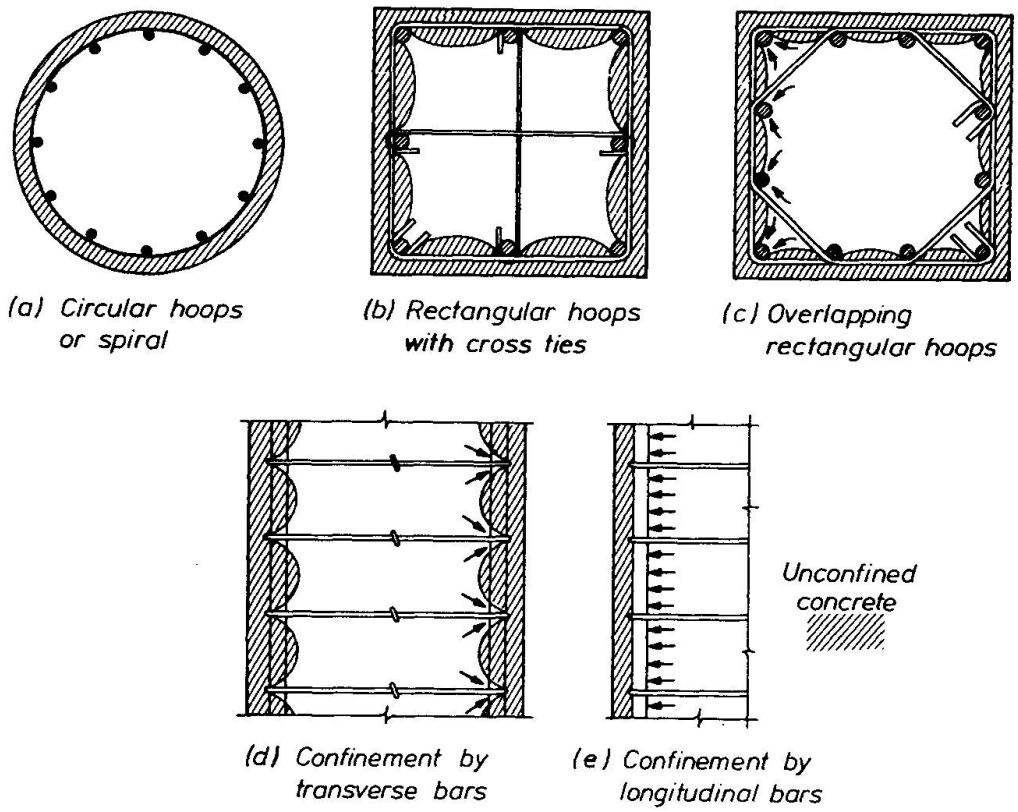

Fig.5 Confinement of Compressed Concrete by Reinforcement

Typical longitudinal stress-strain curves for well confined concrete and identical but unconfined concrete are shown in Fig.6. For confined concrete, eventual fracture of the transverse reinforcement limits the useful concrete compressive strain, but values in the range 0.02 to 0.08 are typically obtained [5,6]. The extent of the improvement in the stress-strain behaviour is a function of the lateral confining pressure, which in turn depends on the volume, yield strength, and efficiency of the arrangement of the transverse reinforcement.

Moment-curvature analyses incorporating models for the stress-strain relation of concrete confined by various quantities and arrangements of transverse reinforcement can be used to compute the quantities of transverse reinforcement required to achieve various curvature ductility levels. This procedure is the basis of several analytical approaches.

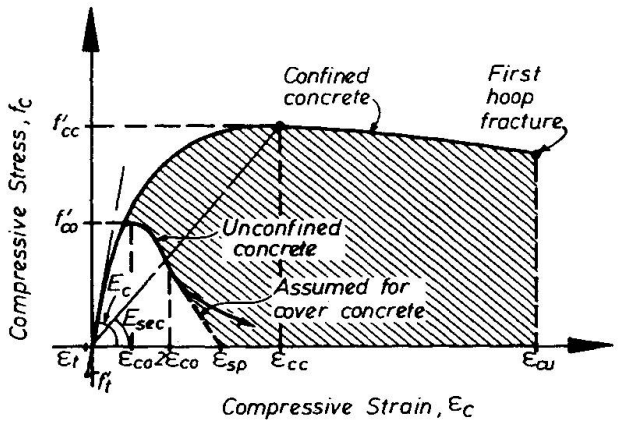

Fig.6 Typical Compressive Stress-Strain Curves for Confined and Unconfined Concrete [6]

5.3 Approach for Ductility Evaluation Based on a Limiting Concrete Compressive Strain

In the past, the maximum available (ultimate) curvature of a structural concrete member has usually been assumed to be reached when a specified "ultimate" compressive strain ε_{cu} has been attained by the concrete. Experimental research by a number of investigators has resulted in the development of several empirical equations for ε_{cu}. A difficulty with this approach is that ε_{cu} depends on several variables, including the ratio of neutral axis depth to member section depth, the shape of the compressed area of the member section, the confined concrete stress-strain relation and the steel stress-strain relation. It is difficult to include all the variables in an equation for ε_{cu}. Generally ε_{cu} values which have been proposed have resulted in conservative estimates of the ultimate curvature [1,5]. However the approach has the merit of simplicity, since the maximum available (ultimate) curvature can be readily calculated from $\phi_u = \varepsilon_{cu}/c$, where c is the neutral axis depth at that stage.

5.4 Approach for Ductility Evaluation Based on the Postpeak Moment-Curvature Behaviour

A more recent method imposes no limit on the concrete compression strain but seeks adequate moment-curvature behaviour. An example of this approach is that proposed by Zahn, et al [7]. Cyclic stress-strain relations for confined concrete were determined [6] which, along with cyclic stress-strain relations for reinforcing steel, permitted analytical predictions of the cyclic moment-curvature behaviour of reinforced concrete members. In addition, it was found that the longitudinal concrete compressive strain at first fracture of the transverse reinforcement could be estimated by energy considerations, by equating the increase in strain energy stored in the confined concrete (represented by the shaded area between the stress-strain curves for the unconfined and confined concrete in Fig.6) to that stored in the transverse reinforcing steel at fracture by tensile straining. These analytical procedures were used to determine the maximum available (ultimate) curvature of reinforced concrete columns containing various arrangements and quantitites of transverse reinforcement. To simulate the effect of severe earthquake loading, a sequence of four identical cycles of bending moment to peak curvatures of equal magnitude in each direction was imposed on the member. The peak curvature for which the moment reduced to 80% of the ideal moment capacity or for which fracture of the longitudinal or transverse reinforcement occurred, was defined as the maximum (available) ultimate curvature (see Fig.7). Design charts have been prepared which relate the maximum available curvature ductility factor ϕ_u/ϕ_y to the column axial load level and to the magnitude of the confining stress from the transverse reinforcement [7].

6. MECHANISMS OF SHEAR RESISTANCE

6.1 Shear Resistance in Plastic Hinge Regions

Tests [1] have demonstrated that cyclic flexure in plastic hinge regions of members can cause a degradation of the shear carried by the conventional shear resisting mechanisms. This is because full depth flexural cracks can exist in the plastic hinge regions, as well as inclined diagonal tension cracks, during much of the reversed loading range. This occurs because when longitudinal steel yields in tension for loading in one direction, open cracks will be present in the concrete "compression" zone when the load is applied in the opposite direction. These cracks will remain open until that steel yields in compression and allows the cracks to close and the concrete to carry some compression (see Fig.8). Thus for parts of the loading cycles the bending moment will be carried by a steel couple alone. If the shear stress at the section is high a sliding shear deformation can occur along a full depth vertical crack (see Fig.8) and the load-deflection hysteresis loops for the structure will show a strength and stiffness degradation.

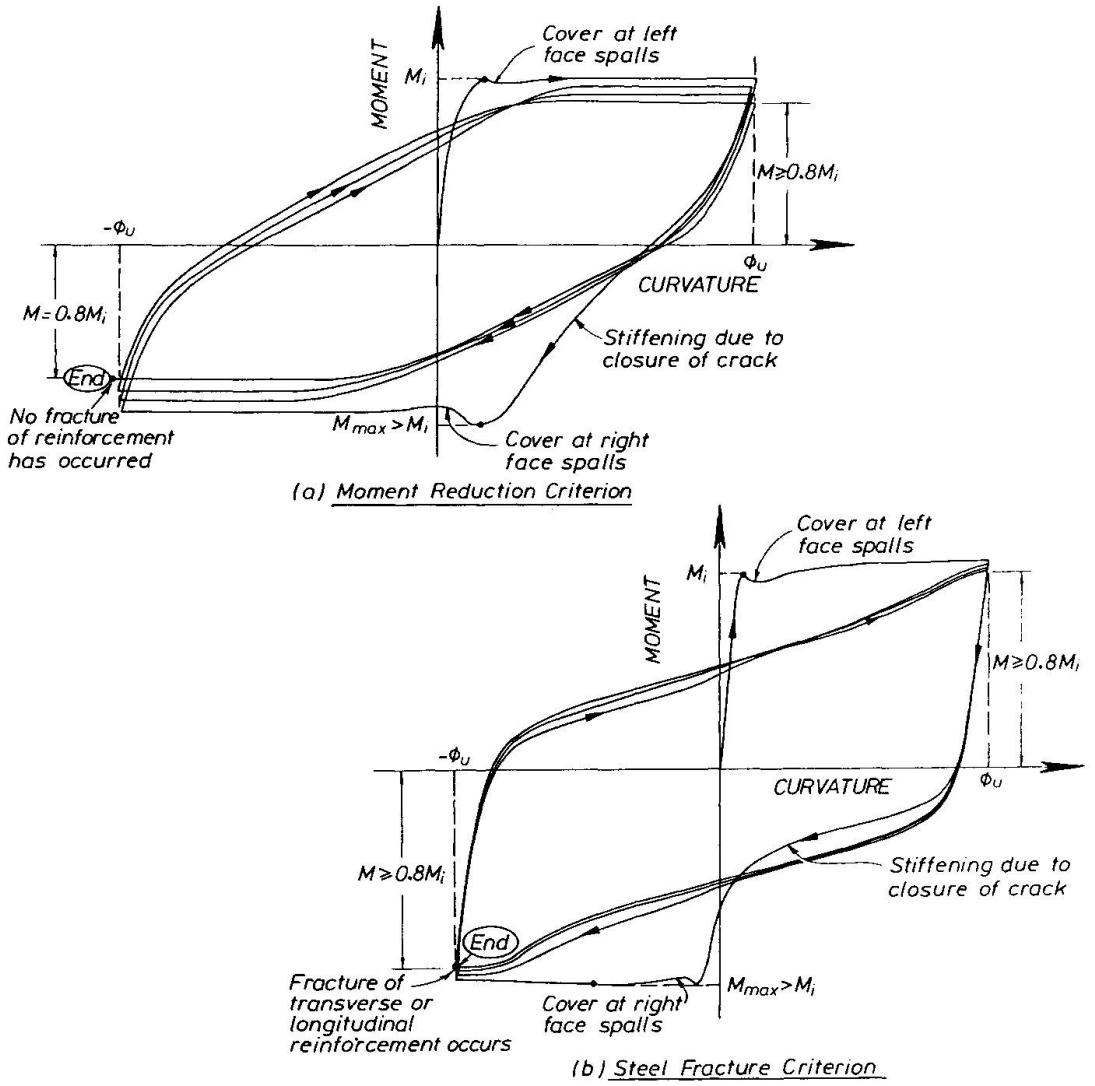

Fig.7 Ductility Evaluation Based on Postpeak Cyclic Moment-Curvature Analysis [7]

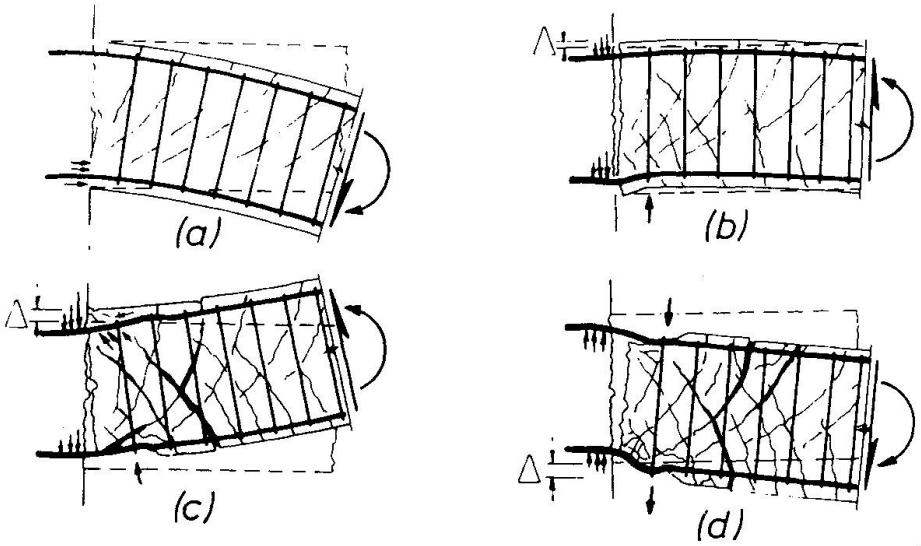

Fig.8 Significant Stages of Development of Deformations at a Plastic Hinge During Cyclic Flexure with High Shear [8]

6.2 Shear and Bond Resistance in Beam-Column Joints of Moment Resisting Frames

Beam-column joint cores can be subjected to extremely high shear and bond stresses when subjected to earthquake loading. If the beams and columns are detailed for adequate ductility the joint cores could become the critical regions of the structure unless also carefully designed. Fig. 9 illustrates an interior beam-column joint core which forms part of a moment resisting frame subjected to earthquake seismic loading. Consideration of the concrete and steel forces acting at the boundaries of the joint core indicates that, to satisfy the equilibrium requirements of the joint core there must be two mechanisms of joint core shear resistance [1], namely :

(a) a diagonal compression strut carrying the concrete compressive forces across the joint core.

(b) a truss mechanism of joint core reinforcement carrying the longitudinal bar forces across the joint core.

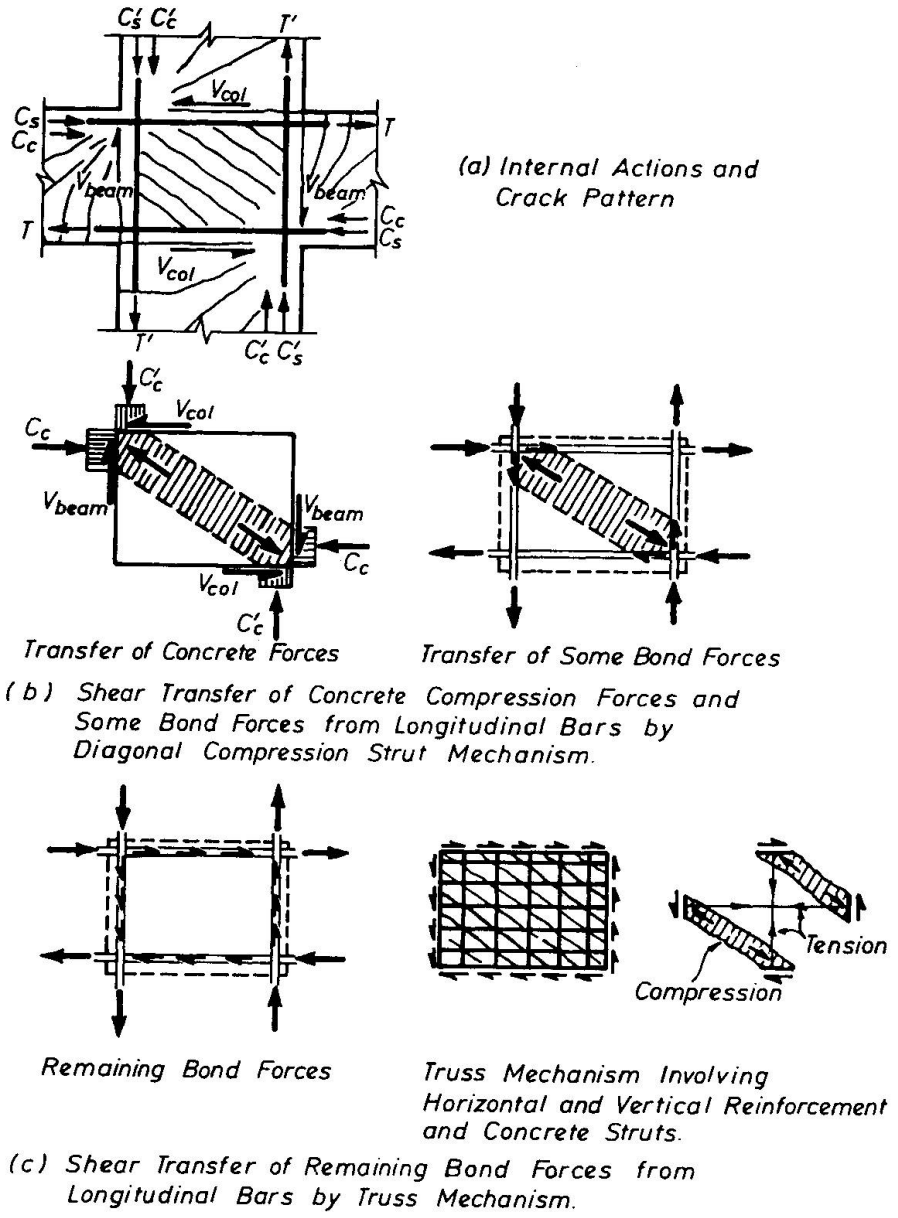

Fig.9 : Idealized Behaviour of a Reinforced Concrete Beam-Column Joint of a Moment Resisting Frame Subjected to Horizontal Loading [1]

It is evident that the truss mechanism requires the presence of both horizontal and vertical shear reinforcement and a diagonal concrete compression field in the joint core to satisfy the equilibrium requirements of the mechanism (see Fig.9c). This can be provided by horizontal column hoops and intermediate longitudinal column bars.

6.3 Strength and Stiffness Degradation Due to Shear and Bond Mechanisms

Significant postelastic deformations due to shear or bond mechanisms lead to severe degradation of strength and stiffness and to pinched hysteresis loops with reduced energy dissipation. Fig.10 shows typical measured experimental load-displacement hysteretic behaviour of two reinforced concrete beam-column assemblies, one controlled by ductile flexural plastic hinging in the beams (Fig.10a) and the other controlled eventually by bond slip of longitudinal beam bars through the joint core (Fig.10b), and a structural wall controlled by shear mechanisms (Fig.10c).

The extent to which shear and bond should be permitted to participate in the hysteretic behaviour is still a controversial matter. Although some variations in hysteresis loop shape may not be a major influence on the postelastic dynamic response of structures subjected to earthquake excitation, there is no doubt that it is much easier to repair flexural damage occurring at a well detailed plastic hinge in a member than to repair damage resulting from inelastic shear and bond mechanisms. Earthquake design codes in New Zealand [3,4] use the capacity design procedure to ensure that yielding of longitudinal flexural reinforcement occurs rather than inelastic shear and bond mechanisms.

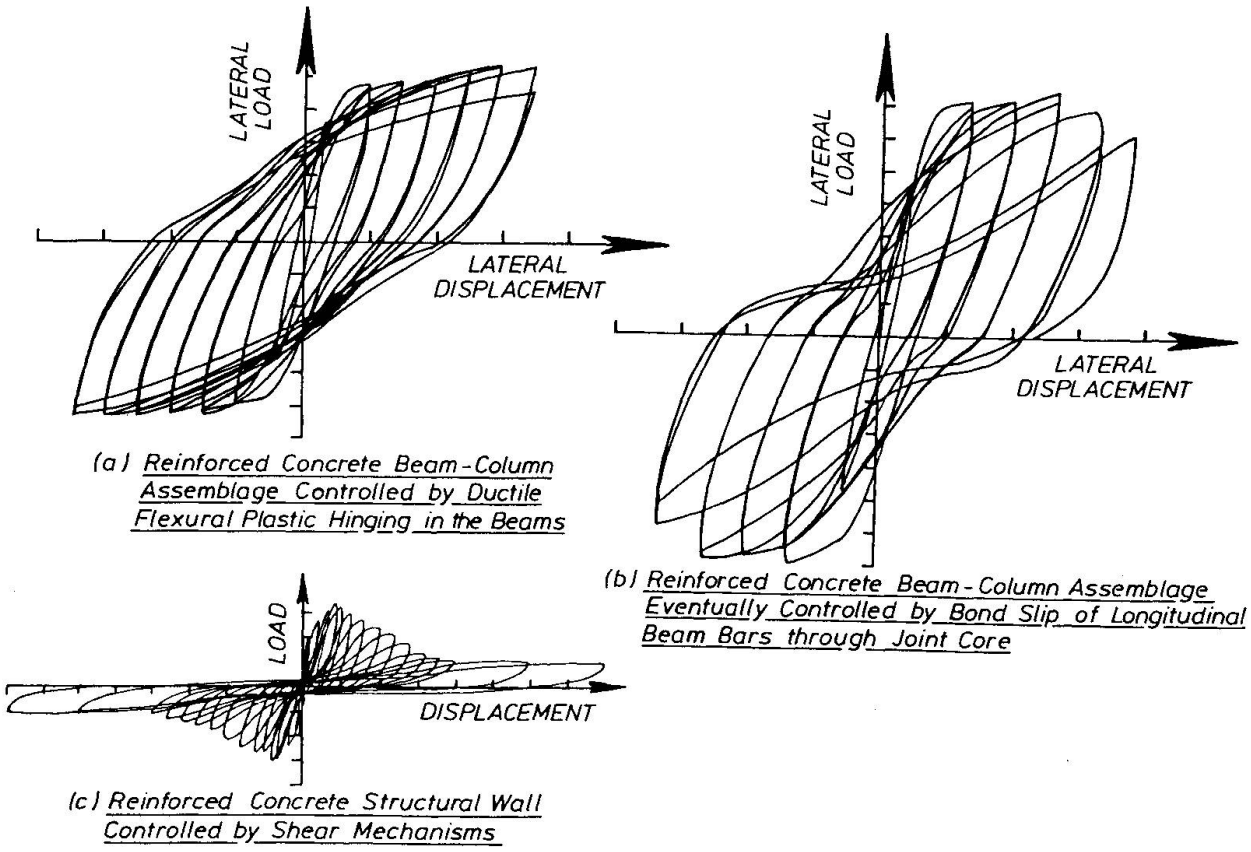

(a) Reinforced Concrete Beam-Column Assemblage Controlled by Ductile Flexural Plastic Hinging in the Beams

(b) Reinforced Concrete Beam-Column Assemblage Eventually Controlled by Bond Slip of Longitudinal Beam Bars through Joint Core

(c) Reinforced Concrete Structural Wall Controlled by Shear Mechanisms

Fig.10 - Typical Measured Hysteresis Loops for Reinforced Concrete Subassemblages

7. CONCLUSIONS

1. Evaluations of ductility have sometimes been confusing in the past due to the various possible definitions for the yield deformation and the maximum available (ultimate) deformation. It is suggested that the yield deformation should be estimated from an equivalent elastoplastic system with elastic stiffness which includes the effects of cracking and with the same ultimate load as the real system. The maximum available (ultimate) deformation should be estimated as that postpeak deformation when load has reduced by a small specified amount, or when the reinforcement fractures or buckles, whichever occurs first.

2. The ductility of concrete structures required for earthquake resistance is best achieved by ensuring in design that it occurs by flexural yielding of plastic hinges. The longitudinal reinforcing steel should have a suitably large elongation at fracture and should be adequately restrained by transverse reinforcement so as to avoid premature buckling. The ductility and strength of compressed concrete can be significantly improved by the presence of well detailed arrangements of transverse reinforcement. The stress-strain relation of confined concrete can be written as a function of the quantity and arrangement of transverse reinforcement. Analytical procedures are available to determine the quantity of transverse reinforcement required to achieve specified levels of curvature ductility.

3. In the design of ductile structures for earthquake resistance, failure modes to be prevented are those due to diagonal tension or diagonal compression caused by shear, excessive plastic hinge rotation of heavily loaded columns, sliding shear along jointing faces or in plastic hinge regions, and bond failures along longitudinal reinforcement. All of these undesirable failure modes lead to premature strength degradation and reduced ductility and can be avoided by use of the capacity design procedures.

8. REFERENCES

1. PARK, R. and PAULAY, T., "Reinforced Concrete Structures", John Wiley, New York, 1975, 769 pp.
2. PARK, R., "State-of-the-Art Report : Ductility Evaluation from Laboratory and Analytical Testing", Proceedings of the 9th World Conference on Earthquake Engineering, Vol.8, Tokyo-Kyoto, August 1988, pp.605-616.
3. "Code of Practice for General Structural Design and Design Loadings for Buildings, NZS 4203:1984", Standards Association of New Zealand, Wellington, 1984, 100 pp.
4. "Code of Practice for the Design of Concrete Structures, NZS 3101:1982", Standards Association of New Zealand, Wellington, 1982, 127 pp.
5. M.J.N. PRIESTLEY and R. PARK, " Strength and Ductility of Concrete Bridge Columns Under Seismic Loading", Structural Journal of American Concrete Institute, Vol.84, No.1, January-February 1987, pp 61-76.
6. J.B. MANDER, M.J.N. PRIESTLEY, and R. PARK, "Theoretical Stress-Strain Model for Confined Concrete", Journal of Structural Engineering, American Society of Civil Engineers, Vol.114, No.8, August 1988, pp.1804-1826.
7. F.A. ZAHN, R. PARK, M.J.N. PRIESTLEY, and H.E. CHAPMAN, "Development of Design Procedures for the Flexural Strength and Ductility of Reinforced Concrete Bridge Columns", Bulletin of New Zealand National Society for Earthquake Engineering, Vol.19, No.3, September 1986, pp.200-212.
8. T. PAULAY, "Developments in Seismic Design of Reinforced Concrete Frames in New Zealand", Canadian Journal of Civil Engineering, Vol.8, No.2, June 1981, pp.91-113.

A Consistent Shear Design Model

Modèle cohérent de dimensionnement à l'effort tranchant

Ein konsistentes Schubbemessungsverfahren

Michael P. COLLINS
Professor
Univ. of Toronto
Toronto, ON, Canada

Frank J. VECCHIO
Associate Professor
Univ. of Toronto
Toronto, ON, Canada

Perry ADEBAR
Assistant Professor
Univ. of British Columbia
Vancouver, BC, Canada

Denis MITCHELL
Professor
McGill Univ.
Montreal, PQ, Canada

SUMMARY

A shear model is presented which takes into account residual tensile stresses in cracked concrete. The model treats both prestressed and non-prestressed members and accounts for the influence of amount of longitudinal reinforcement, magnitude of moment, axial force and member size.

RÉSUMÉ

Un modèle de dimensionnement à l'effort tranchant qui tient compte des contraintes de traction résiduelles dans le béton fissuré est présenté dans cet article. Il traite des éléments de structure précontraints et non-précontraints et tient compte de l'influence de la quantité d'armature longitudinale, de l'intensité du moment, de la force axiale et de la taille de l'élément-même de structure.

ZUSAMMENFASSUNG

Ein Schubbemessungsverfahren wird beschrieben, das Zugeigenspannungen in gerissenem Beton berücksichtigt. Das Verfahren behandelt sowohl vorgespannte wie auch nicht vorgespannte Elemente und berücksichtigt solche Grössen wie Längsbewehrung, Biegemomente, Axiallasten und Bauteilgrössen.

1. INTRODUCTION

In 1973 the ACI-ASCE Shear Committee [1] concluded the introduction to its state-of-the-art report with the words:

> During the next decade it is hoped that the design regulations for shear strength can be integrated, simplified and given a physical significance ...

The shear provisions of the 1984 Canadian Concrete Code [2, 3], which were based on the compression field model, introduced both strain compatibility and the stress-strain characteristics of diagonally cracked concrete, enabling some of the objectives stated above to be achieved. However, because this model neglected the residual tensile stresses in diagonally cracked concrete, it was restricted to members with shear reinforcement.

The modified compression field model [4] considers the influence of residual tensile stresses in the cracked concrete and hence provides the basis for a consistent shear design model. In this paper a design approach based on the modified compression field theory is presented.

2. RESIDUAL TENSILE STRESSES IN CRACKED CONCRETE

Tests of reinforced concrete panels subjected to pure shear [4] demonstrated that even after cracking, tensile stresses exist in the concrete between the cracks and that these stresses can significantly increase the ability of reinforced concrete to resist shear stresses.

Cracked reinforced concrete transmits load in a relatively complex manner involving opening or closing of pre-existing cracks, formation of new cracks, interface shear transfer at rough crack surfaces, and significant variation of the stresses in reinforcing bars due to bond, with the highest steel stresses occurring at crack locations. The modified compression field model attempts to capture the essence of this behaviour without considering all of the details. The crack pattern is idealized as a series of parallel cracks all occurring at angle θ to the longitudinal direction. In lieu of following the complex stress variations in the cracked concrete, only the average stress state and the stress state at a crack are considered. As these two states of stress are statically equivalent, the loss of tensile stresses in the concrete at the crack must be replaced by increased steel stresses or, after yielding of the reinforcement at the crack, by shear stresses on the crack interface. The shear stress that can be transmitted across the crack will be a function of the crack width. Note that shear stress on the crack implies that the direction of principal stresses in the concrete changes at the crack location.

The average principal tensile strain, ϵ_1, in the cracked concrete is used as a "damage indicator" which controls the average tensile stress, f_1, in the cracked concrete, the ability of the diagonally cracked concrete to carry compressive stresses, f_2, and the shear stress, v_{ci}, that can be transmitted across a crack.

3. SHEAR DESIGN OF BEAMS

In applying the modified compression field theory to the design of beams it is appropriate to make a number of simplifying assumptions. As illustrated in Fig. 1, the shear stresses are assumed to be uniform over the effective shear area, $b_w\, jd$. The highest longitudinal strain, ϵ_x, within the effective shear area is used to calculate the principal tensile strain, ϵ_1.

The longitudinal strain, ϵ_x, can be determined from a plane sections analysis (see computer program "RESPONSE" [5]) which accounts for the influence of axial load, moment, and shear. For design, ϵ_x can be approximated as the strain in the "bottom chord" of a truss as

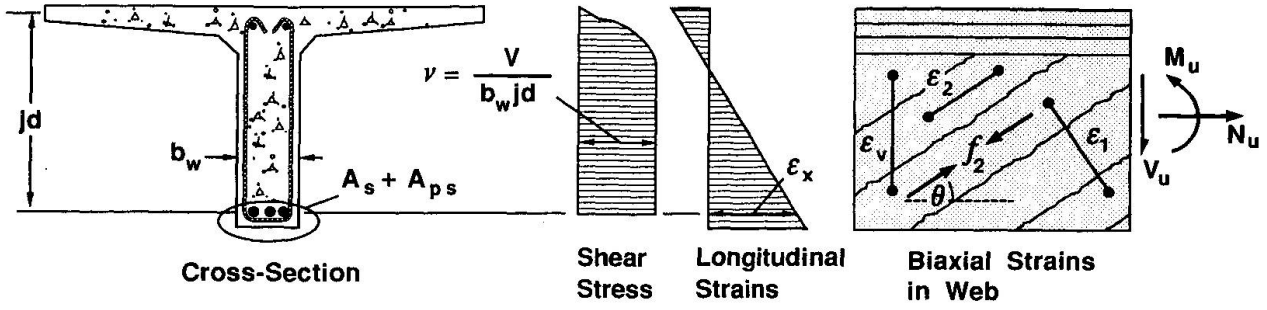

Fig. 1 Beam subjected to shear, moment, and axial load.

$$\epsilon_x = \frac{(M_u/jd) + 0.5N_u + 0.5V_u \cot\theta - A_{ps}f_{se}}{E_s A_s + E_p A_{ps}} \geq 0 \tag{1}$$

where A_s and A_{ps} are the areas of non-prestressed and prestressed longitudinal reinforcement on the flexural tension side of the member.

From strain compatibility, the principal tensile strain, ϵ_1, can be related to the longitudinal compressive stress and the magnitude of the principal compressive strain, ϵ_2, in the following manner:

$$\epsilon_1 = \epsilon_x + (\epsilon_x - \epsilon_2)\cot^2\theta \tag{2}$$

Hence as the longitudinal strain, ϵ_x, becomes larger and the inclination, θ, of the principal compressive stresses becomes smaller, the "damage indicator", ϵ_1, becomes larger.

For design purposes the shear strength, V_u, of a member can be expressed as

$$\begin{aligned} V_u &= V_c + V_s + V_p \\ &= \beta\sqrt{f'_c}\,b_w\,jd + \frac{A_v f_y}{s}jd\cot\theta + V_p \end{aligned} \tag{3}$$

where V_c = shear strength provided by residual tensile stresses in the cracked concrete
V_s = shear strength provided by tensile stresses in the stirrups
V_p = vertical component of force in the prestressing tendons.

The values of θ and β, determined by the modified compression field model are given in Table 1 for members with web reinforcement and in Table 2 for members without web reinforcement.

The tabulated values of the residual tensile stress factor, β, are based on the following expressions:

$$\beta = \frac{0.18}{0.3 + \dfrac{24w}{a+16}} \tag{4}$$

but

$$\beta \leq \frac{0.33\cot\theta}{1 + \sqrt{500\epsilon_1}} \tag{5}$$

Equation (4) is based on the shear stress that can be transmitted across diagonal cracks and hence is a function of the crack width, w, and the maximum aggregate size, a. The crack width is assumed

v/f'_c		Longitudinal Strain $\epsilon_x \times$ 1000				
		0	0.5	1.0	1.5	2.0
≤ 0.05	β	0.437	0.251	0.194	0.163	0.144
	θ	28°	34°	38°	41°	43°
0.10	β	0.226	0.193	0.174	0.144	0.116
	θ	22°	30°	36°	38°	38°
0.15	β	0.211	0.189	0.144	0.109	0.087
	θ	25°	32°	34°	34°	34°
0.20	β	0.180	0.174	0.127	0.090	0.093
	θ	27°	33°	34°	34°	37°
0.25	β	0.189	0.156	0.121	0.114	0.110
	θ	30°	34°	36°	39°	42°

Table 1 Values of β and θ for members with web reinforcement.

z mm		Longitudinal Strain $\epsilon_x \times$ 1000				
		0	0.5	1.0	1.5	2.0
125	β	0.406	0.263	0.214	0.183	0.161
	θ	27°	32°	34°	36°	38°
250	β	0.384	0.235	0.183	0.156	0.138
	θ	30°	37°	41°	43°	45°
500	β	0.359	0.201	0.153	0.127	0.108
	θ	34°	43°	48°	51°	54°
1000	β	0.335	0.163	0.118	0.095	0.080
	θ	37°	51°	56°	60°	63°
2000	β	0.306	0.126	0.084	0.064	0.052
	θ	41°	59°	66°	69°	72°

Table 2 Values of β and θ for members without web reinforcement.

to equal $\epsilon_1 s_{m\theta}$ where $s_{m\theta}$ is the average spacing of the diagonal cracks. Equation (5) is based on the average residual tensile stress in cracked concrete that has a cracking stress of $0.33\sqrt{f'_c}$. See Reference 5 for more details.

In determining the values in Tables 1 and 2 it was assumed that the crack spacing, $s_{m\theta}$, equalled about 300 mm for members containing web reinforcement while, for members without web reinforcement, the spacing of diagonal cracks was assumed to be $s_{mx}/\sin\theta$ where s_{mx} is given in Fig. 2.

To avoid yielding of the longitudinal reinforcement

$$A_s f_y + A_{ps} f_{ps} \geq \frac{M_u}{jd} + 0.5N_u + (V_u - 0.5V_s - V_p)\cot\theta \tag{6}$$

4. INFLUENCE OF MEMBER SIZE

It has been shown [6] that the modified compression field theory can predict the shear capacity of members containing web reinforcement with reasonable accuracy (coefficients of variation about 10%). The influence of axial tension on the shear capacity of members not containing web reinforcement is also predicted accurately (COV 11%) [7].

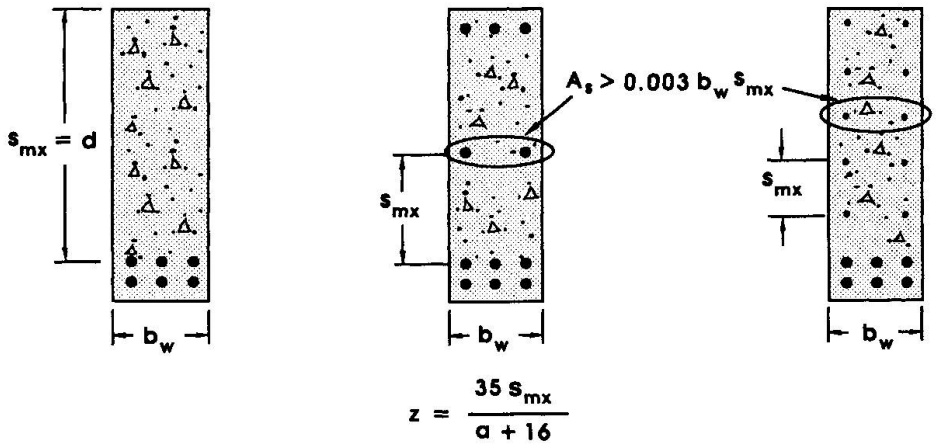

Fig. 2 Crack spacing parameter z.

For the purpose of this colloquium it is of particular interest to discuss the influence of member size upon the shear strength of members not containing web reinforcement. For members not containing crack control reinforcement (Fig. 2), as member size increases the crack spacing, $s_{m\theta}$, will increase and hence, for a given value of strain, ϵ_1, the crack width will increase. An increase in crack width reduces the shear stress that can be transmitted across the crack and hence reduces the shear strength of the member. It can be seen from Table 2 that members containing large amounts of longitudinal reinforcement or prestressed concrete members (i.e., members with low values of ϵ_x) will be less sensitive to member size than lightly reinforced members or members subjected to high moments (i.e., members with high values of ϵ_x). Thus if ϵ_x equals 0 the shear stress at failure increases by a factor of 1.33 as the size decreases by a factor of 16, while if ϵ_x equals 0.002 the shear stress increases by a factor of 3.10.

Figure 3 compares the observed shear stresses at failure for a series of lightly reinforced beams with depths ranging from 200 mm to 3000 mm [8]. Also shown are the shear stresses at failure predicted from the β values in Table 2. It can be seen that the theory predicts the strength of the larger beams very well, but is somewhat conservative for the smallest beam.

5. CONCLUDING REMARKS

The amount of stirrups required to resist a given shear, V_u, can be determined from

$$\frac{A_v f_y}{s} \cdot jd \geq \left(V_u - \beta\sqrt{f'_c} b_w jd - V_p\right) \tan\theta \qquad (7)$$

where both β and θ depend on the longitudinal strain parameter, ϵ_x, which accounts for the influence of moment, axial load, prestressing, and longitudinal reinforcement ratios. In addition, for members without web reinforcement, β and θ are strongly dependent on member size.

The sectional design model summarized above is appropriate for those regions of structures where it is reasonable to assume that plane sections remain plane. In regions where there are substantial static or geometric discontinuities, it is more appropriate to use strut-and-tie design models (see Reference 5).

ACKNOWLEDGEMENT

The long-term research program that resulted in the design method summarized in this paper was made possible by a series of grants from the Natural Sciences and Engineering Research Council of Canada. This continuing support is gratefully acknowledged.

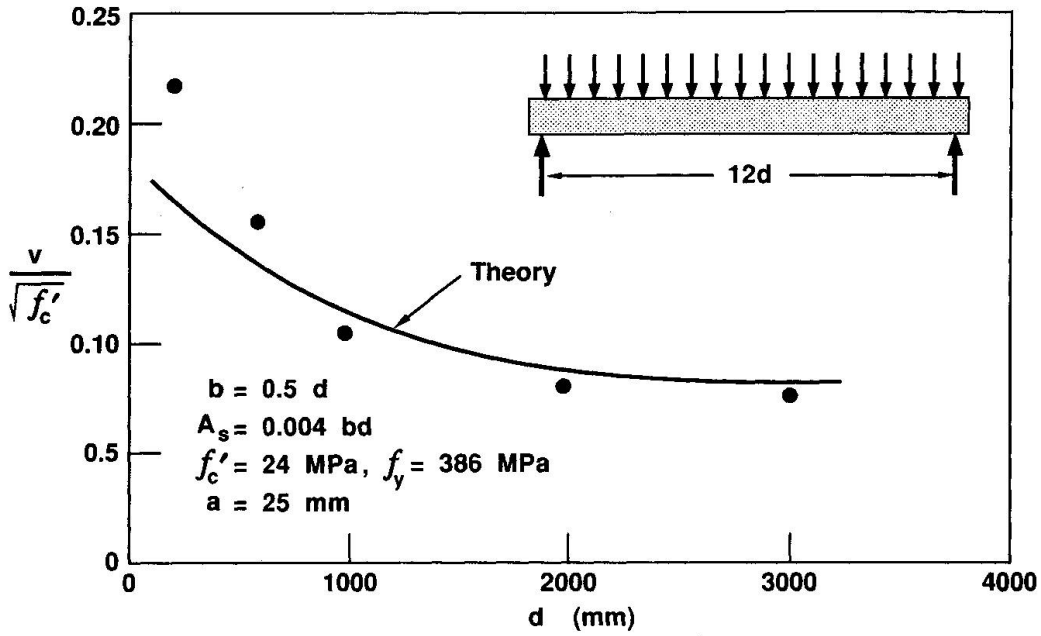

Fig. 3 Comparison of predicted and observed shear stress at failure on section distance d from the support.

REFERENCES

1. ACI-ASCE Committee 426, Shear Strength of Reinforced Concrete Members. Journal of the Structural Division, ASCE, Vol. 99, No. ST6, June 1973.
2. CSA Committee A23.3, Design of Concrete Structures for Buildings, CAN3-A23.3-M84. Canadian Standards Association, Rexdale, Canada.
3. Collins, M.P., and Mitchell, D., Rational Approach to Shear Design – The 1984 Canadian Code Provisions. ACI Journal, Vol. 83, No. 6, Nov./Dec. 1986.
4. Vecchio, F.J., and Collins, M.P., Modified Compression Field Theory for Reinforced Concrete Elements Subjected to Shear. ACI Journal, Vol. 83, No. 2, Mar./Apr. 1986.
5. Collins, M.P., and Mitchell, D., Prestressed Concrete Structures, Prentice Hall, Englewood Cliffs, N.J., 1991.
6. Vecchio, F.J., and Collins, M.P., Predicting the Response of Reinforced Concrete Beams Subjected to Shear Using Modified Compression Field Theory. ACI Structural Journal, Vol. 85, No. 3, May/June 1988.
7. Bhide, S.B., and Collins, M.P., Influence of Axial Tension on the Shear Capacity of Reinforced Concrete Members. ACI Structural Journal, Vol. 86, No. 5, Sept./Oct. 1989.
8. Shioya, T., Shear Properties of Large Reinforced Concrete Members. Special Report of Institute of Technology, Shimizu Corporation, No. 25, Feb. 1989.

Strut-Tie Approach in Higher Strength Concrete Members

Analogie du treillis pour éléments de structures en béton à très haute résistance

Bemessung von Bauteilen aus hochfestem Beton mit Stabwerkmodellen

Julio A. RAMIREZ
Assoc. Prof.
Purdue Univ.
West Lafayette, IN, USA

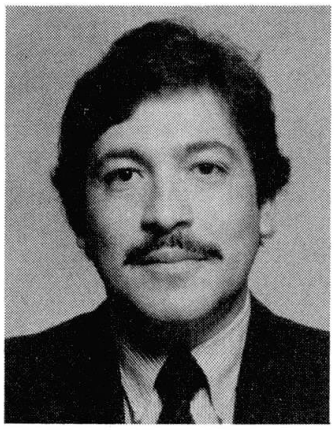

Julio A Ramirez, born 1955, received his Ph.D. in Civil Engineering from the University of Texas at Austin. Dr. Ramirez is a member of the joint ACI-ASCE Committee 445, Shear and Torsion, and the ACI Committee 408, Bond and Development of Reinforcement.

SUMMARY

The different engineering properties observed in higher-strength concretes clearly indicate the need for further basic information on the behaviour of higher-strength structural concrete. This paper makes an immediate contribution with regard to both, performance of higher-strength structural concrete and the use of strut-tie models.

RÉSUMÉ

Les différentes caractéristiques techniques que l'on observe dans les bétons à très haute résistance indiquent clairement la nécessité d'obtenir de plus amples renseignements sur le comportement de structures réalisées de la sorte. Cet article apporte donc une contribution immédiate en ce qui concerne à la fois les performances du béton à très haute résistance et l'application de modèles d'analogie du treillis.

ZUSAMMENFASSUNG

Die besonderen Materialeigenschaften von hochfesten Betonen zeigen die Notwendigkeit grundlegender Untersuchungen über das Tragverhalten von hochfestem Konstruktionsbeton. Es wird vorgeschlagen, die Methode der Stabwerkmodelle, die im Stahl- und Spannbeton eingesetzt wird, auch für die Erforschung von hochfestem Konstruktionsbeton einzusetzen.

STRUT-TIE MODEL

Strut-tie models can be formulated from experimental observations using failure crack patterns, recorded strains in the concrete and the reinforcement, together with actual specimen detailing, loading and support conditions. In design much of this information is not readily available. However, for simple everyday designs an experienced engineer is generally capable of developing strut-tie models based on common engineering sense and knowledge of the behavior of structural concrete. In the more complex design situations, this practical knowledge is often not enough to develop safe and efficient strut-tie models. In such cases, Schlaich et. al [1] suggest that the load-path method can be aided using the principal stress trajectories based on a linear elastic analysis of the structure. The principal compressive stress trajectories can be used to select the orientation of the strut members of the model. The strut-tie model can then be completed by placing the tie members so as to furnish a stable load-carrying structure.

The strut-tie approach for higher-strength concrete members is illustrated with the analysis of a pretensioned beam, specimen I-4A. This specimen was tested to failure using a point load system [2]. The detailing of the specimen is shown in Figure 1, and the material properties are given in Table 1. The strut-tie model for specimen Type I-4A shown in Figure 2(a), is developed first by placing the strut members in the direction of the principal compressive stress trajectories. Next, the vertical ties of the model are placed at the stirrup locations and the horizontal tie is located at the centroid of the strand pattern. In deep beams the usual assumption of linear distribution of strains over the depth of the section is not adequate. The capacity of this type of member in either flexure or shear depends heavily on the detailing of loading and support. This component of the load carrying mechanism, in the form of an inclined strut going from the support to the point load, is clearly shown in the failure crack pattern in Fig. 1.

The development of a strut-tie model is an iterative process because the widths of the struts and the size of the nodes depend on the forces in the struts and ties. A computer program has been developed at Purdue University to help carry out this process [3]. Initially, the truss model is laid out using the centerline dimensions of the strut and tie members. The effects of the prestressing are represented by the equivalent horizontal loads of 310.3^{k} (1380.2 kN) and 74.6^{k} (331.8 kN) shown in Figure 2(a). For the failure load analysis the maximum load of 323^{k} (1436.7 kN) is applied to the strut-tie model and a preliminary analysis is conducted to determine the internal forces in the individual members of the model. Next, the strut members are dimensioned using allowable compressive stresses checking that the resultant dimensions are compatible with the actual geometric constraints of the specimen. The resultant strut-tie model with finite dimensions for the strut members and nodal zones (Fig. 2b) is then analyzed for the applied load and the external forces representing the effects of prestressing. The equivalent prestressing load applied to the tension chord of the strut-tie model is updated by adding to it the force in the tie member next to the support resulting from a first analysis of the model with finite width for the initial prestress force and ultimate load. Finally, the forces in the horizontal tie member obtained from the analysis of the strut-tie model with finite width members for the applied maximum load and updated equivalent prestressing load must be added to the additional tension force calculated from the initial prestressing in order to obtain the actual tension force in the strands at ultimate load. The resultant analysis forces in the vertical ties of the model can be used directly to calculate the required tension force in the transverse reinforcement (stirrups). Next, the principal stresses in the critical nodal zones are determined using the stresses and the geometry of the individual members framing the nodes. This procedure is illustrated in the following section with the test results of specimen I-4A.

EXPERIMENTAL EVALUATION

In the determination of the strut widths of the model for beam I-4A, the compressive stress levels used were $0.9f'_c$ for the diagonals going from the point load to the support, $0.3f'_c$ for all other strut members, and $0.5f'_c$ for the upper compression members. The selection of the stress levels is an iterative process where the measured forces in the strands at the locations shown in Figure 1 were used to refine the estimates. The geometry of the strut-tie model based on the stress levels mentioned above resulted in the calculated forces shown in Table 2. The calculated strand forces were determined using the procedure outlined in the previous section. As can be seen from Table 2, a tension force of 36 kips must be properly anchored at the support. In specimen I-4A a 2 ft. (609.6 mm) overhang on the N-side and more than 2 ft on the S-side was provided to ensure proper anchorage. At failure, no slippage of the strands was observed. The calculated forces at failure in the vertical tension ties of the strut-tie model indicated yielding of this reinforcement. This was confirmed by the strain measurements in the instrumented stirrups. First diagonal cracking in specimen I-4A occurred at a load of 236^k (1049.7 kN) yielding of the stirrup reinforcement was observed immediately after first cracking; however, no stirrup fracture was noted at failure. Failure in specimen I-4A occurred due to crushing of the concrete under the point load followed by crushing of the web section on S-side as shown by the failure crack pattern in Fig. 1. The size of the critical nodal zone under the point load is controlled by the dimensions of the struts framing into it as well as the dimensions of the bearing plate and the width of the specimen. Once the geometry was determined, a finite element analysis was carried out to determine the principal stresses. After an element grid has been laid out in the nodal zone, the axial forces in the individual struts and applied load are discretized into their components parallel and normal to the boundaries of the nodal zone and applied as concentrated loads at the nodes of the elements bordering each strut and the loading plate. Figure 3 shows the chosen finite element grid and applied boundary forces for the portion of the nodal zone where failure was observed. The results of the analysis indicated a state of biaxial compression for most of the nodal zone and a maximum principal compressive stress of 9.76 ksi (67.3 MPa) at element 90, matching the region where failure occurred.

CONCLUSIONS

The use of increased concrete strengths would produce stronger nodal zones and strut members. If the strut-tie mechanism is properly developed this would result in improved ultimate capacity. Hence, adequate detailing of the member is further emphasized with the use of higher-strength concretes. In deep beams the ultimate capacity in either flexure or shear depends heavily on the strength of the main diagonal strut and the proper detailing of loading and support regions. The loading plate determines one of the dimensions of the nodal zone under the point load and at the support, thus affecting the state of stress at the node. Proper anchorage at the support region of the longitudinal tension reinforcement is also critical for the development of the strut-tie mechanism. Although not so critical for deep beams, in more slender members with low amounts of shear reinforcement the use of higher-strength concrete could jeopardize the formation of an adequate strut-tie mechanism upon first diagonal tension cracking. Because of the increased shear force to be transferred at the onset of first diagonal tension cracking and the possible reduction of aggregate interlock contribution the higher shear force to be transferred upon diagonal cracking could cause the first mobilized stirrups to yield and rupture.

REFERENCES

1. Schlaich, J., Schafer, I., and Jennewein, M., "Towards a Consistent Design of Structural Concrete," *Journal of the Prestressed Concrete Institute*, Vol. 32, No. 3, May-June 1987, pp. 74-150.
2. Kaufman, M.K., and Ramirez, J.A., "Re-evaluation of the Ultimate Shear Behavior of High-Strength Concrete Prestressed I-Beams," *ACI Structural Journal*, V. 85, No. 3, May-June 1988, pp. 295-303.
3. Alshegeir, A., and Ramirez, J.A., "Analysis of Disturbed Regions with STRUT-TIE Models," Structural Engineering Research Report No. CE-STR-90-1, Purdue University, West Lafayette, IN, January 1990, 85 pp.

Table 1 - Type I-4A Information

TYPE I - 4A

Geometry:		Concrete:	Transfer	Test
Beam Length (ft)	17	f'_c (psi)	5840	8810
Test Span (ft)	10	E_c (ksi)	5620	5930
Shear Span, a (ft)	5	f_r (psi)	920	-
$\frac{a}{d_p}$	2.35			

Prestressing Strand:	Top	Bottom
Grade	270	270
A_{ps} (in^2)	0.1633	0.1633
d_p,d_p (in)	2.00	26.00
E_{ps} (ksi)	27920	27920
f_{pu} (ksi)	282.0	282.0
f_{si} (ksi)	207.6	193.3
f_{se} (ksi)	199.9	187.8
P_{e1},P_{e2} (kips)	65.3	245.4

Mild Reinforcement:	#5 Bar	#4 Bar
Grade	60	40
A'_s, A_v (in^2)	0.31	0.19
d', rf_y (in, psi)	2.00	165
E_s (ksi)	29020	29500
f_y (ksi)	64	52

SI Equivalents

1 in = 25.4 mm
1 in^2 = 645.2 mm^2
l lb = 4.448N
1 psi = 0.006895 MPa

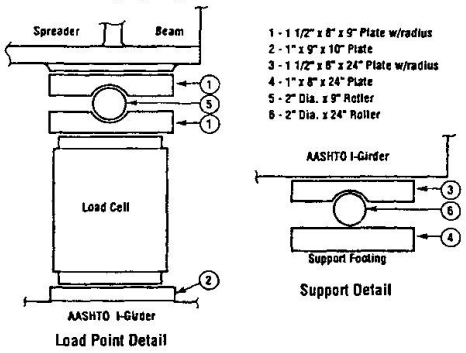

Table 2. Measured and Predicted Strand Forces (kips) for P = 323 kips

Gage #	14	13	12	11	10
Measured	36	39.03	41.75	42.48	36.7
Predicted	35.37	38.16	40.72	41.32	36.91

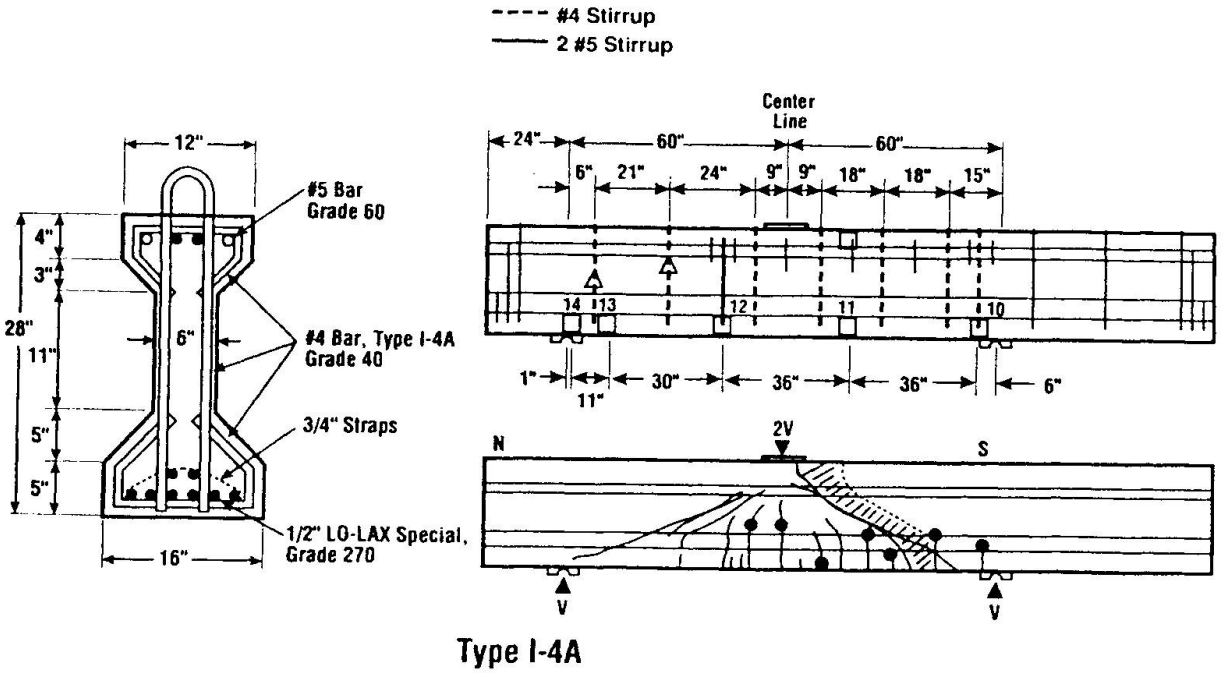

Fig. 1. Detailing and Failure Crack Pattern of I-4A.

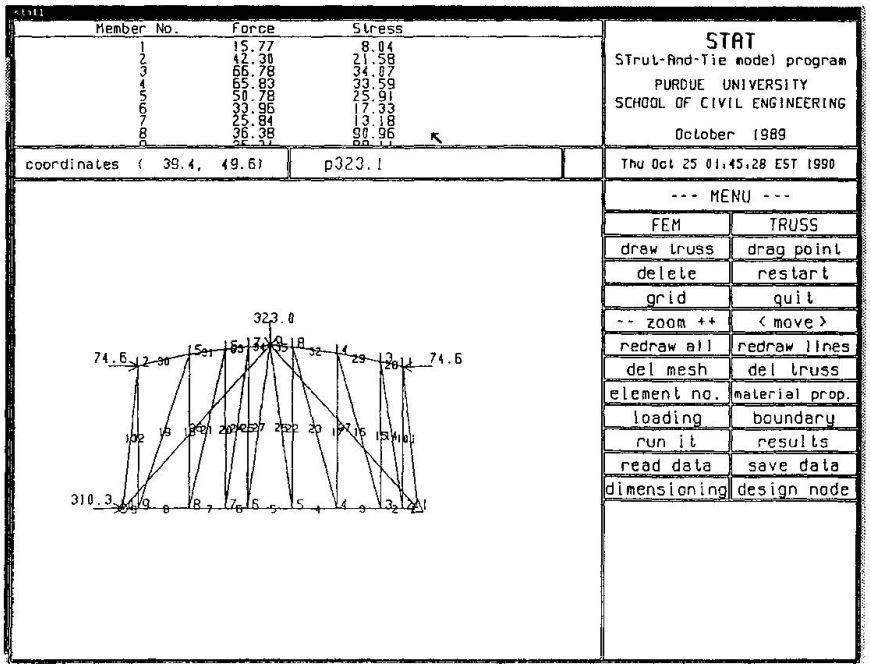

Fig. 2(a). Centerline Dimension Strut-Tie Model

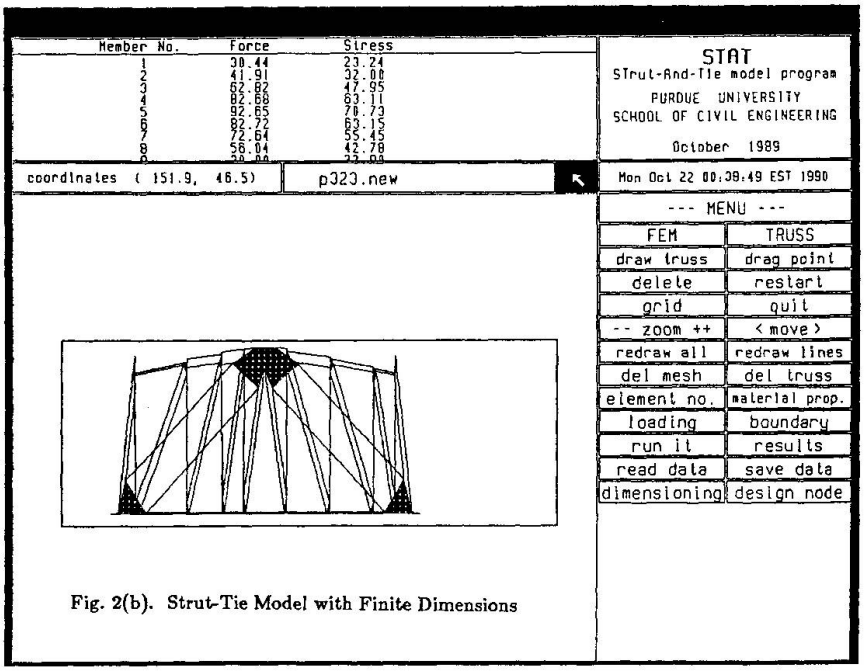

Fig. 2(b). Strut-Tie Model with Finite Dimensions

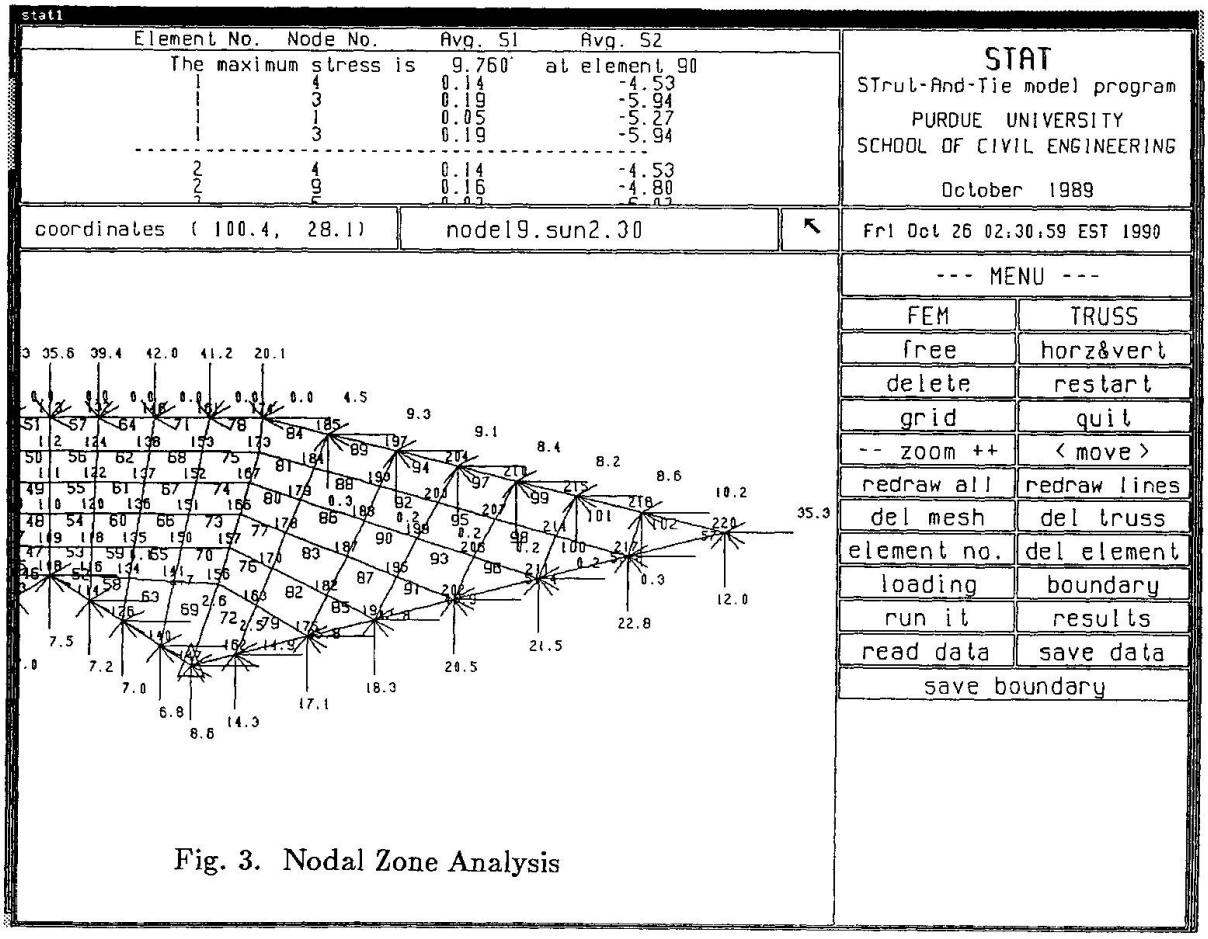

Fig. 3. Nodal Zone Analysis

Design Approaches for Shear Reinforcement in Concrete Beams

Détermination de l'armature à l'effort tranchant

Ermittlung der Schubbewehrung von Betonbalken

Wolfgang MOOSECKER
Prof. Dr.
Fachhochschule Giessen
Giessen, Germany

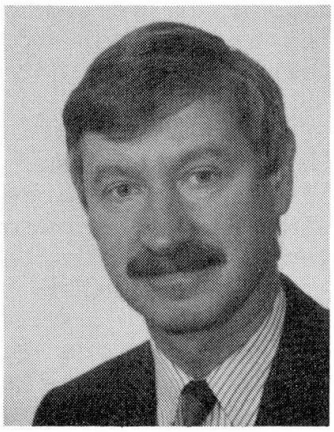

W. Moosecker, born 1948, graduated from Techn. Univ. München and Univ. of Calif. Berkeley. He was a consulting engineer in Krumbach, Germany from 1982 to 1988.

SUMMARY

Most recent approaches to a rational design of shear reinforcement for reinforced concrete beams are formulated in terms of equilibrium of stress fields and compatibility of corresponding strain fields. The review points out common features and differences of these approaches.

RÉSUMÉ

Plusieurs nouvelles méthodes de détermination rationnelle de l'armature à l'effort tranchant des poutres en béton armé sont dérivées de l'équilibre des champs de contraintes et de la compatibilité du champ de déformations correspondant. Les points communs ou divergents de ces méthodes sont successivement traités.

ZUSAMMENFASSUNG

Die meisten neueren Ansätze zur rationalen Bemessung der Schubbewehrung von Stahlbetonträgern sind auf der Grundlage des Gleichgewichtes von Spannungsfeldern und der Verträglichkeit der zugehörigen Dehnungen abgeleitet. Der Überblick behandelt Gemeinsamkeiten und Unterschiede dieser Ansätze.

1. SCOPE

As pointed out in the Introductory Report by MACGREGOR, there is still no general agreement with respect to design of concrete beams for combined shear, bending moment and axial force. But, there is a clear tendency in recent research work on the subject towards physical models with complete description of equilibrium in the shear zone as a rational basis for concrete design.

The review is concerned with recent research work on the description of the equilibrium system of stresses and the compatibility of strains in the web of reinforced concrete beams containing shear reinforcement.

The review is limited to papers published since 1980. This limiting date was deliberately chosen, because the scientific discussion on design of shear reinforcement was decisively influenced by the COLLINS/MITCHELL paper of 1980 [1]. This influence is clearly demonstrated by the fact that all models treated in this review are formulated in terms of stress fields.

Most theories deal with beam regions in constant shear, but - since they are based on physical models - can be adjusted to situations of varying shear. It is assumed that shear failure is due to yielding of shear reinforcement and/or crushing of web concrete. Thus, bending or bond failure is not taken into account.

2. STRESS-FIELD CONCEPTS IN SHEAR DESIGN

In the webs of slender reinforced concrete beams with shear reinforcement, inclined cracks develop prior to shear failure. It is mostly assumed that these cracks are parallel and straight at approximately constant spacing. This simplification is particularly valid for T- or I-shaped beams.

If there are no bending moments in the concrete struts between inclined cracks, the inclined stresses in the concrete web form a continuous inclined compressive stress field σ_c, the angle α to the beam axis of which does not necessarily coincide with the angle α_{cr} of shear cracks. Furthermore, if the spacing of the shear reinforcement is sufficiently close, stresses in the shear reinforcement can be regarded as a continuous tensile stress field σ_t, the angle β to the horizontal of which is equal to the inclination of shear reinforcement.

The traditional truss model for shear design of concrete beams which dates back to the beginning of the century can also be interpreted as a stress field concept in which the inclination of the concrete compressive stress field is taken as 45°.

If the inclination of the compression stress field σ_c is taken as constant over the height of the beam and given the inclination β of the tension stress field σ_t, the stress intensities follow from equilibrium of vertical forces

$$\sigma_c = \frac{V}{b \cdot z} \cdot \frac{1}{\sin^2\alpha \, (\cot\alpha + \cot\beta)} \qquad (1)$$

$$\sigma_t = \frac{V}{b \cdot z} \cdot \frac{1}{\sin^2\beta\,(\cot\alpha + \cot\beta)} \qquad (2)$$

where V = applied shear force
b = web thickness
z = lever arm of bending stress resultants

Hence, there is no fundamental difference between truss analogy and stress field models if the inclination α of the compression stress field in the web is the same. The main problem is to determine this angle α in a rational manner.

3. LOWER BOUND PLASTIC SOLUTION [2],[3]

In theory of plasticity (also called limit analysis), it is assumed that materials exhibit unlimited plastic (i.e. irreversible) deformations when certain stress combinations (yield condition) are reached. Elastic deformations and workhardening effects are normally neglected.

Given that the function describing the yield condition is convex and that the plastic deformations are normal to the yield surface, upper and lower bounds for the failure load of any structure can be derived. The lower bound theorem of plasticity (limit analysis) states that a lower bound to the true failure load can be found from any stress field in equilibrium which does not violate the yield condition.

With respect to web stresses of concrete beams, it follows from the lower bound theorem of plasticity that the inclination α of the web compression field can be freely chosen as long as yield (limit) conditions are not violated. These conditions are usually taken as the yield strength of shear reinforcement and the effective crushing strength f_c^* of concrete in uniaxial compression. The latter cannot be taken directly from normal specimen tests because of cracking and transverse strains in the web concrete.

A maximum of the lower bounds for the failure load of concrete webs in shear is determined, if the angle α of web compression is chosen in such a way that web crushing and yielding of shear reinforcement occurs simultaneously (web crushing criterion). It should be noted that for low amounts of shear reinforcement this assumption leads to inclinations α of web compression well below the crack inclinations observed in tests.

4. THE COMPRESSION FIELD APPROACH OF COLLINS/MITCHELL [1],[4],[5]

Provided that shear crack openings are "smeared" over the web of the beams, compatibility of average strains is governed by Mohr's circle. The compatibility relation between average strain ε_ℓ in the direction of the beam axis, ε_t perpendicular to this axis and the principal inclined compressive strain ε_d can be derived from Mohr's circle as

$$\tan^2 \alpha = \frac{\varepsilon_\ell + \varepsilon_d}{\varepsilon_t + \varepsilon_d} \qquad (3)$$

From eq.(3), the angle α can be determined, if the values of the average strains ε_ℓ, ε_t and ε_d are known.

With the assumption that the directions of the principal compressive strain ε_d and of the inclined web compression field σ_c coincide, this angle α can be used to determine the web stresses from the equilibrium equations (1) and (2). Using this assumption, there is no need to consider the question whether this angle α is equal to the direction α_{cr} of inclined cracks or not.

For stirrups perpendicular to the beam axis ($\beta = 90$), ε_t is equal to the average stirrup strain. It can be determined from the stress-strain relationship of stirrup steel, if the stiffening effect of concrete between cracks and the anchorage slip of stirrups are ignored.

The concrete strain in the direction of the inclined compression field, however, cannot be taken from uniaxial load tests, because the large transverse tensile strains exert a softening effect on the stress-strain relationship of web concrete. VECCHIO/COLLINS [4] propose the following relationship between principal compressive stress σ_c and principal compressive strain ε_d which depends also on the magnitude ε_1 of the principal tensile strain.

$$\sigma_c = \sigma_{c,max} \left[2 \left(\frac{\varepsilon_d}{\varepsilon_c'} \right) - \left(\frac{\varepsilon_d}{\varepsilon_c'} \right)^2 \right] \qquad (4)$$

where $\sigma_{c,max} = \dfrac{f_c'}{0.8 - 0.34\, \varepsilon_1 / \varepsilon_c'}$

$\varepsilon_{c1}' = -0.002$

f_c = concrete cylinder strength

The strength f_{du} of the web concrete in inclined compression is also influenced by the coexisting transverse strain. COLLINS/MITCHELL [1] propose the following relationship

$$f_{du} = \frac{5.5\, f_c'}{4 + \gamma_m / \varepsilon_d} \qquad (5)$$

where $\gamma_m = 2\varepsilon_d + \varepsilon_\ell + \varepsilon_t$

It must be noted that in the normal case of combined bending and shear the longitudinal strains in the concrete web vary over the beam height due to bending. The compatibility equation (3) in this case predicts an angle α which also varies over the beam height as a function of ε_ℓ. For normal design situations, it is recommended by the authors to consider the longitudinal strain at middepth of the beam and take the corresponding angle α as constant over the web height.

5. STRAIN COMPATIBILITY AND AGGREGARTE INTERLOCK [6],[7],[8],[9]

If it is assumed that the angle α of the inclined compression field in the web does not coincide with the angle α_{cr} of inclined cracks, forces must be transferred across the cracks by aggregate interlock. These forces depend on the displacements v and w of the crack faces tangential and normal to the crack direction.

The compatibility of strains can be considered independently for the strains in the concrete struts between cracks and for the average web strains (including "smeared" crack openings). The differences between both strain fields can be summed up to determine the crack displacements. For this, the crack spacing must be estimated from bond considerations.

The forces which are transferred across the inclined cracks by aggregate interlock depend on the crack displacements v and w. KUPFER and coworkers [6],[8] use relationships for aggregate interlock stresses determined by WALRAVEN, while DEI POLI et al. [7] consider equations derived by GAMBAROVA.

Taking into account aggregate interlock forces and strain compatibility, the angle α of the compression field can be determined by an iterative procedure.

Again, strain compatibility is dependent on longitudinal strains which normally vary across the web height. As a consequence, crack displacements, aggregate interlock stresses and the angle of the compressive stress field vary accordingly. To simplify calculations, it is again recommended to consider the strains at middepth and treat all related variables as constant over the web height.

REINECK/HARDJASAPUTRA [9] use a kinematic condition to determine the angle α of the inclined compression field. Following considerations of deformations of truss models, they assume that the resulting crack opening is always perpendicular to α. From this assumption, the angle α can be determined by an iterative procedure. Aggregate forces are taken into account by the model allthough their magnitude is not explicitely considered.

REFERENCES

[1] COLLINS, M.P. and MITCHELL, D., Shear and Torsion Design of Prestressed and Non-Prestressed Concrete Beams. PCI Journal, Vol. 25, No. 5, Sept.-Oct. 1980, pp 32-100.

[2] BRAESTRUP, M.W. and NIELSEN, M.P., Plastic Methods of Analysis and Design. in "Handbook of Structural Concrete", London 1983.

[3] MARTI, P., Zur plastischen Berechnung von Stahlbeton. ETH Zürich, Bericht Nr. 104, Oct. 1980.

[4] VECCHIO, F.J. and COLLINS, M.P., The Modified Compression-Field Theory for Reinforced Concrete Elements Subjected to Shear. ACI Journal, Vol. 83, No. 2, March-April 1986.

[5] COLLINS, M.P. and MITCHELL, D., A Rational Approach to Shear Design - The 1984 Canadian Code Provisions. ACI Journal, Vol. 83, No. 6, Nov.-Dec. 1986.

[6] KUPFER, H., MANG, R. and KARAVESYROGLOU, M., Bruchzustand der Schubzone von Stahlbeton- und Spannbetonträgern - Eine Analyse unter Berücksichtigung der Rißverzahnung. Bauingenieur 58 (1983), p. 143-149.

[7] DEI POLI, S., GAMBAROVA, P.G. and KARAKOC, C., Aggregate Interlock Role in R.C. Thin-Walled Beams in Shear. ASCE Journal of Struct. Eng., Vol. 113, No. 1, Jan. 1987, p. 1-19.

[8] KIRMAIR, H., Das Tragverhalten schlanker Stahlbetonbalken. Deutscher Ausschuß für Stahlbeton, Heft 385, Berlin 1987.

[9] REINECK, K.-H. and HARDJASAPUTRA, H., Zum Dehnungszustand bei der Querkraftbemessung profilierter Stahlbeton- und Spannbetonträger. Bauingenieur 65 (1990), p. 73-82.

Modelling the Transverse Reinforcement in Reinforced Concrete Structures

Modélisation des armatures transversales dans les structures en béton armé

Modellierung von Querbewehrungen in Stahlbetontragwerken

Luc DAVENNE
Civil Engineer
Lab. Méc. et Technol., ENS
Cachan, France

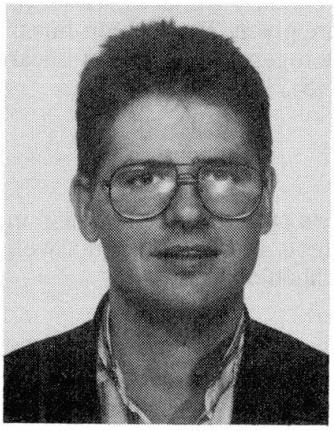

Luc Davenne, born 1963, obtained his Doctorate of the University of Paris 6 in 1990.

Denis BREYSSE
Assist. Prof.
Lab. Méc. et Technol., ENS
Cachan, France

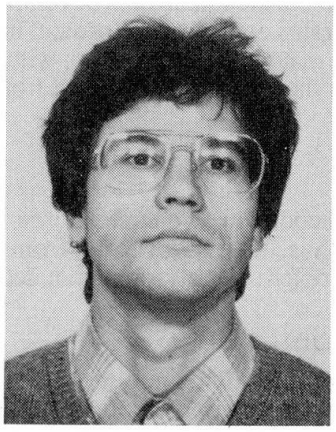

Denis Breysse, born 1958, obtained his Doctorate of the University of Paris 6 in 1986. He his presently teacher at the Ecole Normale Supérieure in Cachan (France).

SUMMARY

The authors present a simplified method to model the influence of transverse reinforcement on the behaviour of reinforced concrete elements. First, a numerical method to compute the three-dimensional stress and strain fields around heterogeneities like transverse reinforcement (stirrups in beams or hoops in columns) embedded in an elastic matrix is developed. Then, a non-linear homogeneous equivalent material is introduced, averaging the local heterogeneities. This unified method allows to treat both the shear reinforcement in beams and the confinement reinforcement in columns.

RÉSUMÉ

Les auteurs proposent une méthode simplifiée pour modéliser l'influence des armatures sur le comportement non linéaire d'éléments de béton armé. Dans un premier temps, une méthode numérique permettant d'obtenir les champs tridimensionnels de déformations et de contraintes localisés autour d'hétérogénéités de type armatures transversales (cadres dans les poutres ou frettes dans les colonnes) incluses dans une matrice élastique est développée. Ensuite, un matériau homogène équivalent rendant compte de façon moyenne des informations fines précédemment obtenues est construit. La méthode permet de traiter de façon unifiée le cas du frettage et celui du cisaillement dans les poutres.

ZUSAMMENFASSUNG

Eine vereinfachte Methode zur Modellierung des Einflusses von den Querbewehrungen auf das nichtlineare Verhalten von Stahlbeton-Konstruktionen wird hier vorgestellt. Zuerst wird eine numerische Methode zur Berechnung der 3D-Verformung- und Spannungsfelder zur Erfassung der Ungleichartigkeiten wie Querbewehrung (Umschnürungsbügel in Stützen oder Bügel in Träger) in einer elastischen Matrix vorgeschlagen. Darauf wird ein gleichartiger Äquivalentstoff mit verschmierten Ungleichartigkeiten formuliert. Die Probleme mit dem Umschnürungsbügel in Stützen und dem Bügel in Träger wird einheitlich behandelt.

1. INTRODUCTION

The behavior of reinforced concrete members including transverse reinforcement (shear reinforcement in beams or confinement reinforcement in columns) is not well understood until now and empirical design methods used in codes and specifications are very different around the world [1]. The concepts that underline current design practice are based partly on rational analysis, partly on test evidence, and partly on successful long-term experience with satisfactory structural performance. A theoretical treatment on the subject is needed.

The purpose of the paper is to model this behavior in the context of a general two-level approach [2] which consists in using for the structures global simplified methods issued from detailed local analysis:

- detailed analyses are first developed to compute the 3D stress and strain fields, warping of cross sections and other local informations in beams and columns taking into account the exact geometry of such elements (spatial distribution of reinforcement for instance).
- then global methods are built using global variables, such as generalized forces on the cross section, and taking into account the previous refined informations. These methods are simpler to use and quicker. The complex local behavior is integrated but not seen by the user who needs only a global response.

Following this general two-level approach, a numerical method to compute three-dimensional stress and strain fields localized around heterogeneities like transverse reinforcement (stirrups in beams or hoops in columns) embedded in an elastical matrix is developed. This method is based on Eshelby works [3, 4] where analytical stresses and strains around an ellipsoidal inclusion in an infinite body are given. Then, a non-linear homogeneous equivalent material is constructed, with an averaging of the local heterogeneities. The non-linear constitutive equations for the concrete are derived from continuous damage theory [5].

2. LOCAL ANALYSIS

A reinforcement bar embedded in a concrete matrix is a local perturbation (there is only a percent of steel in most R/C buildings). Thus, the use of tools from the "micromecanics of defects in solids" seems well adaptated to solve this problem. Equations are not detailed here, interested readers should refer to [4].

2.1 Ellipsoidal heterogeneity

The most popular author in this domain of the mechanics is Eshelby. He obtained in 1959, in an elegant way, the distribution of perturbations around an elipsoidal heterogeneity embedded in an uniformly loaded infinite elastic media [3] (Fig.1).
It can be expressed with:

$$\varepsilon(x) = S(x)\,[(K^*-K)S(x)+K]^{-1}\,(K-K^*)\,\varepsilon^o = H(x)\,\varepsilon^o \qquad (1)$$

where $\varepsilon(x)$ is the strain perturbation at point M with coordinates x, ε^o the uniform strain at infinity, K^* and K the Hooke tensors of the heterogeneity and the matrix respectively and S is the Eshelby tensor which can be expressed from the two elliptic integrals:

$$\Psi(x) = \int_\Omega |x-x'|\,dx' \quad \text{et} \quad \Phi(x) = \int_\Omega \frac{dx'}{|x-x'|} \qquad (2)$$

These integrals are analytical for specials ellipsoids like sphere or infinite cylinders for instance.

2.1 Transverse reinforcement in concrete

In the case of transverse reinforcement studied here (Fig.2), the assumptions must be revised. These hypothesis are treated and discussed in [6] and will be the object of further publications. Only their list is given here.

2.2.1 Assumptions on geometry

- A stirrup or a hoop is not an ellipsoid: the tensor H of eq.1 must be computed with special technics (numerically).
- Reinforcement bars are not unique: interactions are neglected and perturbations are added.
- They are embedded in a finite body: the approximation of infinite media is still acceptable.

2.2.2 Assumption on loading

- In the case of a beam, the loading is not uniform: the beam is discretized in layers where the gradient of loading is supposed small.

2.2.3 Assumption on materials

- The behavior of concrete is not elastic: the continuous damage theory coupled with an homogeneisation procedure is used.

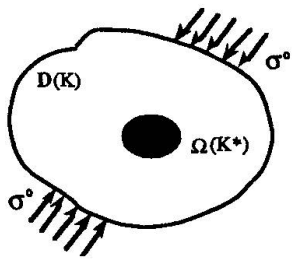

Fig.1 Ellipsoid in an infinite media

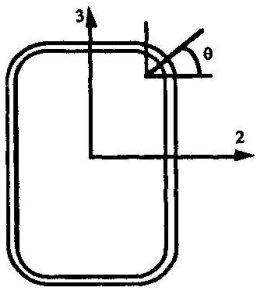

Fig.2 General shape for hoops and stirrups

3. GLOBAL ANALYSIS

3.1 Homogeneous equivalent material

The beam or the column is divided into elementary cells whose height depends of the number of layers choosen (depending on the sollicitation), whose width is the width of the beam and whose length depends on longitudinal distribution of transverse reinforcement (Fig.3,4).

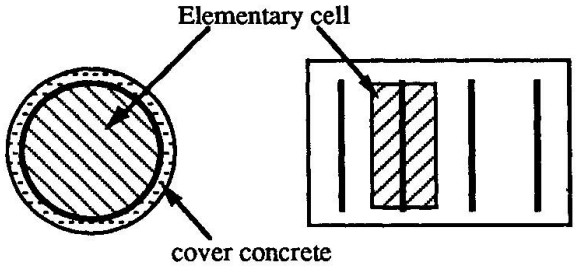

Fig.3 Hoop confined specimens

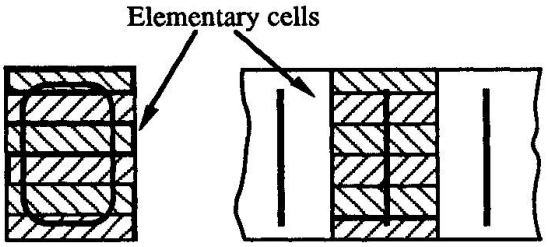

Fig.4 Beams subjected to shear

In relation with the choosen constitutive equations for concrete [5], the homogeneisation variable k is an average on the cell of the leading scalar variable of the damage model, which is calculated at each point within the cell from the positive principal strains $\langle \varepsilon_i \rangle_+$:

$$\tilde{\varepsilon} = \sqrt{\sum \langle \varepsilon_i \rangle_+^2} \tag{3}$$

$$k = \frac{1}{V} \int_{V_t} \frac{\tilde{\varepsilon}}{\tilde{\varepsilon}^0} \, dv \tag{4}$$

where V is the volume of the cell and $\tilde{\varepsilon}^0$ the value of $\tilde{\varepsilon}$ in the concrete alone (if there were no stirrup or hoop).

Thus, during the monodimensionnal calculation described in the following, the variable $\tilde{\varepsilon}_c$ of the cell with transverse reinforcement influence will be calculated from $\tilde{\varepsilon}^0$ (case with no stirrup):

$$\tilde{\varepsilon}_c = k \ \tilde{\varepsilon}^0 \tag{5}$$

The homogeneisation variable k varies with the geometry (% and distribution of steel), with the state of the materials (toughness or damage of the concrete matrix) and with the sollicitation of the cell (traction, compression or shear). k is less than one, so it is called the damage delaying indicator. On Fig. 5, one can see the variation of k with the damage variable:

$$D = \frac{E_c - E_{c0}}{E_{c0}} \tag{6}$$

where E_c and E_{c0} are the actual and initial Young modulus of concrete respectively. It can be seen that the more the concrete is damaged, the more the transverse reinforcement effects are great (k<1).

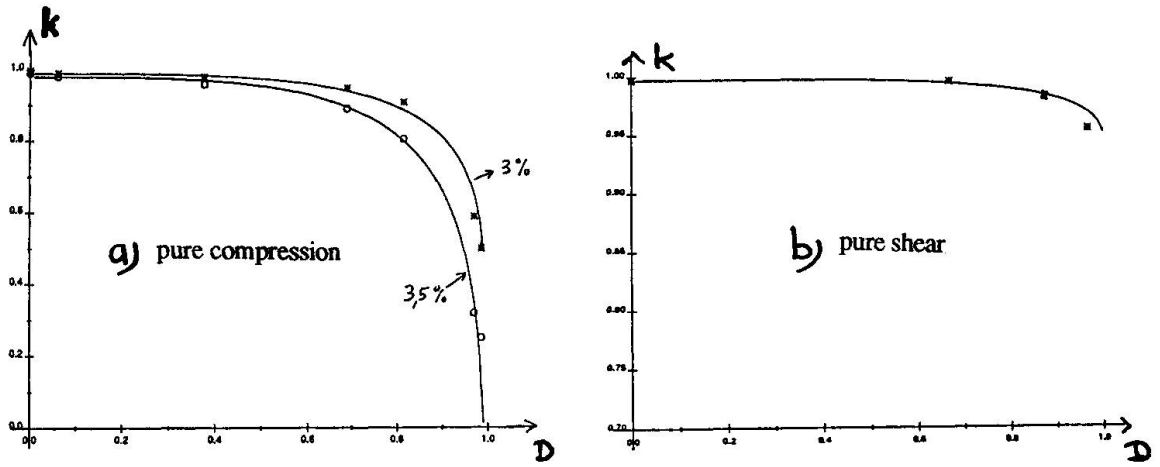

Fig.5 Homogeneisation variable k versus damage $D = \frac{E_c - E_{c0}}{E_{c0}}$

3.2 Global calculation

The heterogeneous elementary cell is replaced by an equivalent homogeneous cell with the same dimensions and whose behavior is affected by the presence of the steel. The transverse steel has no influence on the secant modulus of the cell which is the one of the matrix. But the degradation of the matrix is considerably delayed by the presence of transverse reinforcement.

3.2.1 Hoop confined specimens

The computation of a hoop confined specimen or column is first shown for simplicity:
- First stage: local computation (3D) and building of relations k(D) of Fig.5a.
- Second stage: global computation (1D):

i) The equivalent homogeneous cell is loaded in compression with ε^o, $\tilde{\varepsilon}^o$ is computed with eq.3
ii) The damage D_0 is calculated with the choosen damage law
iii) k is obtained from the curves Fig.5a (numerically stored at the first stage)
iv) The new state of the cell is computed with eq.5: $\tilde{\varepsilon}_c = k\ \tilde{\varepsilon}^o$
v) The damage of the cell D_c is calculated with the choosen damage law
vi) Return to step iii) until convergence (very fast in practice)
vii) Calculation of the stress $\sigma_c = E_{b0}\ (1 - D_c)\ \varepsilon^o$

The first and second stage are completely independant. The (long) three-dimensionnal local computation is done only once. The global monodimensionnal computation is very fast but takes into account the refined information of the first stage.

3.2.2 Beams subjected to flexure and shear

The procedure is about the same but a little more complicated because the cells are loaded with an axial strain ε and a shear strain γ. The corresponding stresses are deduced from:

$\sigma = E_{c0}\ (1-D_c)\ \varepsilon$ and $\tau = G_{c0}\ (1-D_c)\ \gamma$ ()

where E_{c0} and G_{c0} are the Young and shear modulus of the sound concrete and D_c the damage of the cell.
The distribution of the strains along the height of a section of the beam are obtained following the iterative method described in [7]: ε is proportional to the rotation ω of the section (supposed to remain plane) and γ is obtained by equilibrium conditions on a layer.

The homogeneisation variable k of a cell subjected to σ and τ is obtained by combination of the curve for pure compression (Fig.5a) and the curve for pure shear (Fig.5b) computed during the first stage.
Interested readers should refer to [6, 7].

4. RESULTS AND COMPARISON TO TEST DATA

4.1 Hoop confined specimens

The method was applied to the hoop confined cylinders described in Fig.6. The parameters of the damage law were identified from the stress-strain curves of the plain concrete. The stress-strain curves of the confined concrete (core concrete) were then calculated by the proposed method. This was done for two different concretes, one with low qualities (f_c = 26 MPa, Fig.7a) and the other with better qualities (f_c = 52 MPa, Fig.7b).
One can see that numericals results are in good agreements with experimental data [8]: the presence of hoops increases just a little the strength of the concrete (pic stress) but a lot its ductility. The better the concrete, the more prononced these effects.

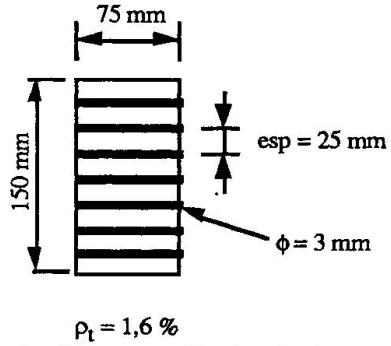

Fig.6 Hoop confined cylinder

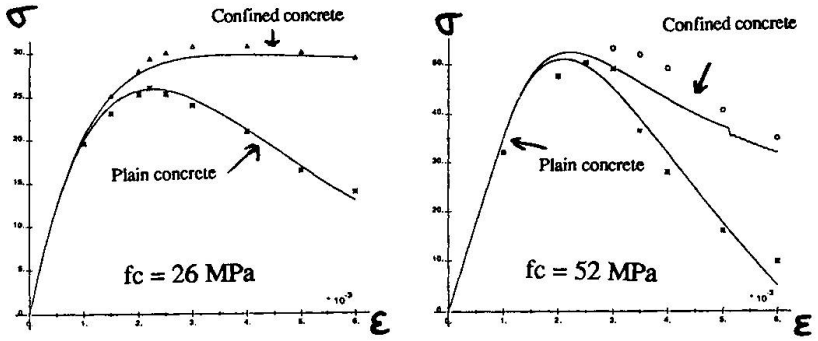

Fig.7 Stress-strain curves — numeric ×○ exp.

4.2 Beams subjected to flexure and shear

With the proposed method, it is also possible to study beams subjected to shear (Fig.8). In this isostatic case, the sections of the beam differ by the ratio M/Vd where M is the bending moment in the section, V the shear effort and d the effective depth of the beam. The greatest M/Vd ratio is the shear span to depth ratio of the beam a/d (in the section under the applied load), which is a well known influencing parameter in such a problem.

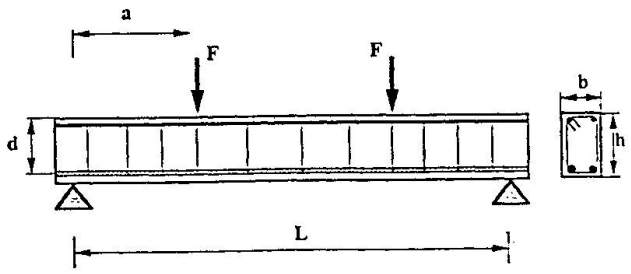

b = 150 mm
h = 300 mm
d = 270 mm
Stirrup: ϕ 6 mm
Longi. bars: top ϕ 10 mm
bottom ϕ 22 mm

Fig.8 Beam subjected to shear

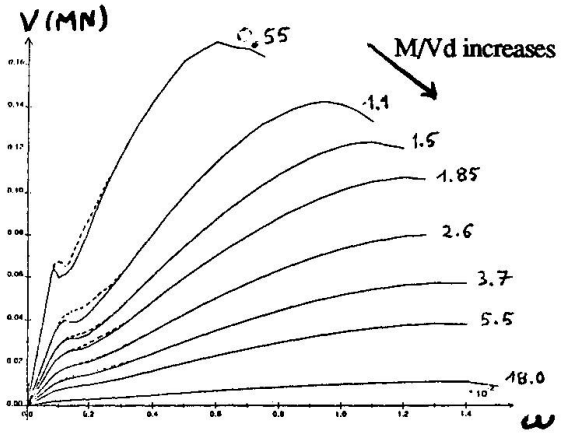

--- with stirrups
— without stirrup

Fig.9 Shear effort V versus rotationof the sections ω

On Fig.9 one can see the simultaneous evolution of the different sections of the beam: the shear effort V is directly related to the applied effort F (V = -F) and loading the beam increases V on the diagramme 9. The sections which have a small M/Vd ratio have two pics. The first pic is due to crushing of concrete under shear in the middle of the section and the second pic correspond to plastification of longitudinals bars or failing of the concrete in compression. The sections with a large M/Vd ratio have only the second pic, the influence of shear being lower.

The ultimate state of the beam is reached when one of the sections reaches a pic. If a/d is large, the beam fails in bending in the sections located in its middle (vertical cracks, Fig.10a). For beams with a small a/d ratio, sections with large M/Vd ratio do not exist and the beam fails in shearing of a section located between the support and the point of application of the load (horizontal cracks, Fig.10b).
The presence of transverse reinforcement has a significant influence only on the first pic in the sections where the M/Vd ratio is small (Fig.10). Thus, the stirrups modify the failure mode of the short beams.

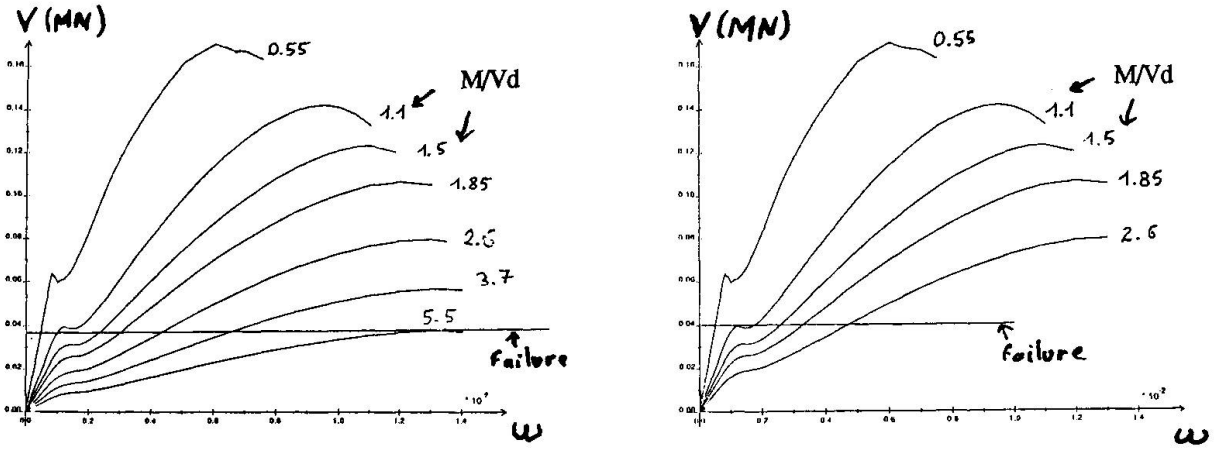

Fig.10 a) Beam with a/d = 5.5 $\frac{Mu}{Mfl} = 1.$ b) Beam with a/d = 2.6 $\frac{Mu}{Mfl} = 0.51$

5. CONCLUSION

Usually, the shear reinforcement in beams and the confinement reinforcement in columns are treated using very different concepts. In the present paper, a unified approach is proposed and the two problems are treated in the same way. This simplified method allows to treat these problems rapidly but with a good accuracy The first results are in good agreement with experimental observations.

REFERENCES

1. BREEN J. E., Why structural concrete. Introductory report, IABSE Colloquium, Stuttgart, April 1991.
2. BREYSSE D., DAVENNE L. and SUN Z., Analysis of Industrials Structures: Accurate and Simplified Methods. Second International Conference on Computer Aided Analysis and design of Concrete Structures, Zell Am See (Austria), 4-6 april 1990.
3. ESHELBY J.D., Elastic inclusions and inhomogeneities. Progress in Solids Mechanics 2, ed. I.N. Sneddon & R. Hill, North-Holland, Amsterdam, pp. 89-140, 1961.
4. MURA T., Micromechanics of defects in solids. Second, Revised Edition, Martinus Nijhoff Publishers, 1987.
5. MAZARS J., Application de la mécanique de l'endommagement au comportement non linéaire et à la rupture du béton de structure. Thèse de Doctorat d'Etat, L.M.T./C.N.R.S./Univ.Paris 6, Cachan (Fra), 1984.
6. DAVENNE L., Modélisation de l'influence des armatures transversales sur le comportement non linéaire d'éléments de béton armé. Thèse de Doctorat de l'Université Paris 6, L.M.T./C.N.R.S./ Univ.Paris 6, Cachan (Fra), 1990.
7. VECCHIO F. J. and COLLINS M. P., Predicting the response of reinforced concrete beams subjected to shear using modified compression field theory. ACI Structural Journal, Vol. 85, No. 3, pp. 258-268, 1988.
8. AHMAD S. H. and SHAH S. P., Stress-strain curves of concrete confined by spiral reinforcement. ACI Structural Journal, Vol.82, No.5, pp. 484-490, 1982.

Modelling of Members with Transverse Reinforcement

Modélisation d'un élément en béton pourvu d'armatures transversales

Modellieren von Konstruktionsbauteilen mit Stegbewehrung

Karl-Heinz REINECK
Dr. Eng.
Univ. of Stuttgart
Stuttgart, Germany

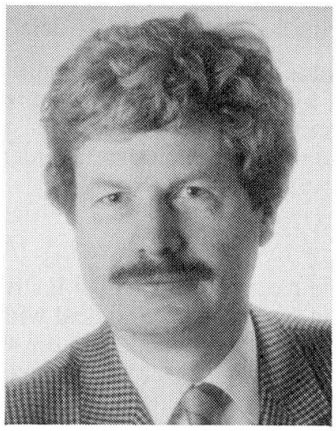

Karl-Heinz Reineck received his Dipl.-Ing. and Dr.-Ing. degrees from the University of Stuttgart. He is involved in both research and teaching at the Institute for Structural Design. His research covers theoretical work and several experiment projects on the shear-behaviour of structural concrete members as well as large-scale tests on reinforced concrete-shells for offshore platforms. He is a member of the CEB-Commission «Member Design».

SUMMARY

The biaxial state of stress in the webs of structural concrete members is described, which is presented by a truss model with the combined action of the stirrups and concrete tensile ties. The magnitude of the load carried by concrete in tension is determined by the friction of the crack faces and therefore the state of strain in the web and crack width have to be determined. However, this allows the calculation of the behaviour from cracking until failure. The influence of axial forces and of the prestress on the ultimate resistance can be consistently described as well as the effective concrete strength explained.

RÉSUMÉ

L'état de contrainte biaxial au sein d'éléments en béton est traduit par l'analogie du treillis, qui modélise les efforts de traction apparaissant soit dans les étiers, soit dans le béton. L'amplitude de la charge reprise par le béton en traction est déterminée par le frottement des surfaces des fissures, ce qui impose la détermination de la largeur des fissures ainsi que de l'état de contrainte au sein de l'élément considéré. Or cette démarche permet le calcul du comportement allant de la fissuration à la rupture; par conséquent, on pourra décire l'influence des forces axiales et de la précontrainte sur la résistance ultime aussi bien que la résistance effective du béton de l'élément étudié.

ZUSAMMENFASSUNG

In Stegen von Konstruktionsbetonteilen herrscht ein zweiachsiger Spannungszustand, der durch ein Fachwerk mit Zugkräften in den Bügeln sowie im Beton modelliert wird. Der vom Beton auf Zug getragene Lastanteil wird aus den durch die Reibung in den Rissen übertragbaren Spannungen bestimmt, und deshalb müssen der Dehnungszustand im Steg und die Rissbreiten bestimmt werden. Dies erlaubt jedoch die Berechnung des Tragverhaltens von der Rissbildung bis zum Bruch. Der Einfluss von Längskräften und der Vorspannung auf die Tragfähigkeit kann konsistent angegeben und die «effektive Betonfestigkeit» erklärt werden.

1. INTRODUCTION

The well-known truss for members with transverse reinforcement is a basic model for structural concrete as shown by MacGregor, Marti and Schlaich in /1/. However, it is also a simple model with only two variables to cover all design cases: the strut inclination Θ and the strength σ_{cw} of the compression struts. This simplicity may lead to contradictions with the real behaviour of members and even to inconsistencies with other models used in the design concept. An important case are the members with moderate shear, which only require light transverse reinforcement: until now most codes provide an empirically derived V_c-term; yet for a truss model unrealistic low values for have to be assumed, which allow almost no staggering of the tension chord reinforcement. A further example is the "effective strength" of the compression fields or struts, where either simply different values depending on the stress situation are proposed or refined strain-considerations are made. Finally, the truss with an uniaxial compression field is an insufficient model for the limit state of serviceability and therefore in codes mostly detailing rules are given (MacGregor /1/).

The aim of this article is to contribute to a clear understanding of the structural behaviour of B-regions with shear forces by presenting a model for the stresses and strains of cracked webs with transverse reinforcement. It will be shown that tensile stresses occur in the web due to the friction of the crack-faces, and that by modelling this the above mentioned inconsistencies are avoided as explained in /2/.

2. EQUILIBRIUM

The equilibrium in the B-region of a r.c.- or p.c.-member is investigated according to the well-known method by Mörsch, to cut the member along the cracks and to deal with the resulting elements in free-body diagrams. For a typical B-region at an end-support the elements are the solid concrete struts between the cracks (Fig.2). For simplicity straight cracks are assumed, whereby their inclinations depend on the degree of prestress and on the magnitude of the axial compressive or tensile force N. Mörsch was satisfied with the capacity of the truss formed by the stirrups and the struts between the cracks (Fig.2a), but now generally the contribution of the friction of the crack faces (Fig.1) is taken into account by assuming flatter strut- than crack-inclinations. (The dowel force of the longitudinal reinforcemnt is neglected in the following for simplicity.) The term "friction" is used here as a general term covering all types of concrete, e.g. also lightweight concrete with no aggregate interlock. Such frictional stresses were so far mostly regarded as components of an uniaxial compression field with an inclination flatter than that of the cracks, like by Kupfer/Mang/Karavesyroglou /3/, Kirmair/Mang /4/, as well as dei Poli/Gambarova/Karakoc /5/. In the following the biaxial state of stress in the web is derived.

From the vertical equilibrium in Fig.1 follows:

$$V = \frac{A_{sw}}{s_w}\,\sigma_{sw}\cdot z\cdot \cot\beta_{cr} + V_f + V_p \qquad (1)$$

whereby V_p is the vertical component of the total force in an inclined prestressed reinforcement. Prestressing is here considered internally in the strains, which is here of advantage since later the strains and relative displacements of the crack-faces have to be determined. The strain in the tension-chord follows from the force, which can be calculated from the equilibrium of moments of the end-support region (Fig.1). Similarly the force C and the corresponding strain in the compression chord are determined from the horizontal equilibrium.

The vertical component V_f of the friction forces can be expressed in terms of the friction stresses in the middle of the web

$$V_f = b_w\, z\, [\tau_{f0} + \tau_{f\sigma}\,(1 - \cot\beta_{cr}/\mu_f)\,] \qquad (2)$$

Thereby the well-known relation for friction was assumed

$$\tau_f = \tau_{f0} + \mu_f\cdot\sigma_f = \tau_{f0} + \tau_{f\sigma} \quad \text{with} \quad \mu_f = \cot\psi = 1,7 \qquad (3)$$

which, however, contrary to the usual applications depends on the crack displacements. The relatively high value for μ_f was derived from Walraven's constitutive laws for crack widths up to 0,5 mm (see /2, 15/).

Now all the forces and stresses along the crack are defined, and the stress field in the solid concrete strut between the cracks can be determined. In Fig.2 all stresses are given with respect to the crack direction. The truss-action (Fig.2a) is made up by the stirrups and the uniaxial compression field between the cracks. The stress fields due to the friction (Fig.2b) are looked at seperately for a better understanding: the shear stresses τ_f result in a biaxial tension-compression field with an inclination of $\beta_{cr}/2$ of the compression field; the normal stresses σ_f result in principal compressive stresses σ_2 and tensile stresses σ_1 parallel to the crack. Altogether a biaxial stress field exists, whereby the principal stresses and the principal inclination φ_1 (Fig.2b) may be determined acc. to the linear elastic theory. This is valid since the principal tensile stresses remain smaller than the concrete tensile strength once the crack pattern has formed.

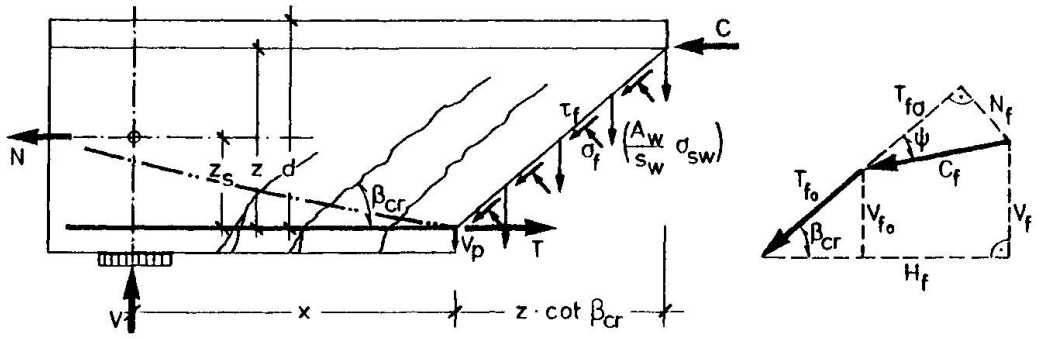

a) end-support region and forces b) forces due to friction

Fig.1: Free-body diagram for an end-support region of a structural concrete member

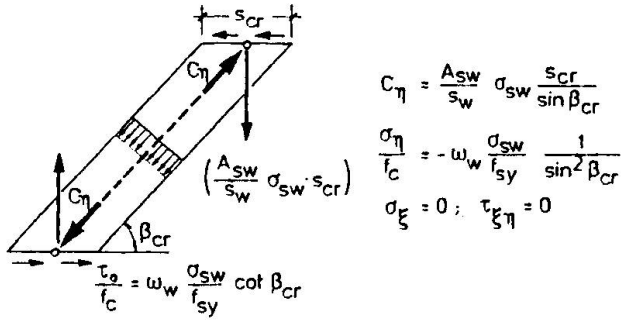

a) forces and concrete stresses due to truss-action

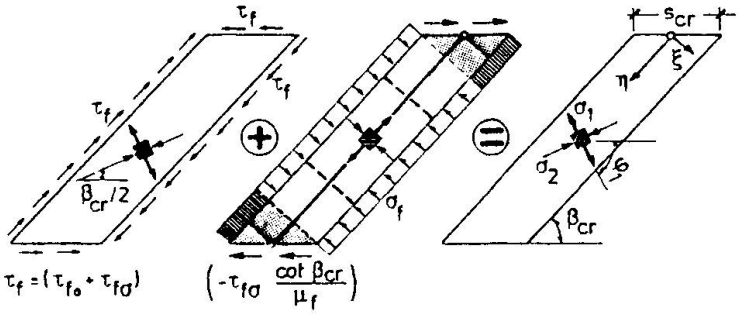

b) stresses due to friction

Fig.2: Forces and stresses for the concrete strut between the cracks

The stress field resulting in the web from all the actions in Fig.2 is that of a principal compression σ_2 inclined at the angle Θ and a principal tension (for higher shear also small compression) perpendicular to that. This was already described by Reineck in /6/, and even earlier by Lipski /7/ who, however, gave a different explanation for the tension field. This state of stress results in the two models shown in Fig.3: the well-known truss model formed by an uniaxial compression field and the stirrups (Fig.3a), as well as a truss-model with concrete tensile ties (Fig.3b). These are the two load paths referred to by Schlaich/Schäfer/Jennewein /8/. The models in Fig.3 are statically equivalent to the model shown in Fig.1, and this also means that there is no principal contradiction between the two well-known approaches in the shear design: the "shear-friction theory" leading e.g. to a V_c-term on one side, and the truss-analogy on the other side. In these truss-models the discrete cracks are not modelled but these must be looked at in order to determine the magnitude of the tensile stress σ_1, which only depends on the friction stresses along the crack. However, these trusses visualize the flow of the forces in a member more clearly and simpler. So the overall model (Bruggeling /1/) and the sectional approach are both necessary.

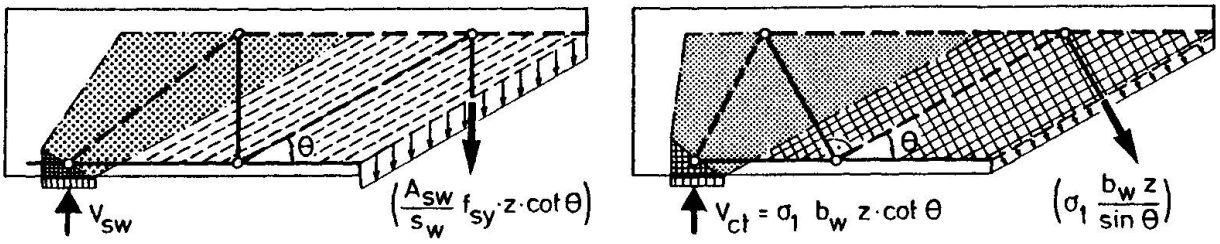

a) stirrups and uniaxial compression field b) biaxial concrete stress field

Fig.3: Truss models following from the principal stresses between the cracks

It must be mentioned that further tensile stresses occur in the struts due to the bond of the stirrups (see /3, 4, 9, 10/). These tensile stresses reduce the stirrup stresses and strains between the cracks (tension stiffening effect), but they do not contribute to the load transfer.

With this model for the biaxial state of stress in the web of structural concrete members with transverse reinforcement a clear transition to the model for members without transverse reinforcement is achieved as also explained in /2, 15/. So apart from being transparent, this model enables a consistent treatment from members with transverse reinforcement to unreinforced members.

3. KINEMATICS AND CONSTITUTIVE RELATIONS

3.1 Kinematics

The strains of an element in the B-region can be calculated from the strains of the truss formed by the stirrups and the solid concrete struts between the cracks (Fig.2a). The stresses due to friction (Fig.2b) are then considered by the deformations of the concrete struts:

$$\epsilon_{cw} = \epsilon_\eta = (\sigma_\eta - 0,2 \cdot \sigma_\xi)/E_c \tag{4}$$

The complete state of strain of a beam-element in a B-region with shear forces is as follows:

- longitudinal strain in the middle of the web: $\epsilon_x = (\epsilon_s - \epsilon_c)\ /2$ (5a)
- curvature: $\bar{\kappa} = \kappa \cdot z = (\epsilon_s + \epsilon_c)\ /2$ (5b)
- vertical strain: $\epsilon_z = \epsilon_{sw}$ (5c)
- shear strain: $\gamma_{xz} = \epsilon_x/\tan\beta_{cr} + \epsilon_{cw}/\sin\beta_{cr} \cdot \cos\beta_{cr} + \epsilon_{sw} \cdot \tan\beta_{cr}$ (5d)

For the vertical strain the beneficial tension stiffening effect between cracks was neglected, because the anchorage slip of the stirrups has a controversial effect; more refined considerations were e.g. made by Kupfer et al. /3, 4/.

With these equations the bending- and shear-stiffnesses of the beam-element are principally given and may be used either for a non-linear analysis or for calculating deformations, since the equations are not limited to the ultimate limit state. The difference to many well-known works, e.g. also by Collins/Mitchell /11/ is, that the crack-inclination is considered and that the direction of the principal strain does not coincide with that of the compression field; further explanations were given by Hardjasaputra /12/ and Reineck/Hardjasaputra /13/.

Since the strains are known also the crack width n and the slip s in the middle of the web can be calculated for a given crack-spacing s_{cr} (measured horizonally):

$$\frac{\Delta n}{s_{cr}} = (\epsilon_x + \epsilon_{sw} + \epsilon_{cw}) \cdot \sin\beta_{cr} + \bar{\kappa}\frac{s_{cr}}{z}\cos\beta_{cr} \tag{6a}$$

$$\frac{\Delta s}{s_{cr}} = -\epsilon_x \cdot \cos\beta_{cr} + (\epsilon_{sw} + \epsilon_{cw})\sin^2\beta_{cr}\ /\cos\beta_{cr} + \bar{\kappa}\frac{s_{cr}}{z}\sin\beta cr - 2,4\frac{\tau_f}{E_c}\sin\beta_{cr} \tag{6b}$$

These crack displacements determine the magnitude of the friction transferring the biaxial stress field over the cracks.

3.2 Constitutive Relations

For the concrete and the steel bi-linear stress-strain curves can be used /2/. The strength of the solid concrete struts between the cracks (see also /14/ and section 6) is not lower than:

$$f_{cw} = 0,85 \cdot f_c \quad \text{or} \quad f_{cw} = 0,80 \cdot f_c \tag{7}$$

The constitutive equations for the friction of the crack-faces were already explained in /15/ and so here only the result is given:

$$\frac{\tau_f}{f_c} = \frac{\tau_{f0}}{f_c} \cdot \frac{\Delta s - 0,24\Delta n}{0,096 \cdot \Delta n + 0,01} \quad \text{with} \quad \Delta n, \Delta s \ [mm] \tag{8}$$

The stress σ_f or $\tau_{f\sigma}$ follows then from Eq.(3). The friction stress τ_{f0} is the limiting value without normal stresses σ_f on the crack face and was set to

$$\frac{\tau_{f0}}{f_c} = 0,45 \frac{f_{ct}}{f_c} \left(1 - \frac{\Delta n}{0,9}\right) \quad \text{with} \quad \Delta n \ [mm] \tag{9}$$

This is a much lower value than that given by Vecchio/Collins/Bhide /9, 10/. With these formulations the whole response of the B-region in a member may principally be determined from cracking until failure, and this is demonstrated in the following by two examples.

4. STIRRUP STRAINS AT SERVICE LOAD

For determining the crack width of the inclined cracks in a web all strains must be known acc. to Eq. (6a), but the stirrup strains play of course a dominant role. Presently a semi-empirical approach is used for predicting the stresses and strains for in the stirrups under service load conditions: the stresses are calculated for a truss model with struts at 45° and the actual load V is reduced by a V_c-term. The presented combination of truss models with additional tensile struts in the web can be used for checking the requirements at the serviceability limit state. As an example for this the well-known test series of identically reinforced beams with varying web thicknesses (varying b/b_w-ratio) by Leonhardt/Walther /16/ was calculated, and Fig.4 shows the comparison of the measured and calculated stirrup stresses with increasing load. Contrary to a truss-model, the presented model yields the typical characteristic of the measured curves. It can also be seen that the usually used V_c-term is not equal to the cracking load as often pretended. However, the calculated values are partly very conservative because the tension stiffening effect was not considered for the stirrup strains. If this is improved the model may serve as a relatively simple tool for determining crack widths. Of course, additionally to the strains also the crack spacing must be determined.

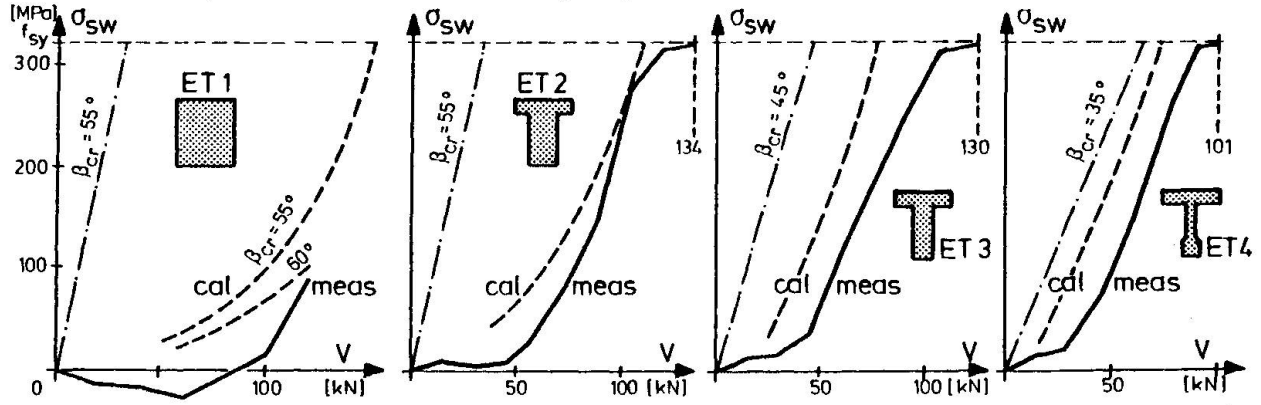

Fig.4: Development of stirrup stresses with the load for test-beams with varying web-thicknesses of Leonhardt/Walther /16/

These results may be interpretated in terms of the load proportions taken by the models with the stirrups or the tensile struts (Fig.3), and such values are given in Fig.5 for the load step 60kN (service load) and the load at yielding of the stirrups. For the two beams with the thick webs the truss with the concrete tensile struts carry quite a considerable part of the load, although the tensile stresses remain low; for the thin-webbed beams the load is almost totally carried by the truss with stirrups. From this it is obvious that the model with the concrete tensile struts is especially relevant for members with moderate shear like in buildings and for foundations.

beam	β_{cr}	Service load V~60 kN					Yielding ε_{sw} = 1,6 ‰				
		θ	σ_1/f_c	V_{ct}	σ_{sw}/f_{sy}	V_{sw}	V	θ	σ_1/f_c	V_{ct}	V_{sw}
ET 1	55°	31,7	0,0180	52,6	0,106	7,4	151,9	24,3	0,0140	56,2	95,7
ET 2	55°	26,0	0,0201	37,2	0,256	22,6	113,9	26,0	0,0137	25,5	88,4
ET 3	45°	25,2	0,0014	1,9	0,634	58,2	75,9	27,4	-0,0062	-7,1	83,0
ET 4	35°	30,5	0,0028	1,5	0,794	58,2	72,1	30,8	-0,0002	-0,1	72,2

Fig.5: Calculated values for two load stages of the test-beams in Fig.4

5. DIMENSIONING AT THE ULTIMATE LIMIT STATE

The main results for the ULS are summarized in the well-known dimensioning diagram (Fig.6) which is simplified by assuming a constant shear force component q_f with increasing ultimate shear force. However, this is quite a good approximation as comparisons with similarly derived diagrams by Kupfer et al /3, 4/ and Gambarova /5/ show. Also Hardjasaputra/Reineck /12, 13/ came to similar results based on a simple kinematic condition proposed by Hardjasaputra /12/, which includes the slip in the cracks and thereby the direction of the principal strain deviation from the direction of the principal compression.

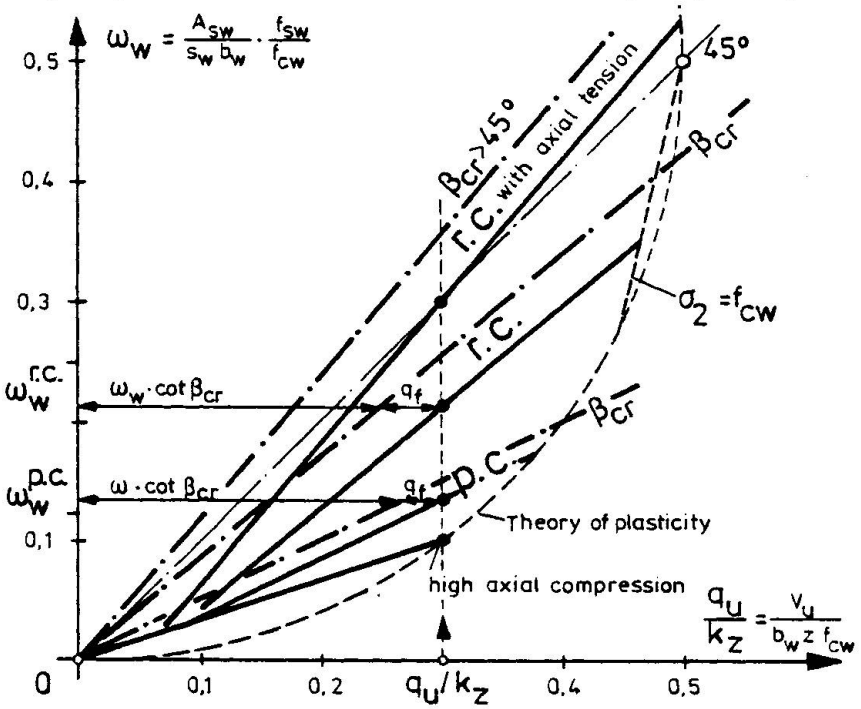

Fig.6: Principal sketch of a dimensioning diagram for the tranverse reinforcement in B-regions and influence of prestress and axial tensile and compressive forces

Since p.c.-beams exhibit a flatter crack inclination than r.c. beams, less stirrups are required although the value for q_f is smaller. For medium values of q_u the friction capacity defines the ultimate load, and only for high values q_u the concrete between the cracks really fails in compression. This occurs at slightly lower shear forces than according to the theory of plasticity because the web is here in biaxial compression (due to high stresses σ_f on the crack face). Of course, in test beams the difference between both "failure types" is not always clearly recognizable, especially not for p.c. beams and webs or panels with small crack spacing.

Axial forces are also constantly considered in the equilibrium equations (see Fig.1), leading e.g. to higher axial strains ε_x as well as steeper crack inclinations for tension flanges of box-girders. It is expecially worth mentioning that for high axial compression very small crack inclinations and therefore also small inclinations Θ for the compression field are possible; therefore a lower limit for Θ is not necessary according to this proposal, since it is taken into account by the limitation of the friction transfer. (Why not 10^o for box-columns of bridges with high axial compression? Here the model is that of a very flat strut as explained by Schlaich /1/). However, since structural concrete is capable of some redistribution, also higher strut inclinations than that of the cracks can occur as pointed out by Kupfer/Guckenberger /17/, who tested and clearly explained the structural behaviour of highly compressed structural concrete members.

Finally it may be concluded that the presented model explains the "V_c-term" and that the simple demanded ways of accounting for it (MacGregor /1/) are possible, as demonstrated by a joint proposal from Kupfer and Reineck for the CEB MC 90.

6. EFFECTIVE CONCRETE STRENGTH

When applying the theory of plasticity to structural concrete, an effective concrete strength for the compression field is taken, which is lower than the uniaxial compression strength (Marti and MacGregor /1/). For a compression field crossing cracks it is now obvious from before, that this value is not constant but depends on the strain condition as well as on the direction and spacing of the cracks, if the friction capacity is decisive. If the compression struts between cracks govern the failure, the reduction of the strength of struts

between cracks is only up to to 0,85 f_c and 0,8 f_c according to many tests by different researchers as explained in /14/; therefore lower values are unnecessarily restrictive.

If now the ultimate loads according to the diagram (Fig.6), are interpretated by the well-known truss with a uniaxial compression field as shown in Fig.7, then the so-called effective concrete strength ($\nu \cdot f_{cw}$) varies with the ultimate load or the inclination Θ. The value ν now cannot be constant, since the friction characteristics cannot only be formulated in terms of strength values, like normally in "shear-friction theories", but a complete description of the strength as well as relative crack displacements is required. Therefore a crack direction has to be assumed and the crack spacing has to be calculated, in order to evaluate the crack width for a given strain condition.

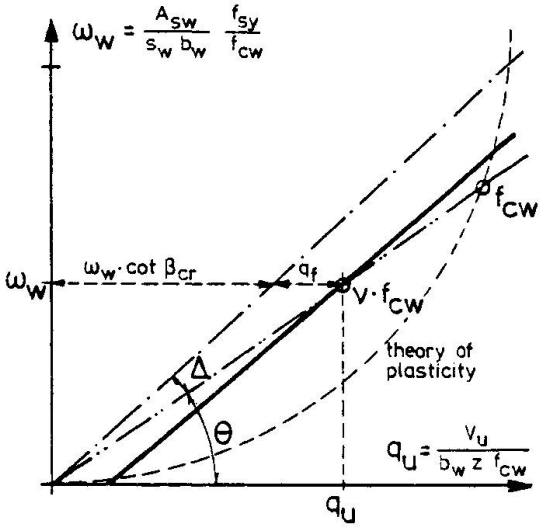

Fig.7: Interpretation of the dimensioning diagram in Fig.6 in terms of an effective concrete strength

All these influencing parameters may simply be described by their effect on the friction component q_f, acc. to Fig.7, and this is shown in Fig.8. The influence of the crack spacing as well as of the crack inclination follows from Fig.8a; thereby the crack spacing is of principal importance because by this parameter a "size-effect" is induced: for larger member depths the crack widths are larger for same rotations or curvatures (as explained in /15/) and also larger bar diameters are used resulting in larger crack widths and smaller values for the friction component q_f. This also follows from the works of Gambarova /5/ and Kupfer et al /4/. The vertical or stirrup strains (Fig.8b) also limit the friction capacity, if large values are reached (unless a second crack field appears and the original cracks close). The longitudinal strains (Fig.8c) reflect mainly the influence of axial forces, which furthermore have an additional effect on the crack inclination. In case of axial compression the crack inclination and also q_f acc. to Fig.8a or 8c decreases, but this is more than made up by the capacity increase of the truss (see Eq.(1) and Fig.2a).

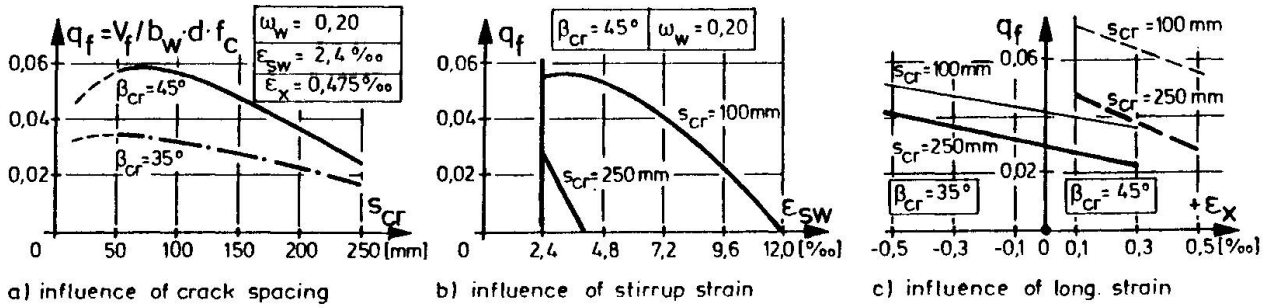

Fig.8: Influence of crack spacing, crack inclination and strains on the shear force component q_f carried by friction

All this shows, that the limited friction transfer also explains the reduction of the effective concrete strength with increasing tranverse strain, which was pointed out by Collins et al /9, 10, 11/; a direct comparison was given in /14/. Furthermore however, the crack spacing and thereby the crack width have an influence, since friction is involved and it is not only a problem of "compression with transverse tension" (as also only in most tests) or of "compression-softening". Consequently it means reversing cause and effect if the "shear

transfer strength" is explained by the "softening" of the concrete as done by Hsu /18/. The force transfer over cracks is a discrete problem and must be dealt with as such, similar to the force transfer over joints as discussed by Ruth /19/. Both problems require a model for the structural behaviour of the whole member, but they also have an influence on it, e.g. in terms of a low "effective strength". Finally it must be mentioned that there might be further causes for a strength reduction as shown by Thürlimann /20/.

RFERENCES

1. IABSE Colloquium "Structural Concrete". Introductory Reports. Stuttgart, April 1991
2. Reineck, K.-H.: A mechanical model for the behaviour of reinforced concrete members in shear (in German), Dr.-thesis., Univ. Stuttgart, 1990, 1-273
3. Kupfer, H.; Mang, R.; Karavesyroglou, M.: Failure of the shear-zone of r.c.- and p.c.-girders - an analysis with consideration of interlocking of cracks (in German). Bauingenieur 58 (1983), 143-149
4. Kirmair, H.; Mang, R.: The structural behaviour of the shear-zone of slender r.c.- and p.c.-girders with bending and axial force (in German). Bauingenieur 62 (1987), 165-170
5. dei Poli, S.; Gambarova, P.G.; Karakoc, C.: Aggregate interlock role in r.c. thin-webbed beams in shear. ASCE-Jour. Struc.Div. 113 (1987), 1-19
6. Fenwick, R.C.; Paulay, T.: Mechanisms of shear resistance of concrete beams. ASCE-Journal Struct.Div. V.94, 1968, ST 10, Oc., 2325-2350
7. Lipski, A.: Poutres a âme mince en béton armé ou précontraint. Ann. d. Travaux Publ. d. Belgique No.1-2, 1971/72
8. Schlaich, J.; Schäfer, K; Jennewein, M: Toward a consistent design for structural concrete. PCI-Jour. 32 (1987), No.3, p.75-150
9. Vecchio, F.J.; Collins, M.P.: The modified compression field theory for reinforced concrete elements subjected to shear. ACI Struct.Jour. 83 (1986), March-April, 219-231
10. Bhide, S.B.; Collins, M.P.: Influence of axial tension on the shear capacity of reinforced concrete members. ACI Struct.Jour. 86 (1989), Sept.-Oct., 570-581
11. Collins, M.P.; Mitchell, D.: Shear and tension design of prestressed and non-prestressed concrete beams. PCI Jour. 25 (1980), Sept.-Oct., 32-100
12. Hardjasaputra, H.: Consideration of the state of strain in the shear design of r.c.- and p.c.-girders (in German). Dr.-thesis, University of Stuttgart, 1987
13. Reineck, K.-H.; Hardjasaputra, H.: State of strain in the shear design of r.c.- and p.c.-girders (in German). Bauingenieur 65 (1990), H.2, 73-82
14. Reineck, K.-H.: Theoretical considerations and experimental evidence on web compression failures of high strength concrete beams. CEB Bull. 193, 61-73, Lausanne 1989
15. Reineck, K.-H.: A mechanical model for structural concrete members without transverse reinforcement. IABSE Colloquium "Structural Concrete", Stuttgart, April 1991
16. Leonhardt, F.; Walther, R.: Shear tests on simple r.c.-beams with and without shear reinforcement (in German). DAfStb H.151, Berlin 1962
17. Kupfer, H.; Guckenberger, K.: Tests on the structural shear behaviour of profiled r.c.- or p.c.-girders with compressed flanges (in German). DAfStb H.377, Berlin, Ernst & Sohn, 1986
18. Hsu, T.T.C.: Softened truss model theory for shear and torsion. ACI Struct. ACI Struct.Jour. 85 (1988), Nov.-Dec. 624-625
19. Ruth, J.: Influence of contract surface problems on design practice. IABSE Colloquium "Structural Concrete", Stuttgart, April 1991
20. Thürlimann, B.: Theory of plasticity for reinforced concrete (in German). Course summerterm 1985, Univ. Stuttgart, Institut für Massivbau.

Deformation and Bending-Shear-Torque Failure

Déformation et rupture sous l'action de flexion, cisaillement et torsion

Verformung und Versagen unter Biegung, Schub und Verdrehung

Petr RERICHA
Senior Lecturer
Czech Techn. Univ.
Prag, Czechoslovakia

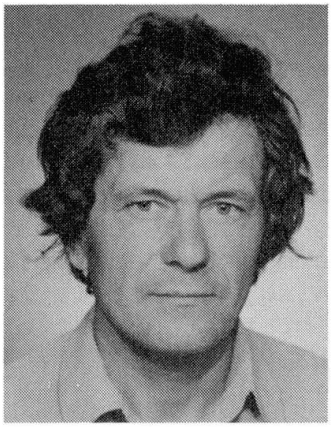

Petr Rericha, born 1944, received his engineering degree from the Faculty of Civil Eng., Technical University Prague. Ever since he has been active in structural mechanics, particularly FEM. He is now back at his alma mater.

SUMMARY

It is proposed that nonlinear continuum analysis by the finite element method will become the standard method for the analysis and dimensioning of structural concrete. Potential simplifications of the method are indicated. A simple, unified, continuum model is proposed for beams, slabs and shells.

RÉSUMÉ

Une analyse non linéaire de la structure, utilisant la méthode des éléments finis est proposée afin d'obtenir un modèle unifié de dimensionnement du béton armé Les simplifications potentielles introduites par la méthode sont indiquées; un modèle de continuité unifié est ensuite introduit pour le cas des poutres, dalles et coques.

ZUSAMMENFASSUNG

Die nichtlineare Analyse des Kontinuums mit Hilfe der Methode der Finiten Elemente wird als einheitliche Methode für die Berechnung und Bemessung des Konstruktionsbetons vorgeschlagen. Mögliche Vereinfachungen der Methode werden aufgezeigt. Es wird ein einfaches und einheitliches Kontinuum-Modell für Balken, Platten und Schalen vorgeschlagen.

1. INTRODUCTION

The assessment of the present design practice as well as the objectives presented in the Breen's introductory report reflect actual, real and even acute needs of the building industry and research. The present paper adresses two of the objectives set forth in the report which call for the consideration of the overall structural behaviour and for new transparent methods.

It is common practice that the overall structural behaviour is analyzed by conventional elasticity models. They provide cross-sectional variables for dimensioning but hardly reflect the actual flow of the forces throughout the structure even at service load level not to speak of the ultimate limit load state. This practice entails strictly sectional approach in dimensioning and detailing. Apparently, it also is inconsistent from the purely mechanical point of view in regard to statically indeterminate structures. Actual flexibility of a reinforced concrete structure is far from that assumed in the elastic analysis. If some more global models are used for dimensioning, typically strut-and-tie models (STM), then in effect some of the conventional elasticity analysis might be eliminated. Marti [3], for example, suggests the application of the STM for continuous beams. The sole purpose of the elastic analysis then is to determine the residual forces (reactions at intermediate supports in the above example). Even these moments can be modified (to some extent arbitrarily) owing to redistribution.

Another substantial flaw of this inconsistent mixture of the elastic analysis and limit state dimensioning turns up when the limit state of deformations is considered. Here the results of the elastic analysis are literally useless. Moreover, the rules for the evaluation of deformations of reinforced concrete members are a real maze in the Czechoslovak standards. These considerations suggest that a consistent unified approach to structural concrete should avoid the traditional elasticity methods of analysis.

2. NONLINEAR CONTINUUM APPROACH

At present there is no feasible method that could replace the elasticity methods. It also seems to be too daring an idea to develop what in fact would be 'another nonlinear mechanics', specific for reinforced concrete. In the long perspective, however, taking into account the amazing advance of the computer technology it seems more imaginable. What should feature such a method?

First, it must be nonlinear since reinforced concrete simply is not linear elastic even at service loads. This brings about the problem of variable loads. Various load cases must be analyzed separately in the realm of the nonlinear analysis. But even today there is a trend to reduce the number of load cases and an exact evaluation of the absolute maxima of the cross-sectional forces is not deemed necessary. A compromise appers to be attainable in this respect.

Second, the method should be able to furnish strains, deflections, stresses and forces at various load levels. Single computational model can then be used to assess all kinds of limit states. This need has indirectly been emphasized in the 'Performance requirements' of the Breen's introductory report. STM approaches

cannot meet this requirement.

An incremental nonlinear finite element analysis (FEA) meets this requirements at the expense of prohibitive demands on the computer and analyst parts. There is, however, a great potential for reducing these demands if the material models are simplified to the level required for design purposes. Hardly any FEA package has yet tried to do so. An obvious possibility is to neglect the tension strength of the concrete as most building codes do. The cost of the nonlinear analysis may also be greatly reduced if we realize that severe nonlinearity occurs just in the initial phase of the gradual loading when the crack pattern develops. In this phase, a continuum analogy to the STM builds up. Subsequent loading invokes almost linear behavior. An obvious advantage of the nonlinear continuum analysis is that less engineering judgment or intuition is required in comparison to STM. It should also be recalled that the finite element discretization provides a natural support for the visualization of the structure and its displacements, strains and the flow of internal forces. Current computer graphics software and hardware relies on discretizations identical or similar to those adopted in the FEA. This aspect might become decisive in the future.

3.DEFORMATION PATTERN IN RC BEAMS

As already pointed out earlier, specific simple design oriented material models are necessary in order to make the nonlinear analysis acceptable. The models for B regions of beams, plates and shells should employ appropriate kinematic hypotheses. Present model is based on the assumption of plane cross-sections (Timoshenko or Flugge hypothesis in the scope of plane frame beams). In reinforced concrete beams, this assumption is not sufficient. The deformation pattern must include the transverse strains ε_y , ε_z if stirrups and hoops are to be activated. An obvious possibility is to supplement the required displacement modes into the assumed displacement field. Compatibility of deformations is then maintained but special finite elements are required and in effect fully three-dimensional analysis is entailed. We prefer another option.

The assumed displacement field remains that of the space beam and the strains ε_y and ε_z are evaluated from the transverse equilibrium equations $\sigma_y = \sigma_z = 0$. Compatibility is violated by the terms $\partial v/\partial x$ and $\partial w/\partial x$ where v, w denote the transverse displacements relative to the displaced local reference frame of the cross-section. These terms may be neglected if the displacement field varies only gradually along the x-axis. Analogous assumption on the stress field has been utilized in the derivation of the above transverse equilibrium equations and Marti[3], Nielsen[4] and Harmon[1] also adopted it. The strains ε_y and ε_z must be solved for by an iteration since the material laws of concrete and reinforcement steel are nonlinear.

The discretization in the cross-section plane is performed by dividing it into sufficiently small subregions. In each subregion, homogeneous stress and strain are assumed. This is a direct generalization of the layer concept in the analysis of reinforced concrete plates and shells. Perfect bond is assumed. The same

strains thus apply to concrete and reinforcement. Reinforcement bars of any directions are easily included and equally treated. It is important to note that an analogous deformation pattern was developed for reinforced concrete plates and shells. In these structures, there is just one condition of the transverse equilibrium and one corresponding transverse strain component to be solved for. The formulation is simpler. On the contrary, adequate STM are staticaly determinate spatial trusses which may be dificult to construct.

Simple elastic-plastic laws were implemented (principal stresses plasticity condition for concrete) and several sample solutions carried out for the purpose of validation. Most are plane frame beams (no torsion). The T-beam in Fig.1 was tested by Leonhardt[2] for bending-shear failure.

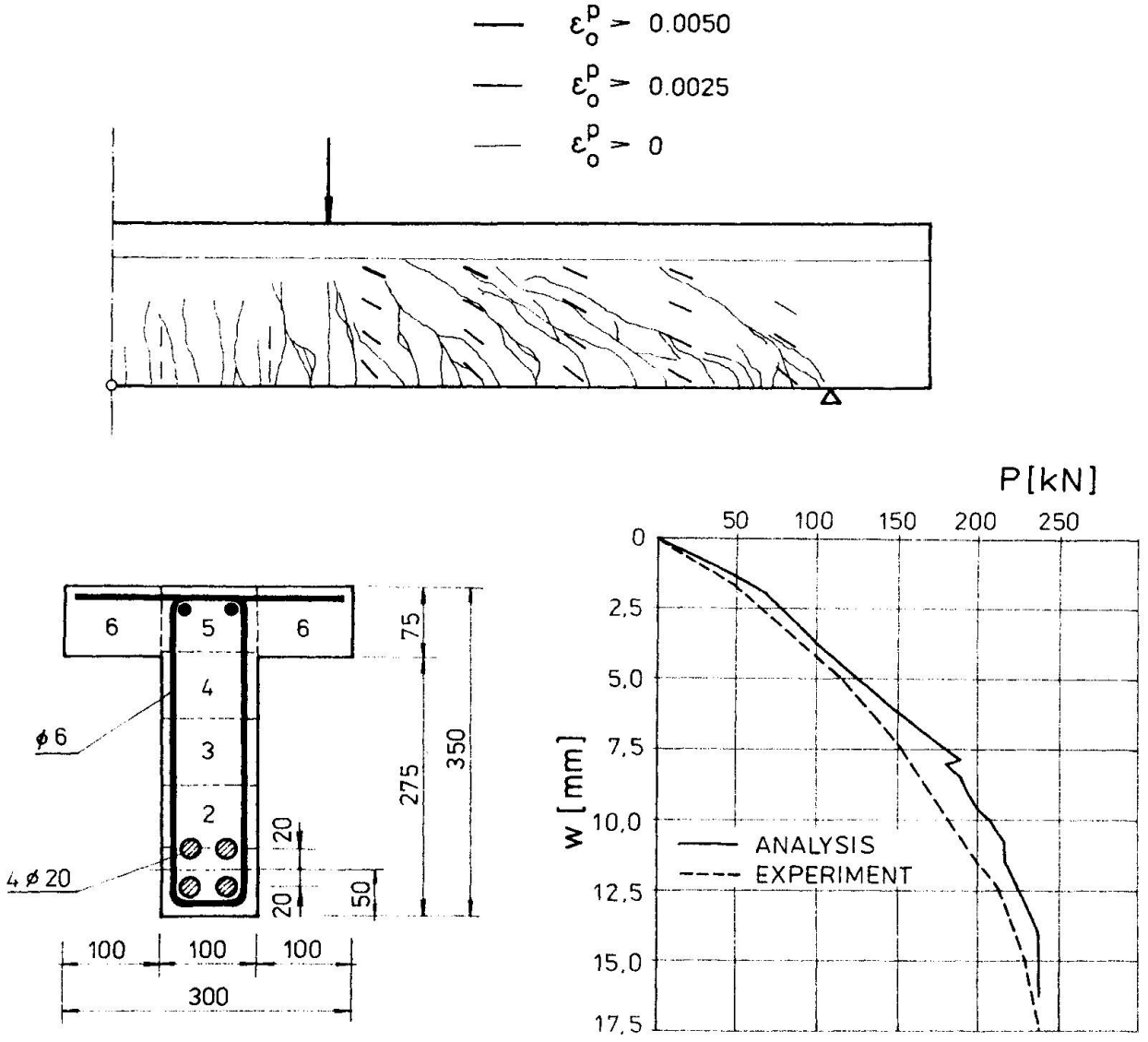

Fig.1 Cross-section, crack pattern (test and analysis) and load deflection curve of a T-beam

The crack pattern at failure compares well to the experimental one

and so does the load-deflection curve. The smeared crack width and the direction of the cracks of the analytical (FEA) solution are indicated by abscissas. Actual stiffness and deformation pattern are well modeled. It is worth mentioning that only 7 finite elements were used in this example. The cross-section was divided into 6 concrete subregion (see Fig.1) and 2 reinforcement layers. Tension strain softening was adopted in this example for concrete and the load-deflection graph is therefore curved. If tension-cut-off concrete is adopted the graph is nearly straight.

4.CONCLUSIONS

Nonlinear continuum modeling of structural concrete is proposed to become a unified analytical and dimensioning tool. Possible simplifications of the nonlinear analysis were indicated which would make it more accesible to designers and engineers. A simple model for beams subjected to simultaneous flexure, shear and torsion is described. The model easily includes arbitrary reinforcement. A sample solution demonstrates that the actual crack pattern and corresponding STM action are well approximated by the proposed model.

REFERENCES

1. HARMON T.G., ZHANGYUAN N., Shear strength of reinforced concrete plates and shells determined by finite element method using layered elements. J. Struct. Engng,ASCE,115,1989,p.1141
2. LEONHARDT F., WALTHER R., Stuttgarter Schubversuche 1961. Beton und Stahlbeton 1962,special issue
3. MARTI P., Paper submitted to the sub-theme 2.4: Dimensioning and detailing, Structural Concrete 1990
4. NIELSEN M.P., Om forskydningsarmering af Jernbetonbjaelker. Bigningsstat. Medd.,38,1967,p.33

Leere Seite
Blank page
Page vide

Combined Loading Effects in Concrete Box Girders

Effets des efforts combinés dans des poutres-caisson en béton

Kombinierte Beanspruchung von Kastenträgern aus Beton

Herbert KUPFER
Prof. of Struct. Eng.
Univ. of Munich
Munich, Germany

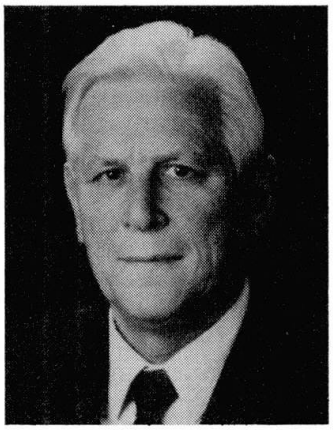

H. Kupfer, born in 1927, obtained his civil eng. degree at the Univ. of Munich in 1949. He was an assistant of Prof. Hubert Ruesch for 6 years. After that he worked at the construction company DYWIDAG, finally as chief engineer. Since 1967 he is full Professor for structural eng. at the Univ. of Munich.

Hans BULICEK
Res. Assist.
Univ. of Munich
Munich, Germany

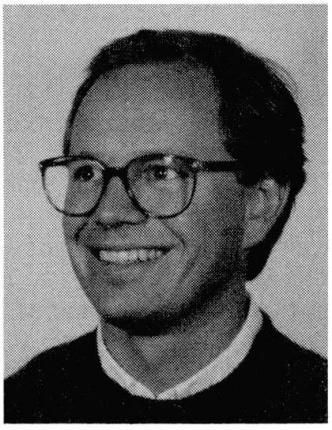

H. Bulicek, born in 1961, obtained his civil engineering degree at the University of Munich in 1988. Since that time he is working as an assistant of Professor Herbert Kupfer.

SUMMARY

Concrete box girders are often subjected to substantial combined loading effects such as bending moments, normal forces, shear forces and torsional moments as, e.g. in the case of cable-stayed bridges suspended in the middle axis. Based on the «shear-wall-model» a consistent design method for the ultimate limit state is presented.

RÉSUMÉ

Les poutres-caisson en béton sont souvent substantiellement soumises aux actions combinées des moments de flexion, de l'efforts normal, des efforts tranchants et des moments de torsion, comme par exemple dans le cas de ponts haubanés soutenus par les câbles d'un support central. Une méthode cohérente de dimensionnement est présentée ici afin d'évaluer l'état de limite ultime.

ZUSAMMENFASSUNG

Kastenträger aus Beton unterliegen oft hohen kombinierten Beanspruchungen aus Biegung, Normalkraft, Querkraft und Torsion wie zum Beispiel bei Schrägkabelbrücken mit Mittelaufhängung. Auf der Grundlage des Schubwandmodells wird ein konsistentes Bemessungskonzept für den rechnerischen Bruchzustand vorgestellt.

1. INTRODUCTION

National codes as well as international codes dealing with concrete structures mostly cover the combined effects of actions by the use of empirical formulas or even neglect the interaction. A standardized consistent design model is missing. A more detailed consideration of the combined action-effects especially is recommended for slender box girders which are substantially subjected to combined effects of actions such as bending moments, normal forces, shear forces and torsional moments.
This paper presents a universal method for the design of concrete box girders in the ultimate limit state by the use of the "shear-wall-model" under consistent consideration of the load transfer by the webs and the chords. Combined action-effects such as slab moments and in-plane load are not treated in this paper.

2. DESIGN PROCEDURE

2.1 Design Principle

As long as bending moments acting in a horizontal plane are not considered, the action-effects such as bending and normal force as well as the longitudinal forces resulting from the diagonal compression field in the webs are allocated to the chords. The webs carry the shear forces. Torsional moments, however, affect webs and chords. Following this rule of distributing the action-effects, slender beams such as box girders can be divided into "shear-walls" being dimensioned for parts of the considered effects of actions. By this way inconsistences and overstresses are avoided. The distribution of the considered action-effects within the respective shear walls is given if a suitable inclination θ of the resulting compressive stress field in each web is derived according to the next paragraph. With regard to the following explanations it is required that the shear reinforcement is located rectangular to the axis of the beam. Furthermore all strengths, strains and action effects are supposed to be derived at "design level" according to reference [1] so that the subscript "d" is renounced within this paper. The action-effects thereby have to be derived taking account of prestressing forces.

2.2 Webs

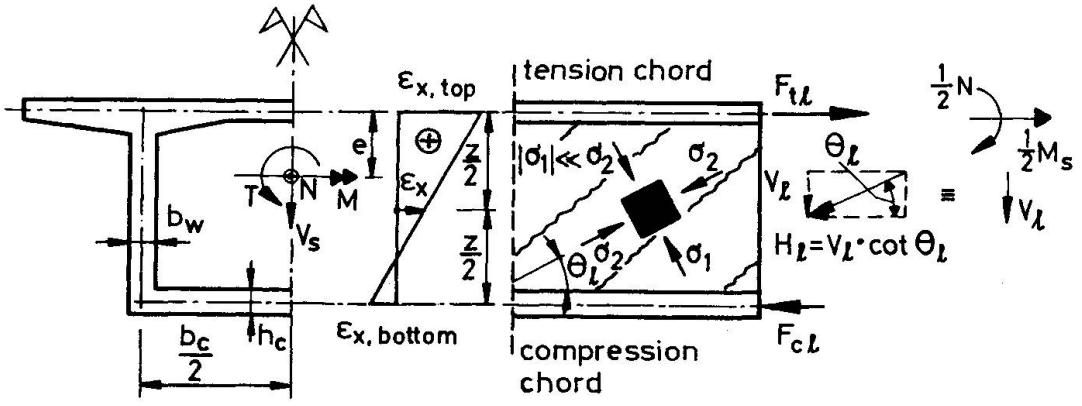

Fig. 1 Notations

Webs of continous beams mainly are subjected to shear forces V_s and the effects V_t of torsional moments T. For bearing this kind of action-effect the modified truss analogy turned out as a suitable model for calculating the magnitude of concrete stresses as well as the amount of the required shear reinforcement in the webs. In reference [2] a consistent model for calculating the resulting stress state in the webs has been developed. The model fulfills the compatibility of deformations in the web and considers the influence of the average axial strain ϵ_x of the chords upon the shear resistance of the webs. It turns out that a biaxial stress field prevails in the web concrete characterized by a predominating principal compressive stress σ_2 and a perpendicular acting subordinated principal compressive or tensile stress σ_1 (see figure 1). For practice design, however, it is confirmed that a uniaxial compressive field in the web concrete is a suitable approximation. Figure 1 illustrates the left part of a box girder (subscript "1") as well as the used notations.
Based on the above mentioned model the following applicable design formula can be derived for calculating the inclinations θ of the uniaxial compression field in the web on the left ($\rightarrow \theta_l$) and on the right hand side ($\rightarrow \theta_r$):

$$\tan\theta = 1 - [\Delta\tan\theta_{plast}] \cdot \frac{0.0015 - \epsilon_x}{0.003}$$

where $$\Delta\tan\theta_{plast} = 1 - \tan\theta_{plast} = 1 - \frac{1 - \sqrt{1 - \nu^2}}{\nu}$$

so that the complete formula is:

$$\tan\theta = 1 - \left(1 - \frac{1 - \sqrt{1 - \nu^2}}{\nu}\right) \cdot \frac{0.0015 - \epsilon_x}{0.003} \qquad \begin{cases} \tan\theta \geq \frac{1}{3} \\ \tan\theta \geq \frac{1 - \sqrt{1 - \nu^2}}{\nu} \end{cases} \qquad (1)$$

where $$\nu = \frac{2V}{b_w \cdot z \cdot f_{cd2}} \qquad (2)$$

The vertical force V in equ. (2) acting in the web has to be determined for the web on the left hand side (V_l) as well as on the right hand side (V_r) according to the following equations:

$$V_l = \frac{V_s}{2} + \frac{T}{2b_c}; \qquad V_r = \frac{V_s}{2} - \frac{T}{2b_c} \cdot \qquad (3)$$

Thereby the average strain ϵ_x of the webs follows from the strains in the chords as:

$$\epsilon_x = \frac{\epsilon_{x,top} + \epsilon_{x,bottom}}{2} \qquad (4)$$

where the chord strains (considered as positive in case of tensile strain) have to be derived taking account of the chord forces given by equ. (7) and (9) respectively. The required iterative calculation of ϵ_x and θ shows a quick convergency since the strain in the chords is influenced only slightly by the value of θ.
Thus the resulting amount of vertical shear reinforcement can be derived from:

$$\omega = \frac{2 \cdot A_{sw} \cdot f_y}{s \cdot b_w \cdot f_{cd2}} = \nu \cdot \tan\theta = \frac{2 \cdot V}{f_{cd2} \cdot b_w \cdot z} \cdot \tan\theta \cdot \qquad (5)$$

Figure 2 illustrates the resulting design curves according to the preceding equations.
The associated strut inclinations θ_l and θ_r for the web on the left as well as on the right hand side can be read from figure 2 taking account of the average axial strain in the chords according to equ. (4). Thus the resulting horizontal tensile force which has to be considered with regard to the chords in addition to the effects of M and N is:

$$\Sigma H = H_l + H_r = |V_l| \cdot \cot\theta_l + |V_r| \cdot \cot\theta_r \cdot \qquad (6)$$

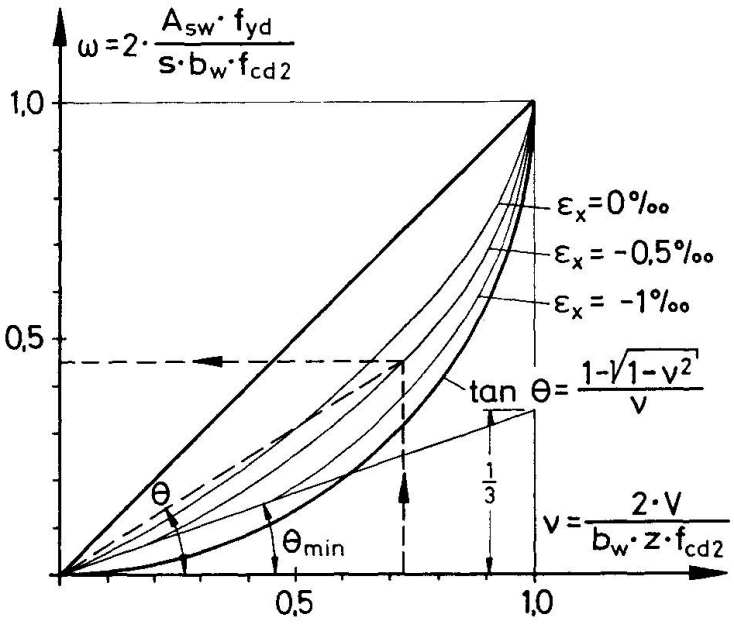

Fig. 2 Required vertical shear reinforcement in the web

2.3 Chords

2.3.1 Compression chords

The compression chords in concrete box girders are subjected to the longitudinal compressive force F_c:

$$F_c = \frac{M_s}{z} - \frac{\Sigma H}{2} \quad \text{whereby} \quad M_s = M + N \cdot e \tag{7}$$

Furthermore they are affected by a variable shear flow having a magnitude of V_l/z on the left and of V_r/z on the right hand side resulting from shear and torsion (see figure 3). With regard to the following evaluation the course of this shear flow is supposed to be approximately linear although strictly speaking a nonlinear course adjusts between the left and the right hand side due to the differential connection to the associated longitudinal stresses σ_x. In a considered element the compressive strength f_{cd1} (according to [1] applying to a uniaxial loaded concrete prism under sustained load) can not be taken as the admissible longitudinal stress σ_x if shear stresses are acting at the same time. Therefore the ultimate longitudinal stresses σ_x (see figure 3) are determined in this paper in terms of the acting shear stresses in the compression chord by the use of a suitable fracture criterion for a combined loaded concrete element as illustrated in figure 4.

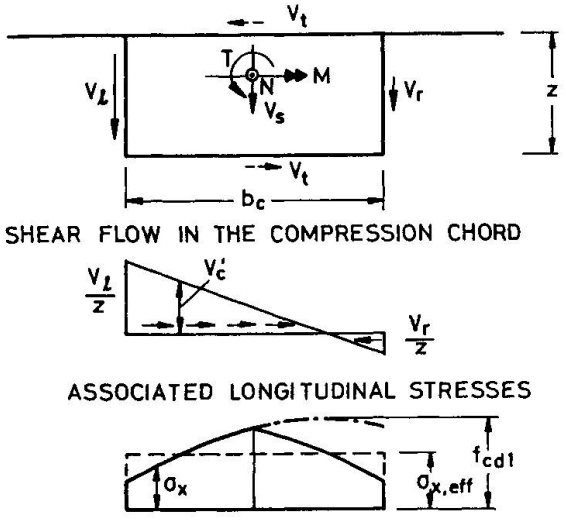

Fig. 3 Stress state in compression chords

In it the concrete compressive strength is supposed to be f_{cd1} in case of pure longitudinal compression of the uncracked concrete whereas it is reduced to $0.8\ f_{cd1}$ in case of pure shear due to the diminishing influence of cracks. The almost elliptic course of the interaction diagram of figure 4 in the range of $0{,}4 \leq \sigma_x/f_{cd1} \leq 1{,}0$ (passed through line) is obtained by the use of reference [3] assuming a magnitude for $\sigma_y = \rho_y \cdot f_y$ (represented by the transverse reinforcement) which leads to concrete failure in the element.

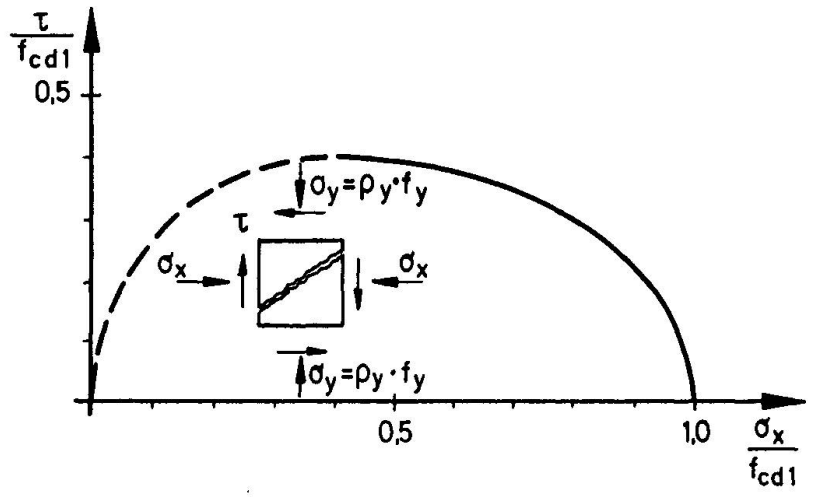

Fig. 4 Fracture criterion for a concrete element in concrete failure

As a simplification on the safe side the course of σ_x along the breadth of the compression chord is supposed to be symmetrically (More favourable values for σ_x could be obtained if the internal horizontal bending moment $(H_l - H_r) \cdot 0{,}5 b_c$ is taken into account for both chords). Thus an average ultimate longitudinal stress $\sigma_{x,eff}$ (see figure 5) is derived applying for combined loaded compression chords by assuming an optimized distribution of load effects within the compression chord according to the theory of plasticity. As a consequence the compressive force F_c according to equ. (7) has to fulfill the following inequality:

$$F_c \leq \sigma_{x,eff} \cdot b_c \cdot h_c \qquad (8).$$

In regions of the compression chord where $V_c' > F_c/b_c$ (for V_c' see figure 3) a longitudinal reinforcement acc. to $\rho_x \cdot f_y \cdot h_c = V_c' - F_c/b_c$ is required assuming a strut inclination of 45° and a uniform stress distribution of σ_x. The required amount of transverse reinforcement in compression chords can be derived by the use of reference [1].

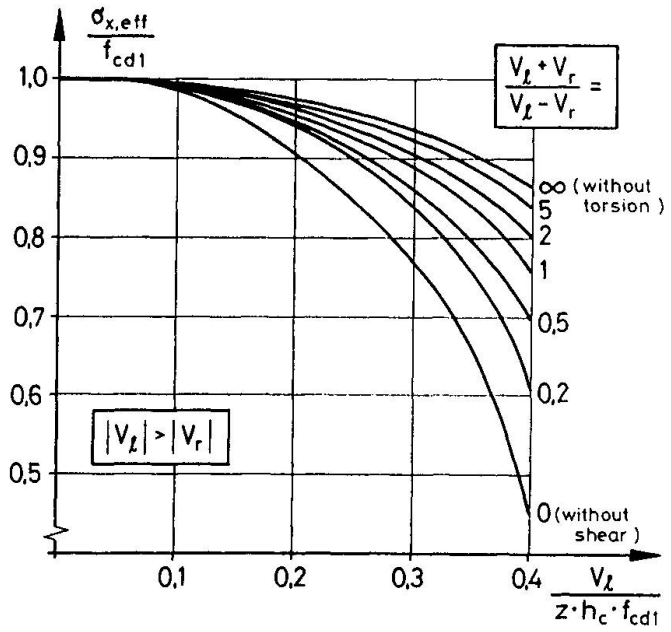

Fig. 5 Average ultimate compressive stress $\sigma_{x,eff}$ in terms of the acting shear forces in the webs

2.3.2 Tension chords

Tension chords in concrete box girders are subjected to the longitudinal tensile force F_t:

$$F_t = \frac{M_s}{z} + N + \frac{\Sigma H}{2} + \frac{T}{2z} \quad . \tag{9}$$

The term $\Sigma H/2$ in equation (9) only covers the horizontal part of the diagonal forces in the webs without including the effects of the diagonal stress field in the tension chord itself. Therefore only those prestressing tendons or reinforcing bars (crossing the decisive section) can be taken into account which are anchored more far from the decisive section than from the nearest web. This is not required for reinforcing bars or prestressing tendons which are curtailed due to a varying magnitude of the torsional moment supposing that this curtailed reinforcement is steady distributed within the tension chord inbetween the webs.

3. SUMMARY

This paper presented a consistent model for the design of concrete box girders which are subjected to combined action-effects. It is based on the shear-wall-model under consistent consideration of the load transfer by the webs and the chords. A simple formula for the determination of the resulting strut inclination in the webs under taking into account the chord strains was given to the designer. The resulting distribution of the inner forces within the cross section was observed and the resulting design forces allocated to the shear walls were obtained. Furthermore an average limit value for the ultimate longitudinal compressive stress in combined loaded compression chords was derived in terms of the acting shear forces in the webs.

REFERENCES

1. CEB-FIP Model Code for concrete structures 1990. Bulletin d'information Nº 196, Comité Euro-International du Béton. Lausanne, March 1990.

2. KUPFER H., BULICEK H., A Consistent Model for the Design of Shear Reinforcement in Slender Beams with I- or Box-Shaped Cross Section. Proceedings to the International Workshop on Concrete Shear in Earthquake, University of Houston, Texas, December 1990.

3. FIALKOW M. N., Crushing Strength of Reinforced Concrete Membranes. ACI Structural Journal, pp. 485-91, September-October 1988.

Reinforced Concrete Plates under Biaxial Bending Moments

Dalles en béton armé soumises à des moments de flexion biaxiaux

Stahlbetonplatten unter zweiachsiger Biegung

Kazuo YOKOZAWA
Manager
Maeda Corporation
Tokyo, Japan

Kazuo Yokozawa, born 1947, received his Dr. Eng. degree from the University of Nihon in 1989. He is engaged in the research on the design of reinforced concrete structures.

Junichiro NIWA
Assoc. Prof.
Nagoya University
Nagoya, Japan

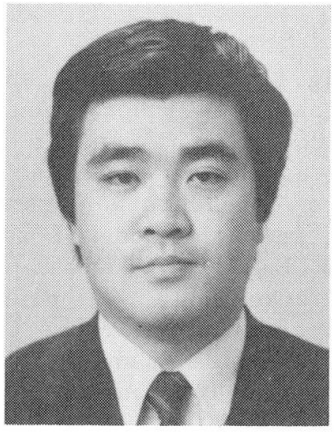

Junichiro Niwa, born 1956, received his Dr. Eng. degree from the University of Tokyo in 1983. He is engaged in research on the analysis of reinforced concrete members subjected to shear and torsion.

SUMMARY

This paper proposes a method of analyzing the strength and deformation of reinforced concrete slabs for out-of-plane biaxial bending moments. In the analytical method, the tension zone and the compression zone were divided into two discrete layers, and compression field theory was employed in analyzing reinforced concrete slabs under in-plane forces. The analytical method was verified using a newly-developed apparatus for out-of-plane biaxial bending tests.

RÉSUMÉ

Cet article présente une méthode d'analyse de la résistance et de la déformation de dalles en béton armé soumises à des moments de flexion biaxiaux hors du plan. Dans la méthode analytique, la zone tendue de même que celle comprimée furent divisées en deux couches discrètes et la théorie du champ de compression fut appliquée dans l'analyse de dalles armées soumises à une force dans le plan. La méthode analytique développé fut vérifiée grâce aux tests effectués à l'aide d'un bâti spécialement développé sous effort de flexion biaxiale hors du plan.

ZUSAMMENFASSUNG

Es wird ein Berechnungsverfahren für das Trag- und Verformungsverhalten von Stahlbetonplatten unter zweiachsiger Biegung vorgeschlagen. Dabei werden die Zug- und die Druckzone als zweiachsig beanspruchte Scheiben nach der Druckfeldtheorie behandelt. Das Berechnungsverfahren wurde durch Versuche in einer neu entwickelten Prüfmaschine bestätigt.

1. INTRODUCTION

With the recent increase of reinforced concrete structures constructed underground, designers are being faced with many problems. Side walls of underground storage tanks for crude oil or LNG, for example, are subjected to out-of-plane biaxial bending or torsional moments. Design methods, however, for reinforced concrete plates (RC plates) under such moments yet remain to be established. In this paper, an analytical method for RC plates under out-of-plane biaxial bending moments is presented. This paper also describes newly developed apparatus for out-of-plane biaxial bending tests, by which the validity of the above analytical method is verified. This study assumes pure bending condition without the influence of out-of-plane shearing force and it considers the deviation of principal moment in the direction of reinforcing bars.

2. ANALYTICAL METHOD FOR OUT-OF-PLANE BIAXIAL BENDING MOMENTS

2.1 Analytical Method

As shown in Fig.1, this method analyzes RC plates, by applying compression field theory, under in-plane forces N_1 and N_2 assumed in the zone of tensile stress due to bending. The method calculates the strength and the deformation of RC plates taking into consideration compatibility conditions for deformation between the zone of tensile and compressive stresses due to bending. Given average strain ε_{ct} perpendicular to cracks in RC plates, the method can calculate the unit compressive force C_1' due to bending from Bernoulli-Eulers' assumption, the stress-strain relationship of concrete and the conditions for equilibrium shown in Fig.2 and equation (1) ~ (3). Since the unit tensile force N_1 due to bending equals C_1 when strain reaches ε_{ct}, the location x of the neutral axis can be obtained by convergence calculation. Using the location x of the neutral axis, bending moment and curvature can be calculated and thus deformational behavior can be traced. Fig. 3 shows a flowchart of the above analytical procedure. The ultimate strength is judged when one of the following conditions was met:

i. Strain at the compressive edge of concrete after the yielding of x-axis reinforcing bars (reinforcing bars at a smaller deviation angle with the maximum principal moment M_1, see Fig. 4) reaches 0.35%.
ii. Y-axis reinforcing bars (reinforcing bars at a greater deviation angle with the maximum principal moment M_1) yields after the yielding of x-axis reinforcing bars.

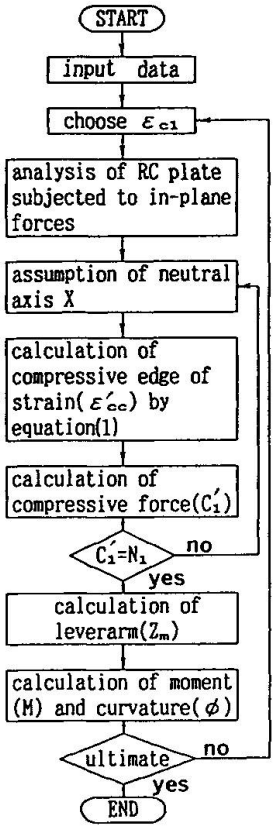

Fig.3 Flowchart for analytical method

$$\varepsilon'_{cc} = \frac{x}{d-x} \cdot \varepsilon_{ct} \quad (1) \qquad \sigma'_c = f'_c\,[2(\varepsilon'_c/\varepsilon_o) - (\varepsilon'_c/\varepsilon_o)^2] \quad (2) \qquad C_1' = \int \sigma'_c \cdot dx \quad (3)$$

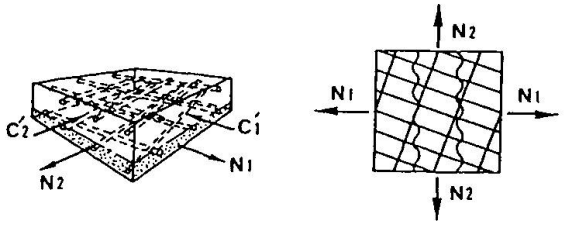

Fig.1 RC plate subjected to biaxial bending and RC plate subjected to in-plane forces assumed in tensile zone due to bending

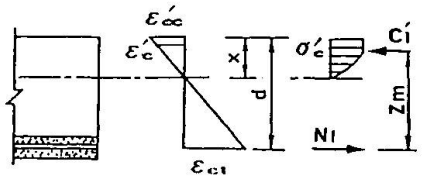

Fig.2 Assumption of strain profile and equilibrium of section

2.2 Analysis of RC Plates Under In-Plane Forces Based on the Compression Field Theory

2.2.1 Modeling of Cracks

A smeard crack model was employed, and RC plates with cracks were assumed to be continuous elements. Strain and stress dealt with in this paper, therefore, were assumed to be average strain and stress which were uniform within the element. It was assumed that the initial cracks occurred when tensile strain in the direction of the maximum principal stress reached 200μ. It was also assumed that even after the maximum principal stress reached the tensile strength, that stress was kept until tensile strain reached 200μ. Reinforcing bars in plates are usually arranged in two directions. It is likely, therefore, that reinforcing bars in the direction perpendicular to the principal moment which are virtually thought to be voids in concrete furthers the development of cracks. The cracking stress was hence determined according to equation (4) which takes this influence into consideration. Experiments conducted by the authors indicated that the direction of cracking, whether in one axis or two axes, remained throughout the cracking process. Consequently, it was assumed that the cracking direction was perpendicular to the maximum principal moment. Biaxial bending with a principal moment ratio of $Km=M_2/M_1=0.5$ or above causes cracking in two directions. To reflect this influence in the analysis, the authors decided to take account of the influence of bidirectional cracks in the evaluation of shear stiffness described later, while assuming that dominant cracks always occurred in a single direction.

$$f_t = 0.5\, f_c'^{\,2/3} \quad (kgf/cm^2) \qquad (4)$$

2.2.2 Stress-Strain Relationship

Stress was calculated using the average stress-strain relationships shown below. In the analysis, Vecchio-Collins Model which considers softening was used as the average stress-strain relationship in a direction parallel to concrete cracks [1], while Okamura-Maekawa Model which considers tension stiffening was used as the average stress-strain relationship in a direction perpendicular to the cracks [2]. For shear stiffness of RC plates after cracking, Aoyagi-Yamada Model was used [3]. It is to be noted, however, that since the average shear stiffness was being considered, the shear stiffness of uncracked portions and the Aoyagi-Yamada Model were serially connected to determine the average shear stiffness (equation (5) with $\beta = 1$).

2.2.3 Influence of Bidirectional Cracks

The analytical method described above is intented for concrete with unidirectional cracks. Experiments showed that cracks occurred in two directions for specimens under biaxial bending with a principal moment ratio of $Km=M_2/M_1=0.5$ or above. A modeling method, however, for bidirectional open cracks yet remains to be established. The authors had presumed that bidirectional cracks reduced the bond between reinforcing bars and concrete, thus decreasing tension stiffening and shear stiffness. From the results of trail calculation for test results, the influence of bidirectional cracks was clearly reflected in the shear stiffness model. When the ratio of the principal moments in two directions was $Km = M_2/M_1 = 1.0$ (cracks fully developed in both directions), the ability of shear transfer seemed to disappear almost. Hence the authors introduced the reduction coefficient β depending on the principal moment ratio Km and gave it as $\beta = 1-Km \leq 1.0$. Then shear stiffness Ga with bidirectional cracks was evaluated using equation (5).

$$Ga = \beta \cdot \frac{Gc \cdot Gcr}{(Gc+Gcr)} \qquad (5)$$

Note here that Gc which represents the shear stiffness of the uncracked portions is given as $Ec/2(1+\nu)$; where Ec is the elastic modulus of concrete,

and ν is Poisson's ratio of concrete. Gcr is the shear stiffness of the cracked portions and is given as $36/\varepsilon_{ct}$ (Aoyagi-Yamada Model).

2.2.4 Analytical Expression of RC Plates Under In-Plane Forces

This analytical method is based on the compression field theory of Vecchio-Collins. However, this method is characterized by clear distinction between the directions of the maximum principal strain (α) and the maximum principal moment (θ). If it is assumed that Mohr's circle applies to the maximum principal strain ε_{c1}, the minimum principal strain ε_{c2}, strains ε_x, ε_y and ε_{xy} in the directions of reinforcing bars, strain ε_{ct} perpendicular to cracks, strain ε_{cv} parallel to cracks, and shear strain γ_{ctv}, compatibility conditions in equations (6) and (7) should be satisfied, where θ is a deviation angle between the direction of the maximum principal moment and the x-axis reinforcing bars and α is an angle between the direction of the principal strain of RC plates and the x-axis reinforcing bars.

$$\varepsilon_x = \varepsilon_{c1}\cos^2\alpha + \varepsilon_{c2}\sin^2\alpha$$
$$\varepsilon_y = \varepsilon_{c1}\sin^2\alpha + \varepsilon_{c2}\cos^2\alpha \quad (6)$$
$$\gamma_{xy} = (\varepsilon_{c1} - \varepsilon_{c2})\sin 2\alpha$$

$$\varepsilon_{ct} = \varepsilon_{c1}\cos^2(\alpha - \theta) + \varepsilon_{c2}\sin^2(\alpha - \theta)$$
$$\varepsilon_{cv} = \varepsilon_{c1}\sin^2(\alpha - \theta) \quad \varepsilon_{c2}\cos^2(\alpha - \theta) \quad (7)$$
$$\gamma_{ctv} = (\varepsilon_{c1} - \varepsilon_{c2})\sin 2(\alpha - \theta)$$

Loads on RC plates are resisted by the stresses of reinforcing bars and concrete, and they can be added. If the principal strain ε_{c1} is given, stress in concrete in the x and y-axis directions can be calculated by equation (8) based on strain's compatibility conditions, the stress-strain relationship and the equilibrium of forces of the free body shown in Fig. 4 and Fig. 5. Equation (9) is obtained from the equilibrium of external and internal forces. If ε_{c1} is established and ε_{c2} and α are assumed, all internal forces can be calculated. The convergence calculation is carried out until the resultant n_x, n_y and n_{xy} equal the principal moment ratio km and the deviation angle θ of the principal moment.

$$\sigma_{cx} = \sigma_{ct}\cos^2\theta + \sigma_{cv}\sin^2\theta - \tau_{ctv}\sin 2\theta$$
$$\sigma_{cy} = \sigma_{ct}\sin^2\theta + \sigma_{cv}\cos^2\theta + \tau_{ctv}\sin 2\theta \quad (8)$$
$$\tau_{cxy} = (\sigma_{ct} - \sigma_{cv})\sin\theta\cos\theta + \tau_{ctv}\cos 2\theta$$

$$n_x = p_x\sigma_{sx} + \sigma_{cx}$$
$$n_y = p_y\sigma_{sy} + \sigma_{cy} \quad (9)$$
$$n_{xy} = \tau_{cxy}$$

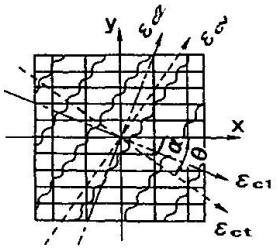

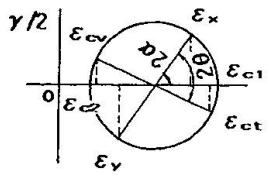

Fig.4 Average strains condition for RC plate element

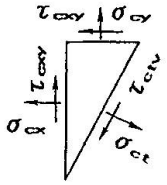

A direction perpendicular to the cracks

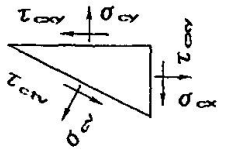

A direction parallel to the cracks

Fig.5 Average stresses acting on free-body in RC plate

3. COMPATISON OF TEST DATA AND CALCULATED VALUES

3.1 Biaxial Bending Test

An analytical model of this type requires verification using test data. However, reliable data on biaxial bending tests had not been available because of difficulty. Therefore an apparatus for biaxial bending tests of RC plates, was newly designed. It did not have the interaction of bending moments between each directions shown in Fig. 7. Using cruciform specimens shown in Fig.6, reliable test data on biaxial bending could be obtained. Table 1 summarizes the type of specimens, the compressive strength of concrete, cracking moment Mcr and the maximum moment M_u.

3.2 Comparison of Test Data and Calculated Values

3.2.1 Comparison on Deformation

When the deviation on angle θ between the directions of principal moment and reinforcing bars under uniaxial bending moment increases, the RC plates show a marked tendency toward decreased flexural rigidity. Comparison of test data and calculated values for the moment-curvature relationship is shown in Fig.8. For RC plates under biaxial bending moments, comparisons on the moment-curvature relationship and the moment-reinforcing bars' average strain relationship are shown in Fig. 9 and Fig. 10, respectively. This analysis can trace deformation until the ultimate state of RC plates because it considers the compatibility conditions of deformation between the tensile and compressive stresses zone due to bending. In this analysis, the reduction coefficient β =(1-Km) is also introduced. As shown in figures, both curvature and average strain calculated accurately represent the actual behavior of deformation from the beginning of cracks through the ultimate state. The figure also shows calculated values which do not consider β. The influence of not considering β is clearly reflected in the results of the evaluation of the reinforcing bars' strain. This implies that if β is not taken into consideration, deformation could be underevaluated when the reinforcement ratio in the y-axis direction is lower than in the x-axis direction.

3.2.2 Comparison on Ultimate Strength

Ultimate strength was estimated on the basis of the definition of the ultimate state described above. Comparison of the estimated values and the test values was shown in Table 1. Note that this comparison included data on not only RC plates under biaxial bending moments, but also those under uniaxial

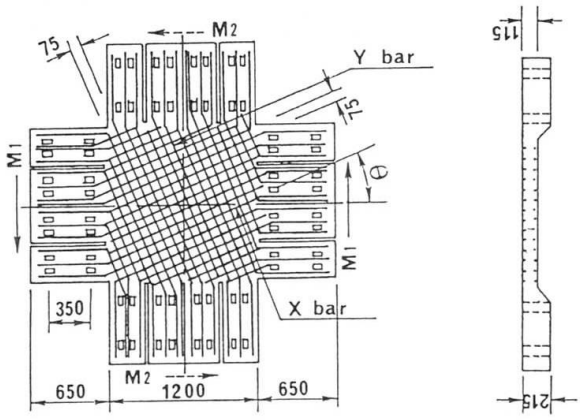

Fig.6 Shape and dimensions of typical specimen

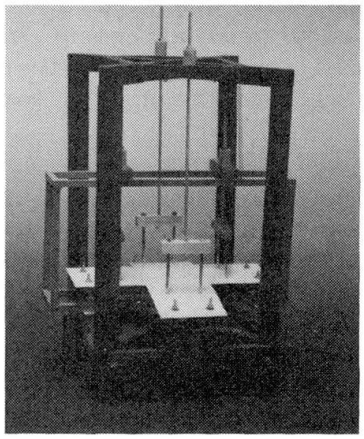

Fig.7 An apparatus for biaxial bending tests

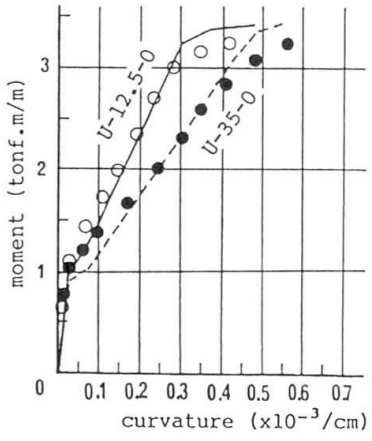

Fig.8 Comparison of test data and calculated values on moment -curvature relationship (uniaxial bending)

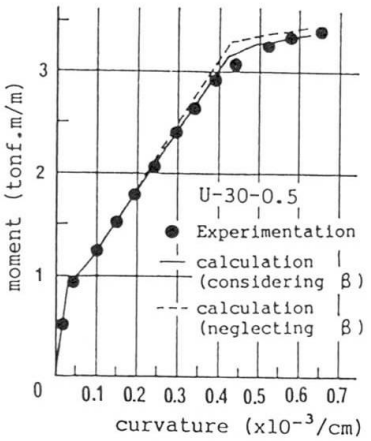

Fig.9 Comparison of test data and calculated values on moment -curvature relationship (biaxial bending)

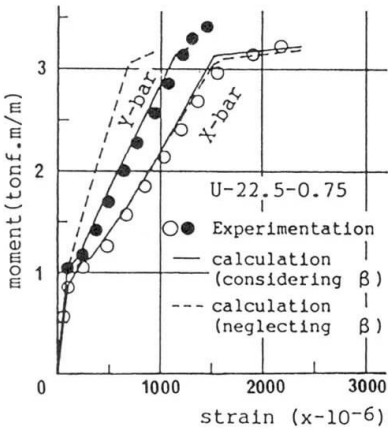

Fig.10 Comparison of test data and calculated values on moment -reinforcing bars' average strain relationship (biaxial bending)

bending moment. The analysis using ten data showed that the ratio of the test values to the calculated values averaged 1.03, giving the coefficient of variation of 4.8%. Although the average value was slightly high, the ultimate strength of RC plates under biaxial bending moment could be estimated with reasonable accuracy.

4. COMPARISON WITH OTHER APPROACHES

The analysis employed is a kind of sandwich method assuming a discrete layer between the compression zone and the tension zone. Some attempts have been made to analyze the behaviors of various members subjected to bending using sandwich models, and one of those was presented by Marti [4]. In his report, slabs were divided into an upper, a middle and lower layers; moment and axial force were resisted by the upper and the lower layers, while out-of-plane shearing force was resisted by the middle layer. In the model, the lever arm dv was assumed at 80% of thickness h. His proposed method of employing a truss mechanism in the middle layer is noteworthy. For the analysis of the upper and lower layers, compression field theory may be required. If the specimens used in this research were analyzed by the above methods, the ultimate strength obtained would show good agreement with test data. It is to be noted, however, that compatibility conditions in the upper and lower layers are not satisfied, those models will not be suited for the examination of serviceability limit state.

Specimen			Test Results			Calculation	M_{1utest}/M_{1ucal}
Mark	θ	K_m (M_2/M_1)	f'_c kgf/cm²	M_{cr} tonf·m	M_{1u} tonf·m	M_{1ucal} tonf·m	
U-0-0	0	0	261	0.98			
U-12.5-0	12.5	0	289	1.09	4.10	3.78	1.08
U-17.5-0	17.5	0	305	1.12	3.75	3.76	1.00
U-22.5-0	22.5	0	252	0.91	3.71	3.62	1.02
U-30-0	30	0	232	0.84	3.54	3.62	0.98
U-35-0	35	0	286	1.02	3.61	3.68	0.98
B-0-0.5	0	0.5	255	0.88	4.02	3.78	1.06
B-12.5-0.5	12.5	0.5	230	0.98	4.03	3.70	1.07
B-22.5-0.5	22.5	0.5	243	0.98	3.98	3.68	1.08
B-30-0.5	30	0.5	262	0.98	3.92	3.69	1.06
B-22.5-0.75	22.5	0.75	248	0.91	3.92	3.77	1.04

the averaged values = 1.03

coeffcient of variation = 4.8%

Table 1 Specimen properties, experimental and calculated value, and comparison of the both values

5. CONCLUSIONS

Here are the conclusions drawn from the study.

(1) Deformational behavior can be accurately traced by analyzing the lower layer of RC plates by compression field theory and by employing compatibility conditions of deformation between the upper and the lower layers.

(2) Accuracy of analysis can be enhanced by introducing the reduction coefficient β considering the influence of bidirectional cracks due to biaxial bending.

(3) Ultimate strength can be accurately represented by defining failure as a state with a strain of concrete's compressive edge of 0.35%, or as the yielding of reinforcing bars in y-axis direction.

The above results indicate that it is possible to unify the design process of RC plates under out-of-plane bending within the framework of the compression field theory as in the case of shear problems of RC plates under in-plane force.

REFERENCE

1. Vecchio,F.J. and Collins,M.P.: Response of reinforced concrete to in-plane shear and normal stresses, Publication No.82-03, University of Toronto, Mar., 1982.
2. Okamura,H.,Maekawa,K. and Izumo,J.: Reinforced concrete plate element subjected to cyclic loading, Proc. of IABSE Colloquium Delft,pp.575 589,Aug.,1987.
3. Aoyagi,Y.and Yamada,K.:Strength and Deformation Characteristics of Reinforced Concrete Shell Elements Subjected In-Plane Force,Proc. of JSCE,NO.331,pp.167~180.
4. Marti,P.: The preliminary paper, Proc.of IABSE colloquium Stuttgart, April.,1991.

Computer Programme for Consistent Design of Surface Structures

Programme d'ordinateur pour dimensionnement de structures planes

Programm zur konsistenten Bemessung von Flächentragwerken

Johann KOLLEGGER
Dr.-Ing.
Ingenieurbüro Mehlhorn
Kassel, Germany

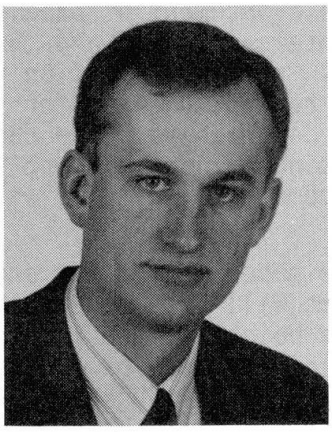

Johann Kollegger obtained his master of Eng. degree from the Univ. of California at Berkeley in 1980, his Dipl.-Ing. from the University of Graz in 1981, and his doctorate from the University of Kassel in 1988. Since 1988 he has been with a consulting firm in Kassel.

SUMMARY

A computer program for the design of the reinforcement of surface structures has been developed. For given thickness, concrete strength, and location of the reinforcement layers, the required reinforcement areas are calculated for any desired combination of in-plane forces and bending moments. The program can be used in a stand-alone version, for example to determine the load carrying capacity of critical points in reinforced concrete panel, plate, or shell structures. It may also be used as a post-processor for finite element programs determining the required reinforcement at each integration point.

RÉSUMÉ

Un programme d'ordinateur qui calcule l'armature des structures planes a été développé. L'épaisseur lui étant donnée de même que la résistance du béton et l'emplacement des nappes d'armatures, il calcule les sections requises d'acier pour toute combinaison de forces dans le plan de la dalle, ainsi que de moments de flexion. Le programme peut aussi être utilisé par exemple pour déterminer la capacité à supporter une charge de points critiques de structures en béton armé de type panneau, dalle ou coque. Il peut aussi être employé comme post-processeur de programmes d'éléments finis capables de déterminer l'armature requise en chaque point d'intégration.

ZUSAMMENFASSUNG

Ein Computerprogramm für die Bemessung der Bewehrung in Flächentragwerken wurde entwickelt. Für vorgegebene Dicke, Betonfestigkeit und Lage der Bewehrungsscharen werden die erforderlichen Bewehrungsflächen für jede beliebige Kombination von Scheiben- und Plattenbeanspruchungen ermittelt. Das Programm kann zur Ermittlung der Tragfähigkeit von einzelnen kritischen Punkten eines Stahlbetonflächentragwerks benützt werden. Es kann aber auch als Nachlaufprogramm eines Finite Elemente Programms zur Bestimmung der Bewehrungsflächen in jedem Integrationspunkt verwendet werden.

1. INTRODUCTION

Many equations for the determination of the reinforcement in panels for deviating principal stress and reinforcement directions have been published. Baumann [1] has presented a thorough treatment of the subject and also an equation for the design of the reinforcement of panels. The subject of dimensioning the reinforcement in panels subjected to general in-plane loading and in particular Baumann's equation are also discussed in Marti's report [2].

The equations for the reinforcement of panels can be applied to plate elements if the lever arm of the internal forces and the thickness of the load carrying covers is known, as is shown in section 4.4 of [2]. This approach leads to satisfactory results if a realistic guess for the internal lever arm and the depth of the concrete compressive zone can be made. If moments and in-plane compressive forces are acting on an element a realistic estimation of the internal lever arm may become difficult, as will be shown for an example below.

In the remainder of the paper a computer program for the design of reinforced concrete surface structures will be described, which is based on rational mechanic assumptions. The height of the internal lever arm and the depth of the concrete compressive zone need not to be guessed but are the result of the design process for an element subjected to arbitrary in plane forces and moments. Although the application of the computer program requires considerably more computations than programs based on Baumann's equation, this is no serious drawback considering the computing power already available in the design offices today.

2. ALGORITHM FOR THE DESIGN OF SHELL ELEMENTS

2.1 Layered shell element

In accordance with [2] the term shell element is used for an element which may be subjected to in-plane forces and moments. A shell element with unit dimensions in the x- and y-directions and the thickness t is shown in Fig. 1. The element is divided into concrete layers and reinforcement layers. The strain and stress state within each layer is uniform. Assuming a linear variation of the strains through the thickness the strain state in each layer can be calculated for known strains and curvatures of the middle surface.

2.2 Concrete layer

Under loading three states - uncracked, cracks in one direction, cracks in two directions - are possible in each concrete layer. A layer with cracks in one direction is shown in Fig. 2, where axes 1 and 2 denote the principal tensile and principal compressive strain directions, respectively.

The uniaxial stress-strain diagram of concrete is also shown in Fig. 2. The parabola-rectangle diagram of the German code [3] has been substituted by a fourth order parabola for numeric reasons. Tensile strength of concrete is set to zero and tension stiffening is also neglected since the program is to be used as a design tool. In accordance with the code [3] an increase of the concrete strength under biaxial compression will not be considered. Concrete under biaxial compression is analyzed with an orthotropic material model using

the stress-strain diagram of Fig. 2 in each principal strain direction and a shear modulus based on the tangent moduli in the principal strain directions.

Initially the cracks in a layer will form in a direction normal to the principal stress in concrete as soon as this stress becomes tensile. Upon increased loading the principal strain direction is adjusted according to the principle of the minimum of the internal energy. The crack direction and the direction of the concrete struts in a layer (Fig. 2) will always remain orthogonal to the principal tensile strain direction. Biaxial tension in a concrete layer will lead to the formation of two orthogonal sets of cracks and a complete loss of stiffness of this layer. The programing of this material model with re-orientation of the principal tensile strain direction, including the tension stiffening effect and an effective concrete strength depending on the transverse stress state has been described in [4].

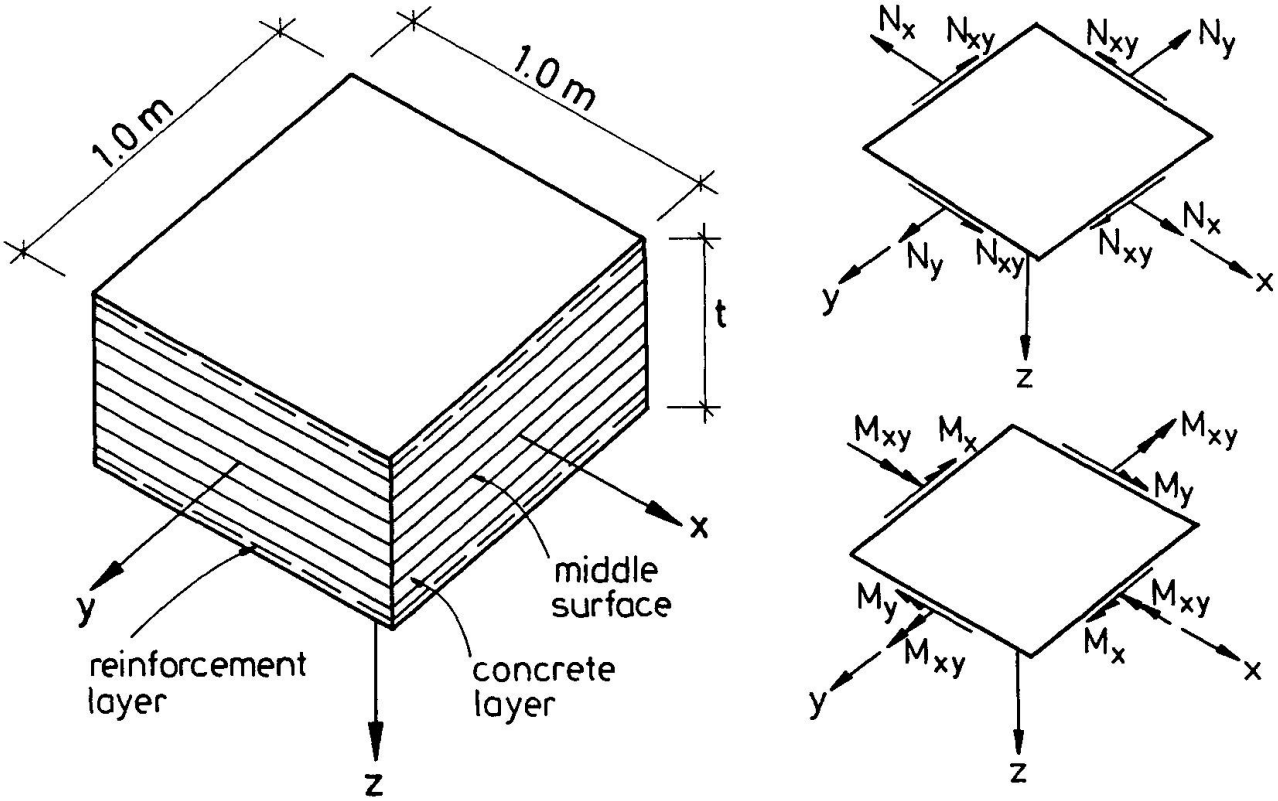

Fig. 1 Layered shell element (left), applied forces and moments (right)

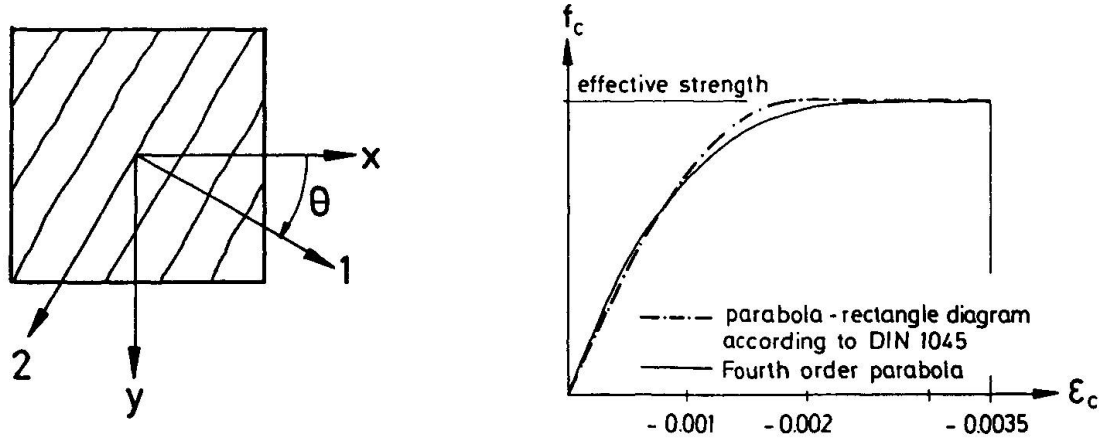

Fig. 2 Concrete layer with cracks in one direction (left) and uniaxial stress-stress strain diagram of concrete (right)

2.3 Reinforcement layer

A reinforcement layer is described by the area of reinforcement, the angle between x-axis and the reinforcing direction, and the distance of the reinforcement layer to the middle surface of the shell element (Fig. 3). An elastic-plastic stress-strain relationship with a hardening modulus is used for tensile and compressive strains as is also shown in Fig. 3. The hardening modulus is set to 1% of the elasitic modulus for numeric reasons. A strain cut-off is assumed for strains larger than 0.005 and smaller than -0.0035 in order to remain compatible with the code [3].

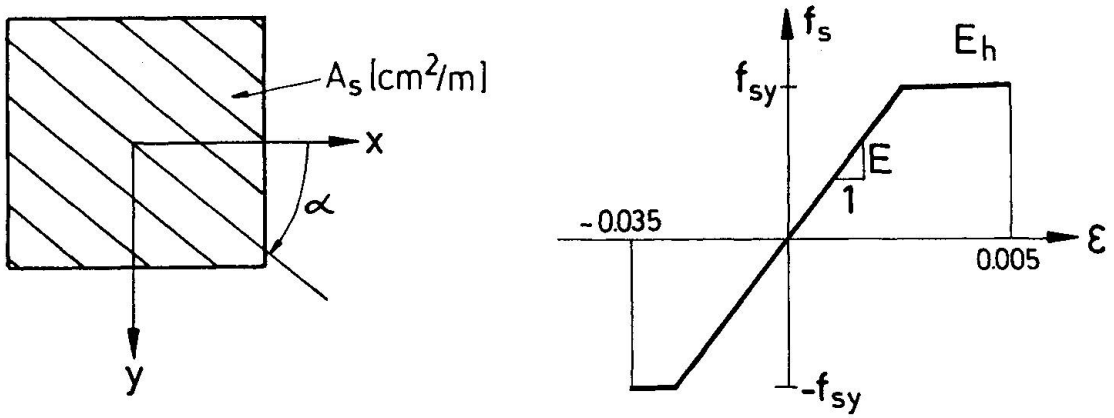

Fig. 3 Reinforcement layer and material model for the reinforcement

2.4 Numerical algorithm to determine the reinforcement of a shell element

The strains in the middle surface and the curvatures of the layered shell element are calculated for any set of applied external forces and moments in an iterative procedure. Starting with linear elastic material properties in the first iteration step, strains and curvatures are calculated. The strains in the individual layers are then determined, and using the material models for the concrete and the reinforcement described above the internal stresses of each layer are calculated. Integrating the internal stresses over the thickness of the element yields the internal forces and moments. Unbalanced forces and moments are calculated as the difference of the externally applied and the internal forces and moments of the element. The unbalanced forces and moments are applied to the layered shell element in the next iteration step. This procedure is repeated until the unbalanced member forces and the differences of the current strains and curvatures with respect to the ones of the last iteration step are smaller than required convergence limits. Then the external member forces of the next load step are applied to the layered shell element and the procedure described above is repeated starting with the element stiffness of the previous load step.

In order to automatically determine the ultimate load of a shell element subjected to proportionally increasing external member forces the following method is used: In the first step the external member forces corresponding to a load multiplier of 1.0 are applied to the shell element. Then the load multiplier is increased in a stepwise manner by 1.0 until no solution can be calculated, i.e. the ultimate load has been overestimated. In the following steps the intervalls are always divided into halves, until the difference between two consecutive load-multipliers remains under a predefined limit. For design examples a value of 0.01 is sufficient for this difference.

In using the layered shell element for the determination of the required reinforcement it is assumed that for each reinforcement layer the reinforcing direction, the distance to the middle surface, and the minimum reinforcement are known. In the first step of the automated design process the load-multiplier for a given set of external forces and moments is calculated with the minimum reinforcement. Then the reinforcement layer with the largest strain is strengthened by adding a reinforcement increment and the load-multiplier is calculated again and compared with the required safety coefficient. The incremental increase of the reinforcement areas of the individual layers and the incremental, iterative determination of the load-multipliers is continued until the required safety coefficient, e.g. 1.75 according to [3], is reached.

The incremental iterative procedure outlined above has been programmed in FORTRAN and implemented on a workstation. The validity of the program has been checked by analyzing numerous experimental tests on panel, plate and shell elements. Comparisons with design examples based on Baumann's theory showed that the same reinforcement areas as determined by Baumann's equation were obtained for panels with in-plane loading and for plates without large reinforcement ratios in the compression zone.

3. ELEMENT SUBJECTED TO AXIAL FORCE AND TWISTING MOMENT

A test program on reinforced concrete plates subjected to torsion was carried out by Marti et al. [5]. Here only plate ML5 will be considered which had a thickness of 20 cm and two reinforcement layers with 20 cm^2/m in in the x-direction and two layers with 5 cm^2/m in the y-direction. In the analysis an effective concrete strength of 25 MPa was used and the strain cut-off acc. to Fig. 3 was disabled. The envelope of the ultimate loads for different combinations of axial force and twisting moment is shown in Fig. 4. The calculated principal strains and the inclination of principal tensile strain direction are indicated for pure axial force, pure twisting moment, and a combination with Mxy=0.05Nx. While the ultimate load for pure axial force can easily be found by a hand calculation and the core model of [2] will predict the ultimate load for pure twisting moment, the intermediate points of the envelope are most easily determined by a nonlinear analyses with the layered shell element.

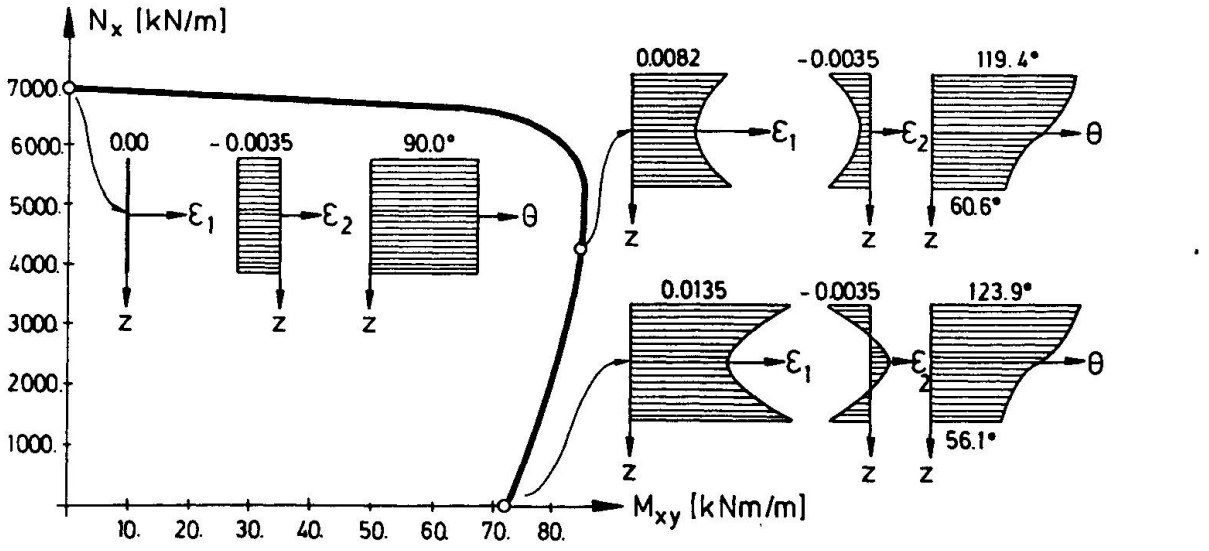

Fig. 4 Calculated ultimate load envelope and selected strain states of plate ML5 [5] subjected to axial force and twisting moment

4. ELEMENT SUBJECTED TO SHEAR FORCE AND BENDING MOMENT

The shell element SE7 was tested at the University of Toronto under a combination of shear force and bending moment [6]. In the following the reinforcement of the shell element will be determined for Nxy=1000 kN/m and Mx=113 kNm/m and a required load-multiplier of 1.75. The effective strength of the 28.5 cm thick specimen is taken as 70% of the cylinder crushing strength which was equal to 41.8 MPa. The yield strength of the reinforcement was 492 MPa and the four reinforcement layers had distances of -12.2 cm, -10.0 cm, 12.2 cm, and 10.0 cm, respectively. The reinforcement areas of the test specimen and the calculated strains at failure are shown in Tab. 1. The failure of the test specimen according to the analysis occured at a load-multiplier of 1.754, whereas a load-multilier of 1.81 is reported from the experiment [6].

For the design task the above mentioned properties remained unchanged. Only the reinforcement areas of the four layers were reduced to a minimum reinforcement of 5 cm²/m. The load-multipliers, reinforcement areas, and calculated strains are shown in Tab. 1 for the first step with minimum reinforcement, intermediate steps with stepwise increased reinforcement, and the final step with a load multiplier larger than 1.75. The determination of the required reinforcement areas took only a few seconds on a workstation.

load-	layer 1		layer 2		layer 3		layer 4	
multiplier	area cm²/m	strain	area cm²/m	strain	area cm²/m	strain	area cm²/m	strain
analysis of ultimate load with reinforcement areas of specimen SE7 [6]								
1.754	41.8	0.0003	13.9	0.0021	41.8	0.0033	13.9	0.0049
incremental, iterative determination of reinforcement areas								
0.283	5.0	0.0004	5.0	0.0011	5.0	0.0049	5.0	0.0020
0.508	5.0	0.0007	5.0	0.0018	11.0	0.0043	5.0	0.0023
1.095	5.0	0.0009	9.0	0.0023	23.0	0.0050	11.0	0.0044
1.539	5.0	0.0015	12.0	0.0038	33.0	0.0046	15.0	0.0043
1.752	5.0	0.0015	14.1	0.0035	37.6	0.0048	16.9	0.0047

Table 1 Analysis of specimen SE7 [6] with reinforcement areas of the test and incremental, iterative determination of reinforcement areas

REFERENCES

1. BAUMANN, T., Tragwirkung orthogonaler Bewehrungsnetze beliebiger Richtung in Flächentragwerken aus Stahlbeton. DAfStb, Heft 217, 1982
2. MARTI, P., Dimensioning and detailing. IABSE Colloquium on Structural Concrete, Stuttgart, 1991
3. DIN 1045, Beton und Stahlbeton, Bemessung und Ausführung, Juli 1988
4. KOLLEGGER, J. and MEHLHORN, G., Material model for the analysis of reinforced concrete surface structures. Comp. Mech., 1990
5. MARTI, P., LEESTI, P. and KHALIFA, W.U., Torsion tests on reinforced concrete slab elements. J. Struct. Div. ASCE, 1987, 994-1010.
6. KIRSCHNER, U. and COLLINS, M.P., Investigating the behaviour of reinforced concrete shell elements. P. 86-09, Dept. Civ. Eng., Univ. of Toronto, 1986.

A Consistent Shear Design Model for Concrete Offshore Structures

Modèle de dimensionnement à l'effort tranchant des structures en mer

Schubbemessungsverfahren für Beton-Offshore Strukturen

Perry ADEBAR
Assist. Prof.
Univ. of British Columbia
Vancouver, BC, Canada

Michael P. COLLINS
Professor
Univ. of Toronto
Toronto, ON, Canada

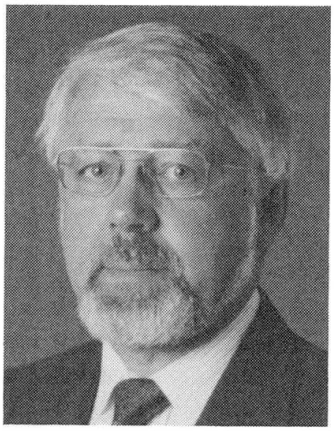

SUMMARY

A strain compatibility procedure for the sectional design of complex concrete structures is presented. The procedure, which is a generalization of the modified compression field theory for membrane elements, is capable of predicting the response of elements subjected to combined membrane forces, bending moments and transverse shear.

RÉSUMÉ

On présente ici une procédure basée sur la compatibilité des contraintes lors du dimensionnement de structures complexes tenant compte des efforts intérieurs. Cette méthode, généralisation de la théorie modifiée du champ de compression applicable aux éléments minces, est capable de prévoir la réponse d'éléments sollicités par des forces de membranes, des moments de flexion et des forces de cisaillement transversales.

ZUSAMMENFASSUNG

Diese Veröffentlichung beschreibt ein Kompatibilitätsverfahren für die Querschnittsberechnung von komplexen Betonstrukturen. Die Methode stellt eine Verallgemeinerung der modifizierten Druckfeld-Theorie für Membranelemente dar. Sie ermöglicht eine Berechnung des Elementverhaltens unter einer kombinierten Beanspruchung durch Membrankräfte, Biegemomente und Schub.

1. Introduction

Traditional sectional design procedures were developed for simple concrete structures such as buildings. The sectional forces (axial load, bending moment, and shear force) at various locations in a building frame are typically determined using a linear elastic analysis. In checking the ability of a particular section to resist the calculated stress resultants, the non-linear behaviour of concrete is taken into account. The response to axial load and bending moment is based on a strain compatibility approach, while shear design has traditionally involved empirical rules.

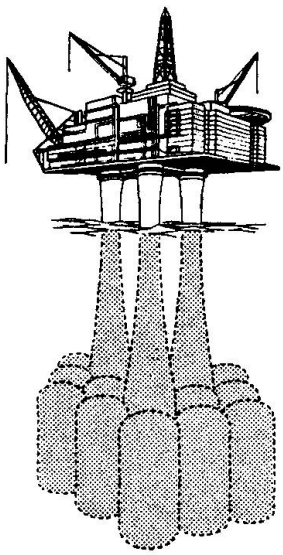

Fig. 1 Concrete Offshore Structure

The design of a more complex structure such as a concrete offshore structure (see Fig. 1) also involves determining the sectional forces at critical locations in the structure. Once again, linear elastic analysis is usually employed. However, the sectional forces for such a structure is considerably more complex. The loading demand at a particular location is expressed in terms of eight stress resultants, three membrane forces, N_x, N_y, N_{xy}, three bending moments, M_x, M_y, M_{xy}, and two transverse shear forces, V_x, V_y, (see Fig. 2). The method currently used to design offshore structures for the three membrane forces and the three bending moments is a generalization of the strain compatibility approach used for beams, while for transverse shear the empirical beam shear design rules are used. This paper describes a procedure in which membrane forces, bending moments and transverse shear can be considered in a consistent strain compatibility approach.

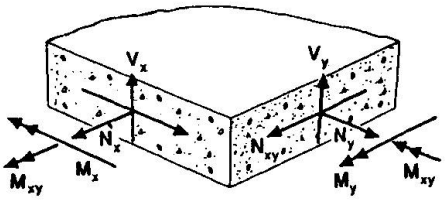

Fig. 2 Sectional Forces

2. Membrane Forces

The simplest "shear problem" is to predict the response of a reinforced concrete element subjected to only membrane forces, N_x, N_y, and N_{xy}. The problem involves relating the uniform biaxial strains ϵ_x, ϵ_y, γ_{xy} to the uniform biaxial stresses n_x, n_y, n_{xy}. A procedure for predicting the response of membrane elements was presented by Vecchio and Collins [1]. In this procedure, called the modified compression field theory, cracked concrete is treated as a new material with its own stress-strain characteristics. Rather than dealing with the variable local stresses (e.g., higher reinforcement stresses at a crack, lower away from the crack) the theory is formulated in terms of average stresses and average strains. In addition, the ability of the section to transmit the required forces across the cracks is specifically checked.

The biaxial stress-strain characteristics of cracked concrete were empirically determined from tests [1]. These tests showed that the principal compressive stress, f_{c2}, in cracked concrete is a function of not only the principal compressive strain, ϵ_2, but also of the co-existing principal tensile strain, ϵ_1. In addition, the tests showed that even severely cracked concrete stiffens the response of reinforcement. In the modified compression field theory this phenomenon is accounted for by assigning an average tensile stress to the concrete. After cracking, the average tensile stress in the concrete reduces as the strains increase (see Fig. 3).

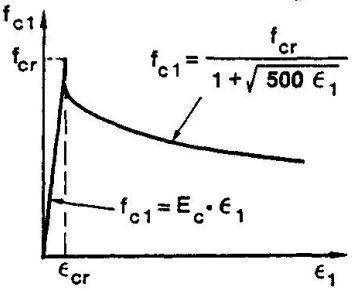

Fig. 3 Average Stress-Strain Relationship for Concrete in Tension

3. Membrane Forces and Bending Moments

A more complex problem exists when there are three bending moments, M_x, M_y, M_{xy}, in addition to the three membrane forces, because the stresses are now not uniform over the thickness of the

element. The problem can be solved using a strain compatibility procedure which is a generalization of the plane sections theory. The membrane strains, ϵ_x, ϵ_y, γ_{xy}, are assumed to vary linearly over the thickness of the element, and therefore can be described by six variables. Given the six strain variables, the stresses in the concrete and the reinforcement can be determined from the biaxial stress-strain relationships. Integrating the stresses over the thickness of the element gives the six stress resultants. The concrete stresses are integrated numerically by dividing the thickness of the element into a number of membrane elements.

Finding the stress resultants which are associated with a given set of strains is a direct procedure. However, if the six stress resultants are given and it is desired to find the six strain variables, trial and error is required. Program SEP [2] was developed based on this approach. It incorporates the procedures of the modified compression field theory as biaxial stress-strain relationships.

4. Equivalent Beam Approach for Transverse Shear

Post-processing design programs based on strain compatibility procedures have been used to check sections of concrete offshore structures for the case of combined membrane forces and bending moments. However, to account for the influence of transverse shear, the empirical beam shear design rules are applied by using the concept of an "equivalent beam."

Consider the element shown in Fig. 4. An equivalent beam strip of unit width taken horizontally from this element would be subjected to the principal transverse shear, but no axial tension. However, the "beam" would be subjected to tension acting across its width. A beam strip taken vertically would be subjected to the highest axial tension, but would not be subjected to transverse shear along its length. The beam strip would be subjected to transverse shear on its "side faces." In neither case is the in-plane reinforcement parallel to the axis of the strip.

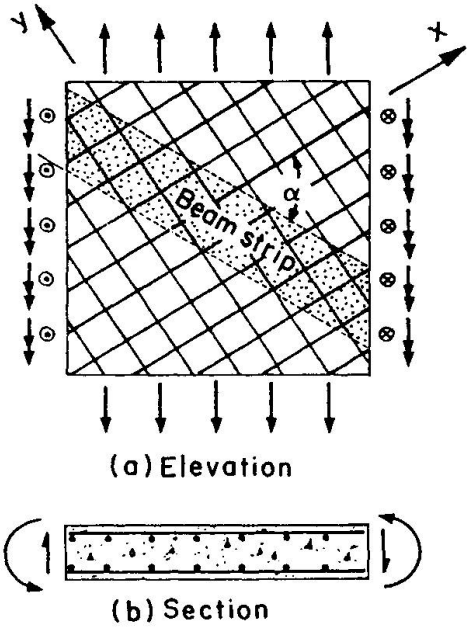

Fig. 4 Equivalent Beam Approach

One procedure currently used to apply the beam shear design rules is as follows. For each beam strip any actions on the side faces are neglected, as is the influence of the orientation of the in-plane reinforcement. The transverse shear per unit width of beam strip is taken as

$$V = V_x \cos\alpha + V_y \sin\alpha$$

and the "axial force" per unit width of beam strip is taken as

$$N = N_x \cos^2\alpha + N_y \sin^2\alpha + 2N_{xy} \sin\alpha \cos\alpha$$

The required amount of stirrup reinforcement expressed in terms of stirrup area per unit area of concrete is determined for every possible beam strip direction using the beam shear equations. The largest amount of stirrup steel is taken as the amount which is needed.

5. Membrane Forces, Bending Moments and Transverse Shear

The case of combined membrane forces, bending moments and transverse shear is complicated by the need to deal with triaxial strains and triaxial stresses. A simple practical solution to the problem is possible by considering, the variation of biaxial strains over the thickness of the element, but triaxial strains at only the mid-plane of the element. The influence of the triaxial strains on the biaxial stresses is assumed to be uniform over the thickness of the element. That is, the transverse strains are assumed to influence only the membrane forces, not the bending moments.

The procedure is done as follows. From the applied bending moments, M_x, M_y, M_{xy}, and the applied membrane forces plus a "first guess" correction to account for the influence of the triaxial strains, $N_x+\Delta N_x^I$, $N_y+\Delta N_y^I$, $N_{xy}+\Delta N_{xy}^I$, the in-plane strains of the middle surface are calculated using the procedure described in the previous section. The in-plane concrete stresses f_{cx}, f_{cy}, v_{cxy} at the middle surface of the shell are first calculated from these biaxial strains neglecting any transverse strains, and then are recalculated considering the influence of the transverse strains (ie. considering triaxial strains). The differences between these two sets of stresses (ie. the additional concrete stresses due to transverse shear) are assumed to be uniform over the effective shear depth. The resultants of these additional concrete stresses, ΔN_x^{II}, ΔN_y^{II}, ΔN_{xy}^{II}, must equilibrate the membrane force corrections. For example, $N_x+\Delta N_x^I+\Delta N_x^{II} = N_x$ which means that $\Delta N_x^I+\Delta N_x^{II} = 0$. Several iterations are generally needed to determine the three membrane force corrections to account for transverse shear.

The triaxial stresses at the mid-depth of the shell are calculated by a trial and error procedure which adjusts the three additional strains ϵ_z, γ_{xz} and γ_{yz} until the required values of the transverse shear stresses v_{cxz} and v_{cyz} are obtained and the resultant normal stress on the z plane is zero (ie. the concrete compressive stress in the transverse direction equilibrates the tensile stress in the transverse reinforcement). The six concrete stresses, f_{cx}, f_{cy}, f_{cz}, v_{cxy}, v_{cxz}, and v_{cyz}, are determined from the six concrete strains, ϵ_x, ϵ_y, ϵ_z, γ_{xy}, γ_{xz} and γ_{yz}, using a three dimensional generalization of the modified compression field theory.

The procedure involves first finding the principal strains, ϵ_1, ϵ_2, ϵ_3, and their directions. The principal concrete stresses, f_{c1}, f_{c2} and f_{c3}, are then found from triaxial concrete stress-strain relationships which are generalizations of the Vecchio and Collins biaxial relationships. In addition, a "crack check" is made to ensure that the loads resisted by the average triaxial stresses can be transmitted across the cracks. When significant transverse shear is present this check is often critical in determining the failure load.

6. Transmitting Forces Across Cracks

The forces resisted by the average stresses are transferred across cracks by a combination of increased reinforcement stresses at the crack and shear stresses on the crack interface. The magnitude of the shear stress depends on the relative increases in reinforcement stress in the various directions as well as the direction of the crack.

The ability of a crack to resist shear by aggregate interlock depends primarily on the crack width. It has been suggested [1] that if there are no compressive stresses on the crack interface the limiting value of the crack interface shear stress, v_{ci}, (in MPa) be taken as

$$v_{ci} \le \frac{0.18}{0.3+\frac{24w}{a+16}}$$

where w is the crack width, a is the aggregate size, and f'_c is the cylinder compressive strength.

The width and direction of a crack can be estimated from the average stresses and average strains. The crack direction is assumed to be normal to the principal average tension direction defined by the three angles θ_x, θ_y, θ_z, while the crack width can be estimated as the product of the principal average strain ϵ_1 and a crack spacing parameter $s_{m\theta}$. That is, $w = \epsilon_1 s_{m\theta}$ where

$$\frac{1}{s_{m\theta}} = \left(\frac{\cos\theta_x}{s_{mx}} + \frac{\cos\theta_y}{s_{my}} + \frac{\cos\theta_z}{s_{mz}}\right)$$

s_{mx}, s_{my} and s_{mz} are indicators of crack control provided by the x, y and z reinforcement directions.

Once the crack direction is known and an assumption is made about the increases in reinforcement stress at a crack, the shear stress on the crack surface can be calculated from

$$v_{ci}=\sqrt{\xi_{xy}^2+\xi_{xz}^2+\xi_{yz}^2}$$

$$\xi_{xy} = (\rho_x \Delta f_{sx} - \rho_y \Delta f_{sy}) \cos\theta_x \cos\theta_y$$
$$\xi_{xz} = (\rho_x \Delta f_{sx} - \rho_z \Delta f_{sz}) \cos\theta_x \cos\theta_z$$
$$\xi_{yz} = (\rho_y \Delta f_{sy} - \rho_z \Delta f_{sz}) \cos\theta_y \cos\theta_z$$

ρ_x, ρ_y and ρ_z are the reinforcement ratios in the x, y and z direction, and Δf_{sx}, Δf_{sy}, Δf_{sz} represent the differences between the average reinforcement stresses and the reinforcement stresses at a crack. Rather than using a strain compatibility approach to determine the reinforcement stresses at a crack, a lower bound approach is used in the modified compression field theory. The relative increases in reinforcement stress are chosen to minimize the required shear stress on the crack surface.

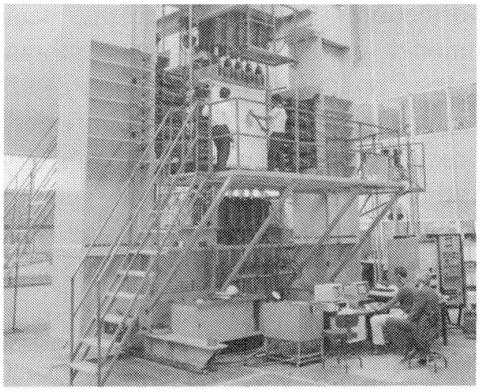

Fig. 5 University of Toronto Shell Element Tester

The increase in reinforcement stress at a crack may be limited by either yielding of the reinforcement or the inability of the crack to transmit the required shear. The average tensile stresses in cracked concrete is in turn limited by the increase in the reinforcement stress at a crack. That is,

$$f_{c1} = \rho_x \Delta f_{sx} \cos^2\theta_x + \rho_y \Delta f_{sy} \cos^2\theta_y + \rho_z \Delta f_{sz} \cos^2\theta_z$$

7. Computer Program SHELL474

The procedures described in this paper have been incorporated into a computer program called SHELL474 [3]. The program operates in two modes. In SLS mode the program calculates the strains (e.g., steel strains, crack widths, etc.) associated with a specified set of eight sectional forces, while in ULS mode the program calculates the complete load-deformation response of a section including the maximum loads which the section can resist.

8. Comparison with Experiments

A large testing machine capable of applying combined membrane forces, bending moments and transverse shear to reinforced concrete elements was constructed in 1984 at the University of Toronto. The machine uses sixty double acting hydraulic actuators to load 1.5 m high by 1.5 m wide elements of varying thickness (see Fig. 5).

Nine specimens were subjected to combined membrane forces, bending moments and transverse shear using the tester [4]. Seven of the specimens were 310 mm thick and had large amounts of in-plane reinforcement ($\rho_x=\rho_y=3.6\%$) but only a small amount of transverse shear reinforcement ($\rho_z=0.08\%$). The concrete (cylinder) strengths were approximately 52 MPa.

The experimentally observed interaction of transverse shear and membrane shear is shown in Fig. 6. Predictions are given from both program SHELL474 (strain compatibility model) and the equivalent beam model. The equivalent beam model gives a reasonable prediction for the pure transverse shear case, but is excessively conservative regarding the influence of membrane shear. This is because

the equivalent beam model makes use of the traditional beam shear design rules, which are excessively conservative regarding the influence of membrane tension. Also, the equivalent beam model does not properly account for the in-plane reinforcement direction or the membrane shear direction. The equivalent beam model predicts that the membrane shear on the right hand side of the interaction (Fig. 6) significantly reduces the transverse shear capacity, while SHELL474 correctly predicts that in this case the membrane shear actually improves the transverse shear response.

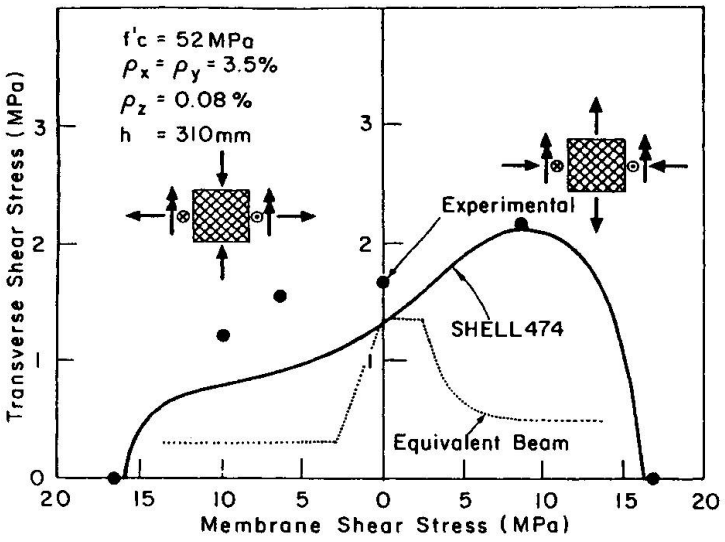

Fig. 6 Membrane Shear - Transverse Shear Interaction

9. Concluding Remarks

Traditional empirical shear design rules developed for simple building components are not appropriate for use in the design of complex concrete structures. If a consistent design approach is to be used for all types of structures then "*a more general approach is required for the (shear) design of structural concrete*" [Breen; Bruggeling].

A general approach to sectional design is possible by considering the following: (1) the compatibility of uniaxial, biaxial or triaxial strains; (2) realistic stress-strain relationships for the materials especially "cracked concrete," and; (3) equilibrium. As was demonstrated in this paper, such a general approach can be consistently applied to structural concrete.

Acknowledgements

The University of Toronto Shell Element Testing Program was jointly developed by Michael Collins and Peter Marti. Professor Marti's contributions are gratefully acknowledged.

References

1. VECCHIO, F.J., and COLLINS, M.P., "Modified Compression Field Theory for Reinforced Concrete Elements Subjected to Shear," ACI JOURNAL, *Proceedings*, V. 83, No. 2, March -April 1986, pp. 219-231.

2. KIRSCHNER, U., and COLLINS, M.P., "Investigating the Behaviour of Reinforced Concrete Shell Elements," *Publication No. 86-9*, Department of Civil Engineering, University of Toronto, September 1986. 209 pp.

3. COLLINS, M.P.; ADEBAR, P.; and KIRSCHNER, U., "SHELL474 - A Computer Program to Determine the Sectional Resistance of Concrete Offshore Structures in Accordance with CSA Standard S474-M89," *Canadian Standards Association Verification Project No. E-2 Report*, March 1989, 125 pp.

4. ADEBAR, P., "Shear Design of Concrete Offshore Structures," *Ph.D. Thesis, University of Toronto*, 1989, 413 pp.

Offshore Structural Concrete

Béton armé des plateformes pétrolières

Offshore Konstruktionsbeton

Terje Aas WARLAND
Civil Eng.
Statoil a.s.
Oslo, Norway

Terje Aas Warland who obtained his civil engineering degree at the Technical University of Hannover spent eight years with civil engineering firms in Germany and Norway. Since 1980 with Statoil. For three years responsible for Statoil Sleipner structural engineering group.

Ove T. GUDMESTAD
Dr. Sc.
Statoil a.s.
Oslo, Norway

Ove T. Gudmestad has a M.Sc. from Univ. of Tromsoe Norway and a Dr. Sc. degree from Univ. of Bergen. He has been with Statoil since 1975 where he has been involved in several projects related to offshore concrete structures.

Knut HOVE
Civil Eng.
Veritec
Oslo, Norway

Engineering training at Univ. of Wisc & Calif. With DnV since 1971 as head of design control of Ekofisk Tank and the first Condeeps. Head of development of DnV Rules Offshore. Major interests: deepwater structures and earthquake engineering.

SUMMARY
This report deals with design and dimensioning methods related to North Sea offshore platforms. Post-tensioning, shear and fatigue in connection with high strength concrete in particular, are assessed. Results from in-situ tests taken from slip are discussed and compared with results regarding bond behaviour of bars in slipform casted concrete.

RÉSUMÉ
Ce document traite les méthodes de dimensionnement et de conception des plateformes pétrolières de la Mer du Nord. Les modes de précontrainte, le mode de cisaillement et la fatigue relatifs au béton à haute résistance sont tout particulièrement traités. Des résultats d'essais in situ réalisés sur les structures érigées suivant la méthode du coffrage glissant sont discutés et comparés avec ceux concernant le comportement d'adhérence de barres d'armatures contenues dans des structures coffrées selon la même méthode.

ZUSAMMENFASSUNG
Dieser Artikel befasst sich mit Berechnungs- und Bemessungsverfahren für Offshore-Plattformen in der Nordsee. Insbesondere werden die Vorspannung, Schub und Dauerfestigkeit von hochfestem Beton behandelt. Es werden Ergebnisse von Baustellenversuchen zum Verbund von Bewehrungsstäben im mit Gleitverfahren hergestellten Beton diskutiert.

1. INTRODUCTION

Design of concrete structures for use in offshore petroleum production involves detailed analytical investigation of complex shell structures subject to dynamic loading from waves and also seismic action. A detailed knowledge of the dynamic response, the local distribution of forces and stresses and resistance to failure in fatigue as well as the ultimate load carrying capacity is therefore of paramount importance.In order to cover these aspects refined global finite element analyses using shell or solid element models are generally required, the results from which must be scaled to cover the structural dynamic response which is determined by use of stocastic methods.

The Sleipner A platform /4/ for 82 m water depth in the North Sea incorporates new features in concrete design and analysis. This platform with a volume of 74000 m^3 of concrete is presently being constructed in Stavanger Norway. Slipform construction is used for the cells and the shafts. The top of the shafts has a near rectangular form to suite the supports of the Modul Support Frame (MSF). This is well covered in the analyses of the structure. The near rectangular top of shafts will be slipformed through application of new slipform technology.The conventional steel transition rings between the MSF and the shafts are eliminated as the steel MSF is placed directly on the concrete shaft. Furthermore the deck is supported on only two, respectively three, supports on each shaft resulting in savings in steel for the MSF. To absorb the high compression forces incurred by few supports and to optimize the design of the walls and the shafts, high strength concrete with quality C65 is necessary.The entire cells up to a level of 48 m are constructed in dry dock. To get sufficient buoyancy out of dock, the four foundation areas are cast in light weight aggregate concrete LC65.

In the following chapters bond strength for slipformed concrete structures will be discussed as well as dimensioning of post-tensioning and application of T-headed bars in cell walls. Shear and fatigue aspects are furthermore reviewed.

2 CONCRETE STRENGTH

2.1 Design strength of concrete

The design strength of concrete should correspond to the concrete strength as obtained in the structure (structural strength) reduced by an appropriate factor of safety to account for undertainties in material characteristics, quality of construction and uncertainties related to prediction of capacity and mode of failure /5/.

The format for the design strength used in the Norwegian concrete design code NS3473 /10/ refers to "structural strength" and differs in this way from the CEB-FIP format. However, the design value is close to that of CEB-FIP 1990.

The grade of concrete - eg C60 - refers in some codes to the cube strength (eg. NS3473) and in others to the cylinder strength. (eg. CEP-FIP, ACI318 and CAN3-A23.3). Uniformity on this simple point is welcome.

2.2 Effects on strength from slipforming

Slipform construction has long tradition. For tower type structures slipforming has been common. Since 1971 slipforming has been used for construction of large offshore structures in the North Sea. The Sleipner A platform described in /4/ which has been in construction since 1989, is shown in Figures 1 and 2.

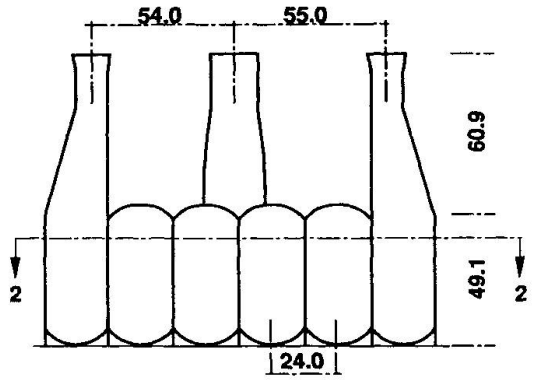

Fig.1 ***SECTION 1-1***

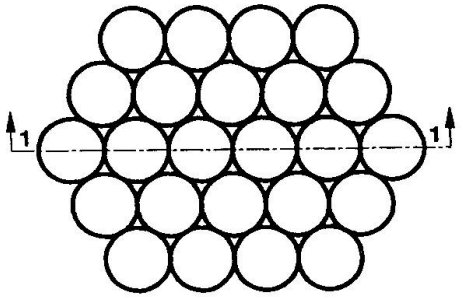

Fig.2 ***SECTION 2-2***

The slipform construction employed for offshore platforms has given high quality well compacted concrete. In /5/ the result of in-situ tests of 1042 cores and 808 cubes from 3 platforms are described. The concrete compressive strength was 5 to 10% higher than for none slipformed parts. There were no indications that the tensile and bond strength should not follow the compression strength. Tests of bond strength of concrete from slipformed structures in Germany, indicate the opposite results. /6/ . The conclusion of the German tests is that the ratio of the computed bond lengths (slipform/ordinary formwork) was found to be 2 for vertical bars and 4 for horizontal bars.

The different results in Germany and Norway indicate that the quality of concrete may be sensitive to the slipform technique. The effective bond length will depend on workmanship and slipform technique as well as wall thickness and specific weight of the concrete.

Statoil is, however confident in using slipform construction with the high quality control of the work maintained for construction of the North Sea structures.

3. PRESTRESSING

Prestressing has been used in the construction of all North Sea concrete structures. The advantages of using prestressing are listed in /2/. Of special importance for offshore platforms is the possibility to reduce structural dimensions and to limit crack widths. According to Statoil requirements, cracks are limited to 0,15mm in the splash zone and 0,30 mm in the submerged zone. Prestressing will also improve the fatigue resistance, due to the better fatigue resistance of the concrete when only exposed to compression.
Global forces (membrane tension) are covered by prestressing imposed by post-tensioned tendons and also by hydrostatic loading. Local moments are taken up by normal reinforcement. Cables are typically located at top and base of shafts and in the ringbeam in the upper and lower domes. Normally, the shafts are also prestressed vertically.

NS 3473, does not prescribe different computational methodology for ordinary reinforced and prestressed concrete. The problems with different design methods for ordinary reinforced and prestressed concrete are thus eliminated, see /1/ and /2/. In determination of capacity in flexure and combination of flexure and membrane action the residual strength of the prestressing steel (the top part of the stress-strain curve not utilized for pretensioning) may be used. This may in many cases, especially for heavy shell structures lead do considerable savings in ordinary reinforcement and avoide congestion of reinforcement. Thus, ensuring better concreting and a better structure.

4. SHEAR

Regarding the Sleipner A platform, several locations are exposed to high shear forces requiring shear reinforcement; the transition areas between the domes and the cell wall as well as in the so called star walls, see Figure 2.

The determination of shear capacity varies between most codes. Also the value of load and material factors are treated differently in the most codes. A comparative study of the shear capacity from the concrete is reported in /8/. According to NS3473 the shear capacity can be calculated by a simplified method, by the truss model method or by a general method for inplane shear. The truss model method is less used in the design of offshore concrete structures. It was first included in NS 3473 in the 1989 edition. The practical use of it in computerized design is more complicated than the simplified method due to the necessity of having in principal one truss model for each load case and the general complexity of the method.The simplified design method given in NS 3473 is partly modifications of the CEB/FIP Model code 1978. The tensile strength is by NS3473 lower than by CIB/FIP Model code 1978 for high strength concrete, /7/.

Shear tests reported in /7/ show that NS3473 predicts well the variation of the diagonal cracking strength for beams with different types of high strength concrete.The determination of ultimate shear strength for high strength concrete above a cylinder strength of 80 MPa is however less well defined. Results reported in /7/ show that shear capacity of high strength concrete beams is more influenced by the scale than beams of normal strength. The more brittle behavior of high strength concrete and the lesser aggregate interlock due to fracture of the aggregate may be part of the reason for reduced shear strength. Further work appears necessary on this subject.

Results reported by M.P.Collins /9/ from a series of thirty-one tests involving concrete panels reinforced in only one direction and loaded in various combinations of tension and shear, provide most valuable information.Use of Collins modified compression field theory on available test results show that the existing reinforced concrete design codes typically are very conservative in their estimate of the shear strengt of elements subjected to combined tension and shear.The modified compression field theory represent the state of the art. The theory takes into account the contribution of the concrete aggregate interlock mechanism in a rational manner. However, as discussed in /3/ the method appears complicated since there is no simple procedure for obtaining transverse strain.
A rational and simple method to predict shear compression and tension based on M.P. Collins theory should be developed in order to get a simple, accurate and economical dimensioning method for shear.

5. FATIGUE

The subject of resistance to fatigue of structural concrete to random loads was first codified in DnV Rules for Offshore Structures 1977. Through joint industrial R and D projects, S-N curves were established for reinforced concrete, normal weight (NW) and light weight (LW) in compression - compression and tension - compression, including the effects of water. During the last 10 years considerable advancement has been made on the subject in terms of refinements of the S-N curves as the data base has been expanded.

At present fatigue of structural concrete is covered in two design codes - i.e. CEB-FIP Model Code 1990 and in NS3473 - for the following modes of loading:

- compression - compression
- compression - tension
- tension - tension

Procedure for estimating the fatigue life for transverse shear and bond based on extrapolations of the unaxial test data are also given. The S-N curves given in CEB-FIP 1990 and in NS3473 differs in some respect. A main difference is the way the stress range or rather the minimum stress is introduced. The NS3473 has also introduced an endurance limit, while the S-N formulation of CEB-FIP assumes a straight S-log N relation.The calculation procedures given in NS3473 is basically a further development of the DnV-77 method, and it is in some respect more detailed than the procedure of CEB-FIP 1990.Recent Norwegian tests on air dry and wet high strength concrete specimens - normal density and light weight tested in cyclic compression are reported in /13/. It is noted that the natural moisture contained in sealed concrete is enough to reduce the fatigue strength to that of wet concrete. Recommended S-N curves including endurance limits for various levels of minimum stress are given in /13/ for concrete in compression. The state of the art is reported in /14/.

Test data and improved computational models should be developed for the following areas:

- out of plane shear action
- 2D cyclic action alternating in tension-compression
- local 3D effects in joints including reinforcement detailing.

6. T-HEADED STIRRUP BARS

Structural elements subject to high out-of- plan shear and those needing confinement for ductility in the post-elastic range require concentrated transverse reinforcement. The traditional hoops of bent stirrups are difficult to place, especially if the tails must be bent back into the core. These conventional stirrups are also relatively inefficient.A T-headed bar with plate anchor at the ends has therefore been developed for use as transverse shear reinforcement. The use of T-headed bars is cost efficient compared to stirrups.Tests described in /11,12/ show these bars to have excellent anchorage under ultimate loads, providing exceptional confinement and ductility to the member, with test specimens yielding displacement ductility factors of over 40. Also tests have indicated that confining effects from T-headed bars have yielded enhancement of concrete strength in the order of 10% as compared to the use of 90° hooked bars. As to the use of 90° hooks these will open up during ultimate strength situations and loose its capacity. Use of 90°- hooks should be limited to ø 12 mm bars.

Structures to be used in the arctic must withstand intense punching shears from the impact from sea ice and iceberg. Offshore structures must withstand the impact from boats and barges, and the base slab and other connecting elements of offshore platforms may have to resist high shear from concentrated reactions. Other extreme load effects that may have to be considered are large earthquakes, explosions, or impact from falling objects. To provide the required strength and ductility the percentages of transverse steel may reach 1.5 to 2.5 % (15000 to 25000 mm^2/m^2). Such reinforcement percentage can only be provided by use of heavy bars fully anchored.

Use of T-headed bar is an effective and structurally reliable method of providing transverse reinforcement to resist shears and to provide confinment of the concrete core. T-headed bars have been used in the North Sea offshore structures, the Gullfaks A and Sleipner A and the Ekofisk Protective Wall.

7 CONCLUSIONS

Slipformed high strength concrete is an excellent material for constructing of offshore platform support structures.

REFERENCES

1. BREEN J.E., Why Structural Concrete.Introductory Report, IABSE Collegium Structural Concrete 1991 Stuttgart.

2. BRUGGELING A.S.G., An Engineering Model of Structural Concrete, Introductory Report, I.B.S.E Collegium.Structural Concrete 1991 Stuttgart.

3. MACGREGOR J.G., Dimensioning Detailing, Introductory Report, IABSE Collegium Structural Concrete 1991 Stuttgart.

4. GUDMESTAD O.T.G., and COKER J.W.A., The Sleipner Platform: An Efficient Gas and Condensate Installation. SPE European Petroleum Conference, London 1988.

5. HAUG A.K. and JAKOBSEN B., In-Site and Design Strength for Concrete in Offshore Platforms, Second International Symposium on Utilization of High Strength Concrete, San Francisco 1990.

6. DEUTCHER AUSSCHUSS FÜR STAHLBETON, Heft 378, Test on the Behavior of Deformed Bars in Slipform Concreted Structures, Berlin 1986

7. THORENFELDT E. and DRANGSHOLT G., Shear Capacity if Reinforced High Strength Concrete Beams, Second International Symposium on Utilization of High Strength Concrete, San Francisco 1990.

8. LEIVESTAD S, VIK B., EKEBERG P.K., The Utilization of High Strength Concrete, a Survey of international Codes and Regulations, International Symposium on Utilization of High Strength Concrete, Stavanger June 1987.

9. BHIDE S.B. and COLLINS M.P. Reinforced Concrete Elements in Shear and Tension University of Toronto, Publication no 87-02.,ISBN 0-7727-7089-1.

10. NORGES STANDARDISERINGSFORBUND: NS3473, Prosjektering av betongkonstruksjoner. Beregning og konstruksjonsregler, 1989.(English version to appear).

11. Gerwik, BenC, Inc. Pheripheral Concrete Wall design Optimization Study - Phase II, Standard Oil Production Company Sponsor AOGA, NO 324, 1987.

12. Hove, Knut, "Ductility Performance of Offshore Concrete Structures" Joint Industry Project (Høvik Norway). Subrestricted D- Column Tests - C90 Concrete, Veritec Report No 86-3689 Vol. 1 and 2, 1987.

13. Gordon Pethovic, Rolf Lenschow, Hans Stensland and Svein Rosseland "Fatigue of High Strength Concrete". Second Symposium on High strength concrete" University of California, Berkely May, 1990.

14. CEB Bulletin No 188 "Fatigue Strength of Concrete Structures" state of the art report 1988.

Experimental Studies of Nodes in Strut-and-Tie Models

Etude des régions nodales dans le cas de l'analogie du treillis

Verhalten von Knotenbereichen und Stabwerkmodellen

James O. JIRSA
Prof. of Civil Eng.
University of Texas
Austin, TX, USA

John E. BREEN
Prof. of Civil Eng.
University of Texas
Austin, TX, USA

Konrad BERGMEISTER
Dr.
University of Stuttgart
Stuttgart, Germany

David BARTON
Staff Engineer
Omega Marine Eng. Systems
Houston, TX, USA

Robert ANDERSON
Bridge Eng.
Greiner, Inc.
Tampa, FL, USA

Hakim BOUADI
Ph.D. Candidate
University of Texas
Austin, TX, USA

SUMMARY

This paper presents the results of a series of tests in which the behaviour of the nodal regions used in strut-and-tie models (STM) was studied. The research program included the construction and loading to failure, of a series of dapped beams and two series of isolated node specimens which simulated CTT and CCT node portions of the dapped beams. The test results supported the use of the STM in detailing. They indicated that the commonly used approach for determining the required development for hooked and straight bars may be overly conservative for node design and showed the beneficial effect of confinement of the concrete in the node and around the tie bars.

RÉSUMÉ

Cet article présente les résultats d'une série de tests étudiant le comportement des régions nodales dans le cas de l'analogie du treillis. Le programme de la recherche incluait la construction et le chargement jusqu'à la rupture d'une série de poutres à décrochement d'extrémité, ainsi que l'étude de deux séries de nœuds isolés simulant les nœuds CTT et TTC de la poutre (T = traction, C = compression). Les résultats confirment la validité de l'application de l'analogie du treillis dans la conception. Ils indiquent que les méthodes communément utilisées pour calculer les longueurs d'ancrage des barres droites ou à crochet peuvent être trop conservatives dans le dimensionnement des nœuds et que l'effet de confinement du béton a un effet favorable sur le nœud et autour des barres formant tirant.

ZUSAMMENFASSUNG

In dieser Veröffentlichung werden die Ergebnisse einer Reihe von Versuchen präsentiert, in denen das Verhalten von Knotenbereichen, wie sie in Stabwerkmodellen auftreten, untersucht wurde. Die Versuche umfassten eine Reihe von Trägern mit ausgeklinkten Auflagern und zwei Testserien, in denen die Druck-Zug-Zug und Druck-Druck-Zug Knoten in den ausgeklinkten Trägerenden isoliert betrachtet wurden. Die Ergebnisse bestätigen die Anwendbarkeit von Stabwerkmodellen für Bemessungs- und Konstruktionsaufgaben. Es wurde beobachtet, dass die üblichen Vorgehensweisen für die Bestimmung der Verankerungslänge von geraden Bewehrungsstäben oder solchen mit Endhaken für die Bemessung von Knotenbereichen sehr konservative Ergebnisse liefern, und dass eine Umschnürung des Betons festigkeitssteigernd wirkt.

1. INTRODUCTION

1.1 Background

Mies van der Rohe restated a traditional German proverb in a positive fashion when he said, "The hand of God is in the details". Clearly, the success of any integrated conceptual approach to the proper design of structural concrete must finally succeed or fail according to the degree of assistance it gives the designer in developing adequate and economic details. Marti [1] states "Dimensioning and detailing of D-regions has often been regarded as an inferior task, while in fact, it is of paramount importance for the quality of any reinforced concrete structure." Schlaich [2] urges that dimensioning be carried out initially on the basis of relatively simple models, such as the strut-and-tie model (STM), with a following step of review at "a suitable level of sophistication" to ensure that the details in fact carry out the intent of the dimensioning model. He quite properly points out that even the most sophisticated non-linear finite element analysis (FEA) has important limits when applied to the capacity of details and expecially to describing the behavior of nodes. The authors have felt that the re-emphasis on STM for D regions provides a golden opportunity for introducing rationality of structural concrete detailing. However, in examining the literature, they came to the identical conclusions voiced by MacGregor [3] and Marti [2] who both call for further experimental investigation of nodal zone strength. The authors have been conducting such experimental studies for several years [4,5].

1.2 Objectives

The basic object of this study was to critically examine the application of STM in the detailing of D-regions. Research cannot be carried out to develop empirical design procedures to cover *every* detailing situation. The STM uses a few basic principles to cover a large range of design problems. While the literature contains considerable general information, there is a lack of test data to corroborate assumptions of the strut-and tie model. Working with a specific application to help verify strut-and-tie procedures, a dapped-end beam detail (See Fig. 1) was selected for testing. The STM principles outlined by Schlaich et al. [6] were used to develop details for the discontinuity regions. It became immediately apparent that the existing state of knowledge was particularly troublesome which applied to the nodes. Major attention was then devoted to tests on isolated nodes (Fig. 1b and Fig. 1c).

1.3 Test Series

1.3.1 Dapped Beam Tests

Three different procedures for the design of dapped beam ends were used. Two different STM and two empirically based methods (PCI and Menon/Furlong) were used. A different dapped end detail was tested for each method [4].

1.3.2 Compression-Tension-Tension (CTT Nodes)

To develop an understanding of an isolated CTT-node, a laboratory investigation identified significant behavioral patterns of the CTT-node, and was used to develop design guidelines. The dapped beams served as the prototype for the node tests. Nine node specimens were designed and loaded to duplicate, as closely as possible, boundary conditions that exist at a critical CTT-

node in the dapped beams. Variables included concrete strength, lateral confinement provided by transverse reinforcement, anchorage details, and node geometry [4].

1.3.3 Compression-Compression-Tension (CCT Nodes)

The CCT node was also isolated from the end reaction region of the dapped beam. Ten specimens were tested in which concrete strength, size of bearing area, amount of transverse reinforcement, and longitudinal reinforcement configuration were varied [4].

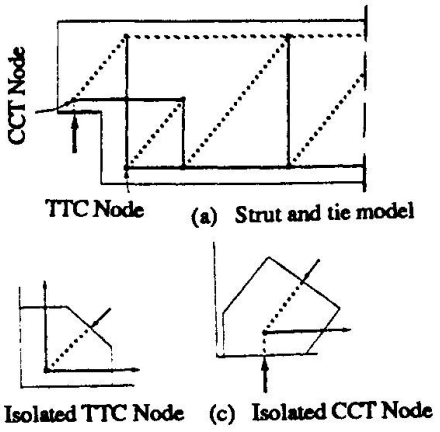

Figure 1 Strut and tie model of the prototype dapped beams.

2. DAPPED END BEAM TESTS

All dapped end details were designed for the same design load levels; a factored ultimate load of 100 kips [4]. The resulting reinforcement layout for the two different STM used, the PCI, and the M/F method designs are shown in Fig. 2. In the actual tests, the dapped end details were provided at the ends of a simply supported beam which was loaded monotonically to failure.

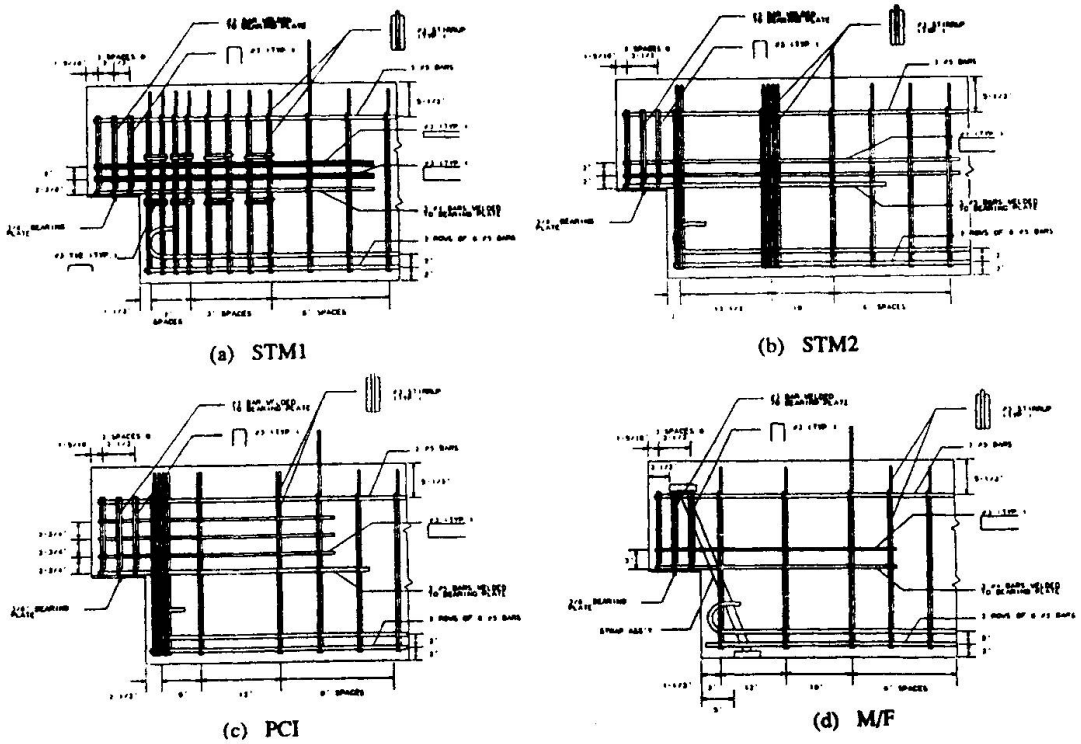

Figure 2. Specimen reinforcement layouts.

The overall behavior of specimens designed using STM was found to be comparable with details designed using current design standards. As shown in Fig. 3 the ultimate capacity of all four specimens substantially exceeded the computed capacity. A ductile failure mode in which the steel yielded before the concrete failed was exhibited by each of the specimens. The STM procedure required slightly more shear reinforcement. The initial cracking load for all specimens ranged from 20 to 30 percent of design ultimate as shown in Fig. 4. In ST-1, cracking was well controlled at service loads. Slightly more cracking was exhibited by ST-2 due to placement of vertical reinforcement farther away from the dap. Initial yielding of reinforcement in both STM specimens was at about 75 percent of design ultimate, substantially earlier than the two empirically designed specimens.

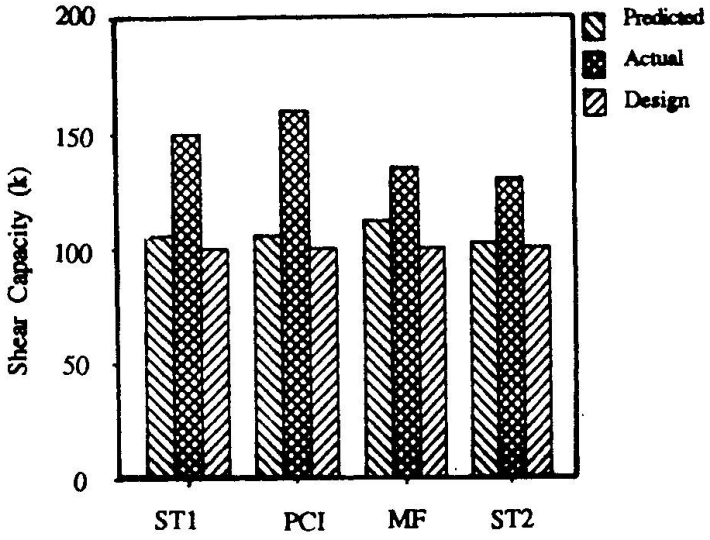

Figure 3 Comparison of specimen shear capacities.

Internal force measurements at the design ultimate load compared well to forces predicted by the design STM. As load was increased beyond the design ultimate load, the distribution of internal forces changed. STM representations of the upper portion of the daps based on measured forces at ultimate were not completely accurate due to the presence of force transfer mechanisms not considered by the STM.

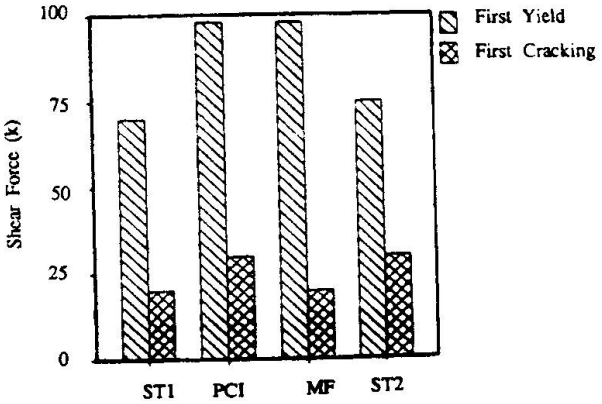

Figure 4 Comparison of cracking and yield loads

Comparison of the behavior of the dapped ends indicates placing the main vertical reinforcement close to the change in section is most efficient. In addition, grouping the reinforcement with as small a spacing as possible appears to offer the best performance. Anchorage requirements based on the STM were found to be conservative and resulted in applied loads well beyond design values. Proper anchorage of the dap horizontal reinforcement and the beam flexural reinforcement was found to be particularly important.

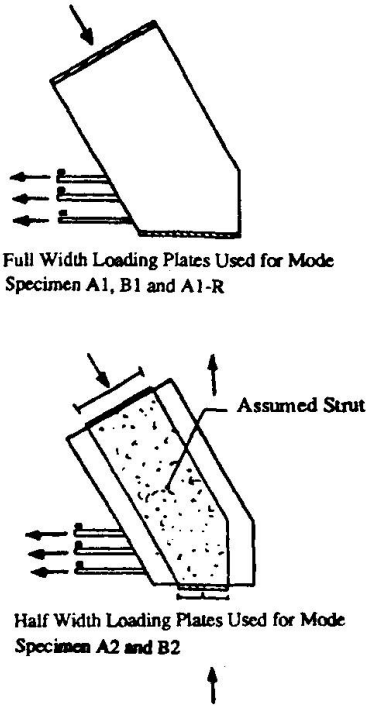

(a) Full Width Loading Plates Used for Mode Specimen A1, B1 and A1-R

(b) Half Width Loading Plates Used for Mode Specimen A2 and B2

Figure 5. General information about the tested CCT-nodes (from Ref. [4]).

3. NODE TESTS

The nodes of the STM represent the locations of change of direction of internal forces, which in the structure occurs over a certain length and width in the node region. The intersecting strut-and-tie forces have to be linked together and balanced in equilibrium in the node region. If one of the struts or ties represents a concentrated stress field (e.g. near a single load, a support or concentrated reinforcement) the deviation of forces tends to be locally concentrated and the node region is relatively small. These kind of nodes are called "singular nodes" and have to be dimensioned with special care. Evaluation of the nodal regions includes checking the nodal boundary stresses and determining reinforcement development requirements for nodes which contain tension ties. Each of these steps requires the determination of the physical boundaries of the node.

3.1 CCT Nodes

The typical critical CCT node in a dapped end beam occurs at the support as shown in Fig. 1(a). This node was isolated as shown in Fig. 1(c). In some presentations of CCT nodes, the tension reinforcement is shown as anchored by use of an external anchor plate. This is seldom found in practice. The usual detail is that straight bars, hooked bars or looped bars are used. Looped bars with confining direct pressure from the bearing plate load are preferred. Sufficient anchorage lengths have to be provided within as well as behind the node. Anchorage lengths can be assumed to begin where the compression struts meet the bars. The effective width of the compression strut can be found by assuming an effective compressive stress in the strut, $\nu_e f_c'$.

The fundamental aspects should allow the designer to determine the geometry of the CCT-node for varying reinforcement distribution and anchorage details (several layers, loops, hooks, etc.). The experimental study by Bouadi [4] provided information about the behavior and transfer of forces within the CCT-node as well as the ultimate strength. Typical test specimens are shown in Fig. 5. Test results with a concrete strength in the range from 2360 to 4680 psi showed crushing of the concrete struts only for the lower concrete strength specimens. In all other cases anchorage failure occurred. The tests indicate the of geometry of CCT nodes shown in Fig. 6. The compressive forces and the tensile force in the reinforcement were increased simultaneously. All specimens experienced post-yield failures including strut crushing, cover splitting, and gross slippage of reinforcement. Statistical examination of the specimens experiencing concrete failure indicated that if $\nu_e = 0.8$ was used, all predictions were conservative with a mean of 1.17 and a standard deviation of 0.14. The CCT node tests indicated:

(1) Specimens were controlled either by anchorage failure or compressive failure;
(2) STM strut orientation angles had been verified as correct in the dapped beam tests. Effective bearing areas based on such orientation gave consistent results for evaluating

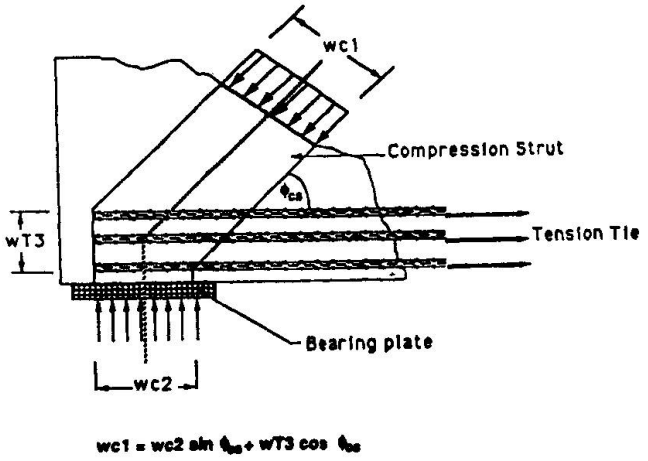

Figure 6. Anchorage detail for CCT-node with directly anchored bars.

tie anchorage and effective compressive strength factors;

(3) The effective compressive stress efficiency factor increased with reduction in bearing area size;

(4) Transverse reinforcement restrained the cracks and increased capacity 35% by preventing anchorage failure;

(5) Anchorage lengths for straight and hooked bars given in the ACI Code were found to be conservative.

3.2 CTT Nodes

The CTT-node is an intersection of a concrete compressive strut and two tensile ties. In steel trusses, bolts, welds, and gusset plates are sized to safely transfer load between the members. In contrast, a CTT-node in a concrete member must rely on anchorage, bond and other internal force transfer mechanisms to transfer strut and tie forces. Anchorage is achieved by providing proper development length or in special circumstances by attaching the reinforcement to bearing plates or other fixed components. The definition of the effective width plays an important factor in the dimensioning process. For the relatively rare case of a CTT-node with anchor plates, the widths of the plates are given as dependent constraints which tend to fix the width of the unknown compression strut. The more practical and generally occurring case is the CTT-node without a bearing plate. For this case the approach of Fig. 7 is proposed.

The efficiency factor for the CTT-node was investigated in an experimental study by Anderson [4]. Figure 8 shows typical test specimens. Other variables included types of anchorages, local confinement and concrete strength. One specimen was subjected to unequal forces in the tension ties in order to induce a different compression strut angle into the specimen. In the tests, general strut failures did not usually occur. The reinforcing anchorage detail was primarily responsible for limiting the ultimate load. However, for design purposes the actual efficiency factor for the concrete compressive strength is of interest. Only one specimen failed by concrete crushing. Using ν_e = 0.8 and taking into account the smaller bearing plate width (4") compared to the compression strut width (6.37"), the experiment/theory-ratio was computed as 1.02.

While data was collected from a relatively small number of CTT tests, the unique nature of the isolated node specimens provides interesting insight into node behavior and design.

(1) Specimens were generally able to reach the design strength which was governed by yielding of tie reinforcement. The ultimate strength of the CTT nodes was affected by concrete strength; however, internal force transfer mechanisms were more affected by the specimen geometry and placement of steel.

(2) In all the specimens, different layers of tie reinforcement were observed to strain at different rates. In the strut and tie model the reinforcement making up a single tie is

normally assumed to be uniformly strained. Major cracks appeared to reduce the available development length for some of the layers of reinforcement closest to the external surface enough to cause a deterioration in the tensile capacity of the tie.

(3) Correlations between the behavior of the node specimens and the prototype dapped beam specimen were quite good.

(4) Evaluation of the strut-and-tie model in the light of the test results indicate that
   (a) cracks were generally parallel with the angle of the compression strut;
   (b) the geometry of the strut is best defined by the strut angle and the width of the outer intersections of the layers of the reinforcement in both directions;
   (c) defining the critical section of the reinforcement by the boundaries of the compression fields appeared to produce reasonable estimates of the capacity of ties anchored through development.

(5) The splitting failures that occurred in several specimens underscored the importance of detailing the CTT-node as a three-dimensional element. Reinforcement should be provided across all planes of weakness to control cracking. Confining reinforcement normal to planes of hooks and bends is especially important.

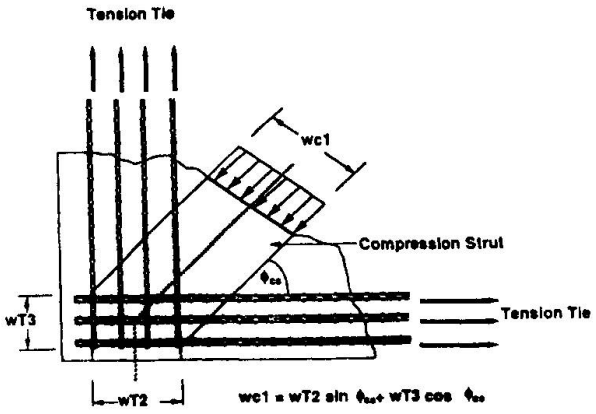

Figure 7 Geometrical approach to define the strut width for CTT-node

4. CONCLUSIONS AND RECOMMENDATIONS

The results of these limited tests show that the STM is useful design procedure for detailing structural concrete. The use of STM along with a knowledge of behavior derived from experimental research seems a good basis for developing efficient design procedures. The STM represents a rational approach which can be extended to detailing situations not covered by existing procedures.

As called for by MacGregor [3] and Marti [1], further experimental verification of other types of details is necessary. In addition, guidelines on analysis and design of nodal regions, serviceability criteria, and tie layout need development. In order to develop comprehensive design criteria for nodes, future studies should include specimens with a number of different bar spacings and amounts of tie reinforcement. Test specimens with high percentages of reinforcement and narrow web widths are also suggested so that effective concrete strength limits could be evaluated more closely. The behavior of specimens with anchor plates and straight or hooked bars needs to be examined. In addition, the effect of strut orientation should be studied more closely. In particular, the effects of skew cracks on the effective concrete strength of the compressive strut should be verified. The isolated node specimens used in this study provide much useful data but admittedly it is never possible to remove a portion of a structural element and isolate it in a manner that does not produce some change in boundary conditions. In spite of that, such node specimens offer a means of acquiring a large amount of data on detailing at a minimal cost.

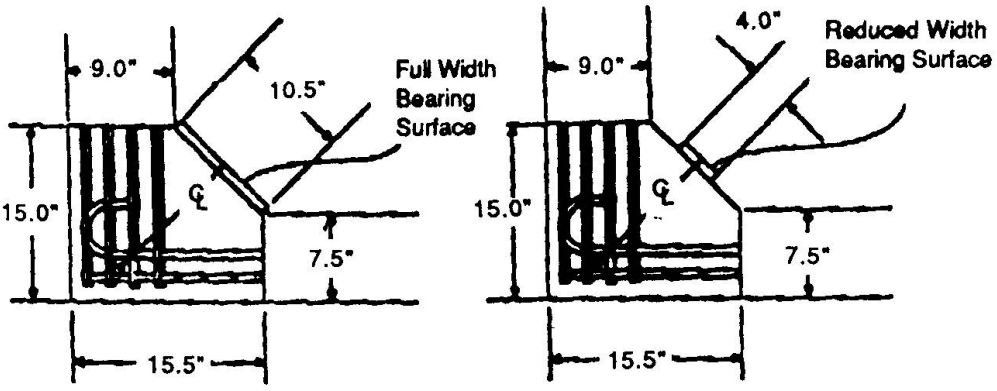

Typical Full Width Bearing Surface Specimens

Reduced Bearing Surface for Specimens HHSR and LHSR

Figure 8 Typical CTT-nodes tested (from Ref. [4]).

5. ACKNOWLEDGEMENTS

The research reported herein was carried out under the sponsorship of the Texas State Department of Highways and Public Transportation and of the Federal Highway Administration. The opinions presented are those of the authors and not necessarily those of the sponsors. Ms. Mary Lou Ralls provided excellent advice on sponsor prototype details and problems.

REFERENCES

1. MARTI, P., "Sub-Theme 2.4: Dimensioning and Detailing," Final Report, IABSE Colloquium *Structural Concrete*, Stuttgart, April 1991.
2. SCHLAICH, J., "Sub-Theme 2.2: Modelling," Final Report, IABSE Colloquium *Structural Concrete*, Stuttgart, April 1991.
3. MAC GREGOR, J.G., "Sub-Theme 2.4: Dimensioning and Detailing," Final Report, IABSE Colloquium *Structural Concrete*, Stuttgart, April 1991.
4. BARTON, D.L., ANDERSON, R.B., BOUADI, A., JIRSA, J.O., AND BREEN, J.E., An Investigation of Strut-and-Tie Models for Dapped Beam Details," Research Report 1127-1, Center for Transportation Research, February 1990.
5. BERGMEISTER, K., BREEN, J.E., JIRSA, J.O., AND KREGER, M.E., "Detailing for Structural Concrete," Research Report 1127-3F, Center for Transportation Research, October 1990.
6. SCHLAICH, J., SCHAFER, K., AND JENNEWEIN, M., "Towards a Consistent Design of Structural Concrete," PCI Journal, May-June 1987, pp. 75-150.

Design of Disturbed Regions

Conception des zones de discontinuités

Bemessung von Diskontinuitätsbereichen

Denis MITCHELL
Prof. of Civil Eng.
McGill Univ.
Montreal, PQ, Canada

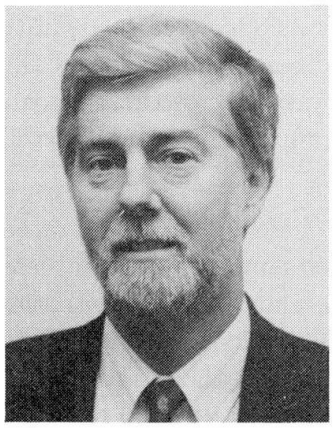

Denis Mitchell has received a number of awards from ACI, ASCE and PCI for his research on structural concrete. He is currently Chairman of the Canadian Concrete Code Committee.

William D. COOK
Res. Eng.
McGill Univ.
Montreal, PQ, Canada

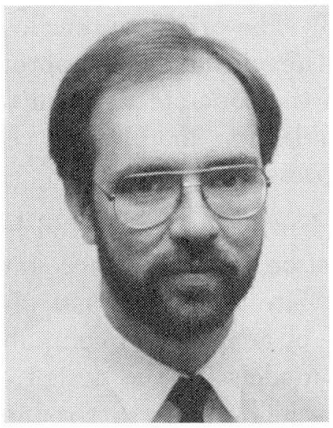

William D. Cook obtained his doctorate in Civil Engineering at McGill University in 1987. His research interests relate to nonlinear analysis of reinforced and prestressed concrete structures.

SUMMARY

The design method for disturbed regions in the Canadian concrete code is first described and the need to consider strain compatibility is explained. The transition from regions where sectional analysis is applicable to regions where strut-and-tie models apply, is discussed. Examples of the application of strut-and-tie models and non-linear finite element analysis, are presented.

RÉSUMÉ

On décrit la méthode de calcul de zones de discontinuités proposée par le Code Canadien du béton, ainsi que la nécessité de considérer la compatibilité des déformations. La transition entre des zones où l'on peut appliquer l'analyse sectionnelle et celles où l'on prend en considération l'analogie du treillis est discutée. L'application de modèles d'analogie du treillis et d'analyse non-linéaire par éléments finis est illustrée par des exemples.

ZUSAMMENFASSUNG

Das Bemessungsverfahren in der kanadischen Betonnorm für Diskontinuitätsbereiche wird beschrieben und die Notwendigkeit erläutert, die Verträglichkeit der Dehnungen zu berücksichtigen. Es wird der Übergang von den Bereichen, in denen eine Querschnittsbemessung durchgeführt werden kann, zu den Bereichen, in denen Stabwerkmodelle verwendet werden, diskutiert. Beispiele für die Anwendung der Stabwerkmodelle und nichtlinearer Finite Element Methoden werden vorgestellt.

1 INTRODUCTION

The design of a structural concrete member typically involves separating the member into two distinct zones. Regions removed from both geometric and loading discontinuities are usually designed for flexure assuming that plane sections remain plane and designed for shear assuming that the shear stresses are uniform over the nominal shear area of the cross-section. Because the plane-sections analysis for flexure satisfies both equilibrium and compatibility, engineers are able to apply this method to a large variety of loadings and cross-sectional configurations. The 1984 Canadian Concrete Standard (CSA)[1] provides the designer with a sectional design approach for shear based on the compression field model[2], which uses a variable angle for the diagonal compressive stresses in the concrete and satisfies both equilibrium and compatibility. The strain-softening of the diagonally cracked concrete is based on the influence of the principal tensile strain in reducing the compressive load carrying capacity of the concrete as developed by Vecchio and Collins[3]. The principal tensile strain is determined by considering compatibility of strains. However, this current code approach does not consider the beneficial effects of the tension that exists in the concrete between the diagonal cracks. The presence of these tensile stresses has been included in a more recent version of this shear design approach[4] and is based on the modified compression field model[3].

Regions adjacent to discontinuities caused by abrupt cross-sectional changes or concentrated loads or reactions must be designed to account for the resulting disturbed flow of forces. In these regions it is inappropriate to assume that plane sections remain plane and that shear stresses are uniform. In spite of advances in computer analysis techniques, engineers are reverting to simple strut and tie models for the design of disturbed regions, similar to those introduced by Ritter[5] and Mörsch[6] and further refined by Thürlimann *et al.*[7], Marti[8] and Schlaich *et al.*[9]. Marti[8] suggested a truss model with a limiting compressive stress in the concrete diagonals of $0.6f'_c$. Schlaich *et al.*[9] suggested choosing the geometry of the truss model such that the angles of the compressive diagonals are within $\pm 15°$ of the angle of the resultant of the compressive stresses obtained from an elastic analysis. These methods, which satisfy equilibrium, do not necessarily satisfy compatibility. The strut and tie model of the 1984 CSA Standard uses compatibility of strains in the determination of the limiting compressive stress in the cracked compressive struts.

2 STRUT AND TIE MODEL OF THE CSA STANDARD

The steps in design of a disturbed region, such as the deep beam shown in Fig. 1, are:

1. Sketch flow of forces in disturbed region and locate nodal zones which are regions bounded by struts, tension ties or bearing areas.
2. Choose dimensions of loading and reaction areas such that nodal zone stresses stay below permissible limits (i.e., $0.85\phi_c f'_c$ in nodal zones bounded by compressive struts and bearing areas, $0.75\phi_c f'_c$ in nodal zones anchoring only one tension tie and $0.60\phi_c f'_c$ in nodal zones anchoring tension ties in more than one direction).
3. Determine geometry of truss model and determine forces in struts and ties. If truss is statically indeterminate, estimate relative stiffnesses of truss members in order to solve forces in struts and ties.
4. Determine required areas of tension ties ($A_s = T/\phi_s f_y$) and check details of tension reinforcement to ensure adequate anchorage into nodal zones.

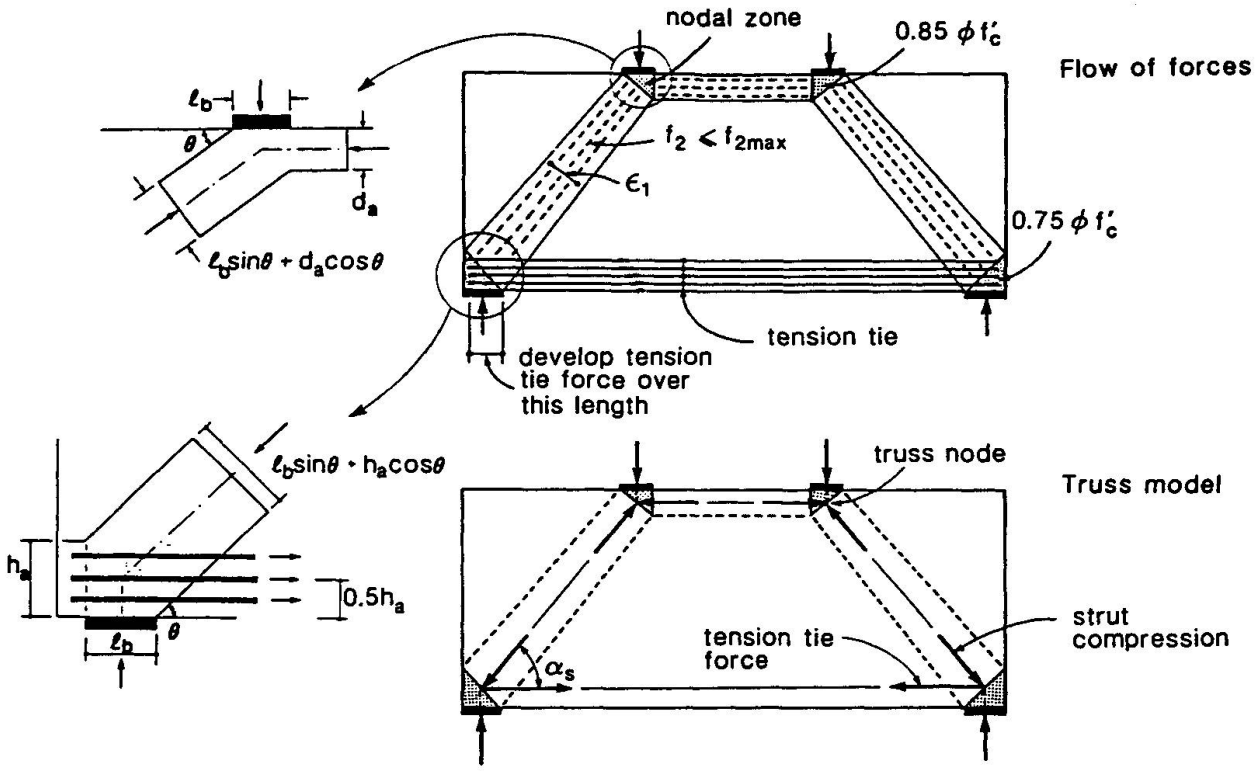

Figure 1: Strut and tie modeling of a deep beam.

5. Check strut compressive stresses from $f_2 = C/\phi_c A_c$ where A_c is effective area of strut as determined by end anchorage conditions (see Fig. 1). Check that f_2 does not exceed crushing strength, f_{2max}, of cracked concrete where:

$$f_{2max} = \frac{\lambda \phi_c f'_c}{0.8 + 170\epsilon_1} \leq 0.85 \phi_c f'_c \tag{1}$$

where ϵ_1 is the principal tensile strain and λ is a factor varying from 1.0 for normal density to 0.75 for structural low-density concrete.
Compatibility of strains is used to determine the principal tensile strain as:

$$\epsilon_1 = \epsilon_s + (\epsilon_s + 0.002) \cot^2 \alpha_s \tag{2}$$

where ϵ_s is the required strain in tension tie (usually taken as ϵ_y) and α_s is the angle between the strut and the tie crossing the strut.

Although design using strut and tie models appears simple, it takes considerable experience in choosing an appropriate model. Guidance on the use of strut and tie models is given by Schlaich *et al.*[9], Marti[8,10], MacGregor[11], Collins and Mitchell[12] and Cook and Mitchell[13].

3 SECTIONAL ANALYSIS VERSUS DISTURBED REGION ANALYSIS

Figure 2 compares the experimentally obtained shear strengths of a series of beams tested by Kani[14] with the predicted capacities from both sectional and strut and tie analyses[4]. In these tests the shear span to depth ratio, a/d, was varied from 1 to 7 and no web reinforcement was provided. At a/d ratios less than about 2.5 the resistance is governed by strut and tie

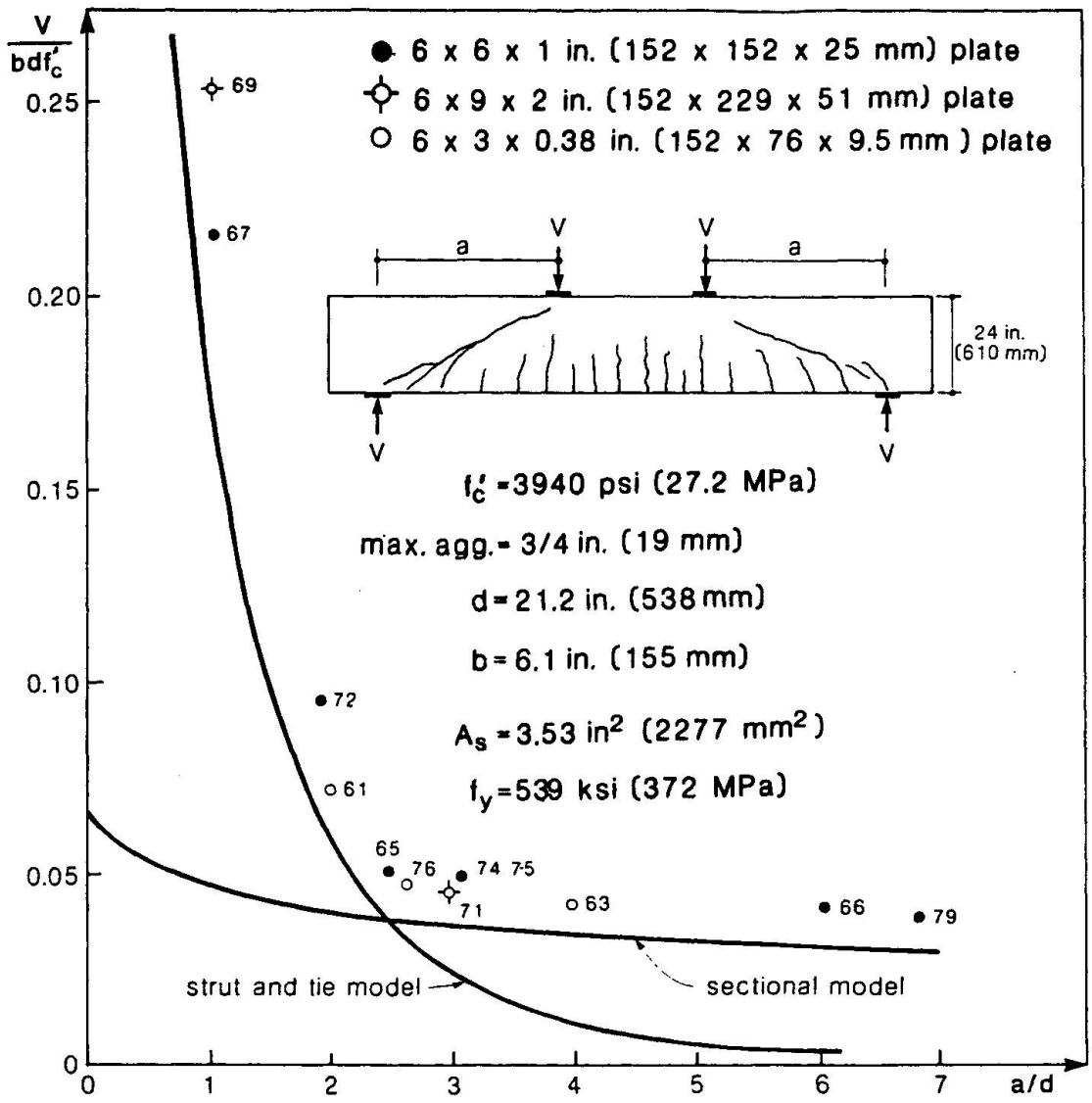

Figure 2: Predictions[4] of shear strength versus a/d ratio for tests reported by Kani[14].

action, with the resistance dropping off rapidly as a/d increases. The failures in this range were governed by crushing of the compressive struts, which were sensitive to the size of the bearing plates. Using the CSA code approach[1] in determining the strength of a member with $a/d = 2.0$ and having a 152 mm long bearing plate resulted in a value of f_{2max} of 10.2 MPa, or only $0.38f'_c$. This relatively low value of the crushing strength of the strut emphasizes the importance of considering strain compatibility in determining the strain softening effect. For a/d values greater than 2.5 the strength is governed by the conditions away from the disturbances created by the support reactions and the applied loads. Because of the significant amount of longitudinal reinforcement failure is governed by shear and the details of the support and loading bearings have little influence on the shear capacity of the member.

4 DESIGN VERSUS ANALYSIS

Elastic finite element analysis is useful for assessing the serviceability conditions of disturbed regions. It has also been used to approximate the required reinforcement for service and fac-

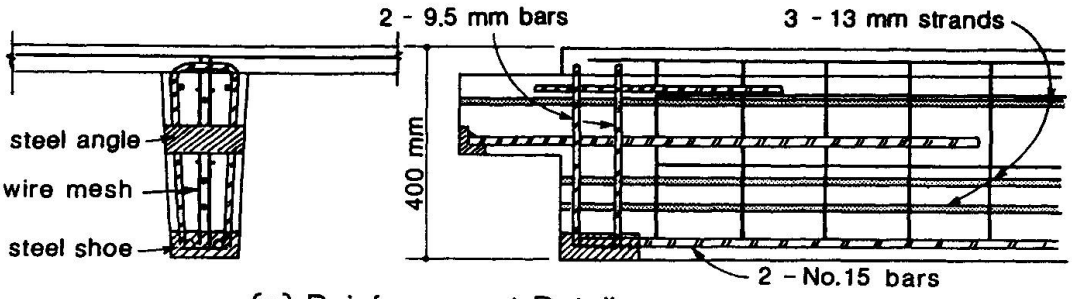

(a) Reinforcement Details

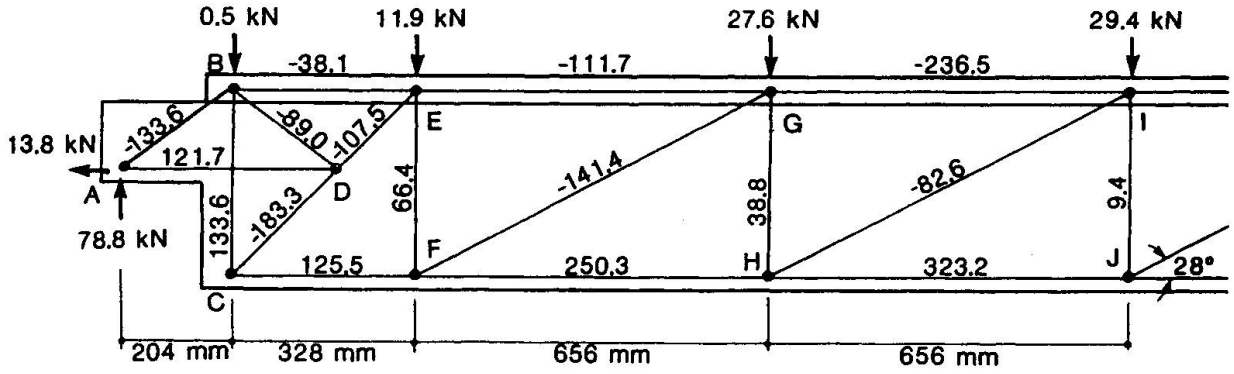

(b) Strut and Tie Model

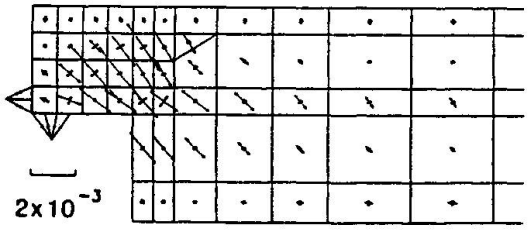

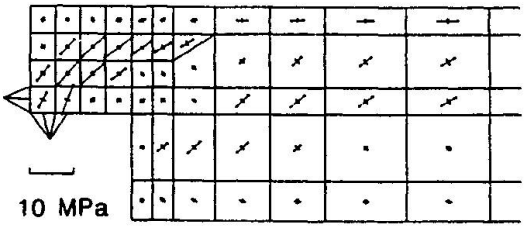

(c) Principal Concrete Strains (d) Principal Concrete Stresses

Figure 3: Analyses of thin stemmed precast pretensioned beam with dapped end[16].

tored loading conditions, however, it does not realistically predict the redistribution of stresses that takes place near ultimate. Non-linear finite element analyses[13,15], based on the modified compression field theory, naturally satisfy both equilibrium and compatibility and take into account the strain softening of the concrete compressive stress-strain relationship (see Eq. (1)). The complex transfer of forces across crack interfaces, including the influence of surface roughness and the increased tensile stresses in the reinforcement at crack locations, is approximated and the tensile stresses between the cracks (tension stiffening) is accounted for. This analysis provides the complete response through all stages of loading, including redistribution of stresses after cracking and yielding. Non-linear finite element analysis is an analysis tool, rather than a design tool, useful for verifying the behaviour of regions designed using strut and tie models.

Figure 3 shows a thin-stemmed dapped-end precast pretensioned beam tested at McGill University[16]. In order to permit the development of the strut and tie model shown (see Fig. 3b), a steel shoe was provided at the bottom of the thin stem (see Fig. 3a) and horizontal and vertical ties, welded to the shoe, provided the bottom chord and the vertical tension tie forces in the truss. Figure 3c and d show the principal concrete strains and stresses predicted by non-linear

finite element analysis. The test beam failed at an end reaction of 79.8 kN. The strut and tie and finite element predictions were 78.8 and 84.5 kN, respectively.

CONCLUSIONS

Strut and tie models, which appropriately account for compatibility in determining the compressive capacity of the struts, provide a simple design method for disturbed regions. Non-linear finite element analysis provides a more sophisticated tool for checking the design for both service and ultimate conditions.

REFERENCES

1. CSA Committee A23.3, "Design of Concrete Structures for Buildings", CAN3-A23.3-M84, Canadian Standards Association, Rexdale, Canada, 1984, 281 pp.
2. COLLINS, M.P. and MITCHELL, D., "Shear and Torsion Design of Prestressed and Non-Prestressed Concrete Beams", PCI Journal, V. 25, No. 5, Sept-Oct. 1980, pp. 32–100.
3. VECCHIO, F.J. and COLLINS, M.P., "The Modified Compression-Field Theory for Reinforced Concrete Elements Subjected to Shear", ACI Journal, V. 83, No. 2, March-April 1986, pp. 219–231.
4. COLLINS, M.P. and MITCHELL, D., "Prestressed Concrete Structures", Prentice Hall, Englewood Cliffs, NJ, USA, 1991, 766 pp.
5. RITTER, W. "The Hennebique Design Method (Die Bauweise Hennebique)", Schweizerische Bauzeitung (Zürich), V. 33, No. 7, Feb. 1899, pp. 59–61.
6. MÖRSCH, E., "Concrete-Steel Construction (Der Eisenbetonbau)", Translation of the third German Edition by E.P. Goodrich, McGraw-Hill Book Co., New York, 1909, 368 pp.
7. THÜRLIMANN, B., MARTI, P., PRALONG, J., RITZ, P., and ZIMMERLI, B., "Anwendung der Plastizitaetstheorie auf Stahlbeton", Institute for Structural Engineering, ETH Zürich, 1983, 252 pp.
8. MARTI, P., "Basic Tools of Reinforced Concrete Beam Design", ACI Journal, V. 82, No. 1, Jan.-Feb. 1985, pp. 46–56.
9. SCHLAICH, J., SCHÄFER, K., and JENNEWEIN, M., "Towards a Consistent Design of Reinforced Concrete Structures", PCI Journal, V. 32, No. 3, 1987, pp. 74–150.
10. MARTI, P., "Sub-Theme 2.4: Dimensioning and Detailing", Proceedings IABSE Colloquium on Structural Concrete, Stuttgart, April 1991.
11. MACGREGOR, J.G., "Sub-Theme 2.4: Dimensioning and Detailing", Proceedings IABSE Colloquium on Structural Concrete. Stuttgart, April 1991.
12. COLLINS, M.P. and MITCHELL, D., "Chapter 4 - Shear and Torsion", CPCA Concrete Design Handbook, Canadian Portland Cement Association, Ottawa, 1985, pp. 4-1–4-51.
13. COOK, W.D. and MITCHELL, D., "Studies of Disturbed Regions near Discontinuities in Reinforced Concrete Members", ACI Structural Journal, V. 85, No. 2, 1988, pp. 206-216.
14. KANI, M.W., HUGGINS, M.W., WITTKOPP, P.R., "Kani on Shear in Reinforced Concrete", Dept. of Civil Engineering, University of Toronto, Toronto, Canada, 1979, 225 pp.
15. ADEGHE, L.N. and COLLINS, M.P., "A Finite-Element Model for Studying Reinforced Concrete Detailing Problems", Publication No. 86-12, Dept. of Civil Engineering, University of Toronto, Toronto, Canada, Oct. 1986, 267 pp.
16. SO, K.M.P. "The Behaviour of Thin Stemmed Precast Prestressed Concrete Members with Dapped Ends", M.Eng Thesis, McGill University, Montreal, Canada, 1989, 155 pp.

Strut-Crack-and-Tie Model in Structural Concrete

Le modèle tirant-bielle-fissure en béton armé

Das Risswerkmodell – materialgerechtes Modell für Stahlbeton

Andor WINDISCH
Civil Engineer
Dyckerhoff & Widmann AG
Munich, Germany

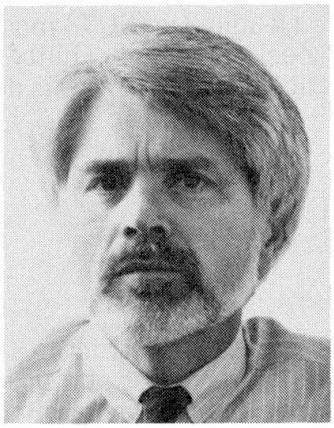

Andor Windisch, born 1942, obtained his Dr. techn. degree at the TU Budapest, Hungary in 1975. He served there as assistant professor for reinforced concrete structures until 1983. For 3 years he was research assistant at TU Stuttgart. He joined the R&D Department of a building company in 1987.

SUMMARY

The strut-crack-and-tie model, a synthesis of section-by-section design and strut-and-tie model, is presented. The geometry of the cracks and correspondingly that of the struts between cracks follow the linear elastic trajectories and can be predicted explicity. The material parameter of the model is the effective steel strength. It depends on the angle between a crack and the reinforcing bar crossing this crack. The concrete struts are assumed to be stressed biaxially. Applicability of the model to design and detailing is presented in an example.

RÉSUMÉ

Le modèle tirant-bielle-fisure est en fait une synthèse du calcul de résistance section par section et du calcul utilisant l'analogie du treillis. La géométrie des fissures, et donc des bielles en béton délimitées par ces fissures, suit les trajectoires linéaires élastiques et peut ainsi être prévue explicitement. Le paramètre de matériau du modèle est la résistance effective de l'acier, qui dépend de l'analyse formé par la fissure et la barre d'armature traversant la fissure. Les bielles de béton subissent une contrainte biaxiale. Un exemple illustre l'application de ce modèle dans le dimensionnement et les détails de construction.

ZUSAMMENFASSUNG

Das Risswerkmodell, eine Synthese der Querschnittsbemessung und des Stabwerkmodells, wird vorgestellt. Die Rissgeometrie und damit auch die Form und Richtung der dazwischenliegenden Druckstreben wird aufgrund des linear-elastischen Trajektorienbildes angenommen. Die wirksame Stahlfestigkeit, die vom Winkel zwischen Riss und Bewehrungsstab abhängt, dient als Materialparameter. Druckgurt und Druckstreben sind als zweiachsig beansprucht betrachtet. Die Anwendbarkeit des Modells zur Bemessung und zum Bewehren wird an einem Beispiel gezeigt.

1. INTRODUCTION

The section–by–section design for flexure and axial load in B regions is simple, rational and general but generally does not work in D regions. Attempts to adapt the classical 45–degree truss model to the results of shear and torsion tests made it complex, empirical and restricted.

Besides the diagonal compression field theory [1] and methods of dimensioning based on equilibrium solutions from the theory of plasticity [2] the strut–and–tie model [3] has been proposed as a unified design concept which is physical and consistent for all types of structures. Its development is not yet finished.

The paper presents the strut–crack–and–tie (SCT) model: a synthesis of the section–by–section design and the strut–and–tie model. The applicability of the SCT model at dimensioning and detailing of geometrical and statical discontinuities is demonstrated on a dapped end.

2. STRUT–CRACK–AND–TIE MODEL

2.1 Basic considerations

During loading of structural concrete (s.c.) structures first the concrete will crack. As a rule, the cracks are not straight (plain) and consist of a flexural crack and a shear crack. The loads can be increased as long as a) the reinforcement which crosses the cracks is able to carry the tensile forces which are necessary for the equilibrium in the cracked sections or b) the compressive strength of the concrete is reached in the compressive zone or in the web. S.c. structures or parts of them, where their failure is announced by yielding of the reinforcement are called normal–reinforced. Those where the reinforcement remains elastic at failure are called over–reinforced.

80–90 per cent of s.c. structures are normal reinforced. They will fail along one of their cracked sections. This section consists of a flexural–shear crack and a sliding (failure) surface across the compression zone. In case of pure bending only a flexural crack and a failure zone in the compression zone develop, their direction is perpendicular to the member's axis. In all other cases the failing sections are curved: in regions with flexure and shear they are cylindrical, while in those with torsion they are distorted. All these failing sections will be called further *sections.*

It was concluded that the load bearing capacity of normal–reinforced s.c. structures cannot be characterized neither with the concrete compressive strength nor with any reduction of this strength. The adjustment of a calculated ultimate bending moment to a test result, which was influenced by anything, will seldom function by the help of any reduction of the effective compressive strength, as it is well known, that the flexural capacity of a normal–reinforced section is quite insensitive to scatters in the concrete strength.

All these circumstances point out that the effective concrete compressive strength cannot be chosen as material parameter in any physical and consistent model for normal–reinforced s.c. structures.

In a second step a possible and reliable reason of the reduced load bearing capacity of D regions with geometrical discontinuity has been found.

Although each member in Figs. 1b–i contains the same bracket shown in Fig.1a, different additional flexural reinforcements are needed in the root sections of the brackets in cases c, d, f, g and i.

Analyzing the crack patterns of these regions it was found that at those members where additional reinforcement was needed, the direction of the flexural crack in the root section (at

the geometrical discontinuity) was not perpendicular to that of the usually horizontal flexural reinforcement (cf. Figs. 2a–i). It is well known, that reinforcing bars are less effective if they cross a crack at an angle less than 90°.

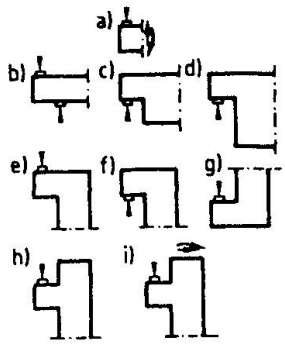

Fig. 1 D regions with the same loading but with partly different reinforcement

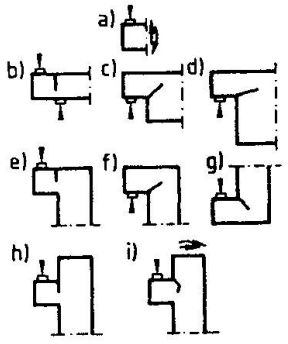

Fig. 2 Direction of flexural cracks in D regions shown in Fig. 1

The idea of the SCT model was born.

2.2 Definition of the SCT Model

The principal characteristic of the SCT model is a system of (cracked) sections. The form of the section depends on the member's geometry and the state of action effects. This form can be simply predicted. The sections are crossed by uniaxially stressed tension ties consisting of reinforcing and/or prestressing steel. The concrete compression struts between the cracks and the compression zone are stressed bi- or triaxially. The tensile strength of the concrete is an integral part of the model, its existence should be guaranteed by both structural and technological measures.

2.3 Selection of Strut–Crack–and–Tie Model

The procedure for laying out SCT models is straightforward omitting any trial and error efforts. Each designer will come with the same model which will reflect the natural load carrying mechanism of s.c. No obscure adaptation of the concrete to the strut–arrangement in the model is demanded. The designer may apply his ingenuity to find the most economic and aesthetic form of the structure.

Starting from a linear elastic analysis of uncracked members and their connections, after applying (if possible) a plastic moment redistribution, the form of the sections can be predicted directly using one and the same model. Instead of looking for the most valid model using minimum strain energy concepts etc. the most convenient reinforcement pattern (e. g. industrialized reinforcement) can be implied directly into the model.

2.4 Interaction of Flexure and Shear

The assumption that flexure and shear can be decoupled and considered separately is assumed to be the source of those troubles which are treated in both invited lectures [4], [5], e.g.:

- shear force carried by concrete
- enhanced shear strength of prestressed members
- shear strength of shear–unreinforced slabs.

If the biaxial state of stress and failure criteria resp. of the compression zone would be rediscovered [6], [7], [8], than all these aforementioned problems and many others could be solved.

In the SCT model the transversal (shear) component of the strength of the compressive zone is fully recognized. The contribution of aggregate interlock along a crack to the shear strength of a member can be easily taken into account at verification of the section's equilibrium.

SCT models indeed allow for consideration of internal forces due to shear, flexure, torsion and axial loads. As when applying this model always the equilibrium of the full member and not a single node is checked, the SCT model provides a real full–member design.

2.5 Material Strength

2.5.1 Steel in Tension

The strength of the steel in tension in ULS is taken as

$$f_{yd} = \Psi \cdot f_{yd}$$

where Ψ is an effectiveness factor, not greater than 1.0. This effectiveness factor accounts for the reduction of the useable strength of a rebar which is not perpendicular to the crack. Factor Ψ, a function of the angle α, shown in Fig. 3, was determined with extended computer calculations using realistic local bond stress – slip relationships, taking into consideration a) the distance between cracks having the characteristic crack width and b) the compatibility requirement that the crack width corresponding to $\alpha = 0$ should remain constant for any α value. The derivation of the effectiveness factor can be found in [9].

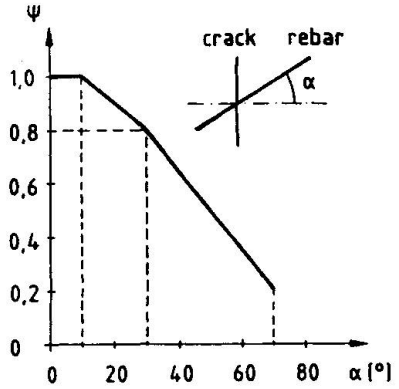

For $10° \leq \alpha = 30°$

$\Psi = 1.00 - 0.01\,(\alpha - 10°)$

for $30° \leq \alpha \leq 70°$

$\Psi = 0.80 - 0.015\,(\alpha - 30°)$

Applying the same factors at checking SLS, the proper performance of D regions can be expected, as it was confirmed by control calculations.

Fig. 3 Effectiveness factor Ψ of a skew rebar

2.5.2 Concrete

Compression struts are considered to be stressed biaxially. The components of the strength of a strut are

a) parallel to the strut's axis $D = b \cdot x \cdot f_{cd}$

b) perpendicular to it $\nu \cdot D$.

The assumption a) can be maintained in webs as well until no improved empirical verification of the opposite is available. It is felt, that the strains perpendicular to the strut will not influence very much the effective compressive strength. No evidence of any reduction in the compression zone due to the anchorage of highly stressed stirrups has been found until now. Obviously, reductions at effective web thickness due to ducts for prestressing elements but even to relative thick rebars which are not perpendicular to the strut's axis should be taken into account.

The factor ν in (b) can be deduced from the Mohr–failure–criterion in a similar way as in [6]. It gives a realistic and physical meaning to the V_c term.

No reduction of the concrete strength under loading plates or supports due to anchored tension bars is necessary. Obviously transverse reinforcement is required to "hang up" longitudinal rebars which lie outside the bearing plate, in order to avert a downward splitting of them.

2.6 D Regions

D regions classified in [3] as a) geometrical discontinuities, b) statical discontinuities and c) combination of a) and b) are interpreted in the SCT model as:

i) the flexural crack at the point of geometrical discontinuity is not perpendicular to any boundary of the region (cf. Fig. 2c, d, f, g and i)

ii) in the neighbourhood of the statical discontinuity only a part of the effective height of the member is really efficient and/or transverse reinforcement (due to bursting and spalling stresses) must be applied when the concrete stress under the loading plate is greater than f_{cd} (cf. deep beams).

Both, variation of the "efficient height", as function of the distance to the concentrated load and inclination of the flexural crack, as function of the linear elastic state of stress at the geometrical discontinuity, can be determined once and for ever and be comprised into quite simple rules.

Knowing the "efficient height" of a given section in a D region, the dimensioning to flexure can be carried out as in a B region: the beam theora can be applied. A similar procedure for deep beams has been suggested in [10].

2.7 Staggering Rule

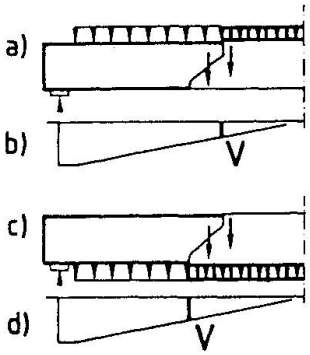

The form of the sections in both, B and D regions gives a direct interpretation of the required extension of the flexural reinforcement in presence of shear and of the staggering rules as well.

The beam shown in Fig. 4a is loaded on its top, that in Fig. 4c on its bottom. Each beam is divided in the same manner into two parts by a section. The inner forces along these sections substitute the loading on the parts at the right. The difference in the shear loads corresponding to the two sections is obvious (cf. Figs. 4b and d resp.).

Fig. 4 Staggering rule in beams loaded on their top and bottom resp.

It should be emphasised that SCT models are clearly intended to be behavioural models, thus they remain simple and transparent. The following example should verify it.

3. DAPPED END OF A PREFABRICATED GIRDER

Intensive linear elastic FE calculations showed that the inclination of the flexural crack at the reentrant corner of a dapped end can be taken as

$$\alpha = 90\, h_k / h \quad [°] \qquad (1)$$

Test results [11] confirmed the applicability of (1).

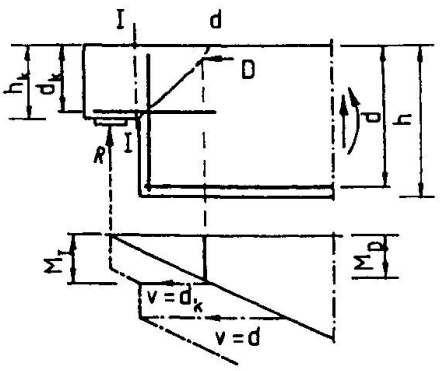

The flexural reinforcement at this corner must be dimensioned for the moment M_D (under the point of application of the compressive inner force on the section d–d shown in Fig. 5a. Applying the horizontal shifts v and v_k resp. due to the effect of the inclined shear crack, approximate the same moment is obtained under the conventional cross section I–I, which is to be dimensioned here actually.

Fig. 5 Dapped end: determination of the design moment for the corner section

At dimensioning the flexural reinforcement in this section the inclined position of the flexural crack relative to the reinforcing bars must be taken into account. If only horizontal reinforcement (A_{sh} in Fig. 6a) will be applied in the dapped end then the flexural equilibrium equation for section d–d in ULS is

$$M_D = M_I = A_{sh} \cdot \Psi_{(90° - \alpha)} \cdot f_{sd} \cdot z_k + A_{sv} \cdot \Psi_{\alpha} \cdot f_{sd} \cdot z_k \cdot \cot \alpha \qquad (2)$$

If inclined reinforcing bars (A_{ss}) will be added (Fig. 6b) then (2) must be extended with

$$A_{ss} \cdot \Psi_{(90° - \alpha - \beta)} \cdot f_{sd} \cdot z_k \cdot (\cos \beta + \sin \beta \cdot \cot \alpha) \qquad (3)$$

The flexural dimensioning of other sections on both sides of the reentrant corner can be performed in the well known manner, as each flexural crack there is perpendicular to the rebars (see Figs. 6c.)

The SCT model gives clear guidance for detailing as well: each rebar may be anchored "behind" that section, where its strength is no more required for maintaining equilibrium in ULS (see Fig. 6d).

Failure loads, calculated with a truss model [11] and SCT model are compared with test results [11] in Fig. 7. The SCT model approximates the test results better.

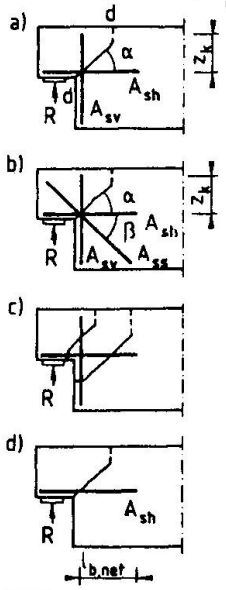

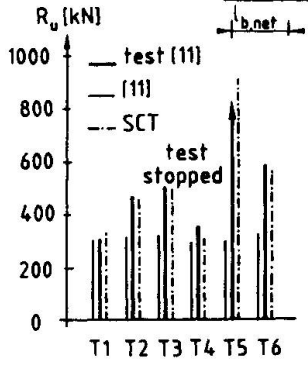

Fig. 6 Dimensioning of a dapped end a) without b) with additional inclined reinforcement at the corner c) at sections on both sides of the corner d) anchorage of the horizontal reinforcement

Fig. 7 Comparison of test results [11] with calculated failure loads

SCT models yielded excellent approximations for test results with other D regions as well [12].

REFERENCES

1. VECCHIO F.J., COLLINS M.P., The Response of R.C. to In–Plane Shear and Normal Stresses. Publ. No. 82–03. University of Toronto
2. NIELSEN M.P. et al., Concrete Plasticity, Beam Shear, .. Spec.Publ. TU Denmark, 1978
3. SCHLAICH J. et al., Towards a Consistent Design of R.C. Structures. JOURNAL PCI 1987
4. MACGREGOR J.G., Dimensioning and Detailing. Invited lecture, Sub–theme 2.4
5. MARTI P., Dimensioning and Detailing. Invited lecture, Sub–theme 2.4
6. WALTHER R., Über die Berechnung der Schubtragfähigkeit .. Beton u Stahlb. 1962.
7. KORDINA, K. et. al., Zur Schubtragfähigkeit von Stahlbeton . Beton u. Stahlb. 1987
8. ELZANATY A.H. et al., Shear Capacity of RC Beams .. ACI Journal, March–April 1986
9. WINDISCH A., Wirkungsgrad eines schiefen Bewehrungsstabs. Bauingenieur, 1991
10. LEONHARDT F., MÖNNIG E., Vorlesungen über Massivbau. Teil 2. Springer 1977
11. STEINLE A., ROSTASY P., Zum Tragverhalten ausgeklinkter Trägerenden. Beton+Fertigteiltechnik, Jun–Jul. 1975
12. WINDISCH A., Das Modell der charakteristischen Bruchquerschnitte. B. u.Stahlb. 1988

Models and Tests of Anchorage Zones of Post-Tensioning Tendons

Modèles et essais de zones d'ancrage des câbles de précontrainte

Modelle und Versuche von Verankerungszonen von Vorspannkabeln

Olivier L. BURDET
Scientific Associate
Fed. Inst. of Technology
Lausanne, Switzerland

Carin L. ROBERTS
Ph. D. candidate
Univ. of Texas
Austin, TX, USA

Gregory L. FENVES
Prof. of Civil Eng.
Univ. of California
Berkeley, CA, USA

David H. SANDERS
Prof. of Civil Eng.
Univ. of Nevada
Reno, NV, USA

John E. BREEN
Prof. of Eng.
Univ. of Texas at Austin
Austin, TX, USA

SUMMARY
This paper presents the results of an investigation of the behaviour and the design of anchorage zones of post-tensioning tendons. The analytical component is a combination of Finite Element Analysis and Strut-and-Tie Models. A total of more than 60 tests of anchorage zones are included in discussion and practical guidelines for the design proposed for incorporation in the AASHTO Bridge Design Specification are outlined.

RÉSUMÉ
Cet article présente les résultats d'un projet de recherche sur le comportement et le dimensionnement des zones d'ancrage des câbles de précontrainte. La partie analytique comprend à la fois une analyse par la méthode des éléments finis et des modèles de treillis. Au total, cet article inclut les résultats de plus de 60 tests expérimentaux de zones d'ancrage et inclut des directives pratiques qui ont été proposées pour être inclues dans la norme américaine de ponts routiers AASHTO.

ZUSAMMENFASSUNG
Im vorliegenden Bericht werden die Resultate eines Forschungsprojektes über das Verhalten und die Bemessung von Verankerungszonen von Vorspannkabeln beschrieben. Der analytische Teil beinhaltet sowohl Finite Element Berechnungen als auch Fachwerkmodelle. Die Resultate von mehr als 60 Versuchen an Verankerungszonen werden aufgeführt. Weiter enthält dieser Bericht praktische Richtlinien, die für die Aufnahme in die amerikanische Strassenbrücken-Norm AASHTO vorgeschlagen wurden.

1. Introduction

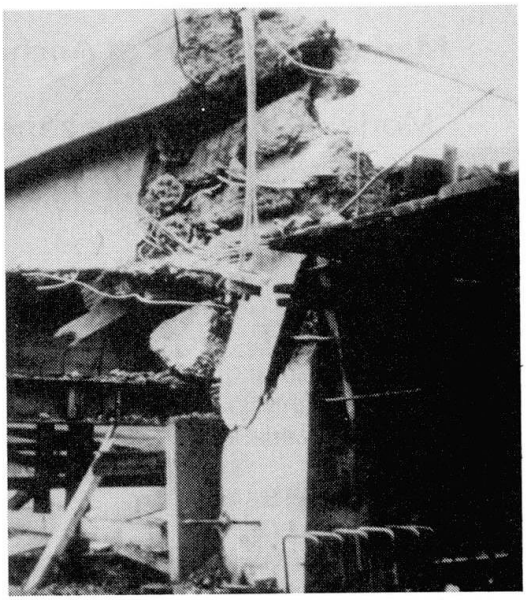

Figure 1: Failure of an Anchorage Zone in a Pedestrian Bridge during Construction

The quest for development of a consistent approach to structural concrete clearly requires a hierarchy of highly transparent design oriented analysis tools [2]. These will range from relatively traditional section mechanics principles suitable for use in B-regions to the more intuitive strut-and-tie models (STM) or more formal elastic or non-linear finite element analyses (FEA) required for the D-regions. Scordelis [12] indicates that while the latter are extremely useful, "... it is imperative that experienced and qualified structural engineers be involved in the interpretation of the results using their judgement and knowledge of structural behavior..." MacGregor [5] reiterates this need but gives special emphasis in the D-regions saying "... the details of the reinforcement in the discontinuities control the strength of these regions and hence must be considered by the structural engineer." Marti [6] suggests that in usual applications of STM, the design is rather insensitive to the assessment of the effective concrete stress, f_c. While this is true in many applications, it is clearly not true in design of post-tensioned anchorage zones. In such discontinuity zones, the very large forces transmitted to the concrete by the tendon anchorages cause very high local stresses on the concrete. The spreading of these forces through the member causes substantial transverse stresses and forces. Problems both at the serviceability limit state, with undesirable cracking, and at ultimate, with possible brittle and explosive failure of the anchorage zone need to be prevented.

Test results and failures during construction (See Figure 1) indicate that compressive stresses in unconfined nodes or at the intersection of confined nodes and unconfined struts often govern actual capacity of anchorage zones. This particular detailing application thus poses much more of a challenge to the development of detailing methods since assessing node and strut capacity is far more difficult than providing proper tie capacity through dimensioning of reinforcement.

This paper describes current progress on an on-going NCHRP sponsored study at the University of Texas at Austin to investigate the behavior of post-tensioning tendons anchorage zones, to provide guidance and to suggest specific provisions for anchorage zone design for the AASHTO Bridge Specification [1].

2. State of Stresses in an Anchorage Zone

The state of stresses in the anchorage zone of a post-tensioning tendon is very complex. Within very short distances, the stresses parallel to the tendon vary from very high compressions (often in excess of the uniaxial compressive strength of the concrete) ahead of the anchorage device to the average compressive stress induced by the post-tensioning, usually in the vicinity of $0.45f_c'$. Perpendicular to the axis, the stresses vary from very high compressive stresses under the device to tensile stresses which often exceed the tensile capacity of the concrete at a certain distance from the anchorage. Figure 2 identifies the major areas of tensile stresses in a simple anchorage zone. The tensile force caused by the lateral spreading of the tendon force from the anchorage device to the entire cross section is often called bursting force in the literature. The force parallel to the concrete surface has in the past often been called spalling force. Because this term implies that this force can cause spalling of the concrete, which is not the case because the force acts parallel to the face of the concrete, and not perpendicular to it, it is more appropriate to call it *edge tension force*. Edge tension forces also occur between anchorages acting on the same concrete surface, and on faces parallel to the axis of the tendon.

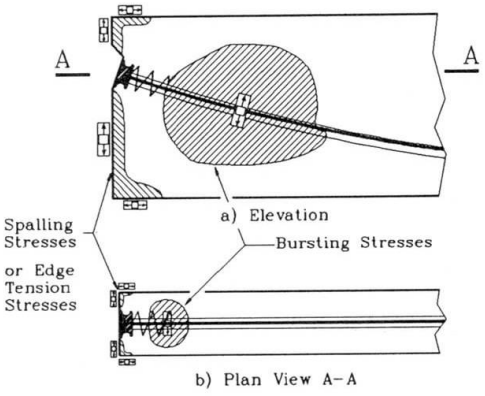

Figure 2: Tensile Stresses in the Anchorage Zone

3. Local Zone - General Zone Concept and Modes of Failure

As a consequence of the complex state of stresses, various modes of failure have been observed for anchorage zones. Aside from failures caused by insufficient material properties or lack of equilibrium, the failures of anchorage zones can be categorized as follows:

- Local compression failure, in which the failure occurs at a very short distance from the anchorage device, and is caused by lack of confinement in the area immediately surrounding the anchorage device.
- Compression failure, similar to the previous mode failure, but with the difference that the failure occurs at a larger distance from the anchorage device, which is itself sufficiently confined.
- Tension failure, in which the reinforcement provided to resist the tensile force induced by the spreading of the concentrated tendon load is insufficient.

Figure 3 shows two regions in the anchorage zone. The *local zone*, in the immediate vicinity of the anchorage device, is highly dependant on the post-tensioning system and is the responsibility of the supplier of the anchorage device. The *general zone* is more remote from the anchorage device and is less influenced by the post-tensioning system. It is the responsibility of the structural engineer. Of the three modes of failure described above, the first one occurs in the local zone, the second mode of failure occurs in the general zone, most often at the interface with the local zone, and the third mode of failure occurs in the general zone.

In order for anchorage devices to be deemed satisfactory, they need to either meet maximum bearing stress and minimum stiffness requirements or to be tested following a prescribed testing procedure described in Section 4. The distinction between local and general zone gives flexibility to the constructor, who can choose the anchorage device and the post-tensioning system, without jeopardizing the integrity of the structure, and without unduly complicating the work of the design engineer.

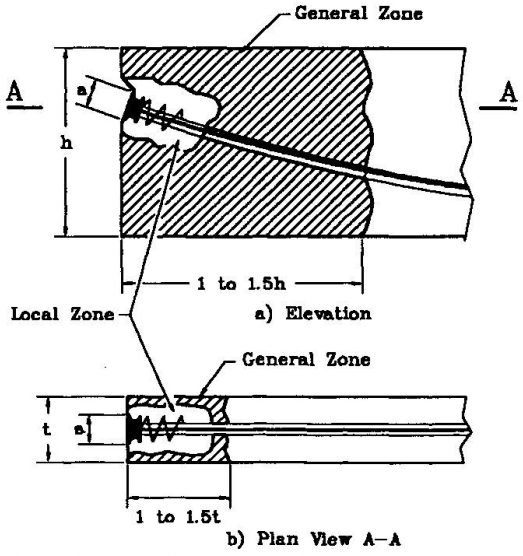

Figure 3: Local Zone and General Zone

4. Local Zone Tests by Roberts

A part of the NCHRP Anchorage Zone research project consisted in an investigation focusing on the behavior of local anchorage zones both at service state and at ultimate. The purpose of this study by Roberts [9] was to define the test procedures and compliance criteria for the testing of anchorage devices. Roberts tested 31 local zone test specimens. The behavior of local anchorage zones was found to be sensitive to the type and amount of confining reinforcement, as well as to the cover provided around the anchorage device. Existing formulae by Richart [8] and Nyogi [7] were enhanced to give a better prediction of the strength of a local zone. Cyclic testing of local zones gives results similar to extended (48 hours) testing, and is more representative of the behavior of anchorage zones under field conditions than monotonic testing. A standardized testing procedure for the local zone was proposed by Roberts for introduction in the AASHTO Bridge Specification.

5. Finite Element Analysis and Strut-and-Tie Models

It is nor practical to test all possible general zone configurations, therefore the design of the general zone must be approached in a different manner than the local zone. The number of variables affecting the design of the anchorage zone remains large even though the local zone has been addressed. A survey of the current design practice in the United States by Sanders [10] showed that the post-tensioning industry is very creative. Tendons often present an eccentricity, an inclination and a curvature in the anchorage zone. Multiple tendons are commonly used, in groups of two to six tendons. Transverse post-tensioning and transverse reactions are often present in the anchorage zone. Special geometries are used to introduce the post-tensioning force to the section, using for example blisters or ribs. The first phase did not consider the expanding field of external post-tensioning. The project was set up to use a combination of elastic finite element analysis, strut-and-tie models and physical tests. Linear elastic finite element analysis offers the advantage of being a well known method of obtaining the internal state of stresses in a body. As pointed out by

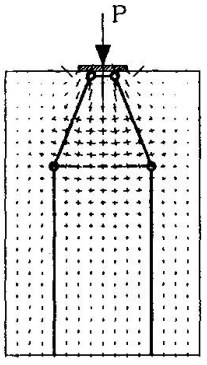

Figure 4: Simple Strut-and-Tie Model with Elastic Stress Vectors

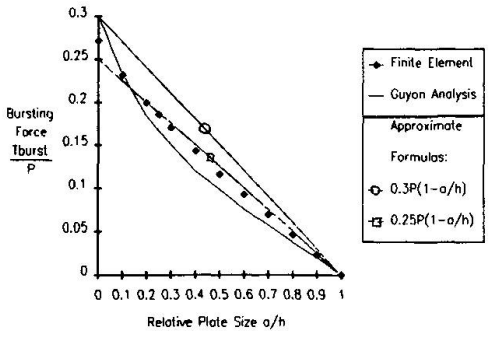

Figure 5: Bursting Force for Concentric Tendons

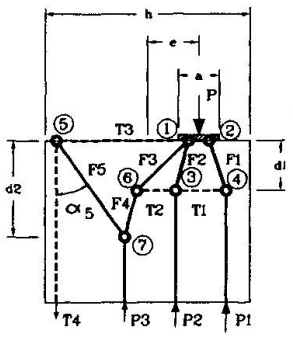

Figure 6: Strut-and-Tie Model of an Eccentric Anchorage Zone

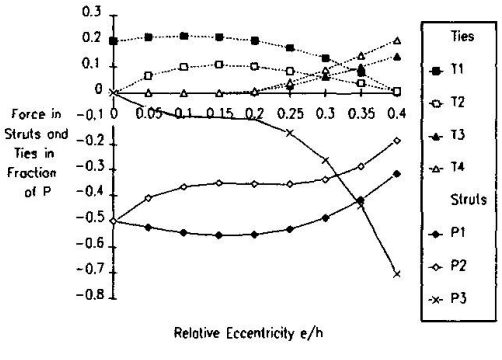

Figure 7: Forces in the Struts and Ties as a Function of the Eccentricity

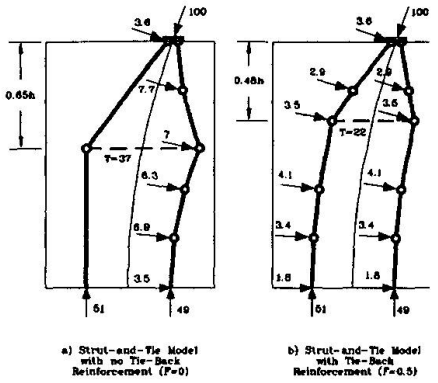

Figure 8: Strut-and-Tie Model of an Anchorage Zone with a Curved Tendon, Eccentricity 0.25h and Initial Inclination 20 degrees

Schlaich [11], the elastic state of stresses constitutes a good starting point for the development of strut-and-tie models. Of special interest is the representation of the principal stress vectors shown in Figure 4. These vectors give a good idea of the flow of forces through the anchorage zone and are helpful in assessing the adequacy of a strut-and-tie model. The physical test specimens by Sanders [10] were used to demonstrate the validity of the models and to calibrate the design formulae.

Figure 5 shows the bursting force obtained by integrating the elastic stresses perpendicular to the tendon path, along with the force obtained from the simple strut-and-tie model shown in Figure 4. As can be observed, the correlation is quite good. The figure also shows Guyon's equation [4] for the same force.

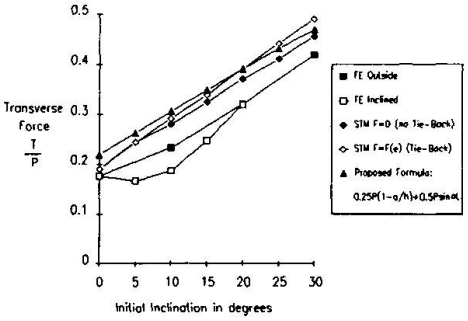

Figure 9: Transverse Bursting Force as a Function of the Initial Inclination for an Initial Eccentricity of 0.25h

The real power of the strut-and-tie model is its ability to model a wide range of anchorage zone configurations. Figure 6 shows a strut-and-tie model for an anchorage zone with an eccentric load. Figure 7 shows the forces in the various members as a function of the eccentricity.

Figure 8 shows two possible strut-and-tie models for an anchorage zone with an eccentricity, an inclination and a curvature of the tendon. If no tie-back reinforcement is provided, all the tendon deviation forces are transmitted to the strut on the inside of the tendon, and the external strut is straight between the reinforcement bars. If tie-back reinforcement is provided, the tendon deviation forces are distributed to both compression struts. If the force in the tie-back reinforcement is added to the bursting force, it is found that the sum is approximately equal to the bursting force in the case without tie-back reinforcement. Figure 9 shows the variation of the bursting force as a function of the initial inclination. The figure also shows the results obtained from the finite element analysis and the values predicted by an approximate formula as outlined in Section 6. In a simplified fashion, the increase in tensile force caused by the inclination of the tendon can be approximated as one half of the net shear on the general zone summing the effect of external loads and the transverse component of the post-tensioning force. This corresponds to the intuitive idea that roughly half of the force is resisted by each compression strut.

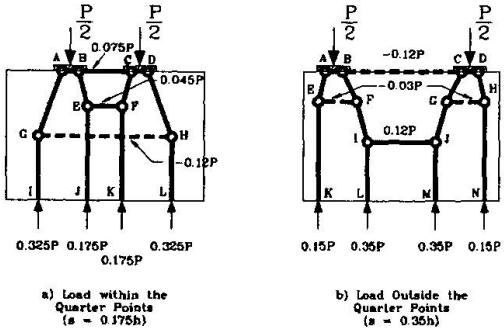

Figure 10: Examples of Strut-and-Tie Models with two Tendons

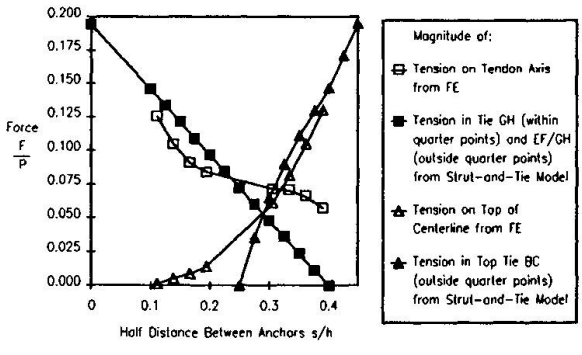

Figure 11: Tension Forces in an Anchorage Zone with Two Tendons

The effect of groups of tendons was investigated, and it was found that, for rectangular sections with straight tendons, the largest tensile forces are induced when only two tendons are used. Figure 10 shows the two basic configurations for two anchorages. If both tendons act within the kern of the section, the state of stresses is similar to that induced by a single anchorage device. As the tendons move outside the kern, an increasingly large edge tension force is induced between the anchorage devices close to the surface of the concrete. Figure 11 shows the edge tension force between the anchorages as a function of the spacing of the anchorages.
Because the compressive stresses in the immediate vicinity of the anchorage device are usually higher than the uniaxial compressive strength of the concrete f'_c, the verification of the capacity of the concrete compression struts is critical. Most authors assume that the limiting stress in the concrete struts is some fraction of f'_c, which is too constraining for anchorage zones. Sanders [10] incorporated the effect of confining reinforcement in a strut-and-tie model. For most practical cases, however, the checks involved in such calculations are beyond the capabilities of the engineer. Therefore, the local zone acceptance tests are relied on for determining the adequacy of the confined node. The critical section for the verification of the compressive stresses in the concrete struts is defined at a certain distance from the anchorage device (in general at one times the lateral dimension of the anchorage device). This allows one to check the compressive stresses in the concrete against the conventional value of $0.70f'_c$ which is commonly accepted for strut-and-tie models.

6. Design Method for Anchorage Zones

The goal of the NCHRP Anchorage Zones research project is the elaboration of a clear, consistent and easily applicable method for the design of anchorage zones of post-tensioning cables. Assuming that the engineer has a good knowledge of the location and magnitude of the force for each tendon, some idea of the size of the anchorage device that will be required to transmit the force and the assurance that the anchorage device used satisfies the testing requirements of Section 4, guidelines for the design of the general anchorage zone are needed. A number of procedures are suggested in the proposed AASHTO revisions. Two general procedures are allowed. One is a detailed elastic analysis such as a valid finite element analysis (FEA). Rules are provided for integrating tensile stresses and selecting appropriate limiting stress values. The second procedure allowed is the strut-and-tie model (STM). Since this equilibrium based procedure is not sensitive to compatibility induced stresses at service load levels, such as edge tension, or spalling stresses around anchorages, certain guidelines are provided requiring supplemental spalling crack control reinforcement. Recognizing that either FEA or STM solutions may require considerable extra effort for the design of some relatively simple but common applications, an approximate procedure is also included. This procedure was developed from the results of FEA and STM parametric studies [3]. It uses relatively simple formulae to determine the magnitude and location of the bursting force and to check the compressive stress at the interface between the local zone and the general zone. It is limited to the case of a single anchorage, or of a single group of closely spaced anchorages acting on a rectangular cross section.

7. Evaluation of the Methodology based on Test Results by Sanders

Sanders [10] conducted a series of 36 tests of anchorage zones. In the specimens modelling single tendon anchorage zones, the reinforcement patterns and the tendon eccentricity, inclination and curvature were varied. Tests of anchorage zones with multiple tendons were also conducted, with the prime variable being the spacing between the anchors. The cracking load of 31 of the specimens by Sanders was estimated based on the elastic stress distribution obtained from a two-dimensional Finite Element Analysis. and the tensile strength of the concrete measured from split-cylinder tests. The average ratio of actual to predicted cracking load is 0.91, with a standard deviation of 0.22. Figure 12 shows the ultimate load reached by the same series of specimens, along with the ultimate load predicted using strut-and-tie models based on elastic stress resultants at the end of the general zone. The average ratio of predicted to ultimate is 1.44, with a standard deviation of 0.44. Sanders [10] developed enhancements to the cracking load prediction, including the effect of the reduction of the tensile strength of the concrete caused by the three-dimensional state of stresses in the anchorage zone. Taking this modification into account, the average ratio of actual to predicted cracking load becomes 1.05 for all tests, with a standard deviation of 0.20. For the ultimate load, Sanders also developed an enhanced STM which includes the effect of a limited plastification of the concrete in the immediate vicinity of the anchorage device. Taking this modification of the model into account brings the average ratio of the predicted ultimate load to the actual ultimate load to 1.19, with a standard deviation of 0.19.
One of the most notable observations made during the evaluation of the test results is the fact that in the large majority of the cases, the capacity of the anchorage zone is controlled by the strength of the compression struts at the interface between the local zone and the general zone. At this location the concrete has no confinement, and is exposed to very large compressive stresses. Thus, increasing the reinforcement of the general anchorage zone will in many case lead to little or no improvement of the overall strength of the anchorage zone. This is confirmed by the observation of Stone and Breen [13], who noted that increasing the amount of orthogonal reinforcement

(the reinforcement provided in the general zone) is not nearly as effective as using longer and heavier spirals, which confine the local zone and have the effect of displacing the interface between the local zone and the general zone to an area of lower compressive stresses. For design purposes, it is in any case advisable to remember that the stresses in the concrete struts often control the design. Also notable is the effect of tensile stresses existing in the anchorage zone. The resistance these stresses provide is usually neglected in the design, but it nevertheless plays an important role in the behavior of anchorage zones. In several cases it was observed that the strength of the anchorage zone exceeded that predicted based on the capacity of the tension ties alone. Burdet [3] suggests that this additional strength is caused by the fact that a part of the concrete at the base of the specimens remained uncracked up to failure, thus providing an additional tensile capacity to resist bursting forces.

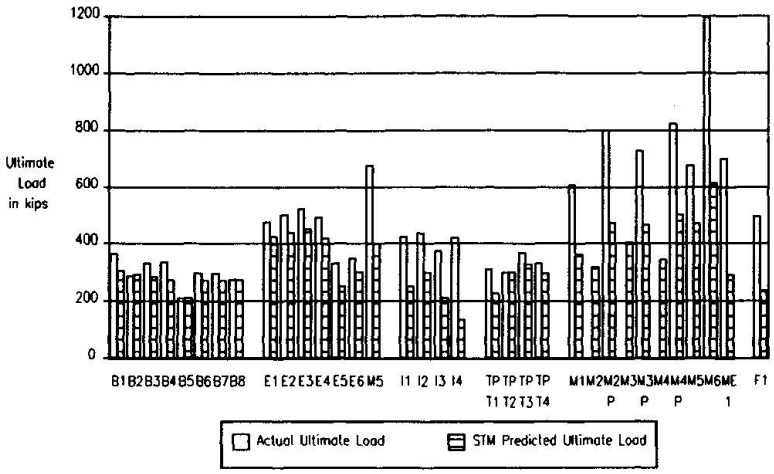

Figure 12: Actual Ultimate Load and Predicted Ultimate Load for Sanders' Test Specimens (1 kip = 4.54 kN)

8. Conclusions

The analysis, behavior and design of anchorage zones of post-tensioning tendons was investigated using a combination of Finite Element Analysis, Strut-and-Tie Models and experimental test specimens. This combination allowed minimization of the number of required experimental specimens and generalization the results in the form of simple design formulae. A consistent design methodology allowing use of finite element analyses, strut-and-tie models, and for certain frequently occurring cases, relatively simple design formulae was developed and has been proposed for inclusion in the AASHTO Bridge Design Specification. A standard testing procedure for anchorage devices and their necessary confinement was also proposed.

The cracking loads computed based on the elastic stresses and the split cylinder strength of the concrete are slightly smaller than the actual cracking loads, possibly because of the detrimental effect of the transverse compression. The ultimate capacity of anchorage zones can be conservatively predicted using the Strut-and-Tie Model. This investigation clearly indicates the critical nature of the compressive struts in anchorage zones. This differs from many other D-region applications in which the struts are not as criotical.

References

[1] American Association of State Highway Transportation Officials (AASHTO),"Standard Specification for Highway Bridges", 13th edition, 1983.

[2] Breen, J.E., "Why Structural Concrete," Final Report IABSE Colloquium on Structural Concrete, Stuttgart, April 1991.

[3] Burdet, O.L., "Analysis and Design of Anchorage Zones in Post-Tensioned Concrete Bridges," PhD dissertation, University of Texas at Austin, May 1990.

[4] Guyon, Y., "Prestressed Concrete," John Wiley and Sons, New York, 1953

[5] MacGregor, J.G., "Sub-Theme 2.4 - Dimensioning and Detailing," Final Report IABSE Colloquium on Structural Concrete, Stuttgart, April 1991.

[6] Marti, P., "Sub-Theme 2.4 - Dimensioning and Detailing," Final Report IABSE Colloquium on Structural Concrete, Stuttgart, April 1991.

[7] Nyiogi, S.K., "Bearing Strength of Reinforced Concrete Blocks," ASCE Structural Division Journal, Vol. 101, No ST5, May 1975.

[8] Richart, F.E., Brandtzaeg, A., and Brown, R.L., "A Study of the Failure of Concrete under Combined Compressive Stresses," Research Bulletin No 185, University of Illinois Engineering Experimental Station, 1928.

[9] Roberts, C.L., "Behavior and Design of the Local Anchorage Zone in Post-Tensioned Concrete," MS thesis, University of Texas at Austin, May 1990.

[10] Sanders, D.H., "Design and Behavior of Post-Tensioned Concrete Anchorage Zones," PhD dissertation, University of Texas at Austin, August 1990.

[11] Schlaich, J., Schäfer, K., Jennewein, M., "Towards a Consistent Design of Structural Concrete," PCI Journal, Vol. 32, No 3, May-June 1987, pp 74-151.

[12] Scordelis, A.C., "Analysis of Structural Concrete Systems," Final Report IABSE Colloquium on Structural Concrete, Stuttgart, April 1991.

[13] Stone, W.C., Breen, J.E., "Behavior of Post-Tensioned Girder Anchorage Zones," Center for Transportation Research Report No 208-2, University of Texas at Austin, January 1981.

Dimensioning of the Nodes and Development of Reinforcement

Dimensionnement nodal et développement de l'armature

Bemessung von Knoten und Entwicklung von Bewehrungen

Konrad BERGMEISTER
Research Associate
Univ. of Stuttgart
Stuttgart, Germany

John E. BREEN
Prof. of Civil Eng.
Univ. of Texas at Austin
Austin, TX, USA

James O. JIRSA
Prof. of Civil Eng.
Univ. of Texas at Austin
Austin, TX, USA

SUMMARY

This paper presents a proposal for the dimensioning process of nodal zones. Based on test results an efficiency factor for cylinder compressive strength from 20 to 80 MPa is proposed. In order to optimize the nodes, some geometrical constraints as well as an equation for the development length for straight bars under lateral pressure (CCT-, CTT-nodes), are also presented.

RÉSUMÉ

Cet article présente une proposition de dimensionnement des zones nodales. Basé sur des résultats d'essais, un facteur d'efficacité pour la résistance en compression de cylindres en béton de 20 à 80 MPa est présenté. On propose aussi quelques restricitions géométriques, ainsi qu'une équation pour les longueurs d'ancrage des barres droites soumises à effort tranchant, et ceci en vue de l'optimisation des nœuds.

ZUSAMMENFASSUNG

In dieser Veröffentlichung wird die Bemessung von Knotenbereichen aufgezeigt. Aufbauend auf Versuchen wird ein Vorschlag für die Wirksamkeit der Zylinderdruckfestigkeit von 20 bis 80 MPa vorgestellt. Sowohl geometrische Bedingungen als auch eine Gleichung für die Verankerungslänge von geraden Bewehrungsstäben mit Querpressung (CCT-, CTT-Knoten) sollen zur Optimierung von Knotenbereichen beitragen.

1. INTRODUCTION

Recent advances in the understanding of the behavior of concrete structures have resulted in more sophisticated methods of analysis. Computer based methods enable the elastic- and inelastic analysis of highly indeterminate and non-linear structures. For the majority of structures however it is unnecessary and inefficient to replicate the entire structure as a strut-and-tie-model (STM). Rather, it is more convenient and common practice to first carry out a general structural analysis, and then to subdivide the given structure into B-regions and D-regions [1]. It utilizes the well-known principle of Saint Venant which provides that local stresses may be assumed negligible at a distance h_D. For practical applications the following approaches as illustrated in Fig. 1 are suggested, and the total area of zone 2 + zone 1 + zone 2 is the effective D-region [2].

2. NODE BACKGROUND

D-regions usually contain either smeared or singular nodes. The singular nodes are more critical and need more attention. The following dimensioning and anchorage requirements must be applied to either smeared or singular nodes. The stress peaks in smeared nodes are less critical because a greater amount of surrounding concrete is normally available. The node of the STM represent the location of change of direction of internal forces. Evaluation of the nodal zones includes checking the nodal boundary stresses an determining reinforcement development requirements for nodes which contain tension ties.

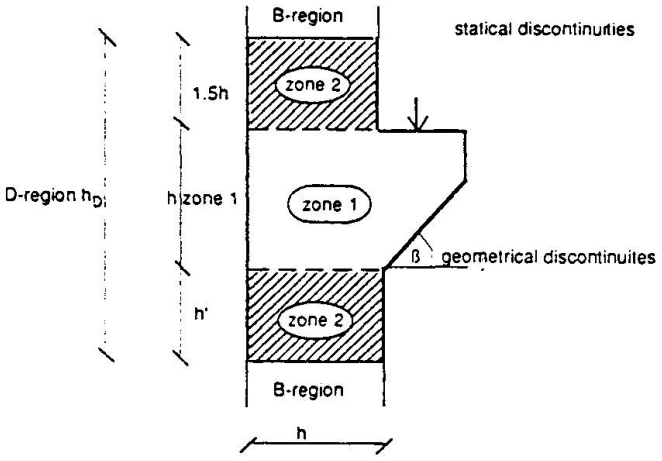

Fig. 1 Suggested subdivison of structure

2.1 Concrete efficiency factor

In general, the effective strength, f_{ce}, available for use in the struts is chosen as some fraction of the concrete compressive strength, f_c. It is given as the product of an efficiency factor, v_e, and the 28 day cylinder compressive strength. The efficiency factor should take into account the following parameters:

- multiaxial state of stress
- disturbances from cracks
- disturbances from reinforcement
- friction forces
- aggregate interlock after cracking
- dowel forces
- time dependence

$$f_{ce} = f_c \cdot v_e \qquad (1)$$

Various proposals for the efficiency factor have been presented. They are usually based on tests of continuous compression fields generated either in thin-web beams or thin

shear panels, although some appear to be based largely on engineering judgement. Empirical relations for the concrete efficiency factor of concrete struts in beam webs as suggested by Nielsen et al. [3], Ramirez and Breen [4], Collins and Mitchell [5] are summarized below:

- Nielsen et al. [3]: $\nu_e = 0.7 - f_c / 200$ $f_c <$ 60 MPa (2)
- Ramirez, Breen [4]: $\nu_e = 2.82 / \sqrt{f_c}$ $\sigma_c < 2.5\sqrt{f_c}$ MPa (3)
- Collins, Mitchell [5]: $\nu_e = 1 / (0.8 + 170\ \varepsilon_1)$ (4)

$$\varepsilon_1 = \varepsilon_x + (\varepsilon_x + 0.002)\cot^2\theta_{cs} \quad \varepsilon_x = 0.002$$

Marti [6] suggested as a reasonable average value for the nodal zone $\nu_e = 0.6$. Schlaich et al. [1] propose values between 0.4 (extraordinary cracks) and 1.0 (undisturbed).

In many applications, substantial confining reinforcement may be present so as to greatly increase the efficiency factor for concrete in compression.
A total of 122 tests have been evaluated using the following approach [2]
(see Fig. 2):

$$f_{ce3} = \nu_e\, f_c\, (A/A_b)^{0.5} + (A_{core}/A_b)\, f_{lat}\, (1 - s/d) \quad \text{[MPa]} \quad (5)$$

$$\nu_e = 0.5 + 1.25 / \sqrt{f_c} \quad \text{[/]} \quad (6)$$

f_{ce3} = confined concrete strength [MPa]
d = equivalent diameter = side length of confined square core [mm]

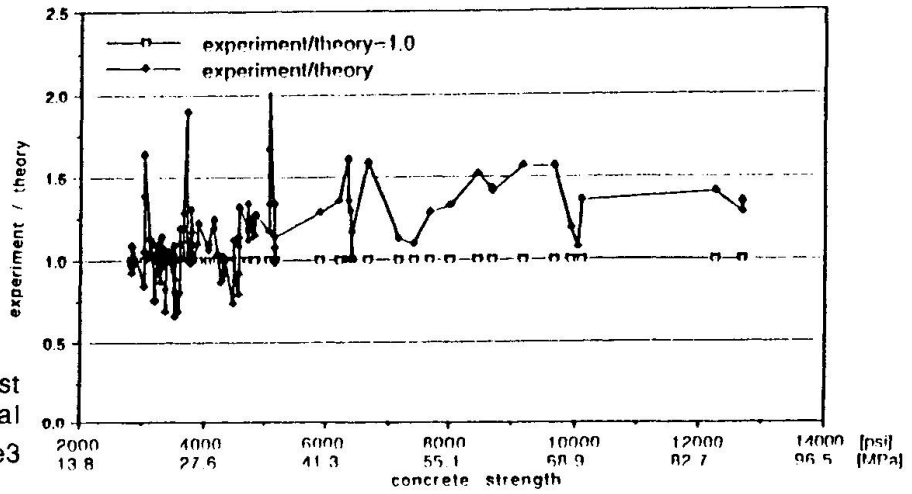

Fig. 2 Comparison of test results with theoretical approaches for predicting f_{ce3}

The proposed equation for the effective confinement strength is a generally conservative and safe approach. The 5%-fractile (m-2σ = 1.124−2*0.238) would be 0.65 which is also the minimum actual test value. The efficiency factor may be used with a concrete strength of up to 80 MPa.

2.3 Anchorage requirements in the nodal zone

All nodal zones are influenced by the tension tie anchorage details. If the resistance to applied tensile force is provided by bearing plates and does not rely appreciably upon bond stresses, then the tie actually provides a compression strut in terms of its action on the nodal zone (positive anchorage details). However, such positive anchorages are not

necessarily required nor are they always desirable or practical construction alternatives for anchoring tensile ties. In CCT- and CTT-nodes the reinforcing bars are under lateral pressure from the compressive strut. When lateral pressure is applied, the bond strength increases approximately in proportion to the square root of the lateral pressure. In addition, the distance between the bearing plate and the reinforcing bar, "e", has an important effect as shown in the study by Lormanometee [7]. Various experimental studies were evaluated to develop a formulation for a possible reduction of the development length for a reinforcement bar under lateral pressure. Only tests in which failure occurred before the bars yielded were included. The lateral pressure acts similar to the action of transverse reinforcement. Based on a comprehensive review of a broad range of test results [2], the development length,"l_d", with transverse reinforcement,A_{tr}, and lateral pressure,f_n, can be expressed as follows:

$$l_d = \frac{d_b \{(3 f_s / [(f_c')^{0.5}] - 50\}}{\{1.2 + 3c/d_b + (A_{tr} f_{yt})/(3.4 s d_b) + [(f_n)^{0.5} (2.4 - e^2/58000)]\}} \quad [mm] \qquad (7)$$

$$(A_{tr} f_{yt}) / (3.4 s d_b) \leq 3.0 \qquad (8)$$

$$0 \leq [(f_n)^{0.5} (2.4 - e^2/58000)] \leq 6.0 \qquad (9)$$

d_b	=	bar diameter	[mm]
f_s	=	stress in the bar at the critical section	[MPa]
f_{yt}	=	yield strength	[MPa]
s	=	spacing	[mm]

The proposed equation take the lateral pressure into account to a distance e = 350 mm.

3. CHECKING AND DIMENSIONING NODES

3.1 Checking and dimensioning CCC-, CCT- and CTT-nodes

The following equation is proposed for confined concrete strength:

a) Unconfined nodes without bearing plates:

$$\sigma \leq f_{ce} / \gamma \qquad (10)$$

$$f_{ce} = \nu_e f_c \leq 2.5 f_c \qquad (11)$$

b) Confined nodes

$$f_{ce3} = [(\nu_e f_c (A/A_b)^{0.5} + (A_{core}/A_b) f_{lat} (1 - s/d)^2)] \leq 2.5 f_c \qquad (12)$$

α = 4.0 for spiral confinement
= 2.0 for square confinement with longitudinal reinforcement
= 1.0 for square confinement without longitudinal reinforcement

$$f_{lat} = \text{lateral pressure} = 2 f_y A_s / (d s) \qquad (13)$$

c) Unconfined nodes with bearing plates (e.g CCT- and CTT-nodes)
For CCT- and CTT- nodes the width of the strut can be found by considering geometrical constraints such as bearing plates and by assuming that the effective

width of the tensile tie is governed by the dimensions from the inside to the outside reinforcement layer.

$$f_{ce3} = \nu_e f_c (A/A_b)^{0.5} \leq 2.5 f_c \quad (14)$$

$$A/A_b \leq 4 \quad (15)$$

d) Triaxially confined nodes
The increase in strength due to three-dimensional states of compressive stresses may be taken into account if the simultaneously acting transverse compressive stresses are considered reliable. This may be particularly appropriate if supplementary transverse prestressing is applied.

$$f_{ce3} = 2.5 f_c$$

In order to optimize the CCT-node both stresses at the C_1 and C_2 faces should be the same (hydrostatic stress). Fig. 3 shows the geometric inter-relation of the strut width, w_{1C}, the tie width w_{T3}, and the angle ϕ_{cs}. If the reinforcement is welded or bolted to the anchor plate, the stress configuration in the node is similar to that in a CCC-node.

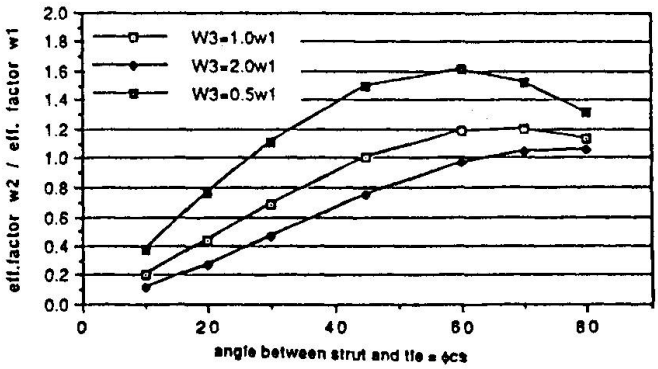

Fig. 3 Dependency of ν_e for CCT-node

When designing a CTT-node the reinforcement in both ties should yield at the same time. Since the compression strut,w2, is dependent on the tension tie widths,w1, and w3, the optimal concrete efficiency is given by the angle with the largest compression strut w2.

Tests by Bouadi [8] with CCT-nodes have shown that confining reinforcement has only a low effect (≈2%) on the failure load. Similarly, for the CTT-node (tests by Anderson [8]) in which the transverse reinforcement anchorage hooks were turned nearly parallel to the longitudinal bars (but not closed), the ultimate load decreased by only 4% compared with closed confining reinforcement.

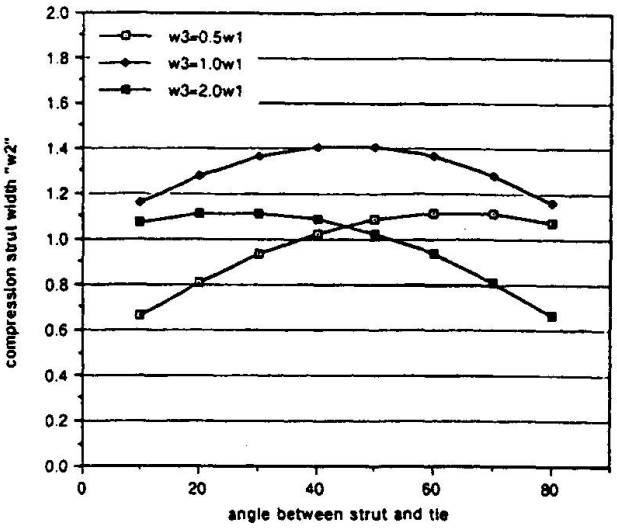

Fig. 3 Dependency of ν_e for CTT-node

By using vertically oriented hooks instead of long bars for the anchorage, the ultimate load decreased by 8% for CCT-nodes. This decrease is probably not significant given the other uncertainties in the design process. The advantage of hooks is that the required anchorage length can be minimized. Using a transverse U for the second tie in CTT-nodes provided lateral confinement, but prying action at the 90° bend can produce splitting cracks. In order to control splitting cracks of the end cover it is suggested that the longitudinal reinforcement be extended a short distance (≈s/2 or 50 mm) past the transverse reinforcement.

3.2 Checking and Dimensioning TTT - nodes

For TTT-nodes it must be evident that satisfactory behavior and adequate strength can be attained only by the efficient interaction of concrete and steel.

In details where the length available for end anchorage may be so short that only special devices can ensure the development of the required bar strength. For TTT-nodes the largest tensile tie should be anchored with looped - or hooked bars (Fig. 4). The stirrup spacing "s" must be so selected that the cover will not break away between two stirrups when the curved bar tends to straighten.

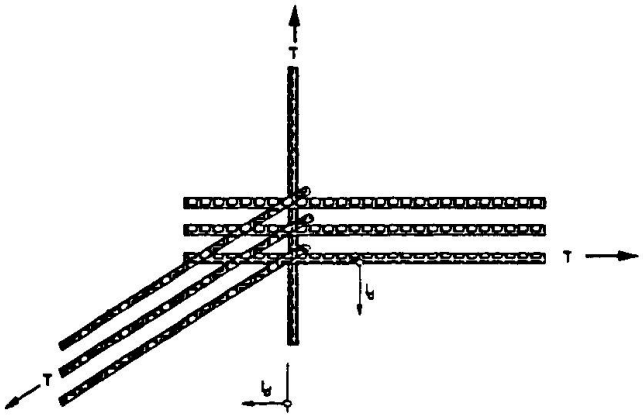

Fig. 4 TTT-node with looped bar

4. CONCLUSIONS

Some guidelines are given for the dimensioning process for the nodal zones. More research on this topic is needed as well as improved guidance for the serviceability control.
In order to satisfy the requirements of the theory of plasticity, a model must be in equilibrium under the applied loads. However, if the selected strut and- tie- model is to fully develop, the load carrying capacity of the strut- and- tie- elements and the rotational capacity of the nodes must not be exceeded before the ties yield. In addition the accepted standards for bar spacing, minimum reinforcement to control creep and thermal stresses should be applied.

REFERENCES

1. SCHLAICH, J.; SCHÄFER, K.: Konstruieren im Stahlbetonbau (Design for Concrete Structures). Betonkalender, 1989, pp. 563-715
2. BERGMEISTER, K.; BREEN, J.E.; JIRSA, J.O.; KREGER, M.E.: Detailing for Structural Concrete. Research Report 1127-3F, Center for Transportation Research, October, 1990
3. NIELSEN, M.; BRAESTRUP, N.; JENSEN, BACH. F.: Concrete Plasticity: Beam Shear-Shear in Joints - Punching Shear. Specialpublication - Dansk Selskab for Bygningsstatik, Lyngby, 1978, 129 pp.
4. RAMIREZ, J.; BREEN, J.: Proposed Design Procedures for Shear and Torsion in Reinforced and Prestressed Concrete. Research Report 248-4F, Center for Transportation Research, 1983
5. MITCHELL, D.; COLLINS, M.: Diagonal Compression Field Theory - A rational Model for Structural Concrete in pure Torsion. ACI-Journal, August, 1974
6. MARTI, P.: Dimensioning and Detailing, Final Report, IABSE Colloquium Structural Concrete, Stuttgart, April, 1991
7. LORMANOMETEE, S.: Bond Strength of Deformed Reinforcing Bar under Lateral Pressure. Master's Thesis, The University of Texas at Austin, 1974
8. BARTON, D.L.; ANDERSON, R.B.; BOUADI, A.; JIRSA, J.O.; BREEN, J.E.: An Investigation of Strut- and Tie Models for Dapped Beam Details. Research Report 1127-1, Center for Transportation Research, February 1990

Current Design Methods for Frame Connections

Méthodes ordinaires de dimensionnement des connexions des cadres

Gewöhnliche Entwurfsmethoden für Rahmenknoten

S.J. PANTAZOPOULOU
Assist. Prof.
Univ. of Toronto
Toronto, ON, Canada

S.J. Pantazopoulou holds a Civil Eng. degree from the National Techn. Univ. of Athens, and M.Sc. and Ph.D. degrees from the Univ. of California at Berkeley. She is a member of ACI Committee 368 and associate member of the joint ACI-ASCE Committee 352.

John F. BONACCI
Assist. Prof.
Univ. of Toronto
Toronto, ON, Canada

John F. Bonacci received B.S., M.Sc. and Ph.D. degrees in Civil Eng. at the Univ. of Illinois-Urbana. He is a member of the joint ACI-ASCE Committee 352 and ACI Committee 408. He is also an associate member of the joint ACI-ASCE Committee 442.

SUMMARY

Current requirements for lateral load design of beam-column joints are either on equilibrium considerations (CEB and New Zealand Codes), or are empirically derived from experimental data (ACI Code). As a result, deformations associated with the design limit states are not considered in evaluating the performance of connections. An alternative approach, satisfying both equilibrium and compatibility requirements is discussed in this paper. The proposed model incorporates the effects of axial load, reduction of concrete compressive strength resulting from diagonal tension, and the influence of indeterminacy which arises in statically redundant structures. Design limits for joint shear stress obtained from the model are compared with those adopted by Design Codes.

RÉSUMÉ

Les codes couramment utilisés pour le dimensionnement sous charge latérale des joints poutres-colonnes sont soit basés sur des principes d'équilibre (CEB et normes de Nouvelle-Zélande), soit dérivés de valeurs expérimentales (Code ACI). Les déformations associées aux états limites de dimensionnement ne sont pas considérées comme véritable résultat lors de l'évaluation de performance des connexions. Une approche alternative satisfaisant à la fois l'équilibre et les conditions de compatibilité est discutée dans cette étude. Le modèle proposé tient compte des effets d'une charge axiale, de la diminution de la résistance à la compression du béton sous l'effet de tensions diagonales, ainsi que de l'indétermination caractérisant les structures hyperstatiques. Les limites de dimensionnement caractérisant les joints soumis à l'effort tranchant obtenues par ce modèle sont comparées à celles adoptées par les codes officiels.

ZUSAMMENFASSUNG

Die derzeit gültigen Anforderungen für die Bemessung von Knoten in seitlich belasteten Rahmen sind entweder auf Gleichgewichtbetrachtungen aufgebaut (CEB und Neuseeland Vorschriften) oder sie wurden empirisch hergeleitet (ACI-Vorschriften). Daraus folgt, dass die mit den Bemessungsgrenzwerten verbundenen Verformungen bei der Beurteilung des Verhaltens der Knoten nicht berücksichtigt werden. Eine alternative Methode, die Gleichgewichts- und Verträglichkeitsbedingungen einschliesst, wird in diesem Beitrag besprochen. Das vorgestellte Modell berücksichtigt den Einfluss der Normalkraft, die Verringerung der Druckfestigkeit des Betons infolge Querzug und den Einfluss der statischen Unbestimmheit von Tragwerken.

1. INTRODUCTION

Requirements for lateral-load design of reinforced concrete (RC) beam-column joints currently implemented in design codes worldwide [1, 2, 3] are based on extensive experimental studies of the inelastic behavior of individual RC frame connections. Because of the complexities associated with controlling tests of statically indeterminate systems, most of the experiments included in the data bases of the various codes have been carried out on highly idealized statically determinate assemblies modelling beam-column connections of frame structures [4, 5, 6, 7].

Forces considered for joint design are illustrated in Fig. 1a. In most contemporary design codes, the magnitudes of these forces are associated with a beam flexural hinging mechanism, implying that beams and columns are dimensioned first. Because a large portion of the forces loading the joint are introduced by bond stresses that develop between concrete and reinforcement, codes require that the magnitude of bond stresses be regulated by controlling the size of longitudinal bar diameter with respect the available development length (column or beam depth). In the following discussion, it will be assumed that the development length requirements are satisfied apriori, and that bond deterioration is not significant (referring both to the derivations and the experimental data discussed in this paper).

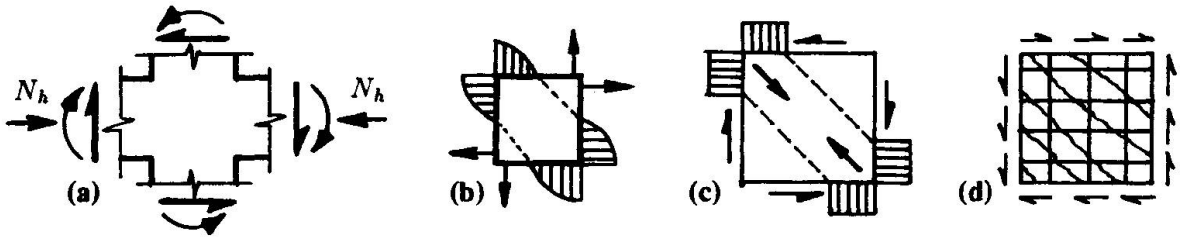

Fig. 1 Shear mechanisms adopted by design codes

Dimensioning and detailing of beam-column joints according to the current design practice is directly linked to evaluation of the so-called joint shear index. This index, which is an estimate of the horizontal and/or vertical joint shear stress, is computed using one of two alternative approaches. The first approach, adopted by the joint ACI-ASCE Committee 352 [1], is characteristic of North American practice. In this approach, the joint-shear index is computed only for a horizontal plane, and is limited by allowable stresses (empirically derived from experiments). The allowable stresses amount to $0.083\ \lambda\sqrt{f'_c}$, (MPa), where λ is 20, 15 and 12 for interior, exterior and corner joints respectively. Furthermore, it has been proposed that development of the concrete strength in the compressed diagonal (Fig. 1b) is facilitated by confining of the concrete core, with closed hoops or other members that frame in to the connection, such as transverse beams and floor slabs [5]. Lateral reinforcement provided in the joint region is the same as that provided in the column critical regions.

The second approach [8], currently adopted by the CEB Model Code [2] and the N. Zealand Code [3], considers both horizontal and vertical joint shear stresses. These stresses, in combination with the normal forces that act at the faces of the joint (Fig. 1a), constitute a loading system for which an admissible state of equilibrium is said to develop from the superposition of a diagonal strut mechanism and a truss mechanism (Fig. 1c, 1d). For the purpose of design, the ultimate joint shear resistance is established by considering the formation of diagonal tension failure inside the joint. For conservatism, the concrete contribution to shear resistance associated with main-strut action (Fig. 1c) is accounted for when the axial force in the column is significant. It has been proposed [8] that axial load improves joint performance by reducing the inclination (from vertical) at which the main-strut mechanism develops. In this model, intermediate horizontal reinforcement is an essential part of the shear-resisting mechanism, comprising the horizontal chords of the idealized truss shown in Fig. 1d. With reference to the role of stirrups or hoops in the overall behavior of beam-column joints, it has been suggested recently that the emphasis which the ACI 352 recommendations place on the confining action of tie reinforcement or other members framing into joint is misleading because the mechanisms of confinement in the critical regions of columns are different from those associated with shear action [9].

The sharp contrast between the two approaches effects different views regarding the definition of acceptable levels of performance, and, to a certain extent, two different interpretations of available experimental evidence as it pertains to the mechanics of joints. Of the two methods, the first is clearly empirical and the latter is based on an admissible equilibrium solution. A consequence of both is that deformations of the joint are not considered in the design process. From the point of view

of structural performance, the amount of deformation required for the joint to develop its resistance is as significant as the magnitude of the resistance. It is therefore desirable that both quantities be reflected in design recommendations.

Although the need for deformation based design criteria for joints has been stated [5], their development has been impeded by the realization that load and deformation demand on the beam-column joints of frames with complex structural configurations is greatly influenced by the three-dimensional effects of the response, and the ability of statically indeterminate structures to redistribute forces. Joint deformation and member expansion are generally unrestrained in statically determinate assemblies, like those used in most experimental studies of joint behavior. Therefore, deformation performance criteria (usually expressed in terms of displacement ductility for the assemblage) quoted by experimentalists in establishing allowable values for joint shear do not directly apply in the case of indeterminate frame structures because of the significant amount of restraint to joint deformation that continuity can cause.

To identify the important parameters that control the behavior of joints, it is instructive to review the available experimental evidence. Early tests conducted in the 1960's on isolated connection specimens illustrated that joint reinforcement in the form of horizontal stirrups, in combination with uniformly distributed longitudinal column reinforcement (so as to form a closed cage), significantly enhanced the shear resistance of joints [4]. Since then, a large amount of research has been conducted, with an aim towards establishing relationships between the degree of deterioration of shear resistance under cyclic loads and the amount of lateral reinforcement provided in the joint. Recent tests (as part of a U.S. - Japan - N. Zealand - China cooperative research effort) of connection specimens simulating Japanese, U.S. and N. Zealand practice (of which the first and last pose the lowest and highest requirements of joint reinforcement, respectively), clearly demonstrate that there is an upper limit in the amount of joint reinforcement, beyond which the overall resistance of a connection is not significantly affected [5]. This manifests the obvious fact that, although large amounts of joint reinforcement can increase the available shear resistance of the joint, this additional strength is not likely to be usable because the demand on the joint is eventually limited by the flexural resistance of adjacent members. All reported specimens (which were designed to fail in beam yielding and had very favorable bond conditions) demonstrated similar overall resistance, with the only significant differences being apparent stiffness of the connections and the amount of deformation. Increased amounts of lateral steel delayed the initiation and propagation of cracking in the joint, and reduced the amount of joint distortion that occurred under a given level of joint shear stress. These results suggest that an important consequence of adding joint reinforcement is an increase of joint stiffness.

Based on this experimental evidence, it is possible to idealize joints as two-dimensional (2-D) panels reinforced in two orthogonal directions, and acted upon by in-plane stresses. However, contrary to familiar 2-D panels, the concrete stiffness contribution is not independent of that of the reinforcement. This is supported by experimental evidence obtained from tests of beam-column joints in which the closed stirrups were replaced by longitudinal beam reinforcement that was uniformly distributed along the height and anchored outside of the joint [7]. Although the joints in these specimens were able to resist the shear demanded to develop beam hinging, a rapid deterioration of joint shear resistance was observed with cycling. Evidently, the stiffening action of closed stirrups occurs not only in the direction of the load but in the perpendicular direction as well, making the confining role of stirrups a more transparent phenomenon. Therefore, the experimental evidence suggests that stirrups contribute to the shear resistance of joints directly (by resisting part of the joint shear), and indirectly (by confining the concrete core, thus enhancing its diagonal compressive strength). However, these two functions are not independent or mutually exclusive of each other - a point that fuels the current debate between differing design philosophies.

From tests of interior beam-column joints with transverse beams, it has been established even joints without any stirrup reinforcement can perform satisfactorily within realistic levels of lateral displacement [5]. This suggests that transverse beams at interior connections and closed hoop reinforcement affect the behavior of joints in a similar manner, by restraining volumetric expansion, which eventually leads to deterioration of joint shear resistance. It has been suggested that this is result of insufficient modeling of boundary conditions in the experimental models, since the enhancement of joint performance occurred only when transverse beams were free of load during the tests. Indeed, experiments in which transverse beams were loaded have been carried out, and in these cases transverse beams had negligible confining contribution. Nevertheless, tests conducted on indeterminate specimens have shown that the excessive deformation that would occur in the beam plastic hinge regions if the assembly was statically determinate, is partially restrained by the presence of adjacent

members. This restraint has been measured experimentally as internal axial forces that developed in beams experiencing inelastic deformation near the connection. The internal forces, N_3 and N_h (Fig. 1a), represent the reactions of adjacent columns to the lateral displacement required to accommodate beam expansion. Because of the presence of these internal actions, the confining effect of transverse beams on the joint is likely to be significant in actual (indeterminate) structures, where each connection is restrained by the presence of adjacent frames.

With respect the overall displacements of beam-column connections, experiments have shown that a satisfactory joint performance is always accompanied by minimal contribution of joint distortion to the overall lateral drift of the structure (joint performance is deemed satisfactory if cracking is controlled and deterioration of resistance does not occur). In statically determinate assemblies of typical proportions, joint distortion accounted for approximately 25% of the total displacement at low levels of lateral drift. At higher displacement levels (corresponding to approximately 2% interstorey drift, which is often considered a design limit), experimental data suggest that the contribution of joint distortion to total drift became less than 15%, when beams developed sustained flexural hinging as a result of sufficiently reinforced joints or joints with low shear stresses (stresses below values associated with cracking of concrete). In contrast, the contribution of joint distortion to the total drift has been observed to increase with increasing magnitude of total displacement, reaching 40% in cases of joints with insufficient hoop reinforcement or excessive levels of joint shear stress (stresses exceeding the empirical limits in the ACI-ASCE 352 Recommendations [1]). This information suggests an opportunity to link connection design to overall structural response. But any such design approach must consider joint deformations as well as internal forces. No current design basis does so explicitly.

2. EQUILIBRIUM AND KINEMATICS OF JOINTS

In this section it is assumed that the joint is properly detailed and that reinforcement is present in quantities sufficient to provide adequate crack control; stresses and strains are averaged over the dimensions of the entire joint [10].

2.1 Equilibrium

Average stresses in the joint are depicted in Fig. 1. Shear stresses are introduced by direct member action and by the bond that develops between the main reinforcement and the joint core concrete. Shear stress, v, is assumed to be uniformly distributed over the boundaries of the joint (Eqn. 1, Table 1). Eqns. 2 and 3 establish equilibrium in the vertical l and horizontal t directions at the center of the joint. σ_l and σ_t represent the average vertical and horizontal compressive stresses of the concrete. ρ_l, ρ_t are the available amounts of vertical and horizontal reinforcement (where $\rho_t = \rho_b + \rho_s$, for which ρ_b and ρ_s are the percentages of horizontal beam reinforcement and horizontal stirrups in the joint, respectively). The corresponding average stresses in the reinforcement are f_l and f_t. Dimensions of the joint (depth, width and height), are denoted by d_w, b and h ; N_v is the column axial force. N_h represents the beam axial force, which results from partial restraint to beam expansion provided by adjacent columns in indeterminate frames.

$v = \frac{V_h}{bd_w} = \frac{V_v}{bh}$ (1)	$\sigma_t = -\rho_t f_t - \frac{N_h}{bh}$ (3)	$\sigma_1 - \sigma_t = v \tan\theta$	$\sigma_t = -v \tan\theta$ (6)
$\sigma_l = -\rho_l f_l - \frac{N_v}{bd_w}$ (2)	$\sigma = \begin{pmatrix} \sigma_t & v & 0 \\ v & \sigma_l & 0 \\ 0 & 0 & \sigma_3 \end{pmatrix}$ (4)	$\sigma_1 - \sigma_l = \frac{v}{\tan\theta}$ (5)	$\sigma_l = -\frac{v}{\tan\theta}$ $\sigma_2 = -v(\tan\theta + \frac{1}{\tan\theta})$

Table 1 Joint equilibrium equations

Furthermore, if the joint reinforcement is of the closed-hoop type, the concrete of the joint is subjected to passive confining stress $\sigma_3 = -\rho_s f_3$. Here, f_3 represents the hoop stress in direction normal to the plane of action of the applied shear force. Eqn. 4 describes the average stress tensor associated with the joint. The maximum principal stress, σ_1, associated with the stress tensor must not exceed the tensile capacity of concrete. If, for the sake of simplicity, it is assumed that this capacity is negligible then, since in any plane stresses are either negative (compressive) or zero, it is evident that $\sigma_2 = \sigma_l + \sigma_t$ (conservation of the first invariant, given that σ_1 is assumed zero). The elements of the stress tensor in the (t, l) coordinate system are related to the principal stresses via Eqns. 5 (Table 1); expressions for σ_t, σ_l and σ_2 in terms of the applied shear stress v are obtained from Eqns. 5 upon substitution of $\sigma_1 = 0$ (Eqns. 6).

2.2 Kinematics

We assume that the overall geometry of the joint after deformation is described by the average angle of shear distortion, γ, and by the average longitudinal and transverse strains denoted by ϵ_l and ϵ_t respectively. Equation 7 (Table 2) describes the tensor of average strains as defined in the (t, l) system. Some useful relations between the entries of the tensor expressed in various coordinate systems are also given in Table 2. The direction of principal strains, which enters the terms of Eqn. 8 is generally unknown. Considering the behavior before yielding of hoops in the joint (of primary interest from the design point of view), it is assumed that, if the reinforcement has not yielded, the direction of principal strains (α) is closely related to that of stresses (θ). If $\theta = \alpha$ is adopted, then it is possible to express θ in terms of the values of stress in Table 1. To do this, $\tan\theta$ is written in terms of strains (Eqn. 8). Strains are substituted with the ratios σ_2/E_c, f_l/E_s, f_t/E_s; v is replaced by $(-\sigma_t/\tan\theta) = [\rho_t f_t + (N_h/bh)/\tan\theta]$. This procedure leads to a quadratic equation for $\tan\theta$ (Eqn. 9), where $n = E_s/E_c$, while the strain ratio $r = e_h/\epsilon_t$ reflects the amount of lateral restraint to joint growth, which is likely to be significant for indeterminate structures. It is evident from Eqn. 9 that such restraint plays the same role algebraically as horizontal joint reinforcement, which is parallel to experimental observation of improved joint performance when transverse beams were present in tests of interior connections. The quantities $e_v = N_v/E_c b d_w$ and $e_h = N_h/E_c h b$ have units of strain, and represent the deformations occurring in the joint under purely axial forces.

$$\epsilon = \begin{pmatrix} \epsilon_t & 0.5\gamma \\ 0.5\gamma & \epsilon_l \end{pmatrix} \qquad \epsilon_1 + \epsilon_2 = \epsilon_l + \epsilon_t \tag{7}$$

$$\gamma = \frac{2(\epsilon_1 - \epsilon_t)}{\tan\alpha} = 2(\epsilon_1 - \epsilon_l)\tan\alpha \qquad \tan^2\alpha = \frac{\epsilon_1 - \epsilon_t}{\epsilon_1 - \epsilon_l} = \frac{\epsilon_2 - \epsilon_l}{\epsilon_2 - \epsilon_t} \tag{8}$$

$$\frac{1 + \frac{1}{n\rho_t} - \frac{r}{n\rho_t(n\rho_t + r)}}{1 + \frac{1}{n\rho_l}} \tan^4\theta + \frac{e_v/\epsilon_t}{(1 + n\rho_l)(n\rho_t + r)} \tan^2\theta - 1 = 0 \tag{9}$$

2.2.1 Behavior before yielding of joint reinforcement

Before yielding of the horizontal joint reinforcement, the magnitude of joint shear stress is related to hoop strain by Eqn. 10 (Table 3). In a similar manner, expressions for the remaining elements of the strain tensor may be obtained as seen in Table 3. The expression for the principal tensile strain (ϵ_1) indicates that the strain is not only affected by the amount of joint shear stress, but also that it increases with increasing vertical axial load, while the influence of lateral restraint on the joint is the reverse. This effect is significant, because the magnitude of diagonal (principal) compression that can develop in the core concrete decreases with increasing magnitude of the tensile strain in the perpendicular direction.

$$\epsilon_t = \frac{1}{\rho_t E_s}\left(v\tan\theta - \frac{N_h}{bh}\right) \qquad \epsilon_l = \frac{1}{\rho_l E_s}\left(\frac{v}{\tan\theta} - \frac{N_v}{bd_w}\right) \tag{10}$$

$$\gamma = \frac{2}{E_s(1 - \tan^2\theta)}\left[v\frac{\tan^2\theta\rho_l - \rho_t}{\rho_l\rho_t} + \left(\frac{N_v}{bd_w\rho_l} - \frac{N_h}{bh\rho_t}\right)\tan\theta\right]$$

$$\epsilon_1 = \frac{1}{E_s(1 - \tan^2\theta)}\left[v\tan\theta\frac{\rho_l - \rho_t}{\rho_l\rho_t} - \frac{N_h}{bh\rho_t} + \frac{N_v\tan^2\theta}{bd_w\rho_l}\right] \tag{11}$$

Eqn. 11a provides a relationship between average joint shear stress and the amount of associated joint distortion. It is evident from the above that column axial load promotes joint distortion, while restraining horizontal loads reduce the amount of distortion at a given level of shear stress.

2.2.2 Behavior after yielding of joint reinforcement

Upon yielding of the joint hoops, the pattern of deformation in the joint is likely to change noticeably. In terms of stresses, it is evident from Eqn. 3 that $\sigma_t = -\rho_t f_y - (N_h/bh) = -v\tan\theta$, which can be solved for the angle of principal stresses $\tan\theta$: $(\tan\theta = [\rho_t f_y + N_h/bh]/v)$. This result can be used to obtain expressions for the average longitudinal (vertical) stress, the average nonzero principal stress, and the amount of hoop strain, ϵ_t, in terms of the joint shear v (Eqns. 12, 13, Table 4).

$$\sigma_l = -\frac{v^2}{\rho_t f_y + N_h/bh} \; ; \; \sigma_2 = -\rho_t f_y - \frac{N_h}{bh} - \frac{v^2}{\rho_t f_y + N_h/bh} \tag{12}$$

$$\epsilon_t = \frac{1 + \frac{1}{n\rho_l}}{E_c\left[\rho_t f_y + e_h E_c\right]^3} v^4 - \frac{e_v v^2}{n\rho_l\left[\rho_t f_y + e_h E_c\right]^2} - \frac{\rho_t f_y + e_h E_c}{E_c} \tag{13}$$

Thus, a dramatic increase occurs in the values of σ_l, σ_2 and ϵ_t, for small increases in the value of joint shear after yielding of hoops, since all terms (except v) in Eqns. 12 and 13 remain constant thereafter.

3. MECHANISMS CONTROLLING SHEAR RESISTANCE

The shear resistance of a joint is likely to be limited by the occurrence of one of two possible mechanisms: (1) bond failure of the main reinforcement, which is responsible for introducing the shear stresses, v, to the joint, or (2) yielding of joint reinforcement. Of these, case (1) was excluded in this study by assuming that pertinent development length requirements are satisfied. For case (2), it has been shown that after initiation of yielding of joint hoops, a substantial increase in the values of σ_1 and σ_2 will occur. Thus, hoop yielding is is likely to be succeeded by either a) yielding of the longitudinal column reinforcement, or b) crushing in the principal direction of concrete compressive stresses. Upper limits to the shear capacity associated with these two mechanisms can be established as follows: for case 2(a), the stress in the longitudinal steel reaches the yielding stress, f_y. Thus,

$$\sigma_l = -\rho_l f_y - \frac{N_v}{bd_w} = -\frac{v^2}{\rho_t f_y + N_h/bh} \text{ therefore, } v_n = \sqrt{\left\{\rho_t f_y + \frac{N_h}{bh}\right\}\left\{\rho_l f_y + \frac{N_v}{bd_w}\right\}} \tag{14}$$

For case 2(b), failure occurs when the principal compressive stress, σ_2, reaches the crushing strength of concrete, f_{max}. This crushing strength, however, depends upon the amount of restraint to volumetric expansion, which here is represented by stress σ_3. Furthermore, f_{max} also depends on the amount of tensile deformation in the perpendicular direction, characterized by ϵ_1 [11]. It is assumed here that the relationship between stress and strain along the principal compressive direction can be described by [11],

$$\sigma_2 = f_{max}\left[2\frac{\epsilon_2}{\epsilon_{max}} - (\frac{\epsilon_2}{\epsilon_{max}})^2\right] \text{ where, } \left\{\begin{array}{l} f_{max} = \alpha f_c' \\ \epsilon_{max} = \alpha\epsilon_o \end{array}\right\} \text{ and, } \alpha = \frac{K}{0.8 + 0.34\epsilon_1/\epsilon_o} \tag{15}$$

where, $K = 1 + \rho_s(f_y/f_c')$. Upon substitution of Eqn. 15 in Eqn. 12, the following alternative expression for the limiting joint shear stress is established:

$$v_n = \sqrt{|(f_{max} + \rho_t f_y + N_h/bh)(\rho_t f_y + N_h/bh)|} \tag{16}$$

4. STUDY OF PARAMETERS IN PROPOSED FORMULATION

In this section, the proposed formulation is used to investigate the influence of various connection-design parameters on conditions corresponding to yielding of hoop reinforcement. Equation 10 can be solved for the amount of shear stress, and Eqn. 11 the corresponding shear distortion, that a joint will tolerate before horizontal reinforcement yields. The "design" variables considered for this hypothetical case study are summarized in Table 5. For this example, the ratio of beam reinforcement (ρ_s) was set at 0.015 (top and bottom combined).

To apply the equations for the purposes of this parameter study, two simplifying assumptions were made:

1. The term E_c is actually a function of ϵ_2, which means that Eqn. 9 should be solved iteratively for the angle θ. Instead, E_c was taken as the secant modulus at the point of peak stress for an assumed parabolic concrete compressive stress–strain relationship (Eqn. 15).

2. The particular response condition examined here corresponds to tensile yield of hoop reinforcement. To account for hoop "pre–strain" that would exist in the presence of vertical axial force, N_v, Poisson's ratio was taken equal to 0.2 to give the expression $\epsilon_t(available) = f_{yh}/E_s - 0.2e_v$ for use in Eqns. 9, 10, and 11.

The influence that each of the variables considered had on tolerable shear before hoop yield is summarized in Table 5. Only cases for which failure by crushing or vertical yield did not occur before hoop yield are included in this analysis of parametric influences. It can be observed that increasing hoop yield stress ($f_{yt}(hoops)$), amount of hoop reinforcement (ρ_s), and beam axial stress ($N_h/f_c'bh$) had similar effects of increasing both tolerable shear distortion and shear stress (Fig. 2a-2c). Indeed, these were the only parameters that resulted in significant and consistent increase of overall joint capacity as limited by hoop yield. By comparison, the proposed formulation shows (Fig. 2d) that column axial stress ($N_v/f_c'bd_w$) had less of an effect on the shear distortion or stress the joint sustained before hoops yielded.

Design Variable	Nominal Value for Study	Range of Values for Study	Effect of increase of variable	
			$v/\sqrt{f_c'}$ @ hoop yield	γ @ hoop yield
f_c'	35 MPa	20 - 100 MPa	Nonlinear decrease	Nonlinear decrease
f_{yt} (hoops)	400 MPa	300 - 600 MPa	Strong linear increase	Strong linear increase
ρ_l	0.04	0.01 - 0.08	Slight nonlinear increase	Slight nonlinear decrease
ρ_s	0.003	0 - 0.010	Linear increase	Linear increase
$N_v/f_c'bd_w$	0.05	0 - 0.25	Slight linear increase	Slight linear decrease
$N_h/f_c'bh$	0.02	0 - 0.25	Linear increase	Linear increase

Table 5 Summary of design parameter study

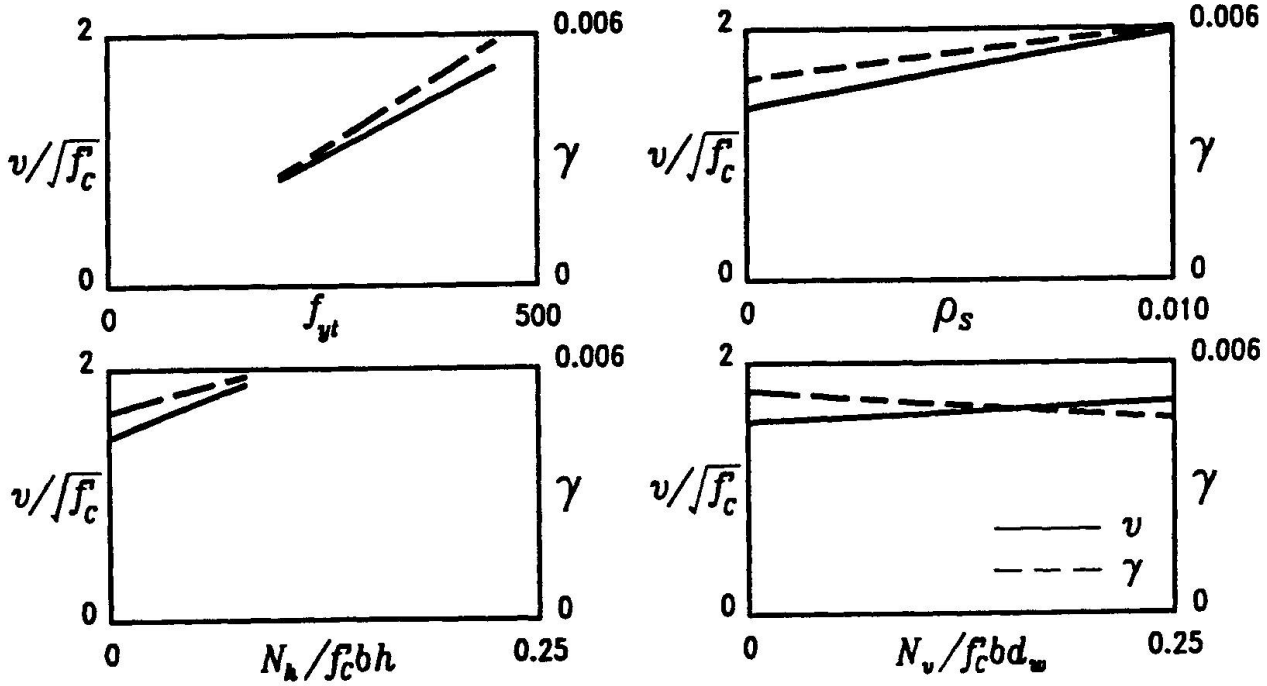

Fig. 2 Results of parametric study

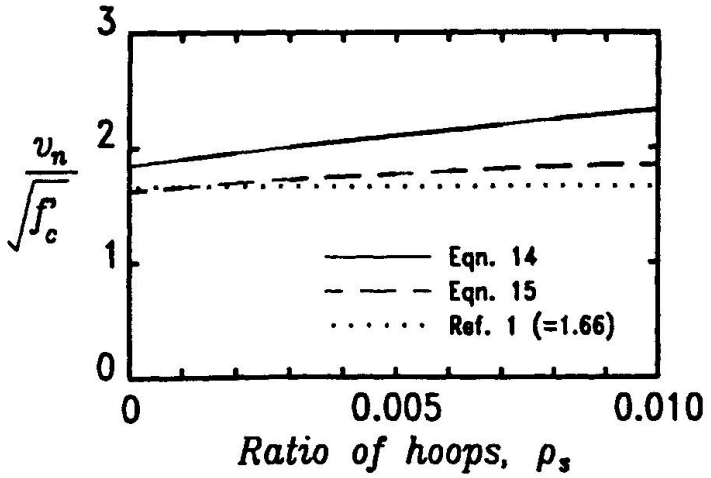

Fig. 3 Shear resistance after hoop yield

Shear capacities associated with connection failure by yield of vertical reinforcement (Eqn. 14) or concrete crushing along the principal diagonal (Eqn. 16) after hoop yield are plotted against the ratio of hoop reinforcement for the sample problem in Fig. 3. For this particular example, it can be observed that capacity will be limited by concrete compression and that, for any ratio of hoops, it is about equal to the value recommended by ACI-ASCE Committee 352 [1]. From the terms of Eqns. 14 and 16, it is apparent that axial stress in the column and beam play an active role, along with the quantity of hoop reinforcement, in determining the shear capacity of connections.

From the terms of Eqns. 14 and 16, it is apparent that axial stress in the column and beam play an active role, along with the quantity of hoop reinforcement, in determining the shear capacity of connections.

5. CONCLUSIONS

At the root of this Colloquium is the pursuit of generalized approaches for design of structural concrete [12, 13]. Connections in framed structures are a good example of a specific problem in need of unified interpretation– as evidenced by the slowly converging, but still diverse, viewpoints recently presented to the American Concrete Institute by researchers from Japan, New Zealand, and the United States [ACI Fall Convention 1989, San Diego]. In this paper, consideration of both the kinematics and equilibrium of a joint resulted in a comprehensive model that makes it possible to gauge the influence of any design variable at any stage of response and provides design equations for joint shear capacity. While the latter is possible from approaches based strictly on equilibrium and empirical summary, the former can only be achieved by attempting to consider joint deformations. The point is transparent to the particular structural element considered in this paper.

ACKNOWLEDGEMENTS

The work presented in this paper was carried out at the University of Toronto, Canada. Financial support for the study was provided by NSERC grants No. OGP0042033 and OGP0042154.

REFERENCES

1. ACI-ASCE COMMITTEE 352, Recommendations for Design of Beam-Column Joints in Monolithic Reinforced Concrete Structures. American Concrete Institute, Detroit, 1985, 18 pp.

2. CEB-FIP Model Code for Seismic Design of Concrete Structures. Bulletin d'Information No. 160, Paris, 1983, 117 pp.

3. STANDARDS ASSOCIATION OF NEW ZEALAND. Code of Practice for the Design of Concrete Structures. Part 1, 127 pp. and Part 2, 156 pp. Wellington 1982.

4. HANSON N. W. and CONNER H. W., Seismic Resistance of Reinforced Concrete Beam-Column Joints. Proceedings, ASCE, V. 93, ST5, Oct. 1967, pp. 533-560.

5. KUROSE Y., Recent Studies on Reinforced Concrete Beam Column Joints in Japan. PMFSEL Report No. 87-8, Phil M. Ferguson Structural Engineering Laboratory, Department of Civil Engineering, The University of Texas at Austin, December 1987, and references thereof.

6. MEINHEIT D. F. and JIRSA J. O., Shear Strength of R.C. Beam-Column Connections. Proceedings, ASCE, V. 107, ST11, Nov. 1981, pp. 2227-2244.

7. WONG P. K. C., PRIESTLEY M. J. N. and PARK R., Seismic Resistance of Frames with Vertically Distributed Longitudinal Reinforcement in Beams. ACI Structural Journal, Vol. 87, No. 4, July-August 1990, pp. 488-498.

8. PAULAY T., PARK R. and PRIESTLEY M. J. N., Reinforced Concrete Beam-Column Joints Under Seismic Actions. ACI Journal, Proceedings V. 75, No. 11, Nov. 1978, pp. 585-593.

9. PAULAY T., Equilibrium Criteria for Reinforced Concrete Beam-Column Joints. ACI Sructural Journal, V. 86, No. 6, November-December 1989.

10. COLLINS M. P., Towards a Rational Theory for RC Members in Shear. ASCE Structures Journal, Vol. 104, No. ST4, April, 1978, pp. 649-666.

11. VECCHIO F.J. and COLLINS M.P., The Modified Compression-Field Theory for Reinforced Concrete Elements Subjected to Shear. ACI Journal, March-April 1986, pp. 219-231.

12. MacGREGOR J. G., Dimensioning and Detailing. Sub-Theme 2.4, Proceedings, IABSE Colloquium, Stuttgart, 1991.

13. MARTI P., Dimensioning and Detailing. Sub-Theme 2.4, Proceedings, IABSE Colloquium, Stuttgart, 1991.

Evaluation of the Rotation Capacity of «D» Regions

Capacité de rotation des zones «D»

Schätzung der Rotationsfähigkeit von «D»-Zonen

Gian Michele CALVI
Researcher
Univ. of Pavia
Pavia, Italy

Gian Michele Calvi received his Master of Science from the University of California, Berkeley, and his Ph.D. from the Politecnico di Milano. His main research interests are related to the seismic design of reinforced concrete and masonry structures, having been active both in the experimental and numerical fields.

Ester CANTU'
Researcher
Univ. of Pavia
Pavia, Italy

Ester Cantu', born in 1952, graduated in Civil Engineering at the University of Pavia. She is a researcher at the Department of Structural Mechanics of the University of Pavia. Her research field concerns masonry and reinforced concrete structures.

Guido MAGENES
Grad. Res. Assist.
Univ. of Pavia
Pavia, Italy

Guido Magenes, born in 1963, obtained his Civil Engineering degree at the University of Pavia and his M.Sc. degree at the University of California, San Diego. His research interests are related to structural concrete and masonry.

SUMMARY
The main objective of this paper is to discuss the effectiveness of some currently applied models in predicting the real rotation capacity of concrete slabs reinforced with welded wire meshes, as a functional of steel properties, reinforcement percentage and load condition. Comparisons are made with the experimental results obtained from 36 tests performed at the University of Pavia. Attention is given to the implications of the results for design codes and practical detailing.

RÉSUMÉ
L'objectif principal de cet article est de discuter l'efficacité de quelques modèles appliqués actuellement pour prévoir la capacité de rotation des dalles en béton armées de treillis, en fonction des propriétés de l'acier, du pourcentage d'armature et des conditions de mise en charge. Des comparaissons sont faites avec les résultats expérimentaux obtenus à partir de 36 essais effectués à l'université de Pavie. On portera son attention sur les conséquences de ces résultats sur les normes de dimensionnement, ainsi que sur les détails constructifs.

ZUSAMMENFASSUNG
Hauptgegenstand dieser Arbeit ist, die Effektivität einiger allgemein angewandter Modelle zu diskutieren, die die tatsächliche Rotationsfähigkeit von mit geschweissten Betonstahlbalken bewehrten Betonplatten als Funktion der Materialeigenschaften des Stahles, des Bewehrungsgehaltes und der Belastung ausdrücken. Es werden Vergleiche mit Ergebnissen aus 36 Versuchen, die an der Universität von Pavia durchgeführt wurden, angestellt. Die Einbindung dieser Ergebnisse in Normen und in die Praxis wird betrachtet.

1. PRELIMINARY REMARKS

The CEB Model Code 78 [1] allowed the redistribution of the bending moments calculated from a linear analysis if some ductility requirements were met by the critical sections.
The available plastic rotation was computed as a function of the neutral axis position according to the experimental results obtained from about 350 tests performed in the sixties [2,3].
Most of these tests had been performed on specimens reinforced with mild steel bars, with very good elongation capacity and large overstrength after yielding.
More recently it has become more and more common in Europe to produce steel with lower elongation capacity and lower overstrength, due to different production processes (cold worked steel) and weldability requirements (welded wire meshes). The applicability of the older results has been therefore questioned and discussed on the base of numerical analyses [4,5].
The plastic rotation capacity available for redistribution purposes has been consequently reviewed in the most recent codes [6,7], adding a second parameter to be considered: the elongation capacity of the steel.

The main objective of this paper is to discuss the ability of current numerical models to predict the real rotation capacity of plastic hinge regions and to examine the implications on codes of practice. Particular attention will be paid to the case of welded wire meshes, for a number of reasons: the steel is usually cold worked and has a lower elongation capacity; the steel percentages are often small; the bond between steel and concrete and the crack pattern can be strongly affected by the presence of the transversal bars.

2. FACTORS AFFECTING THE PLASTIC ROTATION CAPACITY

The basic parameter used in design codes to determine the available rotation capacity of a D region is the neutral axis depth (x/d) [1,6,7]. It has to be noted that the CEB MC 90 recognizes a decreasing rotation capacity if the neutral axis is too high, which means that the steel mechanical percentage is too low. The neutral axis depth is a very comprehensive parameter because it summarizes the effect of the section geometry and of some mechanical properties of the material.

Nevertheless the most recent codes are assuming a second parameter, i.e. the steel elongation capacity. The reason for which the influence of steel elongation was not considered in the past is simply due to the good uniform quality of the steel used up to the seventies.

A third parameter which is implicitly recognized as important is the ratio of the ultimate strength (f_{su}) to the yielding strength (f_{sy}) of the steel: a higher ratio allowes a larger region in which the yielding moment is attained, and the theoretical plastic rotation is consequently higher. Actually only a minimum for this ratio is given by the codes, but a tendency to the production of steel with less and less f_{su}/f_{sy} does exist, particularly for what concerns welded wire meshes.

It is also well known that the bond between steel and concrete plays an important role for the determination of the available rotation capacity, but there has not been in the past any transposition of this fact in the codes of practice. If this may be acceptable for deformed bars (but the bond is in this case proportional to the bar diameter), in the case of smooth bars the

spreading of the yielded region of the bar can significantly affect the rotation capacity. In this case the distance between transversal bars may become the fundamental parameter.

Finally it has to be reminded that the beam slenderness (length over depth, l/d) governs the relation between fiber deformation, section curvature and overall rotation, therefore if the maximum fiber deformation is given (i. e. the steel elongation capacity and the bond relations) the available rotation is proportional to the beam slenderness. Also if the depth of a beam is kept constant the theoretical length of the plastic hinge (distance between the points at which the yielding moment is attained) increases with increasing span. The beam slenderness is usually taken into account in the codes by means of some limit value of slenderness for which the given relations are applicable.

3. MODELS TO PREDICT THE AVAILABLE ROTATION CAPACITY

The most commonly used models able to predict the plastic rotation capacity of D regions are based on a few common hypotheses and follow some common steps:

- plane sections are supposed to remain plane;
- the sections are divided into layers, each of them being characterized by the appropriate stress - strain relation;
- the sectional moment - curvature relations are then constructed by imposing increasing curvatures, getting strains and stresses and computing the corresponding bending moments;
- for a given bending moment diagram is then possible to compute the total rotation integrating the section curvatures on the desired length.

The key issue of such models is a refined consideration of the tension stiffening effect of the concrete around the bars from crack to crack. For this purpose some bond stress-slip relation is needed [8], together with some model to predict the position of the cracks.
If the tension stiffening effect is not considered a rotation for the case of so called "naked" bars is obtained, which is generally always greater than the real rotation. The difference in the curvature for the two cases are qualitatively shown in fig. 1.

Some possible plastic penetration beyond the limit of the yielding moment should also be considered.

A fundamental problem which is far from being solved is to decide if, in which cases, and for what amount a translation of the bending moment diagram has to be considered, as required by the well known "truss analogy". In [4] it is suggested to consider a translation if some shear cracking is expected.

If only one crack is present in the yielded region and if the reinforcement percentage is low (i. e. the neutral axis depth is very small), a simplified model could be used to estimate the maximum available plastic rotation.
The beam could be considered as a combination of two rigid bodies, connected by a hinge in the compressed zone of the critical section and by a deformable steel element at the level of the tensile reinforcement. The length of the steel element should be defined on the base of the distance at which a perfect bond is believed to have been reached.

4. EXPERIMENTAL RESULTS

Tests on thirty six slabs reinforced with welded wire mesh have been recently completed at the Laboratory of the Department of Structural Mechanics of the University of Pavia. The specimens had the same rectangular section (440 mm x 160 mm), slenderness of about 14 and were casted with the same concrete. The spacing of the transversal bars was normally set at 150 mm. All the details on materials, geometry and results are presented in [9]. The variable parameters were as follows.

Steel properties

Three types of steel were used, with different stress-strain relations and different bond characteristics. The main differences can be identified in the mean ultimate elongation capacity (ε_u equal to 3.45, 4.36 and 7.99 %) and in the surface of the wires (smooth or deformed).

Reinforcement percentage

The geometrical percentages of the tensile steel were 0.23, 0.38 and 0.64 %, corresponding to neutral axis depth approximately equal to 0.09 d, 0.12 d and 0.17 d. The steel at the compressed edge was kept constant (geometrical percentage 0.23 %).

Applied load

The load was either concentrated at midspan or divided into four equal loads.

The main results in term of available plastic rotation are given in fig. 2: the experimentally measured rotations are systematically higher than the corresponding values accepted in the CEB MC 90, but the ratio between available and accepted plastic rotation does not seem to be uniform.
The trends given by the CEB are roughly confirmed, but the steel with higher elongation capacity seems to be much more sensitive to a decrease of the reinforcement percentage and of the bar diameters.
The smooth wire meshes deserve a special mention because of the good uniform behaviour.

A comparison of numerical and experimental results is presented in fig. 3.
The numerical model was not refined and did not consider the tension stiffening effect; the complete stress-strain curve of the steel was used.
The numerical simulations should have therefore sistematically overestimated the available rotation. This is not the case for some specimens with smooth bars (LiB) and with the more ductile deformed bars (NeA). For these cases the introduction of a tension stiffening effect in the model would have further underestimated the available plastic rotation. While the substantial approximation of the same values for the experimental and numerical results could have been predicted in the case of smooth bars (i.e. in this case the bond could be neglected), the results obtained from NeA type steel still deserve some explanation.

The tension stiffening effect is experimentally very clear, as shown in fig. 4, where the moment-curvature diagrams for different regions of a beam are shown. It is also clear that only in one crack the steel has been able to reach yielding: the yielded length depends therefore on the bond stress-slip relation rather than on the distance between the points at which the yielding moment is attained. This consideration explains why the numerical predictions are generally too high in the case of smaller deformed bars: in this case the bond is much higher.

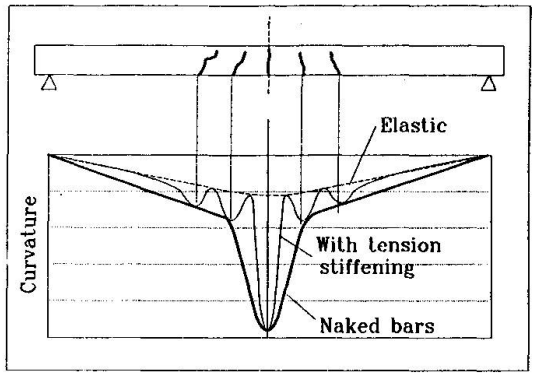

Fig.1 - Comparison of typical curvatures with and without considering the tension stiffening effect

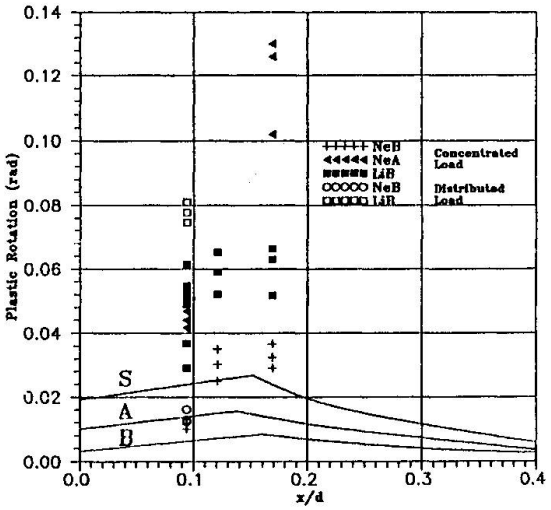

Fig.2 - Experimental plastic rotation vs. the CEB MC 90 design curves

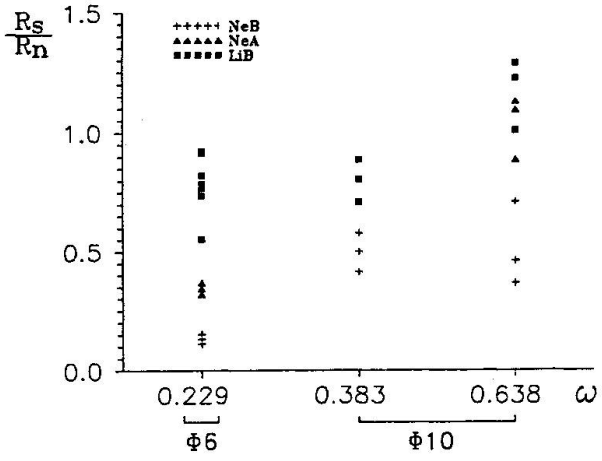

Fig.3 - Ratio between experimental and numerical ("naked bars" with bending moment diagram traslation) rotations as a function of steel percentage (bar diam.) and quality

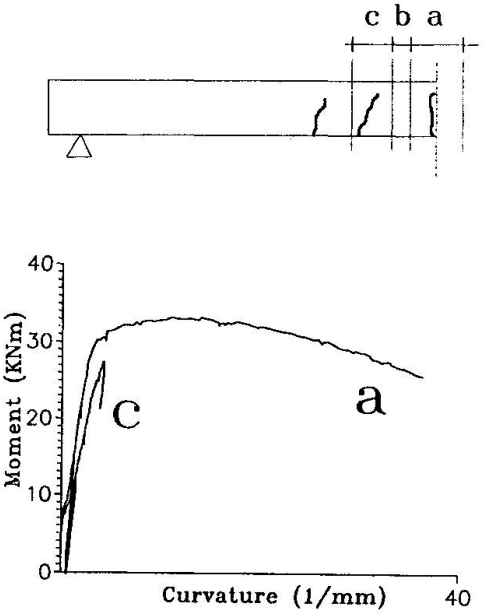

Fig.4 - Evidence of the tension stiffening effect from the experimental results

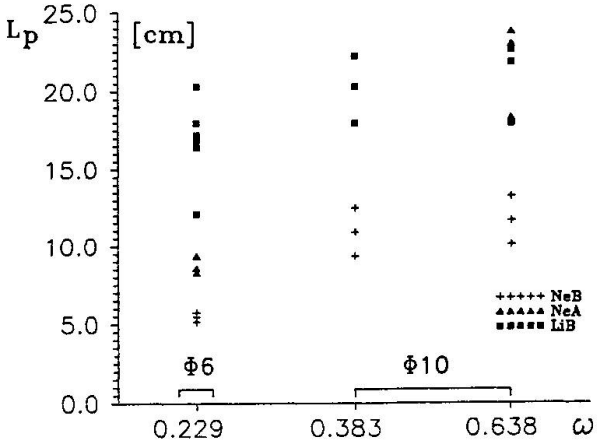

Fig.5 - Yielded lenghts required by the "rigid bodies model" as a function of steel percentage (bar diam.) and quality

The simplified model previously mentioned has been also applied to check the implications of the experimental results. In fig. 5 the lengths of the bars that should have fully yielded to match the experimental results are shown.
In the case of deformed bars, the bond is clearly playing the fundamental role, with required plastic length approximately proportional to the bar diameter.
In the case of smooth bars the required plastic length is about constant, confirming the negligibility of bond stress-slip relations with respect to the mechanical restraints offered by the transversal bars.

5. IMPLICATIONS FOR DESIGN CODES AND CONCLUSIONS

The importance of bond relations in the evaluation of the available rotation capacity in D regions has been generally neglected by codes and this is particularly dangerous in the case of small diameter bars, for which also the mechanical properties of the steel are usually worse.
On the opposite, from experimental results it appears that the use of smooth bars could assure a series of advantages if a mechanical bond is anyway guaranteed by the presence of transversal welded wires.
The definition of minimum values of reinforcement and minimum bar diameters seems to be particularly important in the case of deformed bars, when some plastic rotation is required, even if a good elongation capacity of the steel is provided.

ACKNOWLEDGEMENTS

The experimental tests discussed in this paper have been funded by the Italian Society of Steel Producers (Federacciai). The authors wish also to express their gratitude to Prof. G. Macchi for his support and suggestions.

REFERENCES

[1] CEB-FIP, Model Code for Concrete Structures, Bulletin d'Information CEB No. 124/125, 1978
[2] MACCHI G., Ductility Condition for Simplified Design without Check of Ductility, Bulletin d'Information CEB No. 105, 1976
[3] SIVIERO E., Rotation Capacity of Monodimensional Members in Structural Concrete, ibidem
[4] ELIGEHAUSEN R., LANGER P., Rotation Capacity of Plastic Hinges and Allowable Degree of Moment Redistribution, Bulletin d'Information CEB No. 175, 1987
[5] COSENZA E., GRECO C., PECCE M., Plastic Rotation and Required Ductility in R. C. Continuous Beams, L'Industria Italiana del Cemento, 1, 1990 (in italian)
[6] COMMISSION OF THE EUROPEAN COMMUNITIES, Eurocode No. 2, Common Unified Rules for Concrete Structures, Final Draft, 1988
[7] CEB-FIP, Model Code 1990, First Draft, Bulletin d'Information CEB No. 195/196, 1990
[8] ELIGEHAUSEN R., POPOV E. P., BERTERO V. V., Local Bond Stress-Slip Relationship of Deformed Bars under Generalized Excitations, Report No. UCB/EERC 83/23, University of California, Berkeley, 1983
[9] CALVI G. M., CANTU' E., MACCHI G., MAGENES G., Experimental Investigation on the Rotation Capacity of Concrete Slabs Reinforced with Welded Wire Meshes, Rapporto N. 33, Dipartimento di Meccanica Strutturale dell'Universita' di Pavia, 1990

Ductility of Structural Concrete

Ductilité du béton structurel

Duktilität des Konstruktionsbetons

Igor TERTEA
Prof. Dr.
Polytechn. Inst.
Cluj-Napoca, Romania

Igor Tertea, received his Dipl. Eng. and the Dr. Eng. degrees from the Polytechn. Inst. of Timişoara, Romania, and is since 1956 Professor of reinforced and prestressed concrete at the Polytechn. Inst. of Cluj-Napoca, Romania. He is the author of several publications.

Traian ONET
Prof. Dr.
Polytechn. Inst.
Cluj-Napoca, Romania

Traian Onet, born 1937, received his Dipl. Eng. and the Dr. Eng. degrees from the Polytechn. Inst. of Cluj-Napoca, Romania. He is since 1965 Professor of reinforced and prestressed concrete at the same Institute, and author of several books and publications on reinforced and prestressed concrete.

SUMMARY

The paper presents the ductility computation for B regions and the main parameters influencing the ductility of structural concrete as seen from the correlation of the numerical tests with experimental results.

RÉSUMÉ

Cet article présente une méthode de calcul des zones B, ainsi que les paramètres influençant la ductilité du béton, résultant d'une corrélation entre résultats numériques et expérimentaux.

ZUSAMMENFASSUNG

Der Artikel stellt ein Rechnungsverfahren für die Duktilität der B-Bereiche vor und zeigt die wesentlichen Einflüsse auf die Duktilität von Konstruktionsbeton auf, die aus Vergleichen von numerischen Berechnungen mit Versuchsergebnissen gewonnen werden.

1. INTRODUCTION

In accordance with the ideas expressed in the introductory reports by J.E. Breen and A.S.G. Bruggeling, as well as with the considerations contained in the lectures of J.G. MacGregor and P. Marti, we shoud emphasize the fact that one of the fundamental requirements of structural concrete elements design is the provision of a proper ductility. In fact, one of the most important advantages of structural concrete is offered by the possibility to design the required sectional or/and structural ductility, in accordance with the building's emplacement and the nature of actions.

The above assertion is valid only for the portions of the structural elements subjected to bending moments with or without axial load (B regions), for which there are already clear design models permiting a qualitative and especially a quantitative ductility computation [1,2,4].

For the portions subjected to combined action of bending moment and shear force (D regions) design model recently proposed (full-member design procedure) does not refer to ductility but in case of inclined crack width limitation.

2. DUCTILITY COMPUTATION FOR B REGIONS

The design model used by the authors [4,5] does not essentially differ from that proposed by A.S.G. Bruggeling [1], in which the prestressing can simply be regarded as an artificial loading, from the point of view of load capacity.

For the ductility computation the following assumptions are made:

a) The stress - strain curve of concrete is a parabolic one (Fig.1) and takes into consideration the concrete confinement by transverse reinforcement.

b) The stress - strain diagram for nonprestressed steel is bilinear (corresponding to elasto-plastic behaviour).

c) The stress - strain diagram for prestressing steel is linear for $\sigma_p \leq 0{,}6\ f_{pu}$ and five degree parabolic over this value.

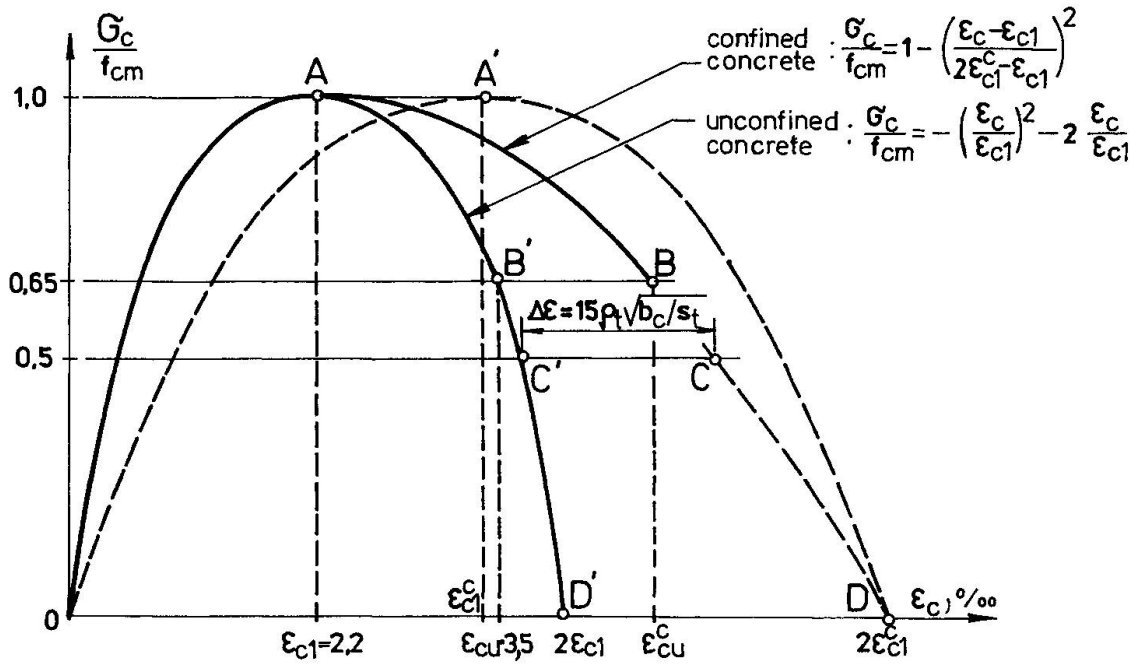

Fig. 1

d) Active and passive reinforcement yield at the same time.

e) Plane sections before flexure remain plane after flexure.

f) The prestressing effect, after losses, is similar to external forces P_{∞} and P'_{∞} (corresponding to the reinforcements A_p and A'_p).

g) There is a good bond between concrete and reinforcements.

h) The cross sectional stress and strain distribution at yield point of reinforcement and at fracture of concrete are represented in Fig.2a and Fig.2b respectively.

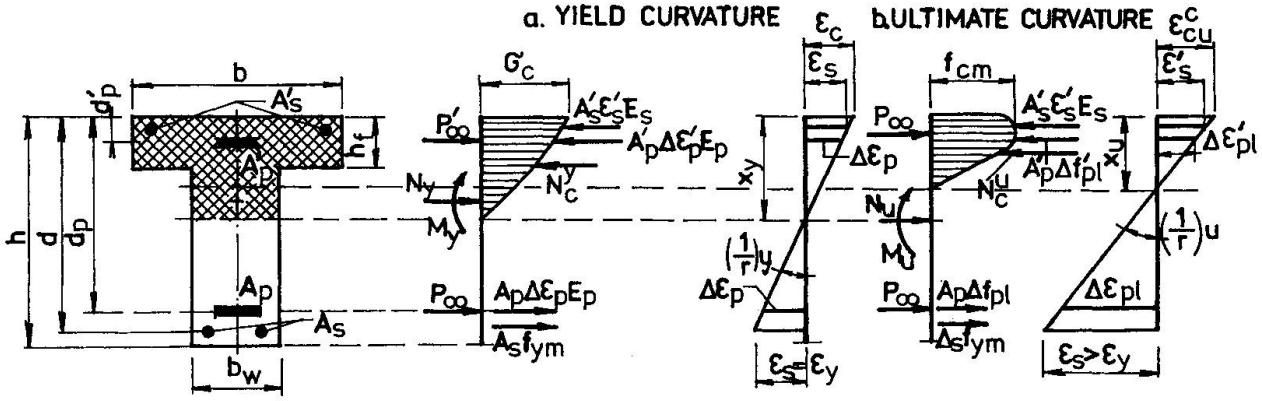

Fig. 2

The ductility ratio for a structural concrete section subjected to bending with axial load can be computed as follows:

$$D = \frac{\varepsilon_{cu}^{c}(1 - \xi_y)E_s}{\xi_u f_{ym}} = \frac{\varepsilon_{cu}^{c}(\delta - \xi_y)E_p}{\xi_u(f_{0.2m} - \sigma_{p\infty})} \qquad (1)$$

where $\xi_y = \frac{x_y}{d}$ and $\xi_u = \frac{x_u}{d}$.

The values of ξ_y and ξ_u are the solutions of the equations:

$$A \xi_y^3 + B \xi_y^2 + C \xi_y + D = 0 \qquad (2)$$

$$E \xi_u^3 + F \xi_u^2 + G \xi_u + H = 0 \qquad (3)$$

where the coefficients have the expressions from Appendix, for one of possible situations depending on section characteristics.

Design procedure is programmable. The set of numerical program [4] is providing the possibility to print the diagrams for estimating the ductility ratio depending on different parameters.

3.PARAMETERS INFLUENCING THE STRUCTURAL CONCRETE DUCTILITY

Numerical tests using the above mentioned programs have been correlated with experimental results obtained in Reinforced Concrete Laboratory of Politechnical Institute of Cluj and also with in other laboratories and we got the following conclusions:

- The ductility of structural concrete sections is drastically diminished by increasing the axial forces intensity (external action effects and/or prestressing effect) which accompany the bending moment. The curvature ductility may be improved by reducing the prestressing degree or (at a given prestressing degree) by proper transverse reinforcement [3,5].
- The beams with unbonded prestressing reinforcement have a greater ductility in comparison with those with bonded prestressing reinforcement.

- The passive or active reinforcement of compressive zone has a favourable influence on ductility due to beneficial effect of the concrete confinement.
- The higher the ratio of passive reinforcement (ρ_w) (at the same quantity of the total reinforcement) and the less the quality of this reinforcement, the greater the value of ductility.
- The effect of small number of repeated loading cycles on the ductility was insignificant.

REFERENCES

1. BRUGGELING A.S.G., Structural concrete: Science into practice. Heron, vol.32, no.2., 1987.
2. COHN M.Z., TRINH J.K.L., Précontrainte partielle: De la théorie a la pratique. Annales de l'ITBTP, no.444, mai 1986, pp. 90 - 115.
3. ONEŢ T., AL-DABBEEK J.N.S., New Data Regarding the Transverse Reinforcement Effect on Ductility of Structural Concrete Elements (in Romanian). The XIV-th Concrete Conference, vol.1, Cluj-Napoca, 1988.
4. ONEŢ T., TERTEA I., Ductility of Structural Concrete (in Romanian). Construcţii, nr.11-12, 1988, pp.72 - 77.
5. TERTEA I., ONEŢ T., Ductility of Partially Prestressed Concrete. International Symposium "Nonlinearity and Continuity in Prestressed Concrete", University of Waterloo, Ontario, Canada, 1983.

APPENDIX

$$\boxed{\varepsilon'_s \geq \varepsilon_y}$$

$$A = \frac{1}{3}\frac{\varepsilon_y}{\varepsilon_{c1}}\left(3+\frac{\varepsilon_y}{\varepsilon_{c1}}\right)$$

$$B = (\alpha+\alpha_p)-(\alpha'-\alpha'_p)-\frac{\varepsilon_y}{\varepsilon_{c1}}+\frac{\varepsilon_y}{\varepsilon_{c1}}\frac{h_f}{d}\left(\frac{b}{b_w}-1\right)\left(2+\frac{\varepsilon_y}{\varepsilon_{c1}}\right)+n_y$$

$$C = -2\alpha-\alpha_p\left(1+\frac{d}{d_p}\right)+2\alpha'-\alpha'_p\left(1+\frac{d'_p}{d}\right)-$$

$$-\frac{\varepsilon_y}{\varepsilon_{c1}}\frac{h_f}{d}\left(\frac{b}{b_w}-1\right)\left(2+\frac{h_f}{d}+\frac{h_f}{d}\frac{\varepsilon_y}{\varepsilon_{c1}}\right)-2n_y$$

$$D = \alpha+\alpha_p\frac{d}{d_p}-\alpha'+\alpha'_p\frac{d'_p}{d}+\frac{\varepsilon_y}{\varepsilon_{c1}}\frac{h_f^2}{d^2}\left(\frac{b}{b_w}-1\right)\left(1+\frac{1}{3}\frac{h_f}{d}\frac{\varepsilon_y}{\varepsilon_{c1}}\right)+n_y$$

$$\alpha = \varrho_w\frac{f_{ym}}{f_{cm}}\ ;\ \alpha' = \varrho'_w\frac{f_{ym}}{f_{cm}}\ ;\ \alpha_p = \varrho_{wp}\frac{\varepsilon_y E_p}{f_{cm}}\ ;\ \alpha'_p = \varrho'_{wp}\frac{\varepsilon_y E_p}{f_{cm}}\ ;$$

$$\varrho_w = \frac{A_s}{b_w d}\ ;\ \varrho'_w = \frac{A'_s}{b_w d}\ ;\ \varrho_{wp} = \frac{A_p}{b_w d}\ ;\ \varrho'_{wp} = \frac{A'_p}{b_w d}\ ;$$

$$n_y = \frac{N_y + P_\infty + P'_\infty}{b_w d f_{cm}}\ .$$

$$\boxed{\varepsilon'_s \geq \varepsilon_y\ ;\ \xi_u > \frac{h_f}{d} > \xi_u\left(1-\frac{\varepsilon_{c1}}{\varepsilon^c_{cu}}\right)}$$

$$E = \frac{1}{3}\frac{b}{b_w}\frac{\varepsilon_{c1}}{\varepsilon^c_{cu}}\left[1-\left(\frac{\varepsilon_{c1}}{2\varepsilon^c_{c1}-\varepsilon_{c1}}\right)^2\right]+\left(\frac{b}{b_w}-1\right)\left[\frac{\varepsilon^c_{cu}}{\varepsilon_{c1}}-\frac{1}{3}\left(\frac{\varepsilon^c_{cu}}{\varepsilon_{c1}}\right)^2\right]-$$

$$-\frac{b}{b_w}\left[1-\frac{1}{3}\left(\frac{\varepsilon^c_{cu}}{2\varepsilon^c_{c1}-\varepsilon_{c1}}\right)^2+\frac{\varepsilon^c_{cu}\varepsilon_{c1}}{(2\varepsilon^c_{c1}-\varepsilon_{c1})^2}-\left(\frac{\varepsilon_{c1}}{2\varepsilon^c_{c1}-\varepsilon_{c1}}\right)^2\right]$$

$$F = \alpha+\alpha_{pu}-\alpha'-\alpha'_{pu}-\frac{h_f}{d}\frac{\varepsilon^c_{cu}}{\varepsilon_y}\left(\frac{b}{b_w}-1\right)\left(2-\frac{\varepsilon^c_{cu}}{\varepsilon_{c1}}\right)+n_u$$

$$G = \frac{\varepsilon^c_{cu}}{\varepsilon_{c1}}\frac{h_f^2}{d^2}\left(\frac{b}{b_w}-1\right)\left(1-\frac{\varepsilon^c_{cu}}{\varepsilon_{c1}}\right)$$

$$H = \frac{1}{3}\frac{h_f^3}{d^3}\left(\frac{b}{b_w}-1\right)\left(\frac{\varepsilon^c_{cu}}{\varepsilon_{c1}}\right)^2$$

$$\alpha_{pu} = \varrho_{wp}\frac{\Delta f_{pl}}{f_{cm}}\ ;\ \alpha'_{pu} = \varrho'_{wp}\frac{\Delta f'_{pl}}{f_{cm}}\ ;\ n_u = \frac{N_u + P_\infty + P'_\infty}{b_w d f_{cm}}\ .$$

Conclusions from Tests on Corbels

Conclusions d'essais sur des consoles courtes

Folgerungen aus Versuchen an Konsolen

Wolfgang ZELLER
Dipl.-Ing.
Univ. Karlsruhe
Karlsruhe, Germany

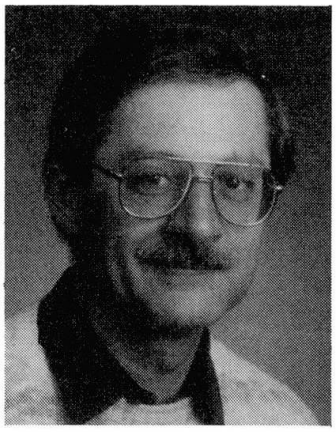

Wolfgang Zeller, born 1942, received his engineering degree from the University of Karlsruhe, Germany. Formerly he was concerned with prestressed concrete bridge construction in a consulting firm and later took up a position as a teaching assistant at the University of Karlsruhe. Presently, he is engaged in research on bridge bearings and corbels.

SUMMARY
Results of tests on reinforced concrete corbels are presented. Load-carrying behaviour after diagonal splitting is explained using a refined strut-and-tie model.

RÉSUMÉ
On présente les résultats d'essais réalisés sur des consoles courtes. Le comportement après la fissuration dans la bielle comprimée est discuté à l'aide d'un modèle de treillis modifié.

ZUSAMMENFASSUNG
Es werden Ergebnisse von Versuchen an Konsolen vorgestellt. An einem verfeinerten Fachwerkmodell wird das Tragverhalten nach dem Auftreten von Spaltrissen erläutert.

1. INTRODUCTION

Research on corbels has been an ongoing concern at the University of Karlsruhe since the early 1960's when Franz/Niedenhoff [1] suggested the simple strut-and-tie model to design reinforced concrete corbels. Tests in the late 1970's [2] have shown that heavily reinforced concrete corbels, with an a/d ratio of 1.0, require not only horizontal but, also, vertical stirrups to prevent failure caused by diagonal splitting in the compression strut. This is due to transversal tensile stresses. More recent tests described in this paper are concerned with investigating the behaviour of the compression strut and the stirrup reinforcement used for different corbel designs.

2. TESTS

Two double corbels with a/d ratios of 0.5 and 1.0, respectively, were loaded to failure (Fig. 1). The tension reinforcement A_s consists of horizontal loops, having equal cross sections for both specimens. Horizontal stirrups were used for corbels K1 to K3 to carry the transverse tensile stresses present in the compression strut. These had an amount of reinforcement equal to 1/3, 1/2 and 1/3 respectively, of the reinforcement A_s. Vertical stirrups were arranged in corbel K4 to resist the transverse tensile stresses. Steel reinforcement strains and concrete strains were measured with electrical resistant strain gauges. Table 1 gives details of the corbel design and failure loads.

Failure modes

Corbel K1 : The horizontal stirrup reinforcement first yielded and deformed extensively after the formation of wide inclined cracks, followed by crushing of the concrete in the compression strut at the column corner. Stresses in the ties were below the yield limit. A special device was then used to strengthen this corbel before the adjoining corbel K2 could be tested to failure.

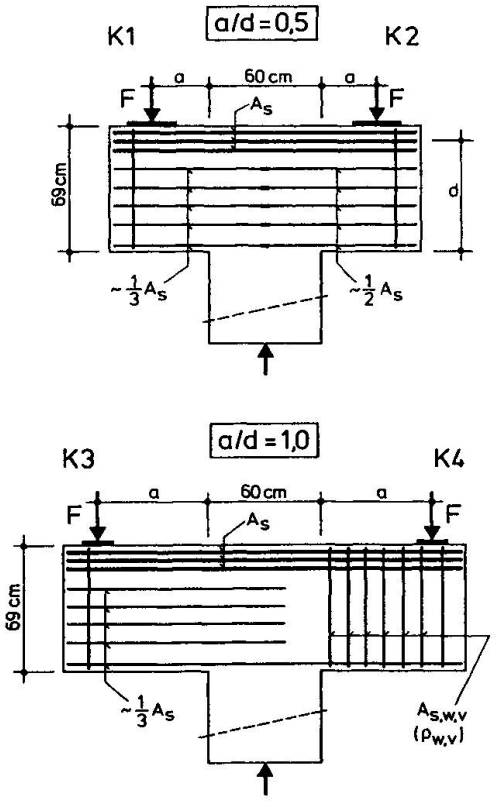

Fig. 1 : Corbel details: reinforcement and dimensions

Corbel No		K 1	K 2	K 3	K 4	units
Ratio	a/d	0,5		1,0		-
Span	a	30		60		cm
Effective depth	d	60		60		cm
Width	b	30		30		cm
Steel						
Tension	A_s	15,5		15,5		cm^2
reinforcement	f_y	~500		~500		N/mm^2
	ρ_l	0,86		0,86		%
Stirrups	A_{swh}/A_s	~1/3	~1/2	~1/3	-	-
(horizontal)	ρ_{wh}	0,38	0,55	0,39	-	%
Stirrups (vertical)	ρ_{wh}	-	-	-	0,37	%
Concrete	f_c	24,5		22,5		MN/m^2
Failure	F_u	948	>1000	455	683	kN
	$\tau_u = F_u/bd$	5,26	>5,55	2,53	3,79	MN/m^2
	τ_u / f_c	0,215	>0,227	0,112	0,169	-

Tab. 1: Experimental test results

Corbel K2 : A maximum load of 1000 kN was reached before the strengthened corbel K1 failed once again. At this load level the stresses in the horizontal stirrups of corbel K2 were just below the yield limit of the steel. The concrete strains in the compression zone at the column corner reached values greater than 4 $^{o}/_{oo}$, suggesting that this corbel would not be able to carry much higher loads.

Corbel K3 : Failure occurred suddenly by diagonal splitting of the compression strut. This was immediately followed by concrete crushing in the zone at the column corner.

Corbel K4 : This corbel failed progressively by crushing of the concrete in the compression zone after extensive yielding of the tension reinforcement (flexural tension failure). Most of the vertical stirrups also exceeded their yield limit.

Crack development

Vertical flexural cracks in the column area began to appear first at very low load levels. These cracks were followed by the formation of inclined cracks at higher load levels and then diagonal splitting cracks which developed near the bearing plate and propagated into the compression zone. The splitting crack widths were geater than those of the flexural cracks. Fig. 2a shows a typical crack pattern of specimen K3 /K4.

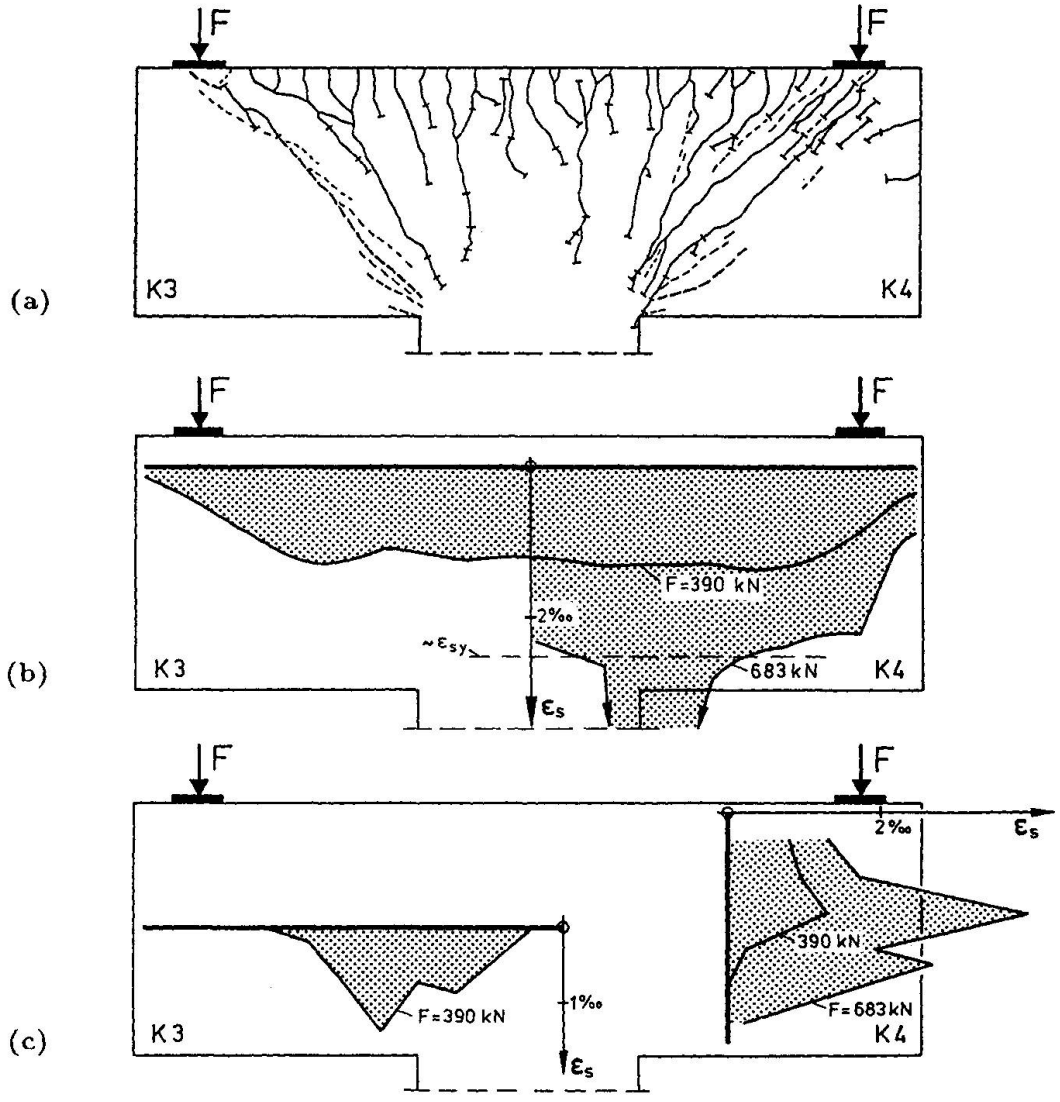

Fig. 2 : Corbels K3 and K4 (a/d = 1.0) : (a) crack pattern; (b) and (c) strain distribution in the tie reinforcement and in both a horizontal and vertical stirrup

Strain measurements

The distribution of the tension tie reinforcement was fairly uniform between the two load bearing plates for corbels K1/K2. However, this was not quite the same case for specimen K3/K4 (Fig. 2b). The maximum strains in both the vertical and horizontal stirrups always occurred in the compression strut area where the bars crossed the splitting cracks (Fig. 2c).

The distribution of concrete strains and stresses is shown in Fig. 3. Stresses are determined from the measured strains and a uniaxial cylinder stress-strain response exhibiting strain softening. Stresses in the compression struts were greatest at the column corner.

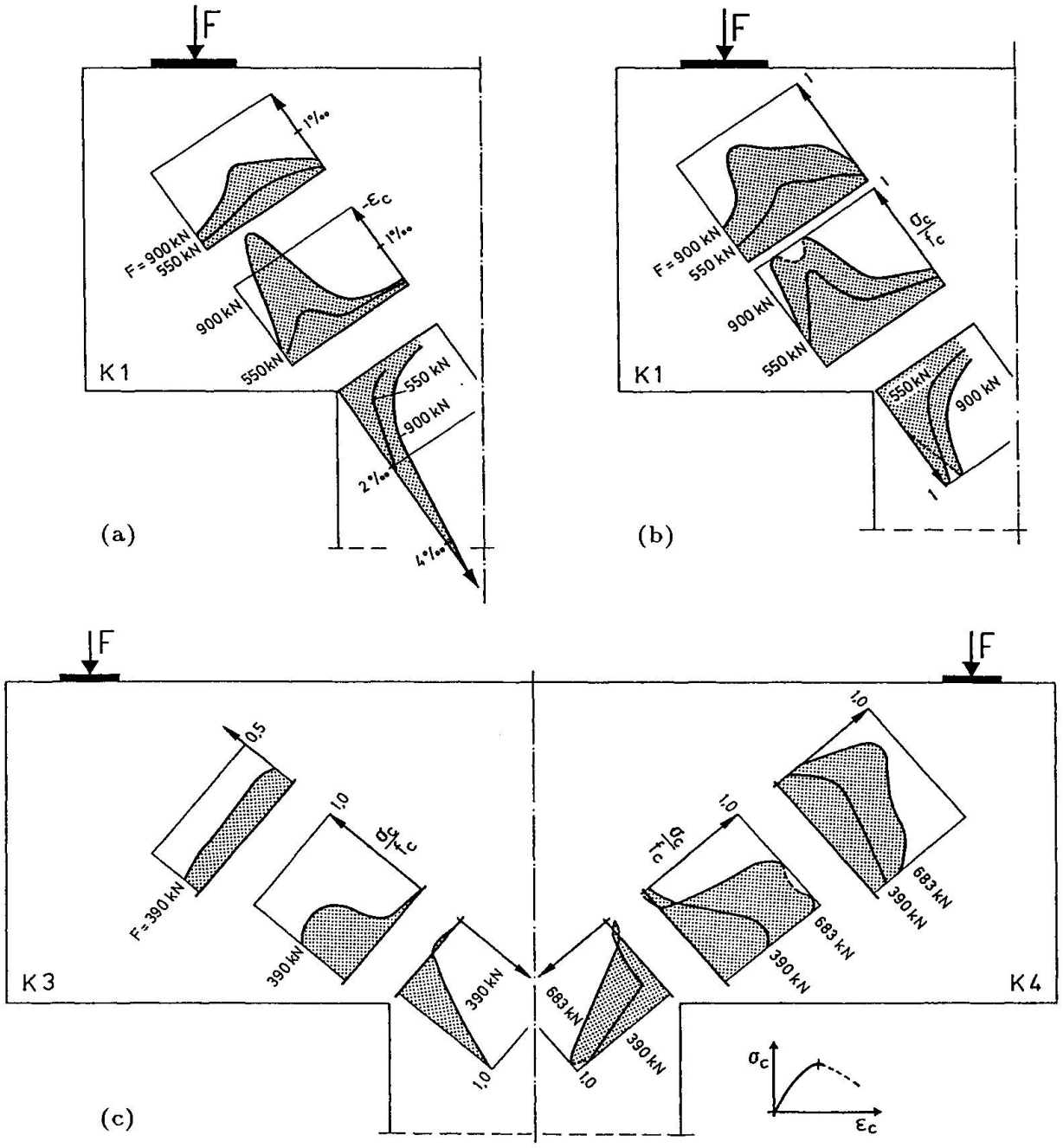

Fig. 3 : Concrete compression strain and stress distribution in corbels K1 and K3/K4

3. DISCUSSION

Results from tests on the corbels demonstrate that stirrups are needed to account for the tranverse tensile forces which develop in the compression strut. The horizontal stirrups used in corbel K1 (a/d = 0.5) were not sufficient to prevent crushing of the concrete in the column corner because of extensive yielding in the stirrups. The same behaviour is assumed for corbel K2. Recall that the stirrup reinforcement used in these corbels was equal to either 1/3 or 1/2 of the tension tie reinforcement. The horizontal stirrups used in corbel K3, having a larger aspect ratio a/d = 1.0, were not very effective, while the vertical stirrups used in corbel K4 resulted in a much higher failure load. The flexural tension failure observed for this corbel was caused by yielding of the tension reinforcement. Hence, corbels should be designed with enough vertical stirrups to allow for this type of failure.

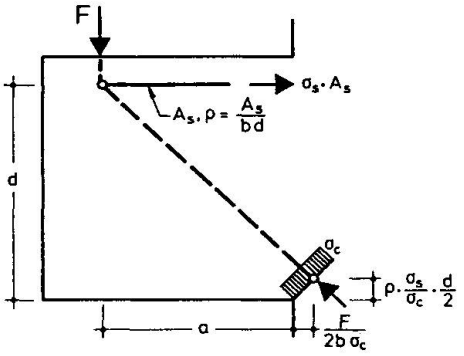

Fig. 4: Simple strut-and-tie model

The simple strut-and-tie model (Fig. 4) is not useful when diagonal splitting occurs. Fig. 5 shows a refined model which is able to analyse post-crack behaviour up to failure. Behaviour at the column corner is only considered since failure should always happen here if the loading node is properly detailed. Rotations occur primarily as a result of deformation in both the tie and transverse tension strut. Rotation on side 1 is greater than that of side 2. Since the struts are not really pinned at the column node, rotation is restrained and consequently strains are greater on side 1. Hence, tensile tie and stirrup reinforcement influence the strains in strut 1 by affecting the rotation of the system. The concrete strains obviously increase greatly when the tranverse tension strut begins to yield, resulting in failure of the concrete.

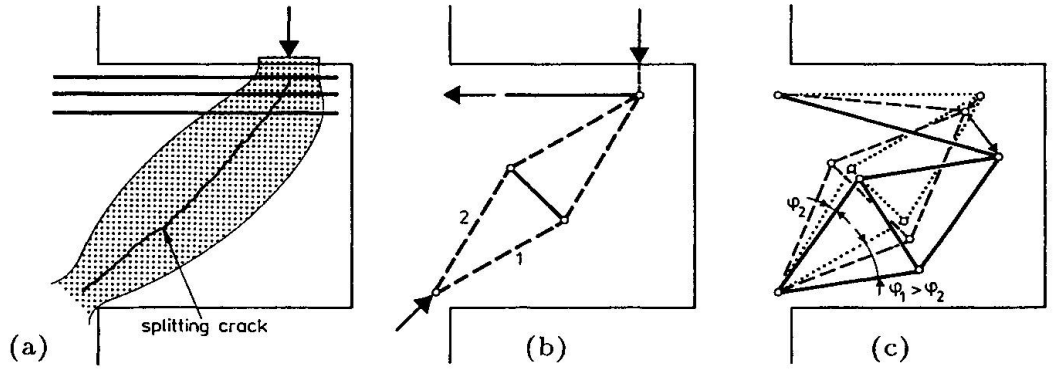

Fig. 5 : Strut-and-tie model explaining diagonal splitting; (a) bottle compression field; (b) refined model; (c) deformation and rotation

Further theoretical research has shown that the magnitude of the tensile splitting force depends on (1) the width of the compression strut at the column corner node and (2) the dimension of the bearing plate and depth of the tension main bars at the loading node.

The width of the compression zone is influenced by the amount of the tensile and the splitting reinforcement. Additionally, the splitting force increases with larger a/d ratios and is not proportional to the force in the main tension bars, as commonly suggested. This assumption leads to an amount of tensile splitting reinforcement which is too small, especially for corbels whith a small a/d ratio.

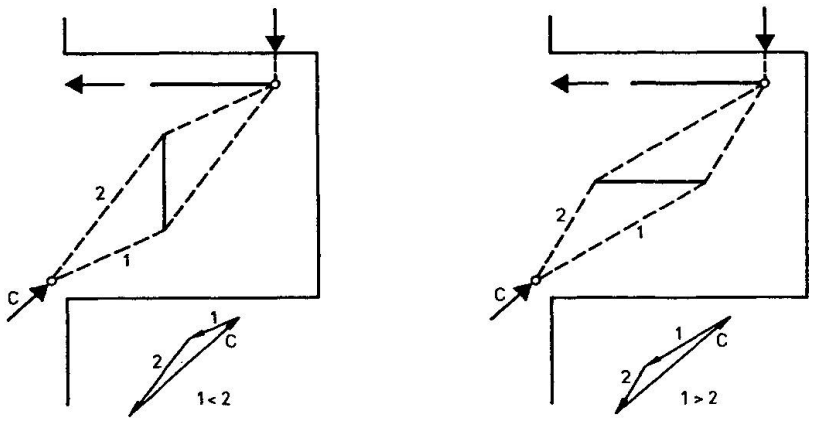

Fig. 6: Strut-and-tie models for corbels reinforced with horizontal or vertical stirrups

The amount of stirrup reinforcement also increases when the orientation of this reinforcement differs from the splitting tensile force vector which is approximately perpendicular to the direct compression strut. In this case, vertical stirrups are more sufficient when the angle of the compression strut is lower than 45°. Conversely, horizontal stirrups are better when the angle exceeds 45°, as is the case for corbels with a/d ratios smaller than about 0.7 to 0.9. Fig. 6 illustrates that when the direction of the splitting reinforcement deviates from the tensile force vector, then not only the splitting forces change but, also, the compresson forces in the column corner.

The tests and analysis described in this paper have shown that the bearing capacity of corbels is greatly influenced by the arrangement of the splitting tension reinforcement, and that the simple strut-and-tie model was not able to account for the actual stresses in the compression zone after diagonal splitting occurred.

4. REFERENCES

[1] FRANZ, G., NIEDENHOFF, H.: Die Bewehrung von Konsolen und gedrungenen Balken, Beton- und Stahlbetonbau 1963, H. 5, S. 112 - 120

[2] EIBL, J., ZELLER, W.: Bruchversuche an Stahlbetonkonsolen bei Veränderung des Bewehrungsgrades, Abschlußbericht 1983, Institut für Massivbau und Baustofftechnologie, Universität Karlsruhe

Dimensioning of the Cable-Stayed Helgeland Bridge

Dimensionnement du pont à haubans de Helgeland

Bemessung der Helgeland Schrägkabelbrücke

H.S. SVENSSON
Sen. Superv. Eng.
Leonhardt, Andrä & Partner
Stuttgart, Germany

Dipl.-Ing. Holger S. Svensson, P.E., P. Eng., born in 1945, received his Diploma in Structural Engineering from Stuttgart University in 1969. He was responsible for the design of several long-span cable-stayed bridges in different countries.

S. HOPF
Sen. Project Eng.
Leonhardt, Andrä & Partner
Stuttgart, Germany

Dipl.-Ing. Siegfried Hopf, born in 1953, received his Diploma in Structural Engineering fromStuttgart University in 1978. He has extensive experience in the design and construction of long-span bridges.

I. KOVACS
Sen. Project Eng.
Leonhardt, Andrä & Partner
Stuttgart, Germany

Dr.-Ing. Imre Kovács, born in 1943, received his Doctorate in Structural Engineering from Stuttgart University in 1973. He has wide experience in all aspects of the dynamic analysis of structures.

SUMMARY
The dimensioning of this cable-stayed bridge with a main span of 425 m and a very slender beam was governed not only by static loads, but also to a great extent by the high dynamic wind loads during construction and after completion. Non-linear effects played an important role in the determination of the stiffness of the structural concrete members.

RÉSUMÉ
Le dimensionnement de ce pont haubané en béton dont la portée principale est de 425 m et dont le tablier est très élancé, a été effectué en tenant compte non seulement des sollicitation de type statique, mais essentiellement des charges dynamiques dues au vent. Les effets non-linéaires jouent un rôle très important sur la détermination de la rigidité des éléments structuraux en béton.

ZUSAMMENFASSUNG
Die Bemessung dieser Beton-Schrägseilbrücke mit einer Hauptspannweite von 425 m und einem sehr schlanken Balken wurde nicht nur durch die statischen Lasten bestimmt, sondern weitgehend auch durch die hohen dynamischen Windlasten während des Baus und nach Fertigstellung. Nichtlineare Effekte spielten eine grosse Rolle bei der Bestimmung der Steifigkeit der tragenden Betonteile.

1. INTRODUCTION

The bridge is located near the town of Sandnessjoen, close to the Polar Circle in Northern Norway. Construction started in April 1989, completion is anticipated for September 1991. A general description is provided in Ref. [1], the layout is shown in Fig. 1.

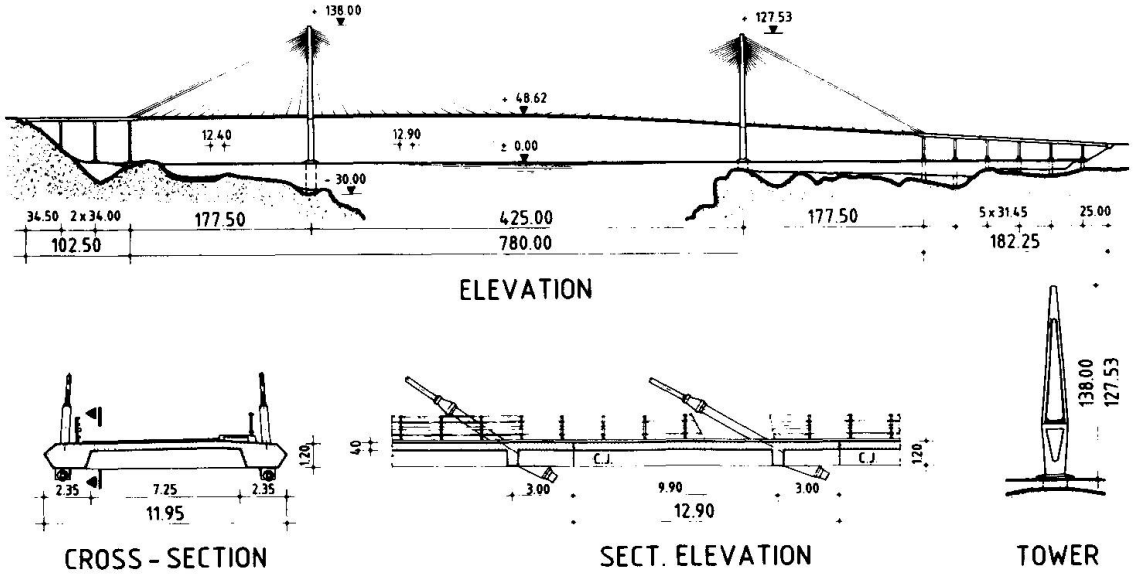

Fig. 1: General Layout

2. DIMENSIONING AND DETAILING

2.1 Towerheads

Three basic tower shapes were investigated: H-, diamond- and A-shapes. The modfied diamond shape was found most suitable, combining economy, esthetics and structural characteristics.
The upper legs are rectangular boxes with 40 cm wall thickness, temporarily post-tensioned during erection with external tendons.

For the cable anchorage area at the tower head a comparison between solid cross sections with overcrossing backstays and forestays, a composite structure, and boxes indicated that concrete box sections with wall thicknesses of 0.42 m and 1.00 m are most economical and have the advantages of anchor head protection from the environment and easy inspection access, see Fig. 2.

At the tower head a large number of concentrated cable forces are introduced. The different models for distributing these forces must be evaluated very carefully, all forces must be followed until they are equally distributed over the cross section, all deviation and tie forces must be taken by steel - rebars or post-tensioned bars - all concrete struts must be checked for compression. Special care must be taken for the design of the nodal zones where the forces are introduced or where several struts and/or ties are intersecting.

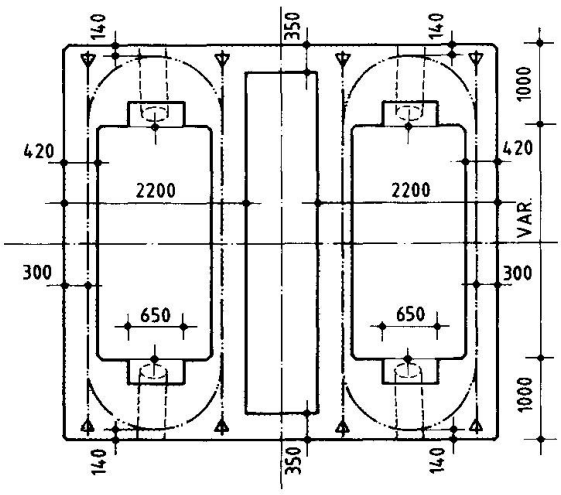

Fig. 2: Section through Towerhead

The system shown in Fig. 2 has been proven to be easy to construct. The number of post-tensioning anchorages is reduced to a minimum, thus reducing the usual congestion in this region. The cable forces are confined by loop tendons, spaced at the same distances as the stays (1.50 m). The question, how much tension is lost along the tight loops due to friction has been investigated in a 1:1 model. With a smooth lubricated duct the standard friction and wobble factors have been confirmed.

The design has been done for different models:
a) truss action (see Fig. 3 and 4)
b) arch action (see Fig. 5)
c) frame action
d) punching.

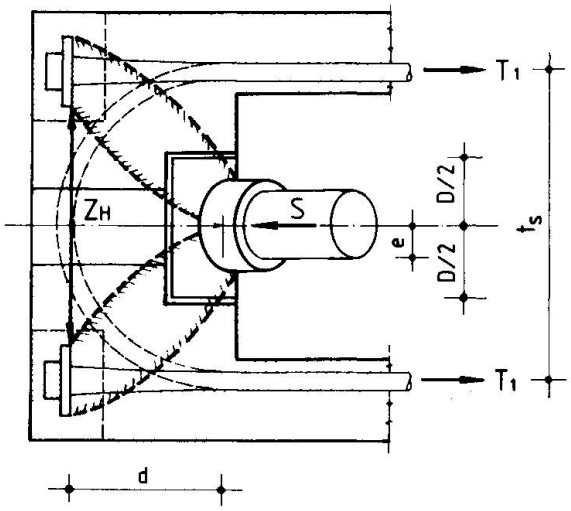

Fig. 3: Truss Action at Towerhead in plan

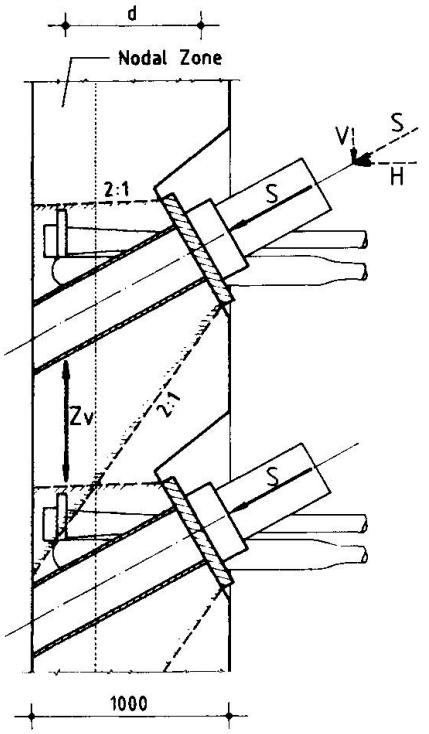

Fig. 4: Truss Action at Towerhead in elevation

a) and b) give each a contribution to the required mild reinforcement, a) more to the horizontal and vertical part outside the loops, b) to the vertical part inside the loop. Local forces have to be covered by separate reinforcement like tie back reinforcement at the loops. The nodal zone is designed as vertical beam acting in tension and bending. It ties together the anchors and gives the possibility to distribute the splitting reinforcement over the total depth of the punching cone. c) and d) are additional investigations which took into account e.g. the double box structure in the upper region.

The reinforcement is designed to satisfy all models a) to d). After the cable forces are introduced into the short walls they must be distributed into the long wall. This design has been done with a multiple truss model.

It was decided by the contractor to use slipforming for all parts of the tower, including the anchorage regions. This was necessary due to the severe wind conditions with very strong, unexpected gusts, during which nobody wanted to take the risk of lifting the more exposed jumping forms.

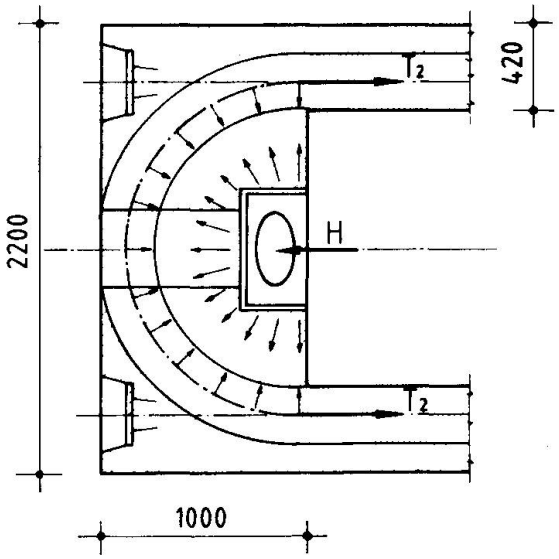

Fig. 5: Arch Action at Towerhead

This slipforming had a very stromg influence on the final rebar arrangement and detailing, especially in the anchorage area. The anchorage pipes have been welded on the ground to a steel frame, lifted up to the tower and bolted to the previous frame in the short walls. All the reinforcement had to be placed around these frames. This was achieved by a very accurate planning of each single bar location.

2.2 Deck Edge Beams

The required two lanes of traffic and a walkway resulted in a beam width of only 11.95 m, which leads to the remarkable slenderness in plan of 1:35.6. For the severe wind conditions the shallow, aerodynamically shaped 1.20 m deep cross-section was developed with a slenderness in elevation of 1:354. Non-linear effects in both directions were investigated using realistic non-linear stress-strain relationships.

Partial prestress was chosen for the beam in both directions to enhance its ductility. Straight tendons in the edge beams are continuous over the full length of the bridge and are coupled in every construction joint. Additional continuity tendons are threaded into empty ducts after completion of the beam across the mid-quarter of the main span. Full depth cross girders are provided at the cable anchorpoints. They contain the only transverse prestress. The reinforced 0.40 m thick roadway slab spans 7.25 m transversely and 12.2 m longitudinally.

The final design was governed by
a) dead plus live load action forces
b) action forces from dynamic wind
c) action forces during construction.

In a) the non-linear effect was taken into account with an estimated reduction of the E-Modulus by 2/3 because in ULS the stress level is above the linear branch of the stress-strain curve. Due to the slenderness of the bridge deck, the non-linear increase of the bending moments reaches 50 % of the linear live load moments, see Fig. 6.

For the first iteration of the wind analysis, an uncracked section without non-linear effects has been investigated. The resulting forces of this study gave the governing moments for the design of the beam almost all along the bridge and lead to the dense reinforcement shown in Fig. 7. The four tendons with 9 x 0.5" strands per edge beam have been provided mainly for erection. Due to partial prestressing the ratio between reinforcement and post-tensioning could be optimized with regard to structural and construction requirements. The combined bar and duct arrangement provides easy access for concreting and vibrating, convenient and economical splices and a simple post-tensioning arrangement.

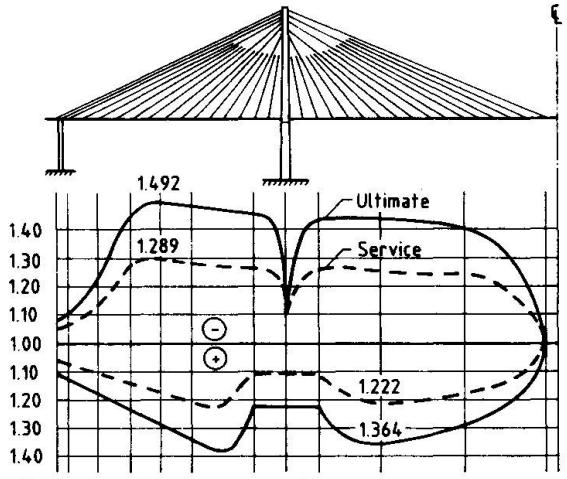

Fig. 6: Non-linear Beam Moments

The design for wind and live load was done in ULS, however the serviceablility had to be checked in SLS. The crack width is limited to 0.2 mm at the rebars and 0.1 mm at the tendons under dead plus 60 % live load. In the cracked section the steel stress is limited to 200 N/mm^2 for this load case. The post-tensioning is sufficient to avoid tension in longitudinal direction under permanent load conditions.

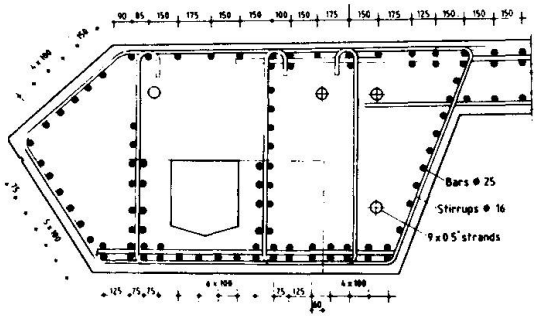

Fig. 7: Reinforcement in Edge Beam

3 AERODYNAMIC INVESTIGATION

The wind climate at the bridge site is very severe. The 50-year design wind speed (10 min. mean) at deck level is 50 m/s, with turbulence intensities horizontally of 10 m/s and vertically of 4 m/s. These rather large turbulences are due to the adjacent mountains.

An analytical time-history wind investigation was performed which is outlined in more detail in Ref. [2].

The non-linear force-deformation characteristics of the beam and the interaction between horizontal and vertical bending as well as torsion in the ultimate limit state were taken into account. For calculations in ULS action force versus deformation behaviour of the structure was followed up through a parametric analysis by a biaxial bending program, under consideration of the governing longitudinal force as well as of cracking of the tensile zone, see Fig. 8. These bending stiffnesses were essentially dependent on the actual reinforcement of the cross section.

A remaining tension stiffness of the concrete between the cracks of up to 1/3 was assumed. Calculations showed that nonlinear behaviour and bending interactions are satisfactorily described through the mathematical model shown in Fig. 9.

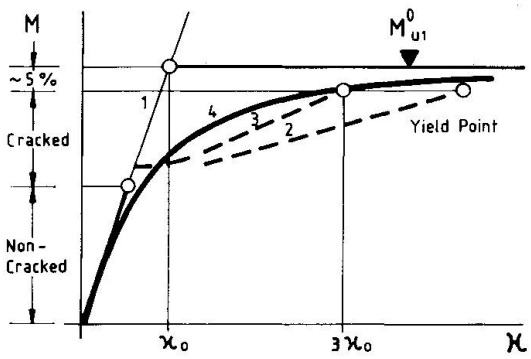

Fig. 8: Beam Stiffness Diagram

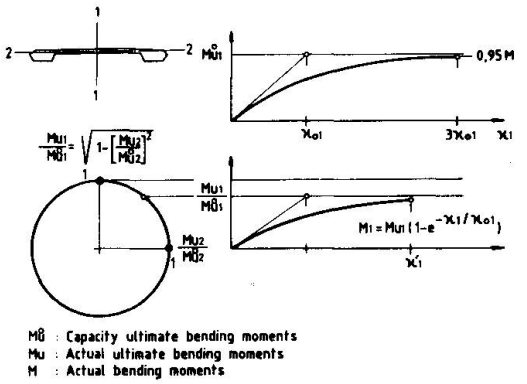

Fig. 9: Moment Interaction, ULS

The nonlinear behaviour in case of one-axial bending was estimated by

$$M_1 = M^0_{U1}\left(1 - e^{-\varkappa_1/\varkappa_{01}}\right)$$

with M_1 actual bending moment in the main plane 1
M_{U1} corresponding bending moment capacity
$\varkappa_1$ actual rotation
$\varkappa_{01}$ fictive roation by bending moment capacity, assuming full-elasticity

In view of a conservative supplementary checking of the ultimate load carrying capacity, the deformations were limited to the elastic limit of the reinforcement; this was found at about
A simultaneous moment in the ortogonal direction was found to be effective essentially through a reduction of the bending moment capacity M_{U1}. In dependence of the reduction factor,

$$\varepsilon = \sqrt{\left(\frac{M_1}{M^0_{U1}}\right)^2 + \left(\frac{M_2}{M^0_{U2}}\right)^2}$$

the reduced bending capacity becomes

$$M_{U1} = |M_1|/\varepsilon.$$

The stiffness receives the same reduction automatically, see definition in Fig. 9. The allowable roatation by achieving the elasticity limit of the reinforcement was found to be at about

$$\varkappa_1' = 3\varkappa_{01}\left(1 - \varkappa_2/3\varkappa_{02}\right).$$

The interaction effect on the torsional stiffness was set to

$$GJ_T = GJ_{T0}\left(1 - \frac{|M_1|}{M_{U1}^0}\right)\left(1 - \frac{|M_2|}{M_{U2}^0}\right).$$

The St. Venant torsional stiffness dropped in the ULS calculations occasionally to 10 - 30 % of the initial value.

The non-linear transverse moments at ULS at mid-span are reduced as a result of redistribution due to degressive stiffness, compared with the moments at service state multiplied by the safety factor of 1.6 as illustrated in Fig. 10.

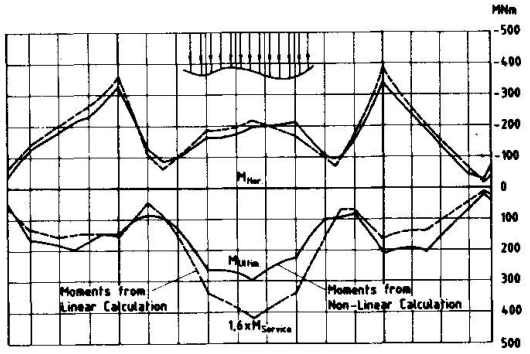

Fig. 10: Transverse Beam Moments, ULS

4. BEAM CONSTRUCTION

In order to facilitate the exact positioning of the stay cables and to provide an economical solution for the transmittal of the horizontal stay force component during casting, the concrete corbels and adjacent parts of the beam with the steel pipe are precast, see Fig. 11.

Governing stages in the erection phase were stressing the cables to final length for max. pos. moments and placing the precast elements and rebars into the catilevered formtraveller for max. neg. moments. The steel stress in the outermost bars was limited to 200 MPa, keeping the crack width at the exterior steel layers smaller 0,1 mm. The erection post-tensioing and the rebars had to be adjusted several times during the final design phase to take care of the changes in the equipment weight.

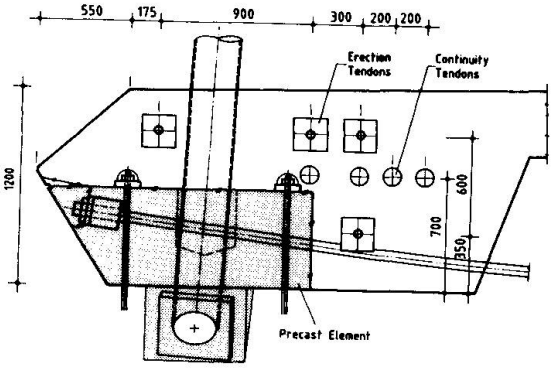

Fig. 11: Edge beam near cable anchorage

5. ACKNOWLEDGEMENT

The owner of the Helgeland Bridge is the Norwegian Road Administration, Nordland, with Mr Wilhelm B. Klaveness in charge. Main consultants are A. Aas Jakobsen, Oslo, Norway. Leonhardt, Andrä and Partners, Stuttgart, Germany, are special consultants for the cable-stayed bridge, including the aerodynamic investigation.

REFERENCES

[1] JORDET, E.A., SVENSSON, H.S.: Helgeland Bridge, a slender concrete cable-stayed bridge in location of severe winds. FIP 90, Vol.1, p. B95 to B99, Hamburg, 1990.

[2] KOVACS, I., SVENSSON, H.S., and JORDET, E.A.: Analytical investigation of the cable-stayed Helgeland Bridge in turbulent wind. To appear soon in the Journal of Structural Engineering, ASCE.